ISSN 2500-316X (Online)

RUSSIAN TECHNOLOGICAL JOURNAL

РОССИЙСКИЙ ТЕХНОЛОГИЧЕСКИЙ ЖУРНАЛ

Information systems.
Computer sciences.
Issues of information security

Multiple robots (robotic centers) and systems.
Remote sensing and nondestructive testing

Modern radio engineering and telecommunication systems

Micro- and nanoelectronics.
Condensed matter physics

Analytical instrument engineering and technology

Mathematical modeling

Economics of knowledge-intensive and high-tech enterprises and industries.
Management in organizational systems

Product quality management. Standardization

Philosophical foundations of technology and society

12+
www.rtj-mirea.ru

12(6) 2024

ISSN 2500-316X (Online)

RUSSIAN TECHNOLOGICAL JOURNAL

РОССИЙСКИЙ ТЕХНОЛОГИЧЕСКИЙ ЖУРНАЛ

- Information systems. Computer sciences. Issues of information security
- Multiple robots (robotic centers) and systems. Remote sensing and nondestructive testing
- Modern radio engineering and telecommunication systems
- Micro- and nanoelectronics. Condensed matter physics
- Analytical instrument engineering and technology
- Mathematical modeling
- Economics of knowledge-intensive and high-tech enterprises and industries. Management in organizational systems
- Product quality management. Standardization
- Philosophical foundations of technology and society

- Информационные системы. Информатика. Проблемы информационной безопасности
- Роботизированные комплексы и системы. Технологии дистанционного зондирования и неразрушающего контроля
- Современные радиотехнические и телекоммуникационные системы
- Микро- и наноэлектроника. Физика конденсированного состояния
- Аналитическое приборостроение и технологии
- Математическое моделирование
- Экономика наукоемких и высокотехнологичных предприятий и производств. Управление в организационных системах
- Управление качеством продукции. Стандартизация
- Мировоззренческие основы технологии и общества

Russian Technological Journal
2024, Vol. 12, No. 6

Russian Technological Journal
2024, том 12, № 6

https://www.rtj-mirea.ru

https://doi.org/10.32362/2500-316X

ISSN 2500-316X (Online)

Russian Technological Journal
2024, Vol. 12, No. 6

Publication date November 28, 2024.

The peer-reviewed scientific and technical journal highlights the issues of complex development of radio engineering, telecommunication and information systems, electronics and informatics, as well as the results of fundamental and applied interdisciplinary researches, technological and economical developments aimed at the development and improvement of the modern technological base.

Periodicity: bimonthly.
The journal was founded in December 2013. The titles were «Herald of MSTU MIREA» until 2016 (ISSN 2313-5026) and «Rossiiskii tekhnologicheskii zhurnal» from January 2016 until July 2021 (ISSN 2500-316X).

Founder and Publisher:
Federal State Budget
Educational Institution of Higher Education
«MIREA – Russian Technological University»
78, Vernadskogo pr., Moscow, 119454 Russia.

The journal is included into the List of peer-reviewed science press of the State Commission for Academic Degrees and Titles of Russian Federation. The Journal is included in Russian Science Citation Index (RSCI), Russian State Library (RSL), Science Index, eLibrary, Directory of Open Access Journals (DOAJ), Directory of Open Access Scholarly Resources (ROAD), Google Scholar, Ulrich's International Periodicals Directory.

The registration number ПИ № ФС 77 - 81733 was issued in August 19, 2021 by the Federal Service for Supervision of Communications, Information Technology, and Mass Media of Russia.

The subscription index of *Pressa Rossii*: **79641**.

Russian Technological Journal
2024, том 12, № 6

Дата опубликования 28 ноября 2024 г.

Научно-технический рецензируемый журнал освещает вопросы комплексного развития радиотехнических, телекоммуникационных и информационных систем, электроники и информатики, а также результаты фундаментальных и прикладных междисциплинарных исследований, технологических и организационно-экономических разработок, направленных на развитие и совершенствование современной технологической базы.

Периодичность: один раз в два месяца.
Журнал основан в декабре 2013 года. До 2016 г. издавался под названием «Вестник МГТУ МИРЭА» (ISSN 2313-5026), а с января 2016 г. по июль 2021 г. под названием «Российский технологический журнал» (ISSN 2500-316X).

Учредитель и издатель:
федеральное государственное бюджетное образовательное учреждение высшего образования «МИРЭА – Российский технологический университет»
119454, РФ, г. Москва, пр-т Вернадского, д. 78.

Журнал входит в Перечень ведущих рецензируемых научных журналов ВАК РФ, в которых должны быть опубликованы основные научные результаты диссертаций на соискание ученой степени кандидата наук и доктора наук, входит в RSCI, РГБ, РИНЦ, eLibrary, Directory of Open Access Journals (DOAJ), Directory of Open Access Scholarly Resources (ROAD), Google Scholar, Ulrich's International Periodicals Directory.

Регистрационный номер и дата принятия решения о регистрации СМИ ПИ № ФС 77 - 81733 от 19.08.2021 г. СМИ зарегистрировано Федеральной службой по надзору в сфере связи, информационных технологий и массовых коммуникаций (Роскомнадзор).

Индекс по объединенному каталогу «Пресса России» **79641**.

https://www.rtj-mirea.ru

Editorial Board

Редакционная коллегия

Contents

Содержание

Information systems. Computer sciences. Issues of information security
Информационные системы. Информатика. Проблемы информационной безопасности

UDC 621.311.1
https://doi.org/10.32362/2500-316X-2024-12-6-7-19
EDN LEDVEZ

RESEARCH ARTICLE

Cybersecurity of smart grids: Comparison of machine learning approaches training for anomaly detection

Sergey V. Kochergin [@], Svetlana V. Artemova, Anatoly A. Bakaev, Evgeny S. Mityakov, Zhanna G. Vegera, Elena A. Maksimova

MIREA – Russian Technological University, Moscow, 119454 Russia
[@] Corresponding author, e-mail: kochergin_s@mirea.ru

Abstract

Objectives. The transformation of modern electric grids into decentralized smart grids presents new challenges in the field of cybersecurity. The purpose of this work is to conduct research and analysis into the effectiveness of different machine-learning methods for identifying anomalies in decentralized smart networks, including cyberattacks and emergency modes, as well as to develop recommendations on the optimal combination of these methods for ensuring effective cybersecurity under conditions of changing electrical loads.

Methods. We consider several machine learning methods for identifying anomalies in power systems that simulate network behavior under conditions of cyberattacks and emergency modes. The relative effectiveness of such methods as multifractal analysis using wavelets, the Isolation Forest model, local outlier factor (LOF), *k*-means clustering, and one-class support vector machine (One-Class SVM), is analyzed.

Results. The comparison of machine learning methods reveals the varying effectiveness of anomaly detection methods used to detect cyber threats and deviations in electrical systems. Isolation Forest is best at detecting abrupt changes related to cyberattacks with high accuracy and a minimum of false positives. While LOF can also be effective in detecting cyberattacks, its increased sensitivity to minor deviations increases the number of false positives. *K*-means and One-Class SVMs are less effective in detecting abrupt anomalies but are useful for general clustering of data and detecting both abrupt and smooth changes, respectively.

Conclusions. The obtained research results indicate the advantages of using a combination of machine learning algorithms to ensure the reliable protection of smart networks from cyberattacks taking into account the nature of the electrical load.

Keywords: smart grids, cybersecurity, machine learning, anomaly detection, Isolation Forest, cyberattacks

• **Submitted:** 12.09.2024 • **Revised:** 25.09.2024 • **Accepted:** 01.10.2024

For citation: Kochergin S.V., Artemova S.V., Bakaev A.A., Mityakov E.S., Vegera Zh.G., Maksimova E.A. Cybersecurity of smart grids: Comparison of machine learning approaches training for anomaly detection. *Russ. Technol. J.* 2024;12(6):7–19. https://doi.org/10.32362/2500-316X-2024-12-6-7-19

Financial disclosure: The authors have no financial or proprietary interest in any material or method mentioned.

The authors declare no conflicts of interest.

НАУЧНАЯ СТАТЬЯ

Кибербезопасность смарт-сетей: сравнение подходов машинного обучения для обнаружения аномалий

С.В. Кочергин [@], **С.В. Артемова**, **А.А. Бакаев**, **Е.С. Митяков**, **Ж.Г. Вегера**, **Е.А. Максимова**

МИРЭА – Российский технологический университет, Москва, 119454 Россия
[@] *Автор для переписки, e-mail: kochergin_s@mirea.ru*

Резюме

Цели. Современные электрические сети, трансформирующиеся в децентрализованные смарт-сети, сталкиваются с новыми вызовами в области кибербезопасности. Цель работы – провести исследование и анализ эффективности различных методов машинного обучения для выявления аномалий в децентрализованных смарт-сетях, включая кибератаки и аварийные режимы, для разработки рекомендаций по оптимальному сочетанию этих методов для обеспечения эффективной кибербезопасности в условиях изменяющейся электрической нагрузки.

Методы. Рассматриваются различные методы машинного обучения для выявления аномалий в энергосистемах, моделирующих поведение сети в условиях кибератак и аварийных режимов. Проведен анализ эффективности таких методов, как мультифрактальный анализ с использованием вейвлетов и модель изолированного леса (Isolation Forest), локальный коэффициент выбросов (local outlier factor, LOF), кластеризация методом *k*-средних и одноклассовая машина опорных векторов (One-Class SVM).

Результаты. Рассмотрены различные методы машинного обучения для выявления аномалий в энергосистемах, моделирующих поведение сети в условиях кибератак и аварийных режимов. Методы обнаружения аномалий показали разную эффективность в выявлении киберугроз и отклонений в электрических системах. Метод Isolation Forest лучше всего обнаруживает резкие изменения, связанные с кибератаками, высокой точностью и минимумом ложных срабатываний. Метод LOF также может выявлять кибератаки, но его повышенная чувствительность к мелким отклонениям увеличивает число ложных срабатываний. Методы *k*-средних и One-Class SVM менее эффективны в выявлении резких аномалий, но полезны для общей кластеризации данных и обнаружения как резких, так и плавных изменений соответственно.

Выводы. Полученные результаты исследований указывают на то, что для обеспечения надежной защиты смарт-сетей от кибератак следует использовать комбинацию алгоритмов машинного обучения с учетом характера электрической нагрузки.

Ключевые слова: смарт-сети, кибербезопасность, машинное обучение, выявление аномалий, Isolation Forest, кибератаки

• **Поступила:** 12.09.2024 • **Доработана:** 25.09.2024 • **Принята к опубликованию:** 01.10.2024

Для цитирования: Кочергин С.В., Артемова С.В., Бакаев А.А., Митяков Е.С., Вегера Ж.Г., Максимова Е.А. Кибербезопасность смарт-сетей: сравнение подходов машинного обучения для обнаружения аномалий. *Russ. Technol. J*. 2024;12(6):7–19. https://doi.org/10.32362/2500-316X-2024-12-6-7-19

Прозрачность финансовой деятельности: Авторы не имеют финансовой заинтересованности в представленных материалах или методах.

Авторы заявляют об отсутствии конфликта интересов.

INTRODUCTION

Modern power grids are being rapidly transformed into decentralized systems with the introduction of smart grids and distributed power generation. Such grids, comprising cyberphysical systems, face new cybersecurity challenges related to the need to protect distributed components from potential multilayered attacks [1–5]. Due to the inadequacy of using traditional antivirus software for protecting such networks, the professional community has been paying more attention to the issue of endpoint protection, including Endpoint Detection and Response (EDR) [6].

A special feature of the EDR system lies in its capability to use behavioral analysis for detecting suspicious activity and detecting changes in the configuration of endpoints and nodes of the electrical network and directly connected electrical equipment. For example, the actions of intruders using fileless methods can manifest themselves in changes in electrical energy parameters (voltage, resistance) and false commands to switch equipment.

Smart grids protection requires the development of new behavioral analysis methods that take into account the peculiarities of their technological modes of operation.

STUDY AND CLASSIFICATION OF HARMONIC DISTORTIONS AND ANOMALOUS SIGNALS CAUSED BY CYBERATTACKS

The primary focus of cyberattacks on smart grids is to create the conditions to maximize the damage of disruption. One cyberattack approach that poses a significant threat consists in tampering with the voltage regulation control system. This exploits a vulnerability connected with the use of transformers with automatic voltage regulation to maintain the required voltage level. The most common regulation method involves the use of load-side regulation transformers [7–9].

Unusual commands and actions during a cyberattack on the electric grid can manifest themselves in a variety of ways that differ from normal system behavior. For example, a command to change a transformer's transformer ratio for no apparent reason or attempts to repeatedly log into the control system may indicate that the attackers are attempting to interfere with the system. Such anomalous actions require prompt detection and analysis to prevent possible threats.

Let us consider an example of power grid operation during a cyberattack. Here the power system is operating in normal mode with all parameters within acceptable limits. Transformer T1 functions stably, providing the necessary voltage at the substation with a transformation ratio of 35(10)/0.4 kV. Suddenly a command is received to change the T1 transformer ratio, although the operator finds no reason for such a change, as the system parameters remain within normal limits. Nevertheless, the command is executed to change the transformer ratio. This causes voltage fluctuations on the low voltage side of the transformer (0.4 kV), which leads to disruption of the connected consumers' operation.

This process can trigger a rolling shutdown of automation and consequent loss of power supply to end consumers. Alarms due to deviations of network parameters appear on the dispatch panel, and operators take measures to restore normal operation. After the incident is eliminated, analysis is performed to identify the cause of sending an unauthorized command. System logs and network traffic are examined for possible cyberattacks or control system failures.

This example demonstrates the vulnerability of electrical grids in the case of intruders penetrating the control system, along with the need for early detection of anomalies (false commands).

Understanding anomalies in power grid protection is not possible without process knowledge. Cyberattacks typically differ from normal system failures due to their lack of association with obvious causal links in the fault chain. Additionally, such attacks occur suddenly, making them difficult to detect using traditional methods [10–14].

In this regard, the task of the present study is to conduct an experiment simulating the deviation of voltage in the network according to a selected anomaly analysis method, allowing it to be distinguished as accurately as possible from the normal emergency mode of operation of the electrical network.

In order to conduct the studies, synthetic data were generated to simulate electrical voltages ranging from −0.9 kV to +0.9 kV (Fig. 1). These data cover three different scenarios: normal system operation (no voltage deviation), sudden voltage deviation due to a cyberattack (no change in electrical load), and emergency operation with prolonged voltage deviation (with change in electrical load).

Under normal conditions, the voltage is described by a sinusoidal time function $U = f(t)$ with the addition of random noise reflecting real fluctuations (Fig. 1a). To simulate a cyberattack, a sudden voltage spike of 0.3 kV was artificially introduced (Fig. 1b). Emergency operation mode with voltage deviation was simulated by increasing the amplitude of the sinusoid for a finite period of time (Fig. 1c).

In this study, several machine learning algorithms were used for the analysis of synthetic data simulating the behavior of the electric grid under cyberattack and emergency mode of electric load deviation. Unlike neural networks, which require significant computational resources, the selected methods such as Isolation Forest method, local outlier factor (LOF), one-class support vector machine (One-Class SVM), and *k*-means clustering, have less computational complexity and do not require a large dataset for learning.

Let us consider each method separately and analyze the results obtained to evaluate their effectiveness in detecting such anomalies.

Multifractal analysis and Isolation Forest method

Fractal methods can be used to detect anomalies in the data, which may indicate a change in the state of the system or the presence of external influences. This makes them useful for monitoring and diagnostics of various processes [15–17].

We apply the discrete wavelet transform for the voltage and calculate multifractal features, including the mean value and the variance of the absolute values of the coefficients. The vector of these features will be used in the Isolation Forest model [18] to detect anomalies.

Let $x(t)$ be a time series representing data (e.g., a voltage time series). In order to analyze the time series, a discrete wavelet transform is used, which decomposes the signal into several levels of detail.

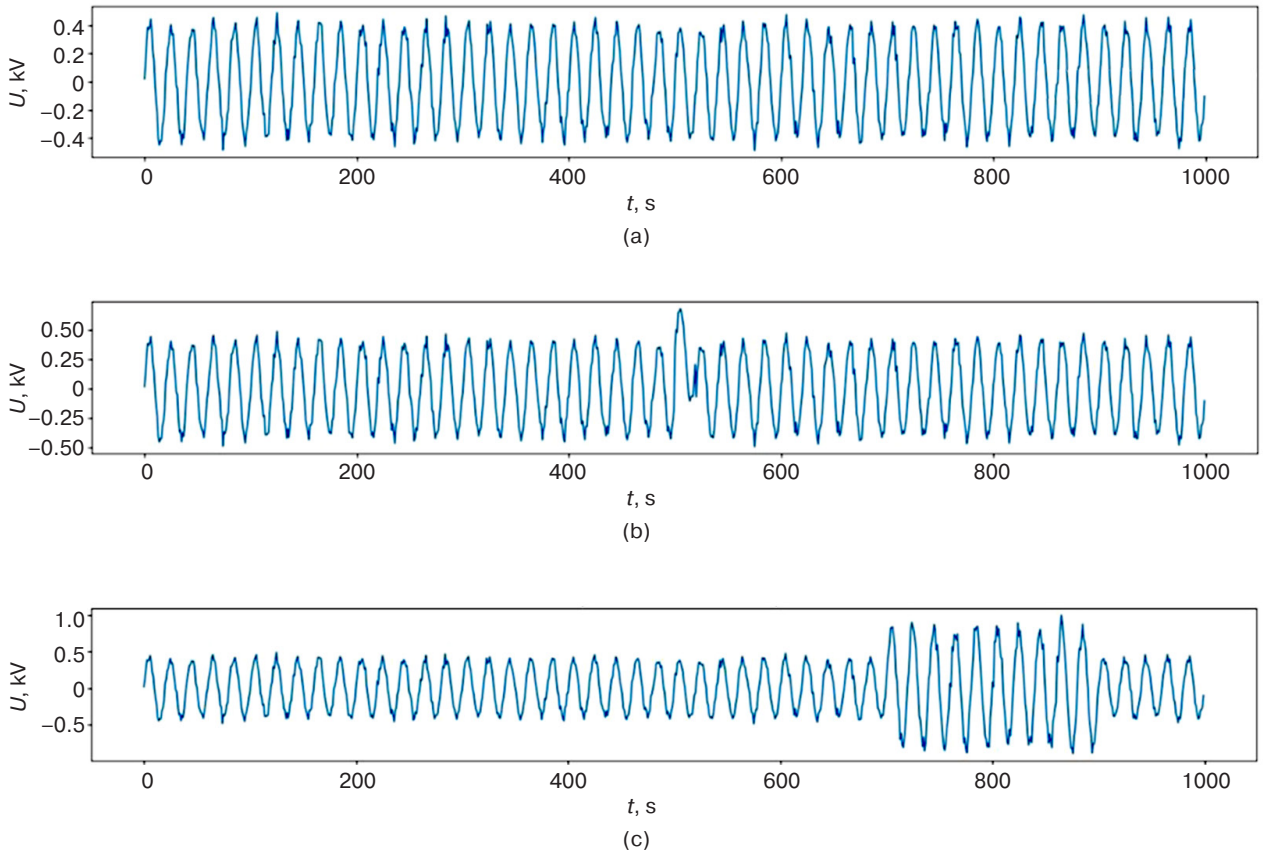

Fig. 1. Simulation of various operation modes of the power grid: normal operation mode (a); mode with cyberattack (b); normal mode with voltage deviation (c)

Wavelet transform W_x of the signal $x(t)$ at the level j can be written as:

$$W_x(t, j) = \Sigma_t x(t)\psi_{j,k}(t), \quad (1)$$

where $\psi_{j,k}(t)$ is a wavelet function, a shifted and scaled version of the mother wavelet.

For each decomposition level j, we obtain a set of coefficients c_j that describe different time scales of the signal:

$$\boldsymbol{c}_j = W_x(t, j). \quad (2)$$

At each level j of the wavelet decomposition, the mean and variance of the absolute values of the coefficients c_j are calculated:

$$\boldsymbol{\mu}_j = \frac{1}{N_j}\sum_{k=1}^{N_j} |\mathbf{c}_{j,k}|, \quad (3)$$

$$\boldsymbol{\sigma}_j^2 = \frac{1}{N_j}\sum_{k=1}^{N_j} (|\mathbf{c}_{j,k}| - \boldsymbol{\mu}_j)^2, \quad (4)$$

where N_j is the number of coefficients at the level j.

These features make up the feature vector for each time series:

$$\mathbf{features} = [\boldsymbol{\mu}_1, \boldsymbol{\sigma}_1^2, \boldsymbol{\mu}_2, \boldsymbol{\sigma}_2^2, ..., \boldsymbol{\mu}_m, \boldsymbol{\sigma}_m^2]. \quad (5)$$

Let $\mathbf{F}_i$ be a vector of multifractal features for the ith time series, then the set of features for all-time series can be written as a matrix:

$$\mathbf{F} = [\mathbf{F}_1, \mathbf{F}_2, \ldots, \mathbf{F}_n]^{\mathrm{T}}. \quad (6)$$

In order to identify anomalies, the Isolation Forest model [18] is trained on the feature matrix $\mathbf{F}_i$. In so doing, the model builds several decision trees according to which the data are sliced based on randomly selected features in an attempt to isolate anomalous data points with the minimum tree depth.

The abnormal scores for each time series are calculated using a decision function:

$$S_i = \text{decision\_function}(\mathbf{F}_i), \quad (7)$$

where S_i is the anomaly estimate for the ith time series.

Abnormal S_i score is used to determine the extent to which a time series deviates from the normal state. Low S_i values indicate a strong anomaly, while high S_i values correspond to normal behavior.

Based on the outlined theoretical principles, a computer program was developed to create a heat map of anomalies using the Isolation Forest model based on multifractal features (Fig. 2). The use of heat maps to visualize anomalies enables visual demonstration of the recurring patterns and the separation of normal events from cyberattacks and emergency modes.

Within the heat map, the horizontal axis represents time steps (0 to 1000) representing successive measurements of the data over time, while the vertical axis represents the anomaly estimates predicted by the model. The gradient scale ranges from black, indicating high anomaly estimates (low probability of normality), to white, which indicates low anomaly estimates (high probability of normality).

Heat map analysis

1. The period is 0–500 s. Most of the data in this period is colored white, indicating low abnormal estimates. This indicates that the model classifies this data as normal.
2. The period near the time mark is equal to 500 s. Within this period, a narrow black band is observed, which corresponds to a high anomalous score.
3. This black band clearly indicates a cyberattack that was synthesized to simulate an abrupt deviation from the norm. The model successfully identified this deviation, as confirmed by the presence of a black area in the heat map.
4. The period is equal to 700–900 s. This section shows a significant variation of the color scale from black to gray, which is associated with the emergency mode in which the amplitude of the sinusoidal signal is changed. In contrast to the narrow black band indicating a cyberattack, a more complex and gradient pattern is seen here, reflecting an anomaly associated with the operating mode of voltage deviation rather than a cyberattack.
5. The period is equal to 900–1000 s. This segment is again dominated by white color, indicating normal data similar to the initial period.

LOF method

The LOF method [19] identifies local anomalies based on a comparison of the data density in the neighborhood of each point.

The LOF for each point x_i is calculated as follows:

1. The distance to the nearest neighbors is determined:

$$d_k(x_i, x_j) = \left\| x_i - x_j \right\|, \quad (8)$$

where k is the number of nearest neighbors.

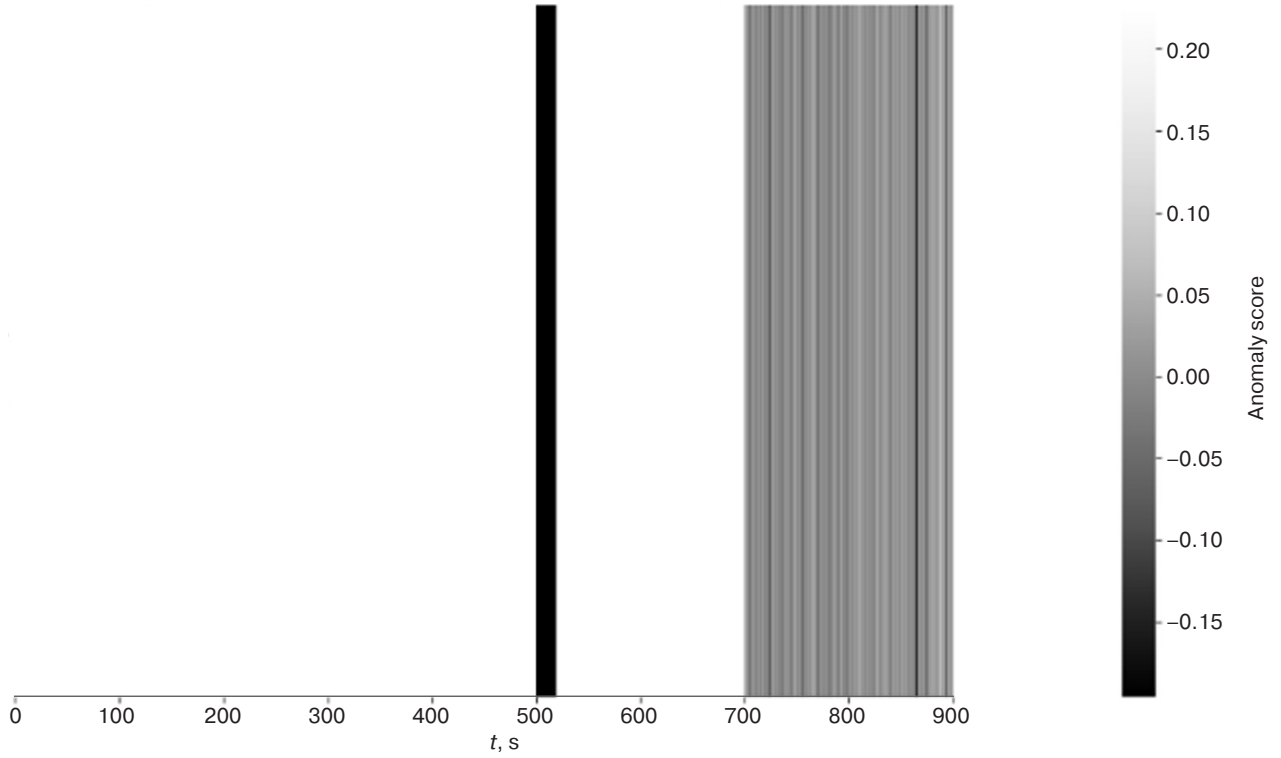

Fig. 2. Thermal anomaly map using the Isolation Forest model with multifractal objects

2. The local reachability density lrd_k for point x_i is determined:

$$\mathrm{lrd}_k(x_i) = \left(\frac{\sum_{j=1}^{k} \mathrm{reach\_dist}_k(x_i, x_j)}{k} \right)^{-1}, \quad (9)$$

where $\mathrm{reach\_dist}_k(x_i, x_j)$ is the distance one has to move from x_i to x_j in order to reach the density of x_j.

3. LOF calculation:

$$\mathrm{LOF}_k(x_i) = \frac{\sum_{j=1}^{k} \frac{\mathrm{lrd}_k(x_j)}{\mathrm{lrd}_k(x_i)}}{k}. \quad (10)$$

A value of $\mathrm{LOF}_k(x_i)$ significantly greater than 1 indicates that point x_i is anomalous.

In order to visualize the results of anomaly estimation, the obtained LOF values are inverted:

$$S_i = -\mathrm{LOF}_k(x_i), \quad (11)$$

where S_i is the anomalous estimate for the point x_i.

Based on these values, a heat map is constructed (Fig. 3), in which anomalous points are displayed in grayscale corresponding to the degree of their deviation from the norm.

The LOF method demonstrated the ability to effectively detect cyberattacks, as can be clearly seen by the black band on the heat map in the region around the 500th point of the time series. However, LOF also detected anomalies across the entire time scale, which can be both an advantage and a disadvantage. In particular, significant changes are observed in the emergency region (700–900 s), although their highlighting is not as contrastive. While the high sensitivity of LOF to local deviations and minor anomalies enables the detection of subtle changes in the data, at the same time it can lead to an increase in the number of false positives, which needs to be taken into account in the interpretation of the results.

K-means clustering method

The *k*-means method is designed to partition a dataset into *k* clusters, in which each cluster is characterized by its center (centroid) [20].

The objective of the method is to minimize the sum of squares of the distances between data points and cluster centers.

Let us have a dataset $\mathbf{X} = \{x_1, x_2, \ldots, x_n\}$, where each data point x_i is a feature vector.

The calculation consists of the following steps:

1. The number of clusters *k*into which the data should be divided is selected.

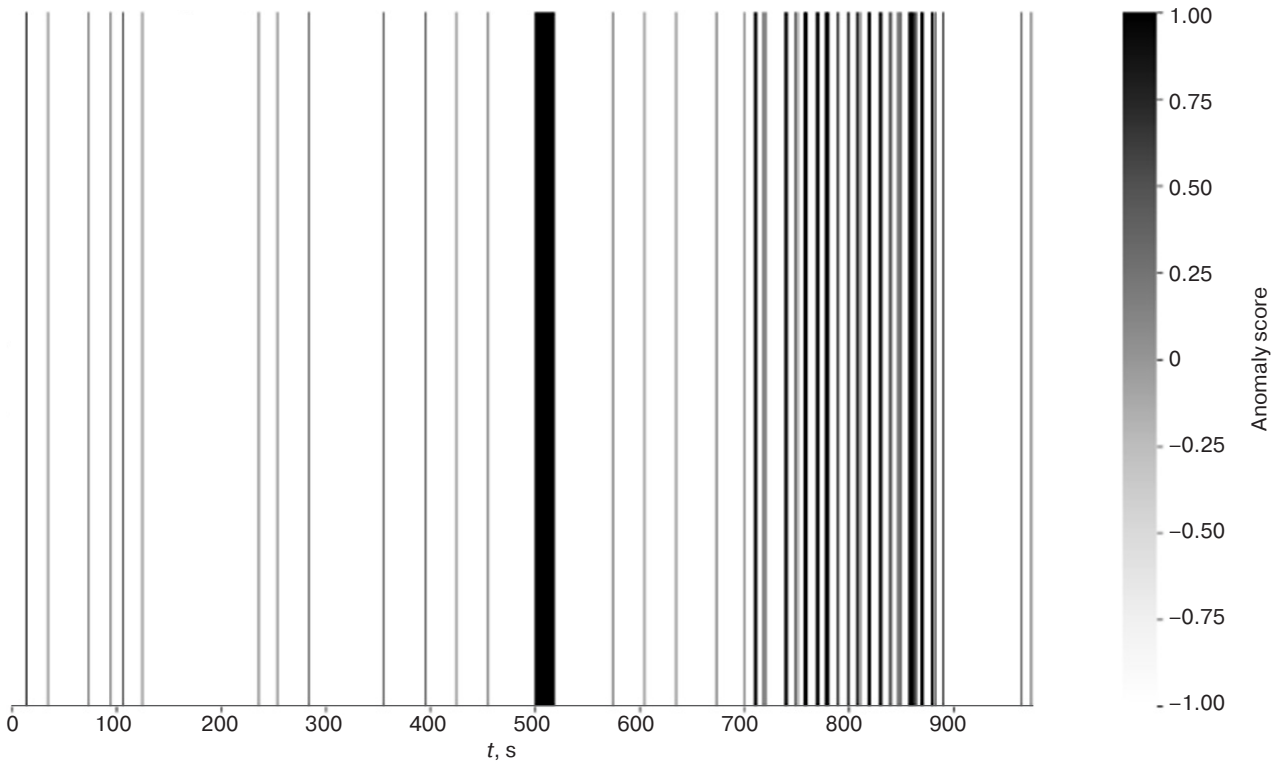

Fig. 3. Heat map of anomaly estimates using LOF

2. Initialization of centroids:

K initial centroids $\{\mu_1, \mu_2, \ldots, \mu_k\}$ are initialized, either chosen randomly from the data points or by other methods such as the *k*-means++.

3. Assigning points to clusters:

For each data point x_i, the distance to each of the centroids μ_j is calculated:

$$d(x_i, \mu_j) = \left\| x_i - \mu_j \right\|. \quad (12)$$

Point x_i is assigned to the cluster with minimum distance:

$$C_i = \arg\min_j d(x_i, \mu_j), \quad (13)$$

where C_i is the cluster to which point x_i belongs.

4. Centroid renewal:

After assigning all points, the centroids for each cluster are recalculated:

$$\mu_j = \frac{1}{|C_j|} \sum_{x_i \in C_j} x_i, \quad (14)$$

where $|C_j|$ is the number of points in the *j*th cluster, and μ_j is the new centroid position.

5. Repeat steps 3 and 4.

Steps 3 and 4 are repeated until the process converges (e.g., until the centroids stop changing or the maximum number of iterations is reached).

K-means method minimizes the following cost function (loss function):

$$J = \sum_{j=1}^{k} \sum_{x_i \in C_j} \left\| x_i - \mu_j \right\|^2, \quad (15)$$

where *J* is the total intra-cluster deviation, and $\left\| x_i - \mu_j \right\|^2$ is the square of the Euclidean distance between a data point and the centroid of its cluster.

The heat map (Fig. 4) shows the distances to cluster centers calculated using the *k*-means clustering method. Time steps are plotted on the horizontal axis are plotted on the vertical axis along with distances to cluster centers. The gradient scale ranges from light gray to black, where black areas correspond to the maximum values of the distances.

While the results obtained via *k*-means clustering method demonstrate its effectiveness in dealing with large anomalies, the approach can produce errors for smooth changes. Therefore, the use of this method should be combined with other methods for a more comprehensive analysis of anomalies.

One-Class SVM method

The One-Class SVM method [21] has a number of features that make it particularly suitable for anomaly detection tasks in critical systems such as electrical

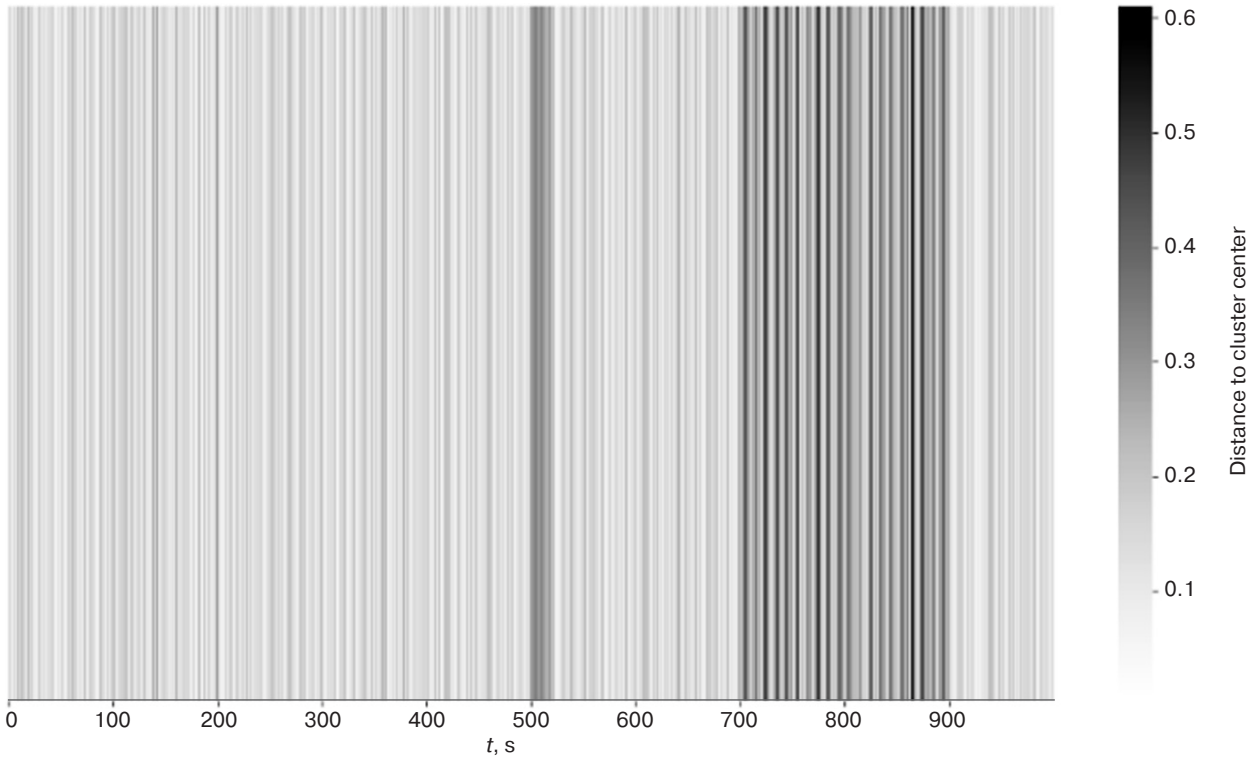

Fig. 4. Heat map of distances to cluster centers using *k*-means clustering

grids. Unlike other methods, One-Class SVM aims to train a model that describes the distribution of normal data and can then be used to detect outliers that do not follow this distribution. This approach is particularly useful in environments where there is limited data on abnormal states or cyberattacks and where the focus is on detecting deviations from the normal state of the system.

In mathematical terms, the One-Class SVM method constructs a hyperplane in feature space that separates all data points from the origin and seeks to maximize the distance between this hyperplane and the closest data points to it. The goal is to have all normal data on one side of the hyperplane and anomalies on the other side.

Formally, let $\mathbf{x}_i$ denote a vector of time series features, where $i = 1, 2, \ldots, n$. One-Class SVM model solves the following optimization problem:

$$\min_{\mathbf{w},\rho,\xi_i} \frac{1}{2}\|\mathbf{w}\|^2 + \frac{1}{\nu n}\sum_{i=1}^{n}\xi_i - \rho \qquad (16)$$

provided:

$$(\mathbf{w} \cdot \phi(\mathbf{x}_i)) \geq \rho - \xi_i,\ \xi_i \geq 0,\ i = 1, 2, \ldots, n. \qquad (17)$$

Here $\mathbf{w}$ is the vector of weights; ρ is the hyperplane offset; ξ_i are the slack variables; $\phi(\mathbf{x}_i)$ is the mapping function to the high-dimensional feature space; ν is a hyperparameter controlling the allowable proportion of outliers and model complexity.

The result of the One-Class SVM is a decision-making function:

$$f(\mathbf{x}) = (\mathbf{w} \cdot \phi(\mathbf{x})) - \rho. \qquad (18)$$

Values of $f(\mathbf{x}) \geq 0$ indicate potential anomalies, whereas values of $f(\mathbf{x}) < 0$ correspond to normal data.

By performing the calculation using the One-Class SVM method, we obtain the results that are shown in the heat map (Fig. 5).

The One-Class SVM method demonstrated high efficiency in detecting both sharp and smooth anomalies in synthetic data modeling the operation of the electrical grid. The ability of this method to detect different types of abnormalities is confirmed by contrasting regions in the heat map corresponding to both cyberattack and fault mode. This approach can be useful for monitoring critical infrastructures, where it is important to detect anomalies in time to prevent system disturbances.

CONCLUSIONS

Based on the heat map analysis, different anomaly detection methods can be concluded to have varying degrees of effectiveness in the context of detecting cyber threats and other abnormalities in electrical systems. The Isolation Forest method performed best in detecting

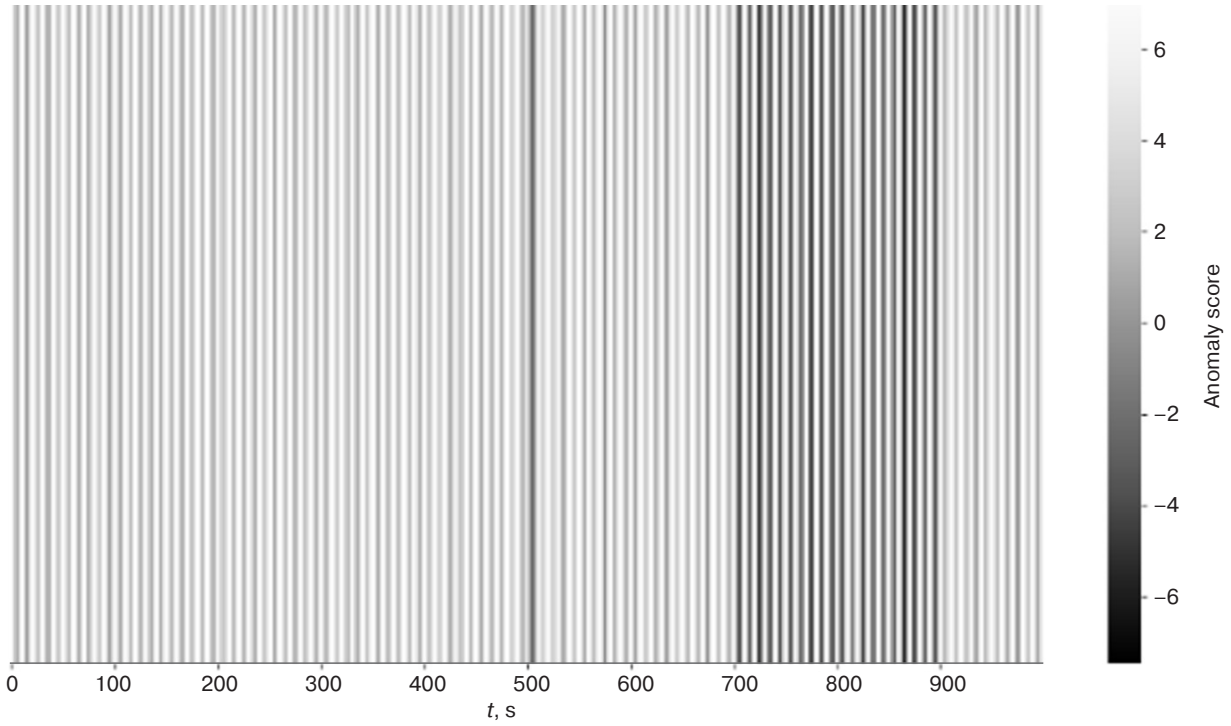

Fig. 5. Heat map of anomaly estimations using the One-Class SVM method

abrupt changes associated with cyberattacks, highlighting such anomalies with high accuracy and producing minimal false positives. While the LOF method also demonstrated an ability to detect cyberattacks, its increased sensitivity to small deviations led to an increased number of false positives, which requires additional attention when interpreting the results.

While the *k*-means clustering and One-Class SVM methods were shown to be less contrastive than Isolation Forest, they also have certain advantages. The *k*-means clustering method proved useful for general clustering of the data but was less effective in detecting sharp anomalies. The One-Class SVM method, on the other hand, demonstrated the ability to detect both abrupt and smooth changes, but with less contrast in highlighting anomalies, which also needs to be considered when selecting the appropriate method for the task of monitoring and protecting critical infrastructures. In general, Isolation Forest can be recommended for detecting cyber threats; however, in order to provide comprehensive anomaly analysis, it is recommended to use several methods in combination.

The presented research confirms the need to combine different methods depending on the nature of electrical load variation in order to effectively prevent cyberattacks on smart grids.

Authors' contributions

S.V. Kochergin—developing the research concept, identifying the main problems, formulating aims and objectives; literature review in cybersecurity for smart grids; preparing the materials for experiments and conducting the experiments.

S.V. Artemova—developing the research methodology, selecting approaches of machine learning for comparison; preparing the article and its editing.

A.A. Bakaev—determining the research topic and discussing the final text of the article.

E.S. Mityakov—interpreting the research results and preparing conclusions.

Zh.G. Vegera—mathematical interpretation of the research.

E.A. Maksimova—analysis of existing anomaly detection methods and identification of the most promising ones for comparison.

Each author uniquely contributed to preparing the research article.

REFERENCES

1. Ihsanov I.I. Security in the electric power industry: current threats and protective measures. In: *Youth and Knowledge – Guarantee of Success – 2023: Collection of Scientific Articles of the 10th International Youth Scientific Conference*. Kursk, September 19–20, 2023. Kursk: Universitetskaya kniga; 2023. V. 2. P. 472–474 (in Russ.). URL: https://elibrary.ru/tfyddx
2. Papkov B.V., Osokin L.V., Kuchin N.N. Cyber security of distribution facilities electrical networks. *Sel'skii mekhanizator = Selskiy Mechanizator*. 2024;5:3–7 (in Russ.). Available from URL: https://elibrary.ru/tfmvhi
3. Kolosok I.N., Korkina E.S. Analysis of cybersecurity of power facilities taking into account the mechanism and kinetics of undesirable processes. *Energetik*. 2024;2:3–8 (in Russ.). http://doi.org/10.34831/EP.2024.60.27.001, available from URL: https://elibrary.ru/ecxvjp
4. Abdrakhmanov I.I. Dangers and threats to cybersecurity in the electric power industry: analysis of modern threats and protection mechanisms. *Nauchnyi Aspekt*. 2024;31(3):3970–3973 (in Russ.). Available from URL: https://elibrary.ru/lrouni
5. Gurina L.A. Assessment of cyber resilience of the operational dispatch control system of EPS. *Voprosy kiberbezopasnosti = Cybersecurity Issues*. 2022;3(49):23–31 (in Russ.). Available from URL: https://elibrary.ru/sapiyh
6. Smetanin D.I. Studying the structure of the System for detecting and countering attacks of ransomware viruses based on Endpoint Detection and Response. In: *Topical Issues of Modern Science: Collection of articles of the 7th International Scientific and Practical Conference*: in 2 v. Penza: Nauka i Prosveshchenie; 2023. V. 1. P. 60–64 (in Russ.). Available from URL: https://elibrary.ru/vuvfpa
7. Lezhnyuk P.D., Rubanenko A.E., Kazmiruk O.I. Optimal control of normal modes of the EES, taking into account the technical condition of transformers with RPN. *Nauchnye trudy Vinnitskogo natsional'nogo tekhnicheskogo universiteta = Scientific Works of Vinnytsia National Technical University*. 2012;4:2 (in Russ.). Available from URL: https://elibrary.ru/pyqugn
8. Kopylova V.V., Parkachev K.N., Tiguntsev S.G. Transformer with thyristor on-load RPN changers. *Elektrooborudovanie: ekspluatatsiya i remont.* 2019;12:35–39 (in Russ.). Available from URL: https://elibrary.ru/vgfudv
9. Arzhannikov B.A., Baeva I.A., Tarasovskii T.S. Thyristor devices for voltage regulation of transformers under load RPN. *Transport Aziatsko-Tikhookeanskogo regiona = Transport of the Asia-Pacific Region*. 2020;4(25):32–38 (in Russ.). Available from URL: https://elibrary.ru/lxmknj
10. Ragozin A.N. Forming a forecast of multicomponent time series of data using digital filtering methods and a predictive auto-encoder in order to detect anomalies in the operation of automated process control systems under the influence of cyberattacks. *Vestnik UrFO. Bezopasnost' v informatsionnoi sfere = Journal of the Ural Federal District. Information Security.* 2021;2(40):44–58 (in Russ.). https://doi.org/10.14529/secur210205, available from URL: https://elibrary.ru/khwhfq
11. Pletenkova A.D. Detection of anomalies caused by cyber attacks in the observed processes of automated control systems using a self-organizing Kohonen map. In: *Security of the Information Space: Proceedings of the 22nd All-Russian Scientific and Practical Conference of Students, Postgraduates and Young Scientists*. Chelyabinsk, November 30, 2023. Chelyabinsk: SUSU Publishing Center; 2024. P. 267–274 (in Russ.). Available from URL: https://www.elibrary.ru/ctpuyj
12. Bukharev D.A., Sokolov A.N., Ragozin A.N. Application of hierarchical cluster analysis for clustering data of ICS information processes affected by cyberattacks. *Vestnik UrFO. Bezopasnost' v informatsionnoi sfere = Journal of the Ural Federal District. Information Security.* 2023;1(47):59–68 (in Russ.). https://doi.org/10.14529/secur230106, Available from URL: https://elibrary.ru/fycuhe
13. Asyaev G.D., Sokolov A.N. Predictive information protection models of automated water management system based on the series using machine learning technologies. *Vestnik UrFO. Bezopasnost' v informatsionnoi sfere = Journal of the Ural Federal District. Information Security.* 2021;4(42):39–45 (in Russ.). https://doi.org/10.14529/secur210404, available from URL: https://elibrary.ru/yjkbtz
14. Sokolov A.N., Ragozin A.N., Barinov A.E., et al. Development of models and methods for early detection of cyber attacks on energy facilities of a metallurgical enterprise. *Vestnik UrFO. Bezopasnost' v informatsionnoi sfere = Journal of the Ural Federal District. Information Security.* 2021;3(41):65–87 (in Russ.). https://doi.org/10.14529/secur210308, available from URL: https://elibrary.ru/kzggpj
15. Shtyrkina A.A., Zegzhda P.D., Lavrova D.S. Detection of anomalies in the traffic of Internet backbone networks using multifractal analysis. *Metody i Tekhnicheskie Sredstva Obespecheniya Bezopasnosti Informatsii.* 2018;27:14–15 (in Russ.). Available from URL: https://elibrary.ru/ypuxqd
16. Basarab M.A., Stroganov I.S. Anomaly detection in information processes based on multifractal analysis. *Voprosy kiberbezopasnosti*. 2014;4(7):30–40 (in Russ.). Available from URL: https://elibrary.ru/tcssen
17. Zegzhda P.D., Lavrova D.S., Shtyrkina A.A. Multifractal analysis of backbone network traffic for denial of service attacks detection. *Problemy informatsionnoi bezopasnosti. Komp'yuternye sistemy = Information Security Problems. Computer Systems.* 2018;2:48–58 (in Russ.). Available from URL: https://elibrary.ru/xtktfz
18. Liu F.T., Ting K.M., Zhou Z.-H. Isolation Forest. In: *Proceedings of the 2008 IEEE International Conference on Data Mining*. IEEE; 2008. P. 413–422. https://doi.org/10.1109/ICDM.2008.17

19. Breunig M.M., Kriegel H.-P., Ng R.T., Sander J. LOF: Identifying Density-based Local Outliers. In: *Proceedings of the 2000 ACM SIGMOD International Conference on Management of Data* 2000. P. 93–104. https://doi.org/10.1145/342009.335388
20. Steinhaus H. Sur la division des corps materiels en parties. *Bull. Acad. Polon. Sci*. 1966;4(12):801–804 (in French.).
21. Oliveri P. Class-modelling in food analytical chemistry: Development, sampling, optimisation and validation issues – A tutorial. *Analytica Chimica Acta*. 2017;982:9–19. https://doi.org/10.1016/j.aca.2017.05.013, hdl:11567/881059. PMID 28734370.

СПИСОК ЛИТЕРАТУРЫ

1. Ихсанов И.И. Безопасность в электроэнергетике: актуальные угрозы и защитные меры. *Юность и знания – гарантия успеха – 2023: Сборник научных статей 10-й Международной молодежной научной конференции*. Курск, 19–20 сентября 2023 г. Курск: Университетская книга; 2023. Т. 2. С. 472–474. URL: https://elibrary.ru/tfyddx
2. Папков Б.В., Осокин Л.В., Кучин Н.Н. Кибербезопасность объектов распределительных электрических сетей. *Сельский механизатор*. 2024;5:3–7. URL: https://elibrary.ru/tfmvhi
3. Колосок И.Н., Коркина Е.С. Анализ кибербезопасности объектов энергетики с учетом механизма и кинетики нежелательных процессов. *Энергетик*. 2024;2:3–8. http://doi.org/10.34831/EP.2024.60.27.001, URL: https://elibrary.ru/ecxvjp
4. Абдрахманов И.И. Опасности и угрозы для кибербезопасности в электроэнергетике: анализ современных угроз и механизмов защиты. *Научный аспект*. 2024;31(3):3970–3973. URL: https://elibrary.ru/lrouni
5. Гурина Л.А. Оценка киберустойчивости системы оперативно-диспетчерского управления ЭЭС. *Вопросы кибербезопасности*. 2022;3(49):23–31. URL: https://elibrary.ru/sapiyh
6. Сметанин Д.И. Изучение структуры системы обнаружения и противодействия атакам вирусов-вымогателей на базе Endpoint Detection and Response. *Актуальные вопросы современной науки: Сборник статей VII Международной научно-практической конференции:* в 2-х ч. Пенза, 10 июня 2023 г. Пенза: Наука и Просвещение (ИП Гуляев Г.Ю.); 2023. С. 60–64. URL: https://elibrary.ru/vuvfpa
7. Лежнюк П.Д., Рубаненко А.Е., Казьмирук О.И. Оптимальное управление нормальными режимами ЭЭС с учетом технического состояния трансформаторов с РПН. *Научные труды Винницкого национального технического университета*. 2012;4:2. URL: https://elibrary.ru/pyqugn
8. Копылова В.В., Паркачев К.Н., Тигунцев С.Г. Трансформатор с тиристорным РПН. *Электрооборудование: эксплуатация и ремонт*. 2019;12:35–39. URL: https://elibrary.ru/vgfudv
9. Аржанников Б.А., Баева И.А., Тарасовский Т.С. Тиристорные устройства регулирования напряжения трансформаторов под нагрузкой РПН. *Транспорт Азиатско-Тихоокеанского региона*. 2020;4(25):32–38. URL: https://elibrary.ru/lxmknj
10. Рагозин А.Н. Формирование прогноза многокомпонентных временных рядов данных с использованием методов цифровой фильтрации и прогнозирующего автокодировщика с целью обнаружения аномалий в работе автоматизированных систем управления технологическими процессами в условиях воздействия кибератак. *Вестник УрФО. Безопасность в информационной сфере.* 2021;2(40):44–58. https://doi.org/10.14529/secur210205, URL: https://elibrary.ru/khwhfq
11. Плетенкова А.Д. Обнаружение аномалий, вызванных кибератаками, в наблюдаемых процессах АСУ ТП с использованием самоорганизующейся карты Кохонена. *Безопасность информационного пространства: Сборник трудов XXII Всероссийской научно-практической конференции студентов, аспирантов и молодых ученых*. Челябинск, 30 ноября 2023 г. Челябинск: Издательский центр ЮУрГУ; 2024. С. 267–274. URL: https://www.elibrary.ru/ctpuyj
12. Бухарев Д.А., Соколов А.Н., Рагозин А.Н. Применение иерархического кластерного анализа для кластеризации данных информационных процессов АСУ ТП, подвергающихся воздействию кибератак. *Вестник УрФО. Безопасность в информационной сфере.* 2023;1(47):59–68. https://doi.org/10.14529/secur230106, URL: https://elibrary.ru/fycuhe
13. Асяев Г.Д., Соколов А.Н. Модели предиктивной защиты информации автоматизированной системы управления водоснабжением на основе временных рядов с использованием технологий машинного обучения. *Вестник УрФО. Безопасность в информационной сфере*. 2021;4(42):39–45. https://doi.org/10.14529/secur210404, URL: https://elibrary.ru/yjkbtz
14. Соколов А.Н., Рагозин А.Н., Баринов А.Е., Уфимцев М.С., Пятницкий И.А., Бухарев Д.А. Разработка моделей и методов раннего обнаружения кибератак на объекты энергетики металлургического предприятия. *Вестник УрФО. Безопасность в информационной сфере*. 2021;3(41):65–87. https://doi.org/10.14529/secur210308, URL: https://elibrary.ru/kzggpj
15. Штыркина А.А., Зегжда П.Д., Лаврова Д.С. Обнаружение аномалий в трафике магистральных сетей Интернет с использованием мультифрактального анализа. *Методы и технические средства обеспечения безопасности информации*. 2018;27:14–15. URL: https://elibrary.ru/ypuxqd
16. Басараб М.А., Строганов И.С. Обнаружение аномалий в информационных процессах на основе мультифрактального анализа. *Вопросы кибербезопасности*. 2014;4(7):30–40. URL: https://elibrary.ru/tcssen

17. Зегжда П.Д., Лаврова Д.С., Штыркина А.А. Мультифрактальный анализ трафика магистральных сетей Интернет для обнаружения атак отказа в обслуживании. *Проблемы информационной безопасности. Компьютерные системы*. 2018;2:48–58. URL: https://elibrary.ru/xtktfz
18. Liu F.T., Ting K.M., Zhou Z.-H. Isolation Forest. In: *Proceedings of the 2008 IEEE International Conference on Data Mining*. IEEE; 2008. P. 413–422. https://doi.org/10.1109/ICDM.2008.17
19. Breunig M.M., Kriegel H.-P., Ng R.T., Sander J. LOF: Identifying Density-based Local Outliers. In: *Proceedings of the 2000 ACM SIGMOD International Conference on Management of Data.* 2000. P. 93–104. https://doi.org/10.1145/342009.335388
20. Steinhaus H. Sur la division des corps materiels en parties. *Bull. Acad. Polon. Sci*. 1966;4(12):801–804 (in French.).
21. Oliveri P. Class-modelling in food analytical chemistry: Development, sampling, optimisation and validation issues – A tutorial. *Analytica Chimica Acta*. 2017;982:9–19. https://doi.org/10.1016/j.aca.2017.05.013, hdl:11567/881059. PMID 28734370.

About the authors

Sergey V. Kochergin, Cand. Sci. (Eng.), Associate Professor, "Information Protection" Department, Institute of Cybersecurity and Digital Technologies, MIREA – Russian Technological University (78, Vernadskogo pr., Moscow, 119454 Russia). E-mail: kochergin_s@mirea.ru. https://orcid.org/0000-0002-3598-8149

Svetlana V. Artemova, Dr. Sci. (Eng.), Associate Professor, Head of the "Information Protection" Department, Institute of Cybersecurity and Digital Technologies, MIREA – Russian Technological University (78, Vernadskogo pr., Moscow, 119454 Russia). E-mail: artemova_s@mirea.ru. Scopus Author ID 6508256085, RSCI SPIN-code 3775-6241, https://orcid.org/0009-0006-8374-8197

Anatoly A. Bakaev, Dr. Sci. (Hist.), Cand. Sci. (Juri.), Associate Professor, Director of the Institute of Cybersecurity and Digital Technologies, MIREA – Russian Technological University (78, Vernadskogo pr., Moscow, 119454 Russia). E-mail: bakaev@mirea.ru. Scopus Author ID 57297341000, RSCI SPIN-code 5283-9148, https://orcid.org/0000-0002-9526-0117

Evgeny S. Mityakov, Dr. Sci. (Econ.), Professor, Acting Head of the "Subject-Oriented Information Systems" Department, Institute of Cybersecurity and Digital Technologies, MIREA – Russian Technological University (78, Vernadskogo pr., Moscow, 119454 Russia). E-mail: mityakov@mirea.ru. Scopus Author ID 55960540500, RSCI SPIN-code 5691-8947, https://orcid.org/0000-0001-6579-0988

Zhanna G. Vegera, Cand. Sci. (Phys.-Math.), Associate Professor, Head of the Department of Higher Mathematics, Institute of Cybersecurity and Digital Technologies, MIREA – Russian Technological University (78, Vernadskogo pr., Moscow, 119454 Russia). E-mail: vegera@mirea.ru. Scopus Author ID 57212931836, RSCI SPIN-code 9076-5678, https://orcid.org/0000-0001-7312-3341

Elena A. Maksimova, Dr. Sci. (Eng.), Associate Professor, Head of the Department "Intelligent Information Security Systems", Institute of Cybersecurity and Digital Technologies, MIREA – Russian Technological University (78, Vernadskogo pr., Moscow, 119454 Russia). E-mail: maksimova@mirea.ru. Scopus Author ID 57219701980, RSCI SPIN-code 6876-5558, https://orcid.org/0000-0001-8788-4256

Об авторах

Кочергин Сергей Валерьевич, к.т.н., доцент, кафедра КБ-1 «Защита информации», Институт кибербезопасности и цифровых технологий, ФГБОУ ВО «МИРЭА – Российский технологический университет» (119454, Россия, Москва, пр-т Вернадского, д. 78). E-mail: kochergin_s@mirea.ru. https://orcid.org/0000-0002-3598-8149

Артемова Светлана Валерьевна, д.т.н., доцент, заведующий кафедрой КБ-1 «Защита информации», Институт кибербезопасности и цифровых технологий, ФГБОУ ВО «МИРЭА – Российский технологический университет» (119454, Россия, Москва, пр-т Вернадского, д. 78). E-mail: artemova_s@mirea.ru. Scopus Author ID 6508256085, SPIN-код РИНЦ 3775-6241, https://orcid.org/0009-0006-8374-8197

Бакаев Анатолий Александрович, д.и.н., к.ю.н., доцент, директор Института кибербезопасности и цифровых технологий, ФГБОУ ВО «МИРЭА – Российский технологический университет» (119454, Россия, Москва, пр-т Вернадского, д. 78). E-mail: bakaev@mirea.ru. Scopus Author ID 57297341000, SPIN-код РИНЦ 5283-9148, https://orcid.org/0000-0002-9526-0117

Митяков Евгений Сергеевич, д.э.н., профессор, и.о. заведующего кафедрой КБ-9 «Предметно-ориентированные информационные системы», Институт кибербезопасности и цифровых технологий, ФГБОУ ВО «МИРЭА – Российский технологический университет» (119454, Россия, Москва, пр-т Вернадского, д. 78). E-mail: mityakov@mirea.ru. Scopus Author ID 55960540500, SPIN-код РИНЦ 5691-8947, https://orcid.org/0000-0001-6579-0988

Вегера Жанна Геннадьевна, к.ф.-м.н., доцент, заведующий кафедрой высшей математики, Институт кибербезопасности и цифровых технологий ФГБОУ ВО «МИРЭА – Российский технологический университет» (119454, Россия, Москва, пр-т Вернадского, д. 78). E-mail: vegera@mirea.ru. Scopus Author ID 57212931836, SPIN-код РИНЦ 9076-5678, https://orcid.org/0000-0001-7312-3341

Максимова Елена Александровна, д.т.н., доцент, заведующий кафедрой КБ-4 «Интеллектуальные системы информационной безопасности», Институт кибербезопасности и цифровых технологий, ФГБОУ ВО «МИРЭА – Российский технологический университет» (119454, Россия, Москва, пр-т Вернадского, д. 78). E-mail: maksimova@mirea.ru. Scopus Author ID 57219701980, SPIN-код РИНЦ 6876-5558, https://orcid.org/0000-0001-8788-4256

Translated from Russian into English by Lyudmila O. Bychkova
Edited for English language and spelling by Thomas A. Beavitt

Information systems. Computer sciences. Issues of information security

Информационные системы. Информатика. Проблемы информационной безопасности

UDC 681.3
https://doi.org/10.32362/2500-316X-2024-12-6-20-25
EDN PWDKPB

RESEARCH ARTICLE

Analysis and selection of the structure of a multiprocessor computing system according to the performance criterion

Grigory V. Petushkov [@], Alexander S. Sigov

MIREA – Russian Technological University, Moscow, 119454 Russia
[@] Corresponding author, e-mail: petushkov@mirea.ru

Abstract

Objectives. Analysis of the various architectures of computing systems (CSs) used in recent decades has allowed us to identify the most common structures. One of the key features is the use of mass-produced equipment to create data processing subsystems (for example, multicore processors and high-capacity semiconductor memory), as well as network equipment to build communication subsystems. This reduces hardware costs and allows typical or cluster configurations to be created, which is especially important for expensive CSs. The desire to achieve high computational speed and performance in such CSs requires minimizing the time to complete the task and balancing time delays both in data processing subsystems and in the communication subsystem which provides data transmission inside the CS. The aim of this work is to analyze computing modules (CMs) and structures on the basis of which the construction of cluster CSs is carried out.

Methods. The main results of the work were obtained using methods of mathematical analysis and modeling.

Results. The study considers the structure of modern multicore microprocessors as the basis for building CMs of cluster CSs. As the number of cores in the microprocessor structure increases, the communication network which unites them into a single structure becomes more complicated. It has been shown that in new developments of microprocessors, communication between cores is performed in the form of a network. The microprocessors themselves are MIMD structures in accordance with the well-known Flynn classification.

Conclusions. The proposed method of selecting an effective structure of a CS allows us to obtain the optimal structure of a CS according to the criterion of performance.

Keywords: InfiniBand network, performance, microprocessors, computing modules, Halstead metrics, analysis

• **Submitted:** 18.10.2024 • **Revised:** 26.10.2024 • **Accepted:** 05.11.2024

For citation: Petushkov G.V., Sigov A.S. Analysis and selection of the structure of a multiprocessor computing system according to the performance criterion. *Russ. Technol. J*. 2024;12(6):20–25. https://doi.org/10.32362/2500-316X-2024-12-6-20-25

Financial disclosure: The authors have no financial or proprietary interest in any material or method mentioned.

The authors declare no conflicts of interest.

НАУЧНАЯ СТАТЬЯ

Анализ и выбор структуры многопроцессорной вычислительной системы по критерию быстродействия

Г.В. Петушков [@], **А.С. Сигов**

МИРЭА – Российский технологический университет, Москва, 119454 Россия
[@] *Автор для переписки, e-mail: petushkov@mirea.ru*

Резюме

Цели. Анализ различных архитектур вычислительных систем (ВС), использовавшихся в последние десятилетия, позволил выделить наиболее распространенные структуры. Одной из ключевых особенностей является использование серийно производимого оборудования для создания подсистем обработки данных (например, многоядерные процессоры и полупроводниковая память большой емкости) и сетевого оборудования для построения коммуникационных подсистем. Это снижает затраты на оборудование и позволяет создавать типовые или кластерные конфигурации, что особенно важно для дорогостоящих ВС. Стремление достичь высокой вычислительной скорости и производительности в таких ВС требует минимизации времени на выполнение задачи и балансировки временных задержек как в подсистемах обработки данных, так и в коммуникационной подсистеме, обеспечивающей передачу данных внутри ВС. Целью работы является анализ вычислительных модулей (ВМ) и структур, на основе которых проводится построение кластерных ВС.

Методы. Основные результаты работы получены с использованием методов математического анализа и моделирования.

Результаты. Рассмотрена структура современных многоядерных микропроцессоров (МП), являющихся основой построения ВМ кластерных ВС. По мере увеличения числа ядер в структуре МП усложняется коммуникационная сеть, объединяющая их в единую структуру. Показано, что в новых разработках МП коммуникация между ядрами выполняется в виде сети, а сами МП представляют собой MIMD-структуры (множественный поток команд, множественный поток данных) в соответствии с известной классификацией Флинна.

Выводы. Предложенная методика выбора эффективной структуры ВС позволяет получить оптимальную структуру ВС по критерию быстродействия.

Ключевые слова: сеть InfiniBand, быстродействие, микропроцессоры, вычислительные модули, метрики Холстеда, анализ

• **Поступила:** 18.10.2024 • **Доработана:** 26.10.2024 • **Принята к опубликованию:** 05.11.2024

Для цитирования: Петушков Г.В., Сигов А.С. Анализ и выбор структуры многопроцессорной вычислительной системы по критерию быстродействия. *Russ. Technol. J*. 2024;12(6):20–25. https://doi.org/10.32362/2500-316X-2024-12-6-20-25

Прозрачность финансовой деятельности: Авторы не имеют финансовой заинтересованности в представленных материалах или методах.

Авторы заявляют об отсутствии конфликта интересов.

INTRODUCTION

Modern multicore microprocessors form the basis for constructing computing modules (CMs) of cluster computing systems (CSs). Along with an increase in the number of cores in the microprocessor structure, the communication network which unites them into a single structure becomes more complex. In improved microprocessor designs, communication between cores is performed in the form of a network. The microprocessors themselves are multiple instruction and multiple data (MIMD) structures in accordance with the well-known Flynn classification [1–3].

At the next level, one or more microprocessors are used as the basis for a CM of a CS cluster cell. In a CM, microprocessors are combined with RAM modules by standard peripheral component interconnect (PCI) class, i.e., Express 3.0 class interfaces. They can also be combined with a switch that provides communication between all microprocessors and all memory modules [4].

At the system level, a relatively large number of CMs in the clustered systems are interconnected by networking facilities. As a rule, this requires several networks, such as [5]:

- a network providing data transfer between CMs in the process of task solving;
- a network that connects individual CMs to a data warehouse used both for initial task data loading and for storing results;
- a service network associated with the control of CS, through which the information on monitoring the performance of the CM and entire CS is circulated.

The fastest of these networks should be the former network, also referred to as a data transfer network and executed as an InfiniBand network (IBA) [6]. This network supports the densest data transfer traffic during the process of task solving in CS. As the number of CM in the CS increases, the processing time for a task decreases due to the increase in the number of processing devices, and the "time overhead" of data transfer between CM will increase [7].

The question then arises about the optimal number of CMs in the CS, providing the minimum time of task execution at known characteristics of CMs and data transmission network. This task is formulated in the work as a cluster CS structure selection problem [8].

METHODOLOGY FOR SELECTING AN EFFICIENT STRUCTURE OF THE ALL-ROUND SYSTEM, OPTIMAL BY THE CRITERION OF FAST PERFORMANCE

Let us evaluate the performance of the CSs using the IBA network when the number of microprocessors and CMs increases [9]. The performance growth of such systems with an increase in the number of CMs is nonlinear. This is because the increase in the number of CMs leads to an increase in the "overhead" associated with the time required for data exchange between modules. The time spent on data exchange especially increases when CMs interact through the network, where delays occur and traffic volume increases.

In order to analyze the influence of these "overheads" [10], let us consider an idealized case of executing a well-parallelized program which consists of N parallel fragments distributed over K CMs, where $N > K$.

The program execution time in the considered case can be estimated as follows:

$$T_{pr} = T_{calc} + T_{exch}, \quad (1)$$

wherein T_{calc} is the time spent on calculations in CMs; T_{exch} is the time spent on data exchange between CMs.

T_{calc} value can be estimated taking into account the capacity of one CM P_{CM} and their number K by the formula:

$$T_{calc} = \frac{G}{KP_{CM}}, \quad (2)$$

wherein G is an estimate of the number of operations in the program.

G value can be obtained by analyzing the program algorithm using, for example, Halstead metrics.

The time consumption for exchanging a data packet T_p in a data network is defined as follows:

$$T_p = T_n + T_d + \frac{Q}{V}, \quad (3)$$

wherein T_n is the delay of data packet formation in the network adapter; T_d is the delay of packet transmission in the network, associated with delays in the switch; Q is the amount of transmitted data in the data packet; V is the velocity of data transmission in the network.

Let us consider the data transmission network as part of the CS [11], since the volume of traffic therein is much larger than that in the service network. Analyzing the time of data exchange as an "overhead" in the process of computation, in the first approximation T_{exch} can be estimated taking the limited network bandwidth into account as follows:

$$T_{exch} = K\frac{Q}{V}. \quad (4)$$

Let us explain the derivation of Eq. (4) in greater detail on the example of a system consisting of K CMs. Since the amount of traffic of each CM is proportional to the number of CMs, let us assume that each CM forwards

packets to other CMs after completing the execution of its program fragment. The total communication time can be estimated by combining the traffic of all CMs [12] forwarded over the network. This time is shown in the form (4).

The amount of data in bytes of the exchange packet is related to the number of operations in the executed program G (computational complexity of the algorithm) as follows:

$$Q = CGL, \quad (5)$$

wherein C is the coefficient characterizing the class of algorithms being executed with respect to data connectivity (algorithms with higher data connectivity are characterized by a higher intensity of exchanges between CMs and a higher value of the coefficient C), and L is the share of computational operations in the executed program fragment ($L \approx 1$).

Taking Eqs. (2)–(5) into account, Eq. (1) can be rewritten as:

$$T_{pr} = \frac{G}{KP_{CM}} + \frac{CGL}{V}K. \quad (6)$$

It follows from the above expression (6) that an increase in K leads to a decrease in the time spent on computation and an increase in the time duration for data exchange in the CS. Thus, the characteristics of the data transmission network will strongly affect the CS performance.

Equation (6) can be used to determine the optimal value of the number of CMs K_{opt}, providing the minimum value of the program execution time T_{pr}. The value of the coefficient k, determining the number of CMs in the full CS, is calculated based on the condition $dT_{pr}/dk = 0$ as follows:

$$K_{opt} = \sqrt{\frac{V}{CP_{CM}L}}. \quad (7)$$

For modern CSs [13], the coefficient values are at the level of unity for network throughput $V = 10$ Gbytes/s and data processing speed of 10 billion operations per second. However, for the coefficient values $C = 0.01$ bytes/operation, characterizing algorithms with weak data connectivity, it can reach 10.

Along with an increase in the data network bandwidth, the number of CMs in the system can be increased without significant performance degradation due to the time spent on data exchange. Using an optical bus with a data transfer rate of $V = 1$, Tbyte/s for the data network can increase the optimal number of CMs by more than 10 times (up to 100 CMs), significantly improving the efficiency of multiprocessor and multi-module CS.

Equation (7) for the coefficient will be referred to as the rule of "selecting the effective structure of the CS" and we note its important practical significance in CS design. The methodology of structure selection for a cluster CS includes several stages [14, 15]:

1. CM performance analysis.
2. Estimation of the data transfer rate in the fastest CS data network.
3. Analysis of the algorithm for determining the data cohesion coefficient C.
4. Determination of the coefficient according to Eq. (7).

In actual CS, the number of CMs, as a rule, exceeds the value of 10. This is due to the development of efficient CS designs. However, with the growth of data transmission speeds in the network, the calculated and actual numbers of CMs will be better coordinated.

CONCLUSIONS

1. The most efficient ratio structures of cluster CSs in terms of "cost/performance" are built on the basis of standard equipment of IBA and Ethernet networks.
2. A methodology for selecting an effective structure of the CS is proposed on the basis of the analysis of time costs for data processing and transmission in the CS. This allows the optimal structure of the CS to be obtained according to the criterion of speed. The methodology includes the following steps:

- analysis of the specifics of data exchange between CMs depending on the algorithm of the task solving;
- analysis of CM performance depending on the equipment used;
- analysis of the bandwidth capacity of the data transmission network in CS;
- selection of the CS structure as a choice of the optimal number of CMs in accordance with Eq. (7).

Authors' contribution
All authors equally contributed to the research work.

REFERENCES

1. Voevodin V.V., Voevodin Vl.V. *Parallel'nye vychisleniya* (*Parallel Computing*). St. Petersburg: BHV-Petersburg; 2002. 608 p. (in Russ.).
2. Orlov S.A., Tsil'ker B.Ya. *Organizatsiya EVM i system* (*Organization of Computers and Systems*). St. Petersburg: Piter; 2016. 688 p. (in Russ.).
3. Henessey J.L., Patterson D.A. *Komp'yuternaya arkhitektura. Kolichestvennyi podkhod* (*Computer Architecture. A Quantitative Approach)*: transl. from Engl. 5th ed. Moscow: Tekhnosfera; 2016. 936 p. (in Russ.).
[Henessey J.L., Patterson D.A. *Computer Architecture. A Quantitative Approach.* 5th ed. Morgan Kaufmann; 2011. 856 p.]
4. Kirk B., Sharad S., Stanley V. How to succeed in an economy of abundance of memory? *Otkrytye sistemy = Open Systems. DBMS*. 2016;2:25–32 (in Russ.).
5. Sugak E.V. *Prikladnaya teoriya nadezhnosti. Praktikum* (*Applied Reliability Theory. The Workshop. Textbook*). Moscow: Lan; 2023. 312 p. (in Russ.). ISBN 978-5-507-47014-3
6. Kovalenko S.M. Evaluation of the reliability of information management systems based on continuous models. *Voprosy radioelektroniki = Questions of Radio Electronics*. 2005;4(2):143–146 (in Russ.).
7. Polovko A.M., Gurov S.V. *Osnovy teorii nadezhnosti* (*Fundamentals of Reliability Theory)*. St. Petersburg: BHV-Petersburg; 2006. 702 p. (in Russ.). ISBN 5-94157-541-6
8. Cherkesov G.N. *Nadezhnost' apparatno-programmnykh kompleksov* (*Reliability of Hardware and Software Complexes*). St. Petersburg: Piter; 2005. 479 p. (in Russ.). ISBN 5-469-00102-4
9. Kovalenko S.M., Platonova O.V. Analysis of the operational efficiency of complex automation systems and the calculation of their reliability on the basis of continuous models. *Izvestiya vysshikh uchebnykh zavedenii. Mashinostroenie = BMSTU J. Mechanical Engineering.* 2014;8(653):75–89 (in Russ.). http://doi.org/10.18698/0536-1044-2014-8-75-79
10. Podgorny Y.V., Antonovich A.N., Petrushin A.A., Sigov A.S., Vorotilov K.A. Effect of metal electrodes on the steady-state leakage current in PZT thin film capacitors. *J. Electroceram.* 2022;49:15–21. https://doi.org/10.1007/s10832-022-00288-5
11. Abdullaev D.A., Milovanov R.A., Volkov R.L., Borgardt N.I., Lantsev A.N., Vorotilov K.A., Sigov A.S. Ferroelectric memory: state-of-the-art manufacturing and research. *Russ. Technol. J*. 2020;8(5):44–67 (in Russ.). https://doi.org/10.32362/2500-316X-2020-8-5-44-67
12. Konyukhova O.V., Kravtsova E.A., Lukyanov P.V. *Tekhnicheskoe i programmnoe obespechenie vychislitel'nykh mashin i system* (*Technical and Software Support of Computers and Systems*). Infra-Inzheneriya; 2023. 200 p. (in Russ.). ISBN 978-5-9729-1186-8
13. Zhuravlev A.A. *Organizatsiya i arkhitektura EVM. Vychislitel'nye sistemy* (*Organization and Architecture of Computers. Computer Systems*). Lan; 2022. 144 p. (in Russ.). ISBN 978-5-507-48089-0
14. Gelbukh C.A. *Seti EVM i telekommunikatsii. Arkhitektura i organizatsiya* (*Computer Networks and Telecommunications. Architecture and Organization*). Lan; 2019. 208 p. (in Russ.). ISBN 978-5-8114-3474-9
15. Andreev A.M., Mozharov G.P., Syuzev V.V. *Mnogoprotsessornye vychislitel'nye sistemy. Teoreticheskii analiz, matematicheskie modeli i primenenie* (*Multiprocessor Computing Systems. Theoretical Analysis, Mathematical Models and Applications*). Moscow: Bauman Press; 2011. 336 p. (in Russ.). ISBN 978-5-7038-3439-6

СПИСОК ЛИТЕРАТУРЫ

1. Воеводин В.В., Воеводин Вл.В. *Параллельные вычисления*. СПб.: БХВ-Петербург; 2002. 608 с.
2. Орлов С.А., Цилькер Б.Я. *Организация ЭВМ и систем*. СПб.: Питер; 2016. 688 с.
3. Хенесси Д.Л., Паттерсон Д.А. *Компьютерная архитектура. Количественный подход*. 5-е изд. М.: Техносфера; 2016. 936 с.
4. Кирк Б., Шарад С., Стенли В. Как преуспеть в условиях экономики изобилия памяти? *Открытые системы. СУБД*. 2016;2:25–32.
5. Сугак Е.В. *Прикладная теория надежности. Практикум.* М.: Лань; 2023. 312 с. ISBN 978-5-507-47014-3
6. Коваленко С.М. Оценка надежности информационно-управляющих систем на основе непрерывных моделей. *Вопросы радиоэлектроники.* 2005;4(2):143–146.
7. Половко А.М., Гуров С.В. *Основы теории надежности*. СПб.: БХВ-Петербург; 2006. 702 с. ISBN 5-94157-541-6
8. Черкесов Г.Н. *Надежность аппаратно-программных комплексов*. СПб.: Питер; 2005. 479 с. ISBN 5-469-00102-4
9. Коваленко С.М., Платонова О.В. Анализ задачи эффективной эксплуатации комплексов систем автоматизации и расчеты надежности на основе непрерывных моделей. *Известия вузов. Машиностроение*. 2014;8(653):75–89. http://doi.org/10.18698/0536-1044-2014-8-75-79
10. Podgorny Y.V., Antonovich A.N., Petrushin A.A., Sigov A.S., Vorotilov K.A. Effect of metal electrodes on the steady-state leakage current in PZT thin film capacitors. *J. Electroceram.* 2022;49:15–21. https://doi.org/10.1007/s10832-022-00288-5
11. Абдуллаев Д.А., Милованов Р.А., Волков Р.Л., Боргардт Н.И., Ланцев А.Н., Воротилов К.А., Сигов А.С. Сегнетоэлектрическая память: современное производство и исследования. *Russian Technological Journal*. 2020;8(5):44–67. https://doi.org/10.32362/2500-316X-2020-8-5-44-67
12. Конюхова О.В., Кравцова Э.А., Лукьянов П.В. *Техническое и программное обеспечение вычислительных машин и систем.* Инфра-Инженерия; 2023. 200 с. ISBN 978-5-9729-1186-8

13. Журавлев А.А. *Организация и архитектура ЭВМ. Вычислительные системы*. Лань; 2022. 144 с. ISBN 978-5-507-48089-0
14. Гельбух С.А. *Сети ЭВМ и телекоммуникации. Архитектура и организация*. Лань; 2019. 208 с. ISBN 978-5-8114-3474-9
15. Андреев А.М., Можаров Г.П., Сюзев В.В. *Многопроцессорные вычислительные системы. Теоретический анализ, математические модели и применение*. Издательство МГТУ им. Н.Э. Баумана; 2011. 336 с. ISBN 978-5-7038-3439-6

About the authors

Grigory V. Petushkov, Vice-Rector, MIREA – Russian Technological University (78, Vernadskogo pr., Moscow, 119454 Russia). E-mail: petushkov@mirea.ru. https://orcid.org/0009-0006-0801-429X

Alexander S. Sigov, Academician at the Russian Academy of Sciences, Dr. Sci. (Phys.–Math.), Professor, President, MIREA – Russian Technological University (78, Vernadskogo pr., Moscow, 119454 Russia). E-mail: sigov@mirea.ru. Scopus Author ID 35557510600, ResearcherID L-4103-2017, RSCI SPIN-code 2869-5663, https://www.researchgate.net/profile/A_Sigov

Об авторах

Петушков Григорий Валерьевич, проректор, ФГБОУ ВО «МИРЭА – Российский технологический университет» (119454, Россия, Москва, пр-т Вернадского, д. 78). E-mail: petushkov@mirea.ru. https://orcid.org/0009-0006-0801-429X

Сигов Александр Сергеевич, академик Российской академии наук, д.ф.-м.н., профессор, президент ФГБОУ ВО «МИРЭА – Российский технологический университет» (119454, Россия, Москва, пр-т Вернадского, д. 78). E-mail: sigov@mirea.ru. Scopus Author ID 35557510600, ResearcherID L-4103-2017, SPIN-код РИНЦ 2869-5663, https://www.researchgate.net/profile/A_Sigov

Translated from Russian into English by Lyudmila O. Bychkova
Edited for English language and spelling by Dr. David Mossop

Information systems. Computer sciences. Issues of information security

Информационные системы. Информатика. Проблемы информационной безопасности

UDC 519.95:621.3
https://doi.org/10.32362/2500-316X-2024-12-6-26-38
EDN BKJTRZ

RESEARCH ARTICLE

Analytical method for analyzing message transmission processes in FDDI networks for digital substations

Alexander S. Leontyev,
Dmitry V. Zhmatov @

MIREA – Russian Technological University, Moscow, 119454 Russia
@ *Corresponding author, e-mail: zhmatov@mirea.ru*

Abstract

Objectives. To develop analytical approaches for the evaluation of probability-time characteristics and fiber distributed data interface (FDDI) network performance with the marker access method, thus enabling communication processes for digital electrical substations to be automated.

Methods. The authors used theory reliability methods, random process theory, mass maintenance theory, the Laplace–Stieltjes transformation for inferring functional equations and the probability-time characteristics calculation for the information transfer processes with the occurring failures.

Results. We conducted a numerical study of packet transfer processes between central processing stations in the FDDI network. We considered the processes of discrete information exchange between electronic devices in the system of electrical digital substations. These included the main technological operations and electrical digital substations operator performed when preparing reports. We described the different modes of operation, both for the individual electrical digital substation and for the system. The authors calculated node loading dependencies, FDDI network performance and temporal characteristics of the packet transfer processes on the incoming message flow intensity and the transmission medium reliability. We conducted a functional analysis of the FDDI networks on two fiber-optic rings which form the main and redundant path of data transfer between the network nodes, significantly increasing network resiliency. The objective of the study was to analyze the information transfer processes in FDDI networks with an accent on ensuring the transmission medium reliability.

Conclusions. We were able to establish the existence of the critical operating network region, which leads to a sharp increase in node load and temporal characteristics, while performance reaches its maximum value and then sharply decreases. We propose the exchange of discrete messages to reflect the electronic devices state and information messages of operator between various remotely spaced electrical digital substation with the FDDI fiber-optic network.

Keywords: digital substations, FDDI networks, token access method, models, time characteristics, failures, performance

• **Submitted:** 30.01.2024 • **Revised:** 24.04.2024 • **Accepted:** 27.09.2024

For citation: Leontyev A.S., Zhmatov D.V. Analytical method for analyzing message transmission processes in FDDI networks for digital substations. *Russ. Technol. J.* 2024;12(6):26–38. https://doi.org/10.32362/2500-316X-2024-12-6-26-38

Financial disclosure: The authors have no financial or proprietary interest in any material or method mentioned.

The authors declare no conflicts of interest.

НАУЧНАЯ СТАТЬЯ

Аналитический метод анализа процессов передачи сообщений в оптоволоконных сетях с маркерным доступом для цифровых подстанций

А.С. Леонтьев,
Д.В. Жматов [@]

МИРЭА – Российский технологический университет, Москва, 119454 Россия
[@] *Автор для переписки, e-mail: zhmatov@mirea.ru*

Резюме

Цели. Цель работы – разработка аналитических методов оценки вероятностно-временных характеристик и производительности оптоволоконной FDDI-сети (fiber distributed data interface) с маркерным методом доступа, позволяющих автоматизировать процессы передачи сообщений для цифровых электроподстанций.

Методы. Использованы методы теории надежности, теории случайных процессов и теории массового обслуживания, преобразование Лапласа – Стилтьеса для вывода функциональных уравнений.

Результаты. Проведено численное исследование процессов передачи пакетов между электрическими цифровыми подстанциями (ЦПС) в оптоволоконной сети FDDI. Рассмотрены процессы обмена дискретной информацией между электронными устройствами в системе электрических ЦПС, включая основные технологические операции, выполняемые персоналом системы ЦПС при подготовке отчетов, характеризующих различные режимы работы как отдельных ЦПС, так и всей системы в целом. Получены зависимости загрузки узлов, производительности FDDI-сети и временных характеристик процессов передачи пакетов от интенсивности входных потоков сообщений и надежности передающей среды. Проведен анализ функционирования FDDI-сетей, построенных на основе двух оптоволоконных колец, которые образуют основной и резервный пути передачи данных между узлами сети, что значительно повышает отказоустойчивость таких сетей. Задача исследования включала анализ процессов передачи информации в сетях FDDI с акцентом на обеспечение надежности передающей среды.

Выводы. Выявлено, что существует критическая область функционирования сети, при достижении которой наблюдается резкое увеличение загрузки узлов и временных характеристик, в то время как производительность достигает максимального значения и затем резко снижается. Предложено осуществлять обмен дискретными сообщениями, отражающими состояние электронных устройств, и информационными сообщениями персонала между различными дистанционно разнесенными ЦПС с использованием оптоволоконной сети FDDI.

Ключевые слова: цифровые подстанции, FDDI-сети, маркерный метод доступа, модели, временные характеристики, отказы, производительность

• **Поступила:** 30.01.2024 • **Доработана:** 24.04.2024 • **Принята к опубликованию:** 27.09.2024

Для цитирования: Леонтьев А.С., Жматов Д.В. Аналитический метод анализа процессов передачи сообщений в оптоволоконных сетях с маркерным доступом для цифровых подстанций. *Russ. Technol. J*. 2024;12(6):26–38. https://doi.org/10.32362/2500-316X-2024-12-6-26-38

Прозрачность финансовой деятельности: Авторы не имеют финансовой заинтересованности в представленных материалах или методах.

Авторы заявляют об отсутствии конфликта интересов.

INTRODUCTION

The digital substation (DSS) is a type of electrical substation where all monitoring, analysis and control processes are performed in a single digital format. The main link for data transmission in such substations is a local area network (LAN) based on Ethernet technology.

One of the main functions of DSS is the exchange of discrete information between digital electronic devices, including voltage and current transformers [1–4]. The GOOSE (generic object-oriented substation event) data transfer protocol described in IEC 61850[1] standard [5–7]. GOOSE model provides a fast mechanism for transmitting events (e.g., commands and warnings) and is used to shut down, start devices, and record alarm events. During the design phase, the utilization and bandwidth of the data transmission paths must be taken into account. The size of a GOOSE message ranges from 573 to 830 bytes. When the message includes 64 discrete signals, the size of a GOOSE message including service information (28–30 bytes, including preamble, sender and receiver addresses, cyclic control code, control fields, limiters, status field) is 1 Kbyte. In this regard, when modeling the exchange of discrete signals between different DSS connected to the fiber distributed data interface (FDDI) network, the synchronous traffic in the network is a GOOSE message of 1 Kbyte or 8 kbits in size. In order to accelerate the development process and improve the quality of the DSS system, methods need to be proposed to analyze the efficiency of the applied information technologies, in particular, standard technologies for preparing information and analytical reports by personnel. The creation of mathematical models to describe the main stages and schemes of report preparation enables the selection of system components for the realization of different modes of operation of both individual DSS and the whole system to be automated on the basis of multivariate analysis. The functioning of individual DSS is based on the use of Fast Ethernet LAN, while the FDDI fiber-optic network is used for the interaction of different DSS.

The main functional tasks performed by DSS system personnel on a daily basis when preparing reports describing various modes of operation of both individual DSS and the entire system include fact-based information retrieval, contextual information retrieval, frequency analysis by report attributes, sorting, clustering, and semantic analysis.

[1] GOST R IEC 61850-5-2011. National Standard of the Russian Federation. *Communication networks and systems in substations*. Part 5. Communication requirements for functions and device models. Moscow: Standartinform, 2020 (in Russ.). The standard describes data flow formats, types of information, rules for describing the elements of an energy object, and a set of rules for organizing an event-based data transfer protocol.

1. METHODOLOGY FOR RECEIVING A MESSAGE TO DSS

The maximum length of lines between DSS is 200 km, provided that the ring does not exceed 100 km. The maximum number of double connection nodes is limited and is 500. According to the IEC 61850 standard [1–3], there are two options for exchanging GOOSE messages between power facilities.

The first option (Fig. 1) relies on tunneling technology. In this context, a broadband Ethernet channel is formed between the objects, through which GOOSE messages are transmitted using network equipment.

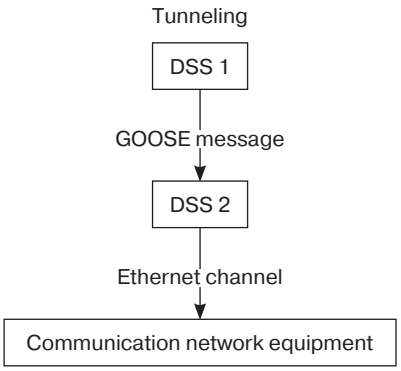

Fig. 1. Tunneling technology for the transmission of GOOSE messages between DSS components

The second scenario, shown in Fig. 2, involves the use of a gateway. In this scenario, an alarm and command device is used to exchange GOOSE messages between objects. The alarm and command devices convert discrete signals from GOOSE messages into coded analog or digital signals for the safe transmission of relay protection commands over the DSS channel. At the receiving end of the alarm and command transmitter, GOOSE messages are generated from the encoded signals received via the channel.

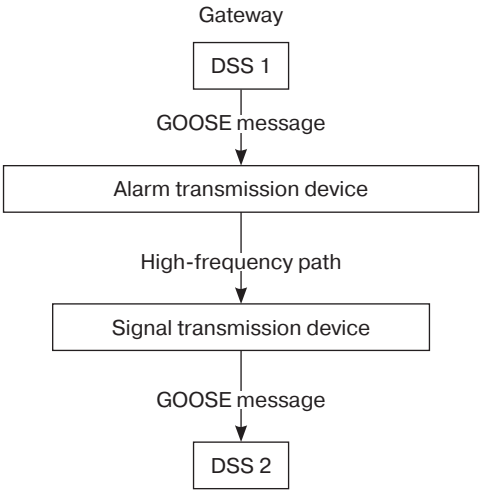

Fig. 2. Use of alarm transmission devices

In order to transmit GOOSE messages using tunneling, digital channels between substations are required. They can be organized by means of digital industrial communication networks or dedicated fiber optic channels. However, the organization of reliable digital high-frequency channels for GOOSE messages is impossible. This is due to the need to transmit relay protection and emergency control commands when short circuits occur on power lines [2–4].

FDDI fiber optic networks can be interconnected with a DSS, in order to enable efficient data transmission in digital power transmission networks. Digital substations can use FDDI networks to exchange data between various devices in the power system, such as monitoring and control systems, security systems, load management systems, and other devices requiring fast and reliable data transmission. Connecting FDDI networks to DSS enables the use of fiber rings to transmit large amounts of data at high speed and reliability, provide high bandwidth, fault tolerance and low latency data transmission. This is especially important for critical power transmission systems.

2. TASK STATEMENT OF THE PROBLEM OF ANALYTICAL STUDY OF THE FDDI NETWORK

When analyzing the performance of FDDI networks, it is paramount that methods, models and algorithms be created which take into account the characteristics of data transmission in these networks, including possible failures.

Simulation methods to determine the temporal characteristics of computer systems and networks under failure conditions are inefficient [8]. Currently known analytical methods are usually applicable to the analysis of local structures and, as a rule, are focused on the analysis of either the time characteristics of local systems with regard to reliability [9–11], or reliability indicators of computer systems and networks [12–14].

Let us consider the problem formulation and analytical model for estimating the time characteristics and performance indicators of FDDI networks with fiber optic rings taking into account the reliability of the transmission medium and limitations on the data transmission time. This approach and its implementation expand the scope of application of the methodology for the study of data transmission processes in local networks using analytical methods [15, 16].

The main indicators in this context are probabilistic and temporal characteristics which are highly dependent on failures of the transmission medium.

A detailed formulation of the problems of research into the probabilistic-temporal characteristics and performance of Ethernet-type LANs and LAN with the token access method, as well as analytical methods of their solution were first developed by A.S. Leontyev and published in 2001 in [15]. The general formulation of the problem of research of probabilistic-temporal characteristics and performance of FDDI networks corresponds to the methodology described in [15]. It can be formulated as follows: **to determine the probabilistic-temporal characteristics of packet transmission, the load of nodes and transmission medium, as well as to evaluate the performance of fiber-optic FDDI networks at a given bandwidth and reliability of the transmission medium, the structure and number of nodes of the FDDI network, streams of transmitted information and limitations on the time of packet transmission.**

The selected performance metric is the total intensity of the flow served in time. The solution of the problem is based on the assumption that the flows λ_n, $n=\overline{1,N}$ entering the network for service and the failures of the transmission medium are of Poisson distribution. It is envisioned that the input to the node is via an accumulator with unlimited capacity. As shown in [15], these assumptions are justified in the development of system modes of operation of the local network. The accuracy of the results obtained with their help is acceptable for engineering calculations.

3. DEVELOPMENT OF MATHEMATICAL APPARATUS FOR FDDI NETWORK RESEARCH

Let us number the nodes of the network in the order of polling, and use the index n to denote the station (node) of the FDDI network. Let N be the number of nodes in the network, λ_n is the intensity of packet flow to the nth node. The average packet transmission time from one node to the neighboring node is determined by the ratio:

$$X^{(1)}=\frac{L_{\text{pac}}}{C},$$

wherein L_{pac} is the length of the packet including the length of the marker; C is the throughput of the transmitting medium.

Obviously, the average interval $Z^{(1)}$ between two consecutive polls of a node is equal to:

$$Z^{(1)}=\sum_{n=1}^{N}\left\{\rho_n X^{(1)}+(1-\rho_n)\frac{L_{\text{m}}}{C}\right\},\quad n=\overline{1,N},\qquad(1)$$

wherein ρ_n is the load of the nth load, L_{m} is the marker length.

In steady-state mode:

$$\lambda_n Z^{(1)}=\rho_n.\qquad(2)$$

From (1) and (2) we obtain:

$$\lambda_n \sum_{n=1}^{N} \left\{ \rho_n X^{(1)} + (1-\rho_n) \frac{L_m}{C} \right\} = \rho_n. \quad (3)$$

The system of equations (3) is an inhomogeneous system of linear algebraic equations with regard to ρ_n.

$$\rho_n = \frac{\lambda_n N \frac{L_m}{C}}{1 - \sum_{k=1}^{N} \lambda_k \left(X^{(1)} - \frac{L_m}{C} \right)}, \; n = \overline{1, N}, \quad (4)$$

λ_k is the maximum number of packets in a node; k is the maximum number of nodes.

By comparing (2) and (4), we obtain:

$$Z^{(1)} = \frac{N \frac{L_m}{C}}{1 - \sum_{k=1}^{N} \lambda_k \left(X^{(1)} - \frac{L_m}{C} \right)}. \quad (5)$$

Formulas (4) and (5) determine the utilization of the network nodes and the average polling cycle of the nodes under the conditions of reliable operation.

Functional equations for determining the cycle of the network with token access method taking into account occurring failures have the following form:

$$Z_f^*(s) = Z^*(\lambda_f + s - \lambda_f Y_f^*(s)), \quad (6)$$

$$Y_f^*(s) = F_f^*(\lambda_f + s - \lambda_f Y_f^*(s)), \quad (7)$$

$$Z_f^*(s) = \int_0^\infty e^{-st} dZ_f(t), \;\; Y_f^*(s) = \int_0^\infty e^{-st} dY_f(t),$$

$$Z^*(\lambda_f + s - \lambda_f Y_f^*(s)) = \int_0^\infty e^{-(\lambda_f + s - \lambda_f Y_f^*(s))t} dZ(t),$$

$$F_f^*(\lambda_f + s - \lambda_f Y_f^*(s)) = \int_0^\infty e^{-(\lambda_f + s - \lambda_f Y_f^*(s))t} dF(t),$$

wherein $Z_f(t)$ is the distribution function (DF) of the network cycle taking into account failures, $Z(t)$ is the DF of the network cycle under conditions of reliable operation, $F_f(t)$ is the DF of the transmission medium recovery time after failures, $Y_f(t)$ is the DF of the transmission medium occupancy period after failures, and s is the complex parameter of the DF of the network cycle taking into account failures.

Functional Eqs. (6) and (7) can be obtained using the catastrophe method [9], in accordance with the technique described in [15]. Differentiating (6) and (7) by s, we obtain:

$$Y_f^{(1)} = \frac{F_f^{(1)}}{1 - \lambda_f F_f^{(1)}}, \quad (8)$$

$$Z_f^{(1)} = \frac{Z^{(1)}}{1 - \lambda_f F_f^{(1)}}. \quad (9)$$

The Laplace–Stieltjes transform of the DF of packet transmission time taking into account the occurring failures $X_f^*(s)$ is defined using the following functional equation:

$$X_f^*(s) = X^*(s + \lambda_f) + \frac{\lambda_f}{s + \lambda_f}(1 - X^*(s + \lambda_f)) F_f^*(s) X_f^*(s), \quad (10)$$

wherein $X^*(s + \lambda_f) = \int_0^\infty e^{-(s+\lambda_f)t} dX(t)$, $X(t)$ is the DF of packet transmission time over the transmitting medium under conditions of reliable operation.

Functional Eq. (10) is easily obtained by using the catastrophe method [9].

Moments $V_n^{(1)}, V_n^{(2)}$ of the service time DF of a packet arriving at the free nth node are defined by the expressions:

$$V_n^{(1)} = X_f^{(1)} + W_{n|\xi_n=1}^{(1)},$$
$$V_n^{(2)} = X_f^{(2)} + 2W_{n|\xi_n=1}^{(1)} X_f^{(1)} + W_{n|\xi_n=1}^{(2)}, \quad (11)$$

wherein ξ_n is the number of packets in node n; $X_f^{(1)}, X_f^{(2)}$ are the DF moments $X_f(t)$; $W_{n|\xi_n=1}^{(1)}$, $W_{n|\xi_n=1}^{(2)}$ are the 1st and 2nd DF moments of waiting time for the arrival of a token at the nth node at $\xi_n = 1$.

The average waiting time of packets in the queue for service in the nth node of FDDI network $W_n^{(1)}$ is given by the Pollaczek–Khinchine formula [15]:

$$W_n^{(1)} = \frac{1}{2} \cdot \frac{\lambda_n V_n^{(2)}}{1 - \lambda_n V_n^{(1)}}, \quad (12)$$

wherein $V_n^{(1)}$, $V_n^{(2)}$ are defined by the formulas (11).

The average packet delivery time $T_n^{(1)}$ in the network is defined by the expression:

$$T_n^{(1)} = W_n^{(1)} + V_n^{(1)}. \quad (13)$$

The total intensity of the timely served packet flow (FDDI network performance) is calculated by the formula:

$$\lambda_{\text{tot}} = \sum_{i=1}^{N} \lambda_i P_i, \quad (14)$$

wherein P_i is the probability of timely delivery of packets arriving to the ith node of the FDDI network, λ_i is the intensity of packets arriving to the ith node of the network.

Analytical relations necessary for estimating the probability P_i of timely delivery of packets arriving at the ith node of the network taking into account emerging failures are presented in [9, 15].

4. SOFTWARE PACKAGE FOR ANALYSIS OF INFORMATION TRANSMISSION PROCESSES IN FDDI NETWORK AND MODELING RESULTS

The authors have developed a set of programs which enable the analytical model considered above to be used in practice, in order to evaluate the efficiency of FDDI network. It can be installed on the FDDI network server for access from workplaces.

Analytical apparatus implemented in the form of this software package enables automated study of the structure and characteristics of FDDI network with two fiber rings, taking into account the reliability of the transmission medium. The screen form of input of initial data and output of modeling results is shown in Fig. 3. The user can enter the input data in the dialog mode using the specified forms.

The calculation results are displayed on the screen as text and in graphic windows. The user can correct the initial data and save the results of calculations in text and graphic files without leaving the modeling system.

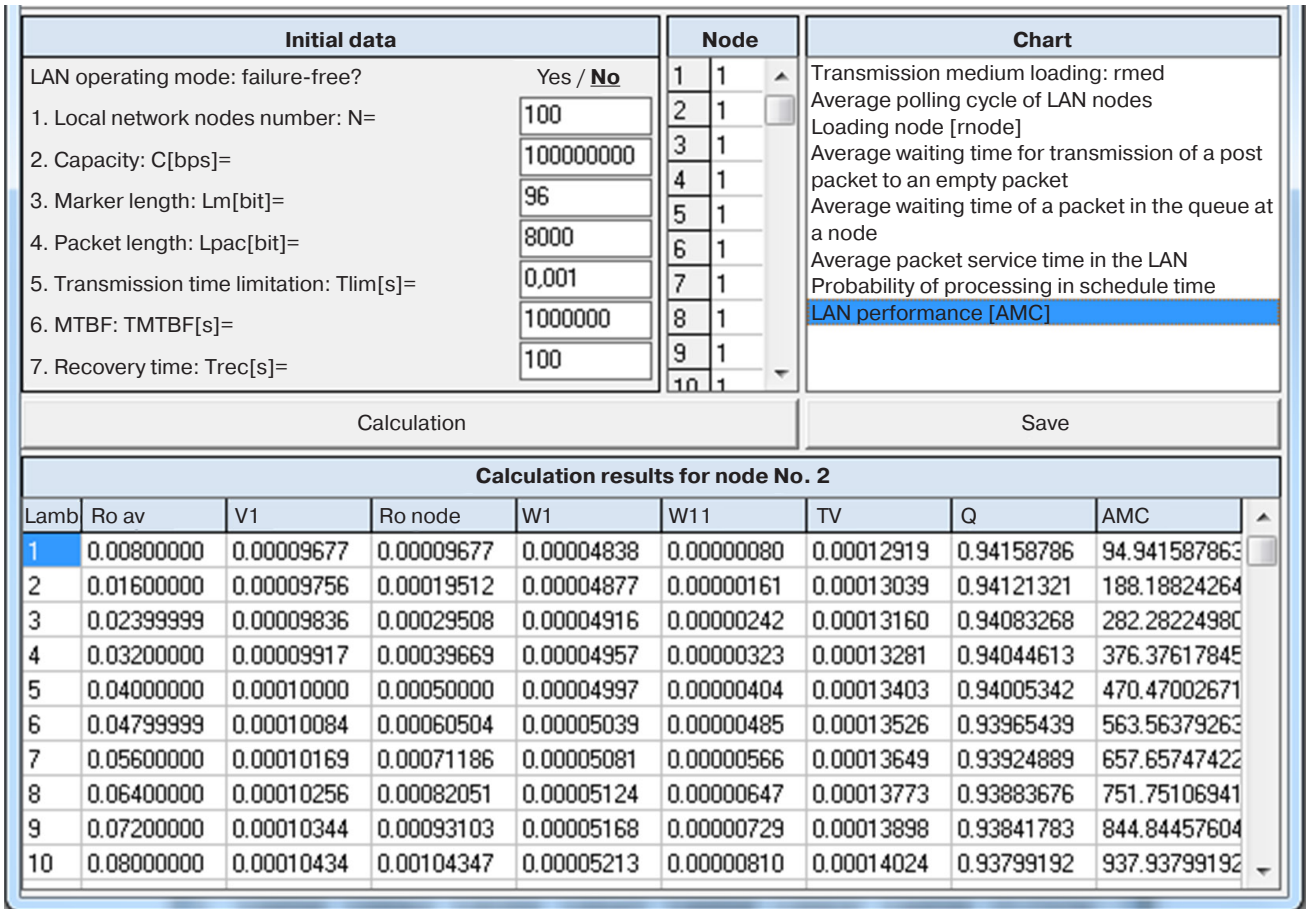

Lamb	Ro av	V1	Ro node	W1	W11	TV	Q	AMC
1	0.00800000	0.00009677	0.00009677	0.00004838	0.00000080	0.00012919	0.94158786	94.941587863
2	0.01600000	0.00009756	0.00019512	0.00004877	0.00000161	0.00013039	0.94121321	188.18824264
3	0.02399999	0.00009836	0.00029508	0.00004916	0.00000242	0.00013160	0.94083268	282.28224980
4	0.03200000	0.00009917	0.00039669	0.00004957	0.00000323	0.00013281	0.94044613	376.37617845
5	0.04000000	0.00010000	0.00050000	0.00004997	0.00000404	0.00013403	0.94005342	470.47002671
6	0.04799999	0.00010084	0.00060504	0.00005039	0.00000485	0.00013526	0.93965439	563.56379263
7	0.05600000	0.00010169	0.00071186	0.00005081	0.00000566	0.00013649	0.93924889	657.65747422
8	0.06400000	0.00010256	0.00082051	0.00005124	0.00000647	0.00013773	0.93883676	751.75106941
9	0.07200000	0.00010344	0.00093103	0.00005168	0.00000729	0.00013898	0.93841783	844.84457604
10	0.08000000	0.00010434	0.00104347	0.00005213	0.00000810	0.00014024	0.93799192	937.93799192

Fig. 3. Screen form for input of initial data and output of modeling results.
AMC—automatic message counting

In order to demonstrate the study of packet delivery processes and performance of fiber optic FDDI networks using the developed analytical method, a simulation of packet transmission is performed. The following initial data were selected for modeling:

- type of transmission medium is two fiber optic rings;
- type of node distribution in the network is random;
- number of nodes in the network $N = 100$;
- bandwidth 100 Mbps;
- MTBF of the transmission medium 100000–1000000 s;
- average recovery time after failure 100 s;
- marker length 96 bits;
- directive time 1 ms;
- synchronous packet length (discrete GOOSE message) 8 kbits;
- intensity of arrival of synchronous packets (discrete GOOSE messages in DSS system) is the same in all nodes of FDDI network (variable parameter).

It should be noted that the group of programs developed enables modeling to be performed at different intensity of the packets arriving to the network nodes for service.

Results of calculations of the probability-time characteristics, performance, node utilization and transmission medium of the FDDI network of the DSS system with given initial data under load variation are presented in Figs. 4–10.

In an FDDI network, packet delivery time depends on the time waiting for transmission in the queue at the network nodes and the time of packet transmission. Therefore, the parameters of information processing in the network should be chosen in such a way that in the whole range of changes in the intensity of the flows of processed packets there are no bottlenecks in the system, i.e., overloads of individual nodes and the transmission medium. In a balanced system, the load of the transmission medium and the load of the nodes when the load increases should be close to each other. As the failure rate decreases and the number of nodes decreases for a given transmission medium capacity, the length of transmitted packets should increase, in such a way that the network is balanced when the load increases.

It should be noted that with an increasing failure rate in FDDI network and increasing number of nodes for a given network throughput to balance the network in the whole range of load changes, and in order to obtain optimal performance, the length of transmitted information packets needs to be reduced, since it will reduce the probability of distortion.

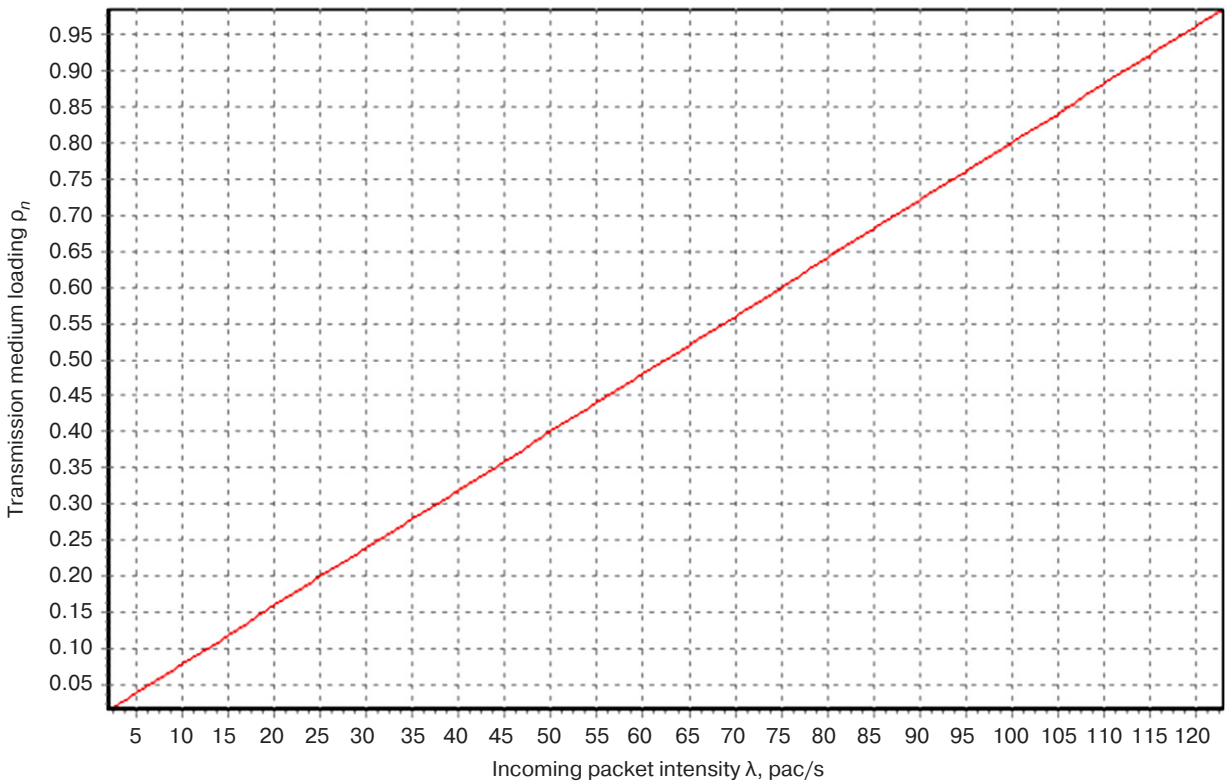

Fig. 4. Dependence of transmission medium load of fiber-optic FDDI network of DSS system on the intensity of synchronous packets arrival to the nodes

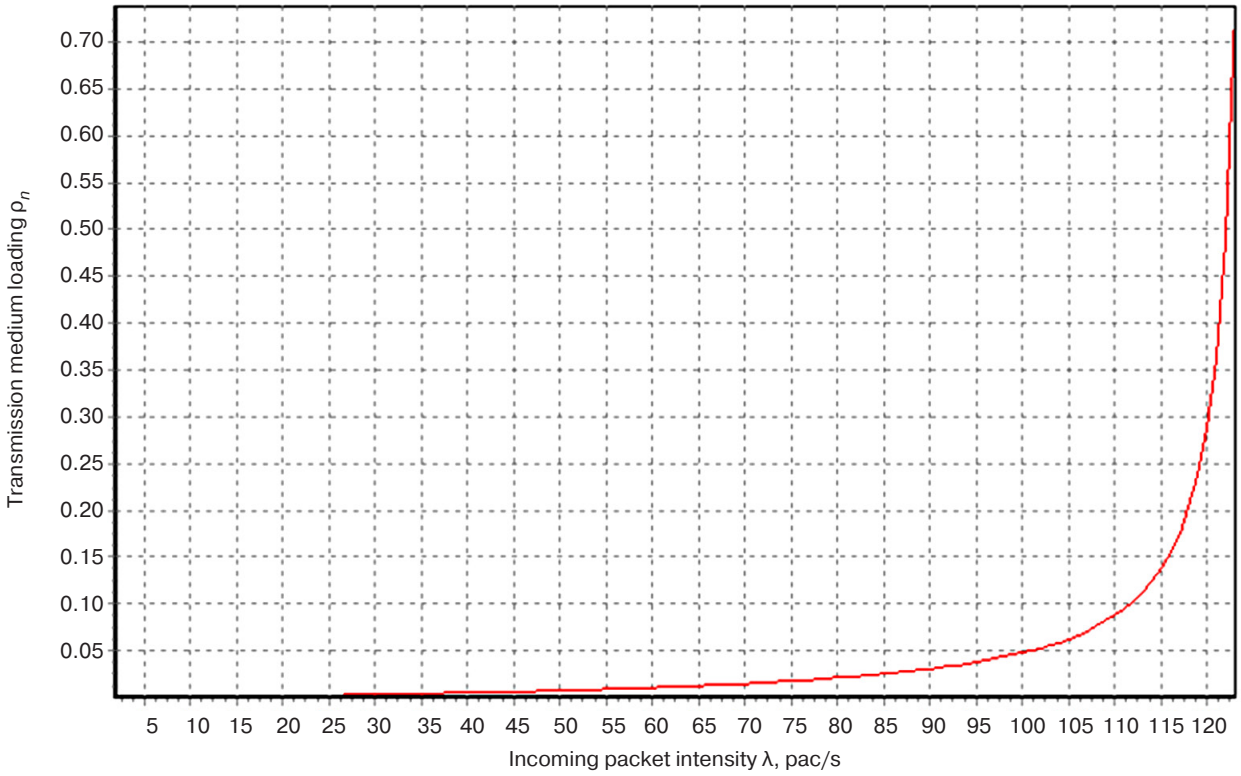

Fig. 5. Dependence of FDDI network node utilization of the DSS system on the intensity of synchronous packets arrival to the nodes

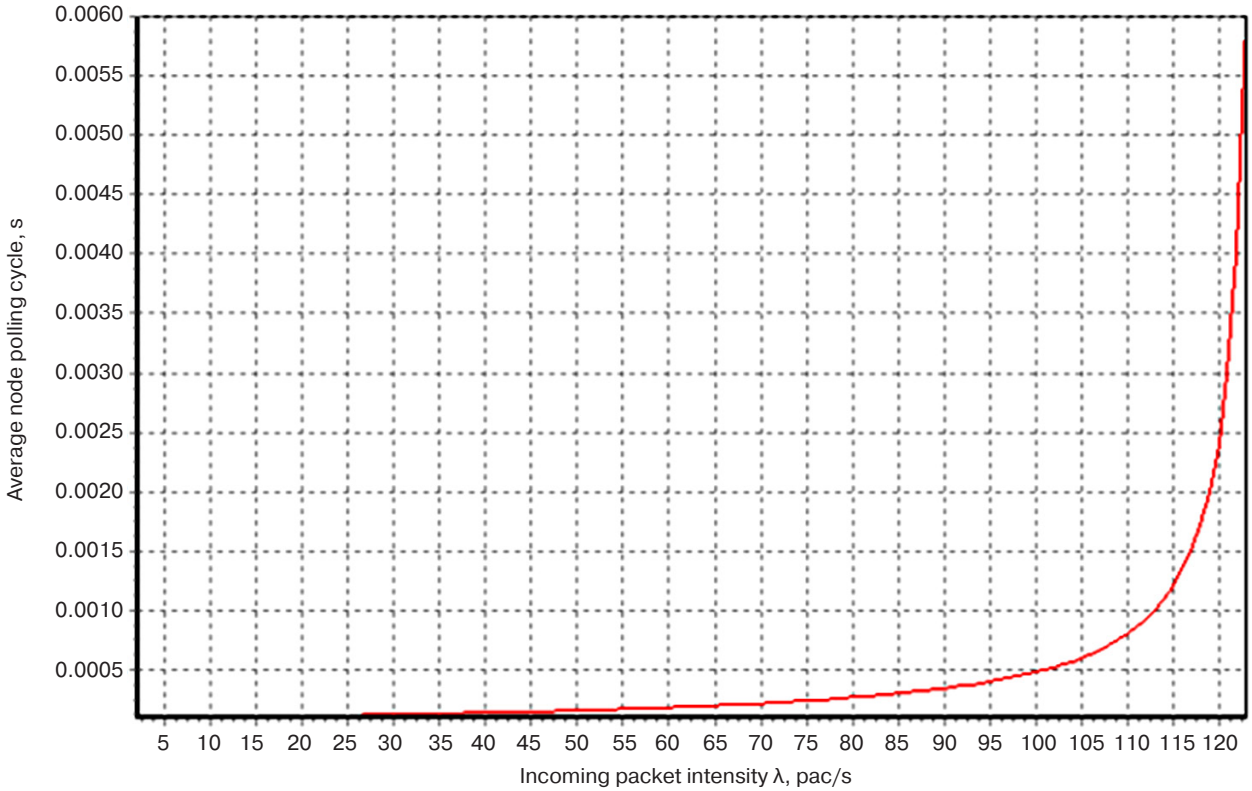

Fig. 6. Dependence of the average polling cycle of the nodes of the FDDI network of the DSS system on the intensity of arrival of synchronous packets to the nodes

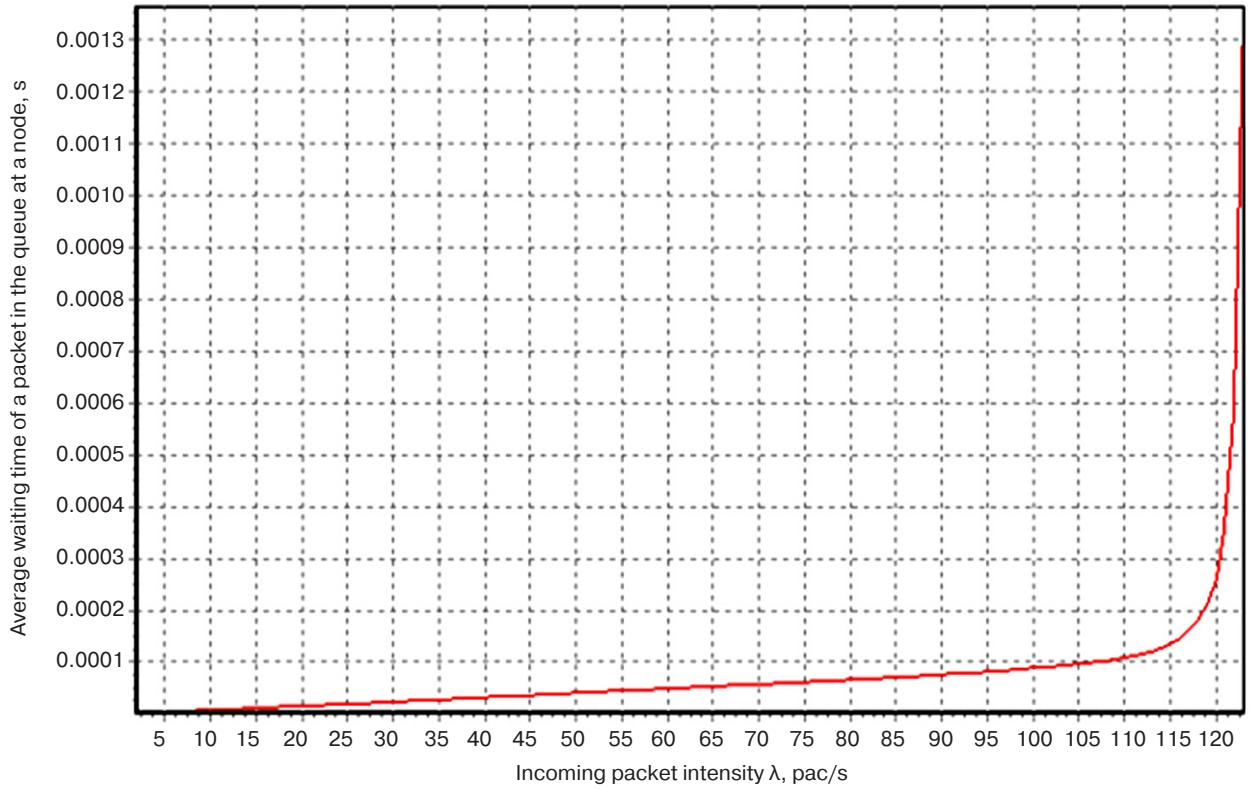

Fig. 7. Dependence of the waiting time for the beginning of synchronous packet transmission in the queue at the node of the FDDI network of the DSS system on the intensity of synchronous packets arrival

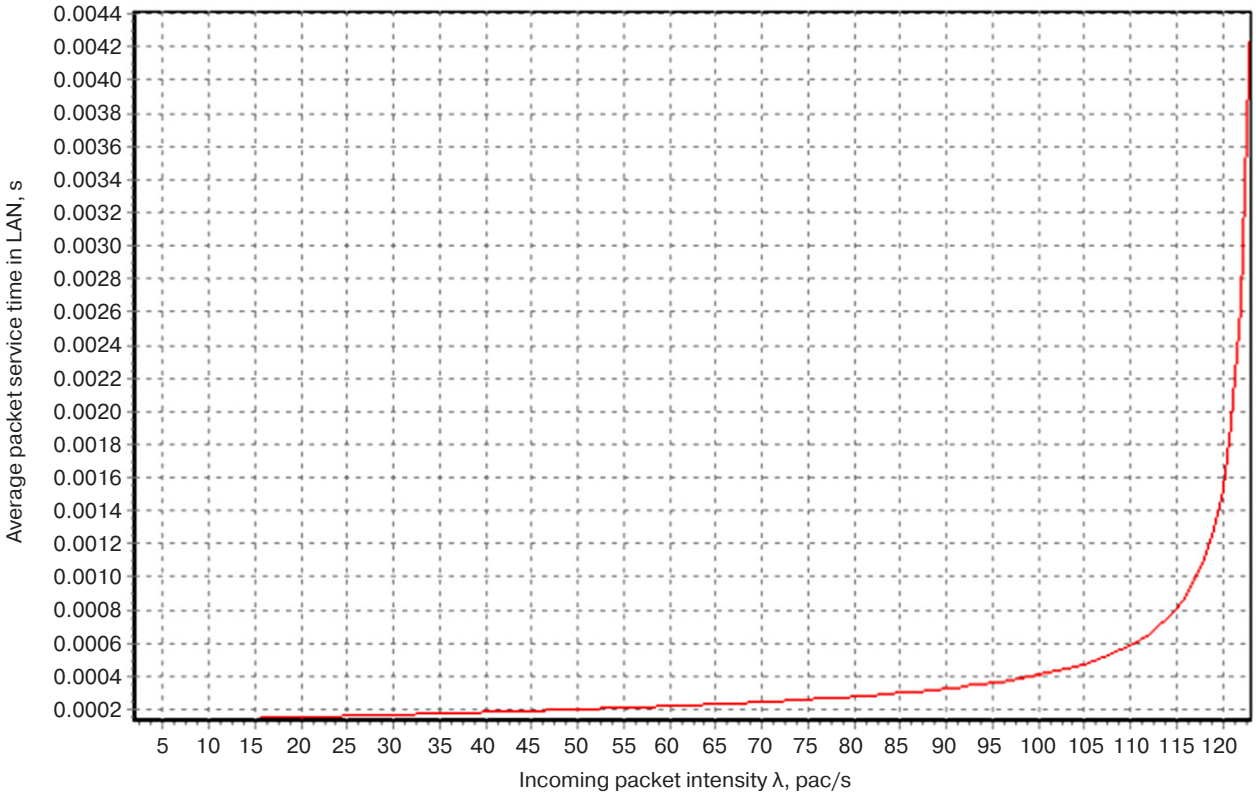

Fig. 8. Dependence of the average service time of synchronous packets in the FDDI network of the DSS system on the intensity of arrival of synchronous packets to the nodes

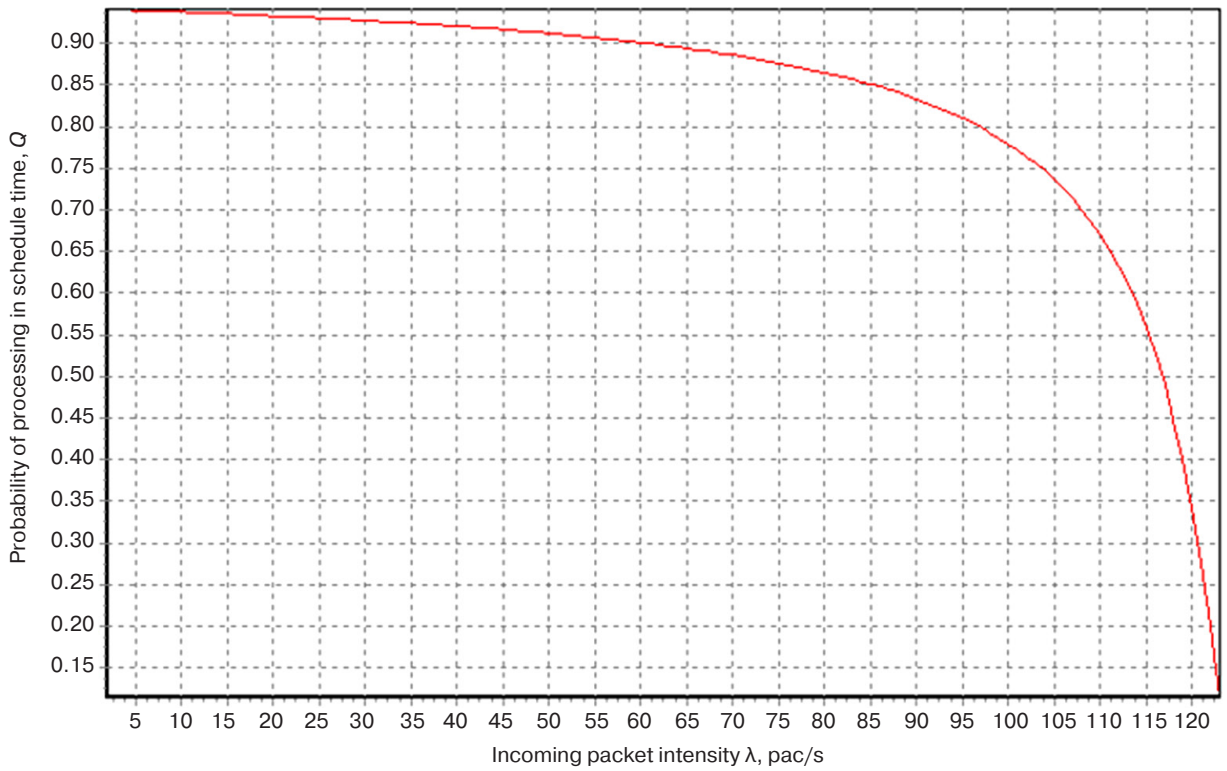

Fig. 9. Dependence of the probability of synchronous packets processing in the given directive terms in the FDDI network of the DSS system on the intensity of synchronous packets receipt

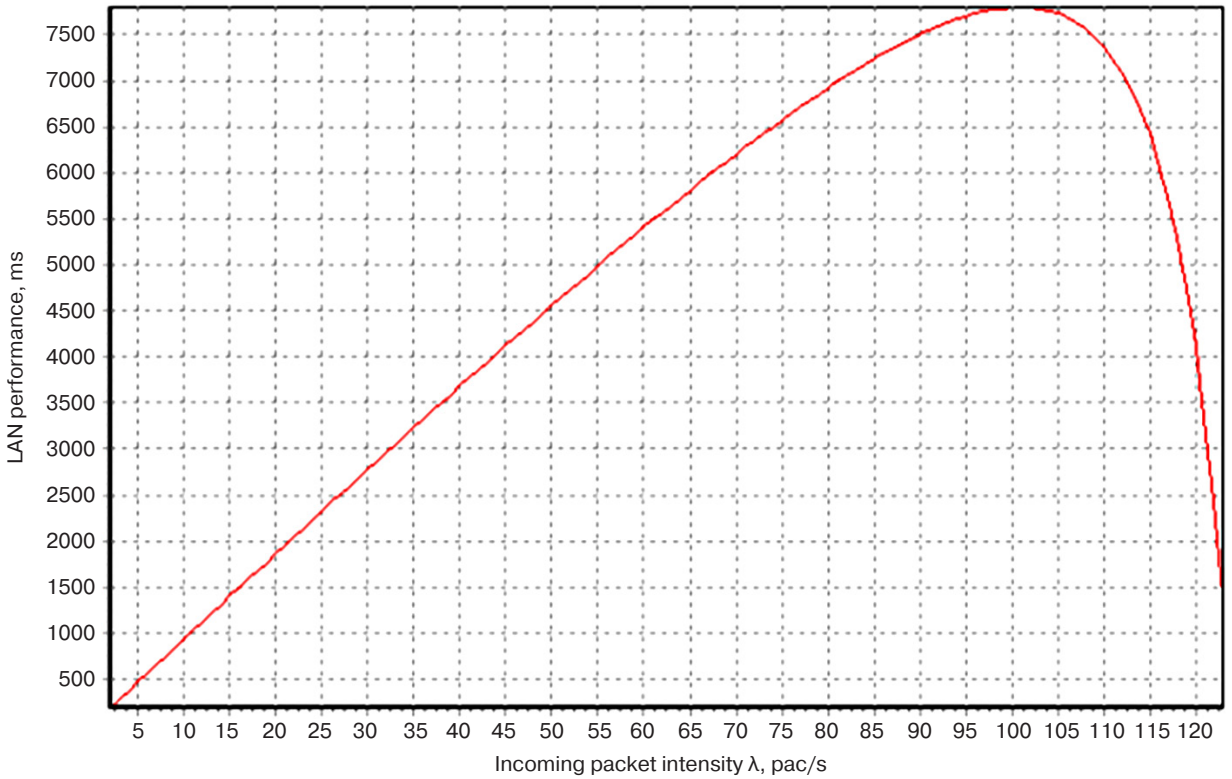

Fig. 10. Dependence of performance, total timely served flow of synchronous packets in FDDI network of the DSS system on the intensity of arrival of synchronous packets

As can be seen from the graphs (Figs. 4–9), as the intensity of packet flows served in the FDDI network increases, the node utilization, node polling cycle and timing characteristics increase, while the network performance (the total timely served packet flow in the network) reaches the maximum value and begins to fall sharply. As the failure rate of the transmission medium increases, the area of abrupt change of FDDI network characteristics shifts to the side of lower utilization.

Consequently, certain modes need to be provided for the operation in FDDI networks of a set of separated DSS when exchanging synchronous packets (GOOSE messages and packets transmitting synchronized parameters of vector measurements for DSS) between different DSS. The objective must be to prevent reaching the area of sharp changes in FDDI network performance, i.e., the need to control the intensity of input flows and limit their growth.

Specific recommendations on the selection of parameters and modes of operation of FDDI network used for information exchange in a distributed system of DSS can be obtained by conducting multivariate analytical calculations using a set of programs implementing the analytical method for the study of fiber-optic FDDI networks, while taking into account the reliability of the transmission medium.

CONCLUSIONS

The study developed a standard technological scheme of report preparation by DSS dispatchers. The authors propose the use of a fault-tolerant FDDI network with two fiber optic rings as a telecommunication component for information exchange between different nodes in the system of remote DSS. Discrete GOOSE messages form a synchronous flow of FDDI network packets, while information messages arising during the performance of basic technological operations in the preparation of reports by dispatchers of the central station do not form such a flow.

The study looked at aspects of development of the analytical models for the estimation of probabilistic-temporal characteristics and performance of FDDI networks with fiber optic rings taking into account possible failures in the transmission medium. The problem was posed and an analytical method was developed, in order to assess the performance of FDDI networks taking into account the reliability of the transmission medium, thus extending the scope of analytical approaches.

The conclusion which can be drawn based on this research is that a mechanism must be implemented to control packet flows entering the network, in order to ensure the efficient operation of FDDI networks. Thus, controlling the intensity of incoming flows and limiting their growth becomes an important aspect of ensuring the efficient operation of the network.

Based on the analytical method developed herein, a set of programs for studying the processes of information transmission in FDDI networks was created. This software enables multivariate analysis of different modes of operation of FDDI networks used for data transmission between remote DSS.

The study also established analytical expressions for estimating node and transmission medium utilization, average packet dwell time in the network, probability of timely packet service and performance. Aspects of FDDI network operation and transmission medium reliability were taken into account when formulating these expressions.

It was found that there is a critical load for FDDI networks at which the network performance reaches a maximum and then decreases sharply. As the failure rate of the transmission medium increases, the critical modes of FDDI network operation shift towards lower loads.

In order to ensure the efficient operation of FDDI networks, the modes of operation need to be regulated in such a way as to avoid reaching critical load at the nodes and in the transmission medium. Controlling the intensity of input flows and limiting their growth are key elements for DSS systems in FDDI networks.

Authors' contribution
All authors equally contributed to the research work.

REFERENCES

1. Gromov I.V., Egorov E.P., Koshelkov I.A. Comparative analysis of the provisions of various editions of the IEK 61850 standard when using the GOOSE and SV protocols. *Releinaya zashchita i avtomatizatsiya = Relay Protection and Automation*. 2019;4(37):46–49 (in Russ.).
2. Sapna, Sharma M. Performance evaluation of a wired network with & without Load Balancer and Firewall. In: *2010 International Conference on Electronics and Information Engineering.* Kyoto, Japan. 2010. P. V2-515–V2-519. https://doi.org/10.1109/ICEIE.2010.5559755
3. Bessoltsev V.S., Khorkov S.A. Digital substation: Structure, protocols, architecture. *Collection of abstracts of the 12th International Scientific and Practical Conference*. Izhevsk; 2022. P. 23–27 (in Russ.).
4. Zhmatov D.V. Technical Condition Monitoring of Electric Equipment in the Digital Substation. In: *2020 2nd International Conference on Control Systems, Mathematical Modeling, Automation and Energy Efficiency* (*SUMMA*). 2020. P. 983–986. https://doi.org/10.1109/SUMMA50634.2020.9280800
5. Kharlamov V.A., Romanov S.E., Khasanov A.K. Ways to transmit GOOSE messages between substations for PAC systems. *Releishchik*. 2022(2):12–17 (in Russ.).
6. Bezdenezhnykh M.N., Egorov A.P., Koshelkov I.A., Doni N.A. GOOSE network load analysis software IEC 61850-8-1:2011. *Avtomatizatsiya i IT v Energetike*. 2019;8(121):22–25 (in Russ.). Available from URL: https://elibrary.ru/ojmxwt
7. Wei M., Chen Z. Study of LANs access technologies in wind power system. In: *IEEE PES General Meeting*. Minneapolis, MN, USA. 2010.
8. Zvonareva G.A., Buzunov D.S. Using Simulation Modeling to Estimate Time Characteristics of a Distributed Computing System. *Otkrytoe obrazovanie = Open Education*. 2022;26(5):32–39 (in Russ.). https://doi.org/10.21686/1818-4243-2022-5-32-39
9. Leontyev A.S. Multilevel Analytical and Analytical-Simulation Models for Evaluating the Probabilistic and Temporal Characteristics of Multimachine Computing Complexes with Regard to Reliability. *Mezhdunarodnyi nauchno-issledovatel'skii zhurnal = International Research Journal*. 2023;5(131) (in Russ.). https://doi.org/10.23670/IRJ.2023.131.8
10. Kul'ba V.V., Mamikonov A.G., Shelkov A.B. Redundancy of program modules and data arrays in a MIS. *Avtomatika i telemekhanika = Automation and Remote Control*. 1980;8:133–141 (in Russ.).
11. Talalaev A.A., Frolenko V.P. Fault-tolerant system for organizing high-performance computing for solving data stream processing problems. *Programmnye sistemy: Teoriya i prilozheniya = Program Systems: Theory and Applications*. 2018;9(1–36):85–108 (in Russ.). https://doi.org/10.25209/2079-3316-2018-9-1-85-108
12. Akimova G.P., Solovyev A.V., Tarkhanov I.A. Modeling the reliability of distributed information systems. *Informatsionnye tekhnologii i vychislitel'nye sistemy = Journal of Information Technologies and Computing Systems*. 2019;3:70–86 (in Russ.). https://doi.org/10.14357/20718632190307
13. Pavsky V.A., Pavsky K.V. Mathematical Model for Calculating Reliability Indicators of Scalable Computer Systems Considering Switching Time. *Izvestiya YuFU. Tekhnicheskie nauki = Izvestiya SFedU. Engineering Sciences*. 2020;2(212):134–145 (in Russ.). https://doi.org/10.18522/2311-3103-2020-2-134-145
14. Ahmed W., Wu Y.W. A survey on reliability in distributed systems. *J. Comput. System Sci*. 2013;79(8):1243–1255. https://doi.org/10.1016/j.jcss.2013.02.006
15. Leontyev A.S. Development of Analytical Methods, Models, and Techniques for Local Area Networks Analysis. In: *Theoretical Issues of Software Engineering: Interuniversity Collection of Scientific Papers*. Moscow: MIREA; 2001. P. 70–94 (in Russ.).
16. Ivanichkina L.V., Neporada A.L. The Reliability model of a distributed data storage in case of explicit and latent disk faults. *Trudy Instituta sistemnogo programmirovaniya RAN = Proceedings of the Institute for System Programming of the RAS*. 2015;27(6):253–274 (in Russ.). https://doi.org/10.15514/ISPRAS-2015-27(6)-16

СПИСОК ЛИТЕРАТУРЫ

1. Громов И.В., Егоров Е.П., Кошельков И.А. Сравнительный анализ положений различных редакций стандарта IEK 61850 при использовании протоколов GOOSE и SV. *Релейная защита и автоматизация*. 2019;4(37):46–49. URL: https://elibrary.ru/icfpna
2. Sapna, Sharma M. Performance evaluation of a wired network with & without Load Balancer and Firewall. In: *2010 International Conference on Electronics and Information Engineering.* Kyoto, Japan. 2010. P. V2-515–V2-519. https://doi.org/10.1109/ICEIE.2010.5559755
3. Бессольцев В.С., Хорьков С.А. Цифровая подстанция: Структура, протоколы, архитектура. *Сборник тезисов XII Международной научно-практической конференции*. Ижевск, 15 апреля 2022 г. Ижевск: Ижевский институт компьютерных исследований; 2022. С. 23–27.
4. Zhmatov D.V. Technical Condition Monitoring of Electric Equipment in the Digital Substation. In: *2020 2nd International Conference on Control Systems, Mathematical Modeling, Automation and Energy Efficiency* (*SUMMA*). 2020. P. 983–986. https://doi.org/10.1109/SUMMA50634.2020.9280800
5. Харламов В.А., Романов С.Е., Хасанов А.Х. Способы передачи GOOSE-сообщений между подстанциями для систем РЗА. *Релейщик*. 2022(2):12–17.
6. Безденежных М.Н., Егоров А.П., Кошельков И.А., Дони Н.А. Анализ сетевой нагрузки GOOSE по МЭК 61850-8-1:2011. *Автоматизация и ИТ в энергетике*. 2019;8(121):22–25. URL: https://elibrary.ru/ojmxwt

7. Wei M., Chen Z. Study of LANs access technologies in wind power system. In: *IEEE PES General Meeting*. Minneapolis, MN, USA. 2010.
8. Звонарева Г.А., Бузунов Д.С. Использование имитационного моделирования для оценки временных характеристик распределенной вычислительной системы. *Открытое образование*. 2022;26(5):32–39. https://doi.org/10.21686/1818-4243-2022-5-32-39
9. Леонтьев А.С. Многоуровневые аналитические и аналитико-имитационные модели оценки вероятностно-временных характеристик многомашинных вычислительных комплексов с учетом надежности. *Международный научно-исследовательский журнал.* 2023;5(131). https://doi.org/10.23670/IRJ.2023.131.8
10. Кульба В.В., Мамиконов А.Г., Шелков А.Б. Резервирование программных модулей и информационных массивов в АСУ. *Автоматика и телемеханика*. 1980;8:133–141.
11. Талалаев А.А., Фроленко В.П. Отказоустойчивая система организации высокопроизводительных вычислений для решения задач обработки потоков данных. *Программные системы: Теория и приложения*. 2018;9(1–36):85–108. https://doi.org/10.25209/2079-3316-2018-9-1-85-108
12. Акимова Г.П., Соловьев А.В., Тарханов И.А. Моделирование надежности распределенных вычислительных систем. *Информационные технологии и вычислительные системы* (*ИТиВС*). 2019;3:70–86. https://doi.org/10.14357/20718632190307
13. Павский В.А., Павский К.В. Математическая модель для расчета показателей надежности масштабируемых вычислительных систем с учетом времени переключения. *Известия ЮФУ. Технические науки*. 2020;2(212):134–145. https://doi.org/10.18522/2311-3103-2020-2-134-145
14. Ahmed W., Wu Y.W. A survey on reliability in distributed systems. *J. Comput. System Sci*. 2013;79(8):1243–1255. https://doi.org/10.1016/j.jcss.2013.02.006
15. Леонтьев А.С. Разработка аналитических методов, моделей и методик анализа локальных вычислительных сетей. *Теоретические вопросы программного обеспечения: Межвузовский сборник научных трудов*. М.: МИРЭА; 2001. С. 70–94.
16. Иваничкина Л.В., Непорада А.Л. Модель надежности распределенной системы хранения данных в условиях явных и скрытых дисковых сбоев. *Труды Института системного программирования РАН*. 2015;27(6):253–274. https://doi.org/10.15514/ISPRAS-2015-27(6)-16

About the authors

Alexander S. Leontyev, Cand. Sci. (Eng.), Senior Researcher, Associate Professor, Department of Mathematical Support and Standardization, Institute of Information Technologies, MIREA – Russian Technological University (78, Vernadskogo pr., Moscow, 119454 Russia). E-mail: leontev@mirea.ru. RSCI SPIN-code 5798-9721, https://orcid.org/0000-0003-3673-2468

Dmitry V. Zhmatov, Cand. Sci. (Eng.), Associate Professor, Department of Mathematical Support and Standardization, Institute of Information Technologies, MIREA – Russian Technological University (78, Vernadskogo pr., Moscow, 119454 Russia). E-mail: zhmatov@mirea.ru. Scopus Author ID 56825948100, RSCI SPIN-code 2641-6783, https://orcid.org/0000-0002-7192-2446

Об авторах

Леонтьев Александр Савельевич, к.т.н., старший научный сотрудник, доцент, кафедра математического обеспечения и стандартизации информационных технологий, Институт информационных технологий, ФГБОУ ВО «МИРЭА – Российский технологический университет» (119454, Россия, Москва, пр-т Вернадского, д. 78). E-mail: leontev@mirea.ru. SPIN-код РИНЦ 5798-9721, https://orcid.org/0000-0003-3673-2468

Жматов Дмитрий Владимирович, к.т.н., доцент, кафедра математического обеспечения и стандартизации информационных технологий, Институт информационных технологий, ФГБОУ ВО «МИРЭА – Российский технологический университет» (119454, Россия, Москва, пр-т Вернадского, д. 78). E-mail: zhmatov@mirea.ru. Scopus Author ID 56825948100, SPIN-код РИНЦ 2641-6783, https://orcid.org/0000-0002-7192-2446

Translated from Russian into English by Lyudmila O. Bychkova
Edited for English language and spelling by Dr. David Mossop

Information systems. Computer sciences. Issues of information security
Информационные системы. Информатика. Проблемы информационной безопасности

UDC 004.056.5
https://doi.org/10.32362/2500-316X-2024-12-6-39-47
EDN IYBIZH

RESEARCH ARTICLE

Modeling incident management processes in information security at an enterprise

Evgeny S. Mityakov [@], Elena A. Maksimova, Svetlana V. Artemova, Anatoly A. Bakaev, Zhanna G. Vegera

MIREA – Russian Technological University, Moscow, 119454 Russia
[@] Corresponding author, e-mail: mityakov@mirea.ru

Abstract

Objectives. The primary aim of the study is to develop a model for managing information security incidents within an enterprise that minimizes damage and costs associated with incident resolution under limited resources and time constraints.

Methods. The paper analyzes existing approaches to managing information security incidents, including mathematical and simulation models, stochastic differential equations, Markov chains, and other methods. The study is based on a systems approach, incorporating analysis of incident parameters, actions for their resolution, response times, damages due to incident occurrence, and the probability of incident elimination. To validate the developed model, synthetic data reflecting various types of incidents and possible actions were used.

Results. The proposed model optimizes incident management by minimizing damage and costs. It considers parameters such as incident criticality, available resources, response time, and the likelihood of successful incident resolution. Testing of the model on synthetic data showed that the proposed approach significantly improves the selection of optimal actions for responding to incidents in situations constrained by budget and time limitations, thereby enhancing the overall effectiveness of incident management.

Conclusions. Implementing the proposed model in enterprises will improve the overall level of information security, enhance incident response efficiency, and strengthen information protection processes. This will ensure the minimization of risks associated with data leaks and other incidents, thus helping enterprises to make informed and timely decisions under conditions of limited resources and time.

Keywords: incident management, information security, incident modeling, damage minimization, limited resources, mathematical modeling, optimization

• **Submitted:** 12.09.2024 • **Revised:** 30.09.2024 • **Accepted:** 14.10.2024

For citation: Mityakov E.S., Maksimova E.A., Artemova S.V., Bakaev A.A., Vegera Zh.G. Modeling incident management processes in information security at an enterprise. *Russ. Technol. J*. 2024;12(6):39–47. https://doi.org/10.32362/2500-316X-2024-12-6-39-47

Financial disclosure: The authors have no financial or proprietary interest in any material or method mentioned.

The authors declare no conflicts of interest.

НАУЧНАЯ СТАТЬЯ

Моделирование процессов управления инцидентами информационной безопасности на предприятии

Е.С. Митяков [@], **Е.А. Максимова**, **С.В. Артемова**, **А.А. Бакаев**, **Ж.Г. Вегера**

МИРЭА – Российский технологический университет, Москва, 119454 Россия
[@] *Автор для переписки, e-mail: mityakov@mirea.ru*

Резюме

Цели. Основной целью исследования является разработка модели управления инцидентами информационной безопасности на предприятии, минимизирующей ущерб и затраты на устранение инцидентов в условиях ограниченных ресурсов и времени.

Методы. В работе проведен анализ существующих подходов к управлению инцидентами информационной безопасности, включая математические и имитационные модели, стохастические дифференциальные уравнения, цепи Маркова и другие методы. Основанием для работы послужил системный подход, который включает в себя всесторонний анализ параметров инцидентов, действий по их устранению, времени реакции, а также ущерба от реализации инцидентов и вероятности успешного их устранения. Для проверки работоспособности разработанной модели использовались синтетические данные, которые отражают разнообразные типы инцидентов и возможные пути их ликвидации.

Результаты. Предложенная модель управления инцидентами позволяет оптимизировать управление инцидентами за счет минимизации ущерба и затрат. В рамках модели учитываются такие параметры, как критичность инцидентов, доступные ресурсы, время реакции и вероятность успешного устранения инцидентов. Апробация модели на синтетических данных показала, что предложенный подход существенно улучшает выбор оптимальных действий для реагирования на инциденты в ситуациях ограничений бюджета и времени, что в свою очередь повышает общую эффективность управления инцидентами.

Выводы. Внедрение предложенной модели на предприятиях позволит повысить общий уровень информационной безопасности, эффективность реагирования на инциденты и улучшить процессы защиты информации. Это обеспечит минимизацию рисков, связанных с утечками данных и другими инцидентами, и поможет предприятиям принимать обоснованные и оперативные решения в условиях ограниченных ресурсов и времени.

Ключевые слова: управление инцидентами, информационная безопасность, моделирование инцидентов, минимизация ущерба, ограниченные ресурсы, математическое моделирование, оптимизация

• **Поступила:** 12.09.2024 • **Доработана:** 30.09.2024 • **Принята к опубликованию:** 14.10.2024

Для цитирования: Митяков Е.С., Максимова Е.А., Артемова С.В., Бакаев А.А., Вегера Ж.Г. Моделирование процессов управления инцидентами информационной безопасности на предприятии. *Russ. Technol. J.* 2024;12(6):39–47. https://doi.org/10.32362/2500-316X-2024-12-6-39-47

Прозрачность финансовой деятельности: Авторы не имеют финансовой заинтересованности в представленных материалах или методах.

Авторы заявляют об отсутствии конфликта интересов.

INTRODUCTION

Information security incident management at enterprises involves processes of identifying, analyzing and responding to incidents involving information systems and data, which includes a set of measures for the prevention and minimization of damage, and restoration of the normal operation of systems following incidents.

In today's reality, such processes represent a key aspect of ensuring the information security of an organization. Contemporary enterprises face many threats involving cyberattacks and unauthorized access to data to information leaks. As well as entailing financial losses, such threats can undermine a company's reputation. Therefore, effective management of information security incidents at an enterprise becomes an integral part of its overall security strategy. Such management ensures a prompt response to current threats, as well as forming a proactive approach to predicting and preventing potential information security incidents in the future.

In the Russian Federation, information security incident management is regulated by a number of state standards. One of these, GOST R 59712-2022[1], is dedicated to computer security incident management, which represents a narrower area within information security. This standard describes a structured approach to the detection, registration, response and analysis of incidents within the framework of the state system GosSOPKA[2]. In turn, GOST R ISO/IEC TO 18044-2007[3] covers a wider range of information security incidents, setting out requirements for their documentation, legal examination, interaction with authorities, and adaptation to contemporary threats. However, the above standards do not take into account mechanisms for assessing damage from incidents and the costs of their elimination, thus limiting their application under conditions where time and resource constraints are critical.

The present work examines information security incident management processes in an enterprise, focusing on an analysis of existing approaches and models aimed at optimizing remediation costs, as well as increasing the responsiveness of incident response and minimizing damage. Here, the main aim is to develop a model that systematizes the incident management process to improve the efficiency of decision-making under resource and time constraints.

INCIDENT MANAGEMENT IN THE ENTERPRISE INFORMATION SECURITY SYSTEM

Information security incident management is critical to maintaining the integrity, confidentiality and availability of enterprise data. Effective incident management involves identifying, responding to and learning from security incidents to improve the overall security posture. An incident in the context of information security is any event or action that harms, or has the potential to harm, the confidentiality, integrity, or availability of information and information systems. The consequences of incidents, which can range from accidental errors to targeted attacks, can be quite serious for organizations.

Examples of incidents include virus attacks, data breaches, DDoS attacks, and unauthorized access. A distinction can be made between incidents and simple violations: an incident is an event that causes (or has the potential to cause) negative consequences to the secure operation of systems, while simple breaches typically do not cause significant consequences or damage and can be addressed without impacting the security of the system. Thus, incidents require more comprehensive analysis, rapid response, and potential application of appropriate remediation and protection measures.

Timely incident responses contribute to improving information security management processes. However, a link between incident response and security management functions is often absent. Therefore, enterprises need to establish integration between these two areas in order to develop a clear plan of action that can increase the trust and support of contractors [1].

[1] GOST R 59712-2022. National Standard of the Russian Federation. *Information protection. Computer incident management. Guide to responding to computer incident*. Moscow: Standartinform; 2023. 20 p. (in Russ.).

[2] https://gossopka.ru/ (in Russ.). Accessed July 15, 2024.

[3] GOST R ISO/IEC TO 18044-2007. National Standard of the Russian Federation. *Information technology. Security techniques. Information security incident management*. Moscow: Standartinform; 2008. 50 p. (in Russ.).

Real-time detection of security incidents is performed through specialized security management centers using information and information security event management systems. These centers, which collect, normalize, store, and correlate security events, are essential for rapid incident detection, loss minimization, vulnerability remediation, and IT service restoration [2].

Effective information security management requires a holistic approach, including the development and implementation of security policies, compliance training, and business-IT alignment[4]. For example, [3] notes that integrating digital forensics with incident handling can improve the effectiveness of incident response strategies.

Paper [4] shows that effective incident management requires a combination of technological solutions and management activities (development of security policies, training and information sharing between departments, etc.). Current incident management practices comply with ISO/IEC 27035 standards[5], but organizations often face certain challenges that are addressed through improved strategies.

Thus, effective enterprise information security incident management involves a combination of thorough incident analysis, strategic use of specialized information systems, and a holistic approach to security management, as well as the integration of technology and management solutions. By addressing communication gaps, using real-time monitoring tools, and implementing best practices, organizations can improve their incident response capabilities and overall security posture [5].

EXISTING INCIDENT MANAGEMENT MODELS

In order to improve the efficiency of incident management processes, various models have been proposed in the specialized scientific literature. For example, [6] considered cognitive modeling of destructive malicious attacks on critical information infrastructure objects and a model of states of critical information infrastructure subjects under destructive attacks in static mode.

Markovian chains and stochastic differential equations are used to describe the dynamics of security information and event management systems [7]. Supervised Markovian chains can be used to formalize and structure the decision support process for security event and incident management. This approach focuses on the dynamics of detecting and preventing cyber-attacks, as well as ensuring timeliness, validity, secrecy, and resource efficiency [8].

A number of studies have proposed simulation models for modeling incident management, which evaluate the effectiveness of incident management operations by analyzing real-world data and various strategies for deploying emergency response teams. Such models can predict the statistical patterns of cyberattacks and the effectiveness of incident response teams, enabling dynamic adjustments to maintain the required level of protection [9].

In [10], the implementation of a three-level incident management model using key metrics is shown to significantly improve the efficiency of incident handling. This model integrates process, technology and service metrics to improve the speed, user satisfaction and availability of incident handling channels.

In addition to the abovementioned models, various approaches based on formal languages and automata theory [11] (providing a structured approach to modeling and analyzing incident management processes to enable the identification and resolution of systemic problems), incident prioritization [12] (using feedback from analysts to correct errors in the assessment process to guarantee prompt resolution of the most critical incidents), etc., can be found in the scientific literature. By integrating feedback mechanisms and comprehensive security event management, organizations can maintain robust incident management processes that adapt to evolving threats and technological changes.

Thus, various models are used in information security incident management tasks, including mathematical, simulation, system dynamic and formal language approaches. These models aim to improve the identification and classification of incidents along with their appropriate responses to ensure effective and proactive security risk management [13]. Information security incident management acts as an important process that is directly related to ensuring three key elements: data integrity, authentication and availability [14]. The application of variation models can improve the processes of incident identification, classification and remediation. In order to achieve maximum efficiency, it is important to take into account the specifics of each organization, the degree of threats and the available resources to adapt the models to real conditions.

INFORMATION SECURITY INCIDENT MANAGEMENT MODEL AT THE ENTERPRISE

For describing information security incident management tasks, a model containing the following components can be used:

[4] Tran D.U. *Holistic Understanding of Information Security Posture*: Thesis Dr. Phil. University of Oslo, Department of Informatics, Series of Dissertations Submitted to the Faculty of Mathematics and Natural Sciences, no. 2696. 2023. https://www.duo.uio.no/bitstream/handle/10852/106520/PhD-Tran-2023.pdf?sequence=3&isAllowed=y. Accessed July 15, 2024.

[5] https://www.iso.org/standard/78973.html. Accessed July 15, 2024.

1. *Set of information security incidents* $I = \{I_1, I_2, \ldots, I_n\}$, where I_i is an information security incident recorded in the organization. Each incident is characterized by the parameters of detection time, degree of criticality, probability of threat realization, etc.
2. *Set of incident management actions* $A = \{A_1, A_2, \ldots, A_m\}$, where A_j is a certain action to eliminate the incident or minimize its consequences. Such actions can include blocking access, restoring data, implementing additional protective measures in the enterprise, etc.
3. *Incident response time* $T(I_i)$. This component of the model depends on the level of criticality of the incident and the resources available for response. Ideally, the higher the criticality of the incident, the shorter the response time should be.
4. *Incident damage function* $D(I_i)$ estimates the real or potential losses to the organization as a result of incident I_i (financial loss, reputational damage, data breach, etc.).
5. *Incident elimination probability function* $P(A_j, I_i)$ describes the probability of success of action A_j in relation to incident I_i. The probability depends on various factors (qualification of employees, execution time, type of incident, etc.).
6. *Incident elimination costs* $C(A_j, I_i)$ reflect how much resource (financial, time, and human) must be expended to implement action A_j in order to eliminate the incident I_i.

The key objective of the model is to minimize the total damage from information security incidents and the cost of their elimination. In order to solve this problem, it is advisable to minimize the following target function:

$$Z = \sum_{i=1}^{n}\sum_{j=1}^{m}\left[D(I_i)(1 - P(A_j, I_i)) + C(A_j, I_i)\right] \to \min,$$

where Z is the total damage and costs for all incidents. It is advisable to take into account the limitations on available resources, response time and risk level:

$$T(I_i) \le T_{\max},$$
$$\sum_{i=1}^{n}\sum_{j=1}^{m} C(A_j, I_i) \le R,$$
$$P(A_j, I_i) \ge P_{\min},$$
$$I_i \in \mathrm{I},\ A_j \in \mathrm{A},$$

where $T_{\max}$ is the maximum allowable incident response time (can be set by the enterprise security policy); R is the total available budget (number of resources) allocated to eliminate information security incident; $P_{\min}$ is the minimum allowable probability of successful incident elimination.

The use of the above model implies the following steps:

1. *Incident detection.*
2. *Incident data collection* (criticality, possible damage, remediation costs).
3. *Assessing the likelihood of a successful resolution of an incident,* taking into account time and cost constraints.
4. *Optimization of actions* (based on the presented model, the action A_j that minimizes damage and costs is obtained).
5. *Monitoring and adjustment* (once all necessary actions to address the incident have been completed, the model can be adjusted to further analyze and prevent future incidents).

The proposed model helps to systematize the process of information security incident management and make optimal decisions for their elimination. However, the model contains a number of limitations and assumptions. The limitations include the need for accurate and up-to-date data, difficulties in estimating damage and probability, and failing to account for the human factor. The assumptions entailed in the model include linearity of damage and cost functions, independence of incidents, unambiguous definition of criticality, and others. When adapting the model to their own information security conditions, enterprises should take these aspects into account.

In order to effectively test the model, a set of synthetic data simulating various types of incidents and possible means for their elimination was used. The choice of synthetic data over real data is due to the limited availability of the latter: enterprises are often unable or unwilling to share information about their incidents for security and confidentiality reasons. In addition, the use of synthetic data enables the construction of more complete and reliable models based on a variety of hypothetical scenarios. When combined with theoretical analysis and development, this approach provides a foundation for a better understanding of information security incident response and management mechanisms. Thus, the use of synthetic data represents a valid method in the face of a lack of real-world information and is aimed at ensuring high-quality and reliable model validation.

Let the analysis at the enterprise reveal a number of information security incidents, each of which requires different actions for elimination, which are limited in resources and time. Initial data for calculations are presented in the Table 1.

Table 1. Initial data

Incident	Potential damage (D), c.u.	Time of reaction (T), h	Criticality
Customer database data leakage	200000	2	High
Virus attack on servers	100000	5	Medium
Unauthorized access to the network	50000	1	Low

Table 2. Possible actions to address information security incidents

Incident	Action	Cost (C), c.u.	Probability of success (P)
Data leakage (I_1)	Disconnecting external connections (A_1)	15000	0.7
	Customer notification and vulnerability correction (A_2)	25000	0.9
Virus attack (I_2)	Reboot servers and start antivirus (A_3)	10000	0.8
	Hardware replacement and data recovery (A_4)	20000	0.95
Unauthorized access (I_3)	Disabling an intruder session (A_5)	5000	0.6
	Network audit and configuration remediation (A_6)	8000	0.85

Suppose the enterprise has limited resources for response: the budget for incident elimination is $R = 50000$ c.u. and the maximum response time for all incidents is 6 h. For each incident, let there be several possible actions with different costs, elimination probabilities and execution times (Table 2).

In order to minimize damage subject to constraints, it is necessary to select actions for each incident. Consider the alternatives.

For I_1. Action A_1 is cheaper, but has a probability of success of 0.7, while action A_2 is more expensive, but has a higher probability of success (0.9). Given the criticality of the incident, it is appropriate to choose action A_2, since data leakage is highly damaging.

For I_2. Action A_3 is cheaper and has a sufficiently high probability of success (0.8). Given the budget constraints, we choose action A_3.

For I_3. Action A_5 is the cheapest, but its probability of success is only 0.6. In this case, it is more appropriate to choose action A_6, since its probability of success is much higher (0.85) and it can be fitted within the budget.

Let us build a model using the initial data. The target function and model constraints will have the following form:

$$Z = \sum_{i=1}^{3}\sum_{j=1}^{2}\left[D(I_i)(1-P(A_j,I_i))+C(A_j,I_i)\right],$$

$$C(A_1,I_1)+C(A_3,I_2)+C(A_5,I_3) \le 50000 \text{ c.u.},$$

$$T(I_1)+T(I_1)+T(I_1) \le 6 \text{ h}.$$

The final model solution will be as follows:

- A_2 for incident 1 (cost is 25000 c.u.; probability of success is 0.9).
- A_3 for incident 2 (cost is 10000 c.u.; probability of success is 0.8).
- A_6 for incident 3 (cost is 8000 c.u.; probability of success is 0.85).

Having calculated the total costs and damage, we get $Z = 90500$ c.u. Thus, application of the model enabled the optimal actions to be selected in order to eliminate incidents with minimal costs and damage within the available budget and reaction time.

CONCLUSIONS

The incident management model proposed in this article can be used to minimize damage and costs through the optimal selection of actions under conditions of limited resources. Although the model has its limitations, its use in practice can significantly increase the level of information security of the enterprise.

The article proposes a model of information security incident management aimed at minimizing damage and costs. However, its practical use raises a number of issues related to simplifications: linearity of damage and cost functions, independence of incidents and unambiguous definition of their criticality. Such assumptions do not always reflect the complexity of real-life situations, where incidents are interrelated, and their consequences may be nonlinear. In addition, the model does not account

for human error or the difficulty of obtaining accurate data during the response phases. Real-world conditions imply resource constraints, stressful situations, and the need for prioritization.

Despite these limitations, the proposed model significantly advances existing information security incident management standards and models. The model includes incident prioritization, criticality assessment, and resource allocation, to enable more informed and timely decision-making under time and resource constraints.

Thus, the model can complement existing approaches by offering tools for more accurate analysis and effective incident management focused on mitigating incidents and improving the overall resilience of the enterprise to information security threats.

In further research, it is planned to conduct testing on real data, which will enable a more accurate assessment of the effectiveness of the developed model. In addition, further research may involve integrating incident management models with other information security management processes. It will also be crucial to assess the impact of the human factor on incidents and develop effective mechanisms for employee training.

Authors' contributions

E.S. Mityakov—conducted the majority of the research, including the development of the concept of the incident management model, the definition of the model's key elements, the analysis of existing approaches, and the formulation of practical recommendations.

E.A. Maksimova—contributed to the literature review, formalization of the model, and the definition of incident management stages.

S.V. Artemova—participated in the analysis of existing incident management models, collecting and systematizing information about the practice of applying models in various organizations.

A.A. Bakaev—supervised the research process, provided guidance on problem formulation and model development, and conducted an expert evaluation of the obtained results.

Zh.G. Vegera—conducted numerical calculations based on the model, contributed to the interpretation of the modeling results, and participated in preparing the article for publication.

REFERENCES

1. Żywiolek J., di Taranto A. Creating value added for an enterprise by managing information security incidents. *System Safety: Human – Technical Facility – Environment.* 2019;1(1):156–162. https://doi.org/10.2478/CZOTO-2019-0020
2. Zidan K., Alam A., Allison J., Al-sherbaz A. Assessing the challenges faced by Security Operations Centers (SOC). In: Arai K. (Ed.). *Advances in Information and Communication. FICC 2024. Lecture Notes in Networks and Systems*. Springer; 2024. V. 920. P. 256–271. https://doi.org/10.1007/978-3-031-53963-3_18
3. Sackey A. Information Security Incident Handling in the Cloud. In: *Book Chapter Series on Research Nexus in IT, Law, Cyber Security & Forensics*. 2022. P. 103–108. https://doi.org/10.22624/AIMS/CRP-BK3-P17
4. Demina A.K. Information security incident management. *Mezhdunarodnyi zhurnal gumanitarnykh i estestvennykh nauk = International Journal of Humanities and Natural Sciences*. 2024;5–1(92):227–231 (in Russ.). https://doi.org/10.24412/2500-1000-2024-5-1-227-231, available from URL: https://elibrary.ru/aizkwa
5. Khorev P.B., Karpeeva V.A. Software tools for analyzing information security incidents based on monitoring of information resources. In: *2022 6th International Conference on Information Technologies in Engineering Education* (*Inforino*). IEEE; 2022. https://doi.org/10.1109/Inforino53888.2022.9782979, available from URL: https://elibrary.ru/qjfmzi
6. Maksimova E.A. Cognitive modeling of destructive malicious impacts on critical information infrastructure objects. *Trudy uchebnykh zavedenii svyazi = Proceedings of Telecommunication Universities*. 2020;6(4):91–103 (in Russ). https://doi.org/10.31854/1813-324X-2020-6-4-91-103, available from URL: https://elibrary.ru/lirtxz
7. Kotenko I.V., Parashchuk I.B. Model of security information and event management system. *Vestnik Astrakhanskogo gosudarstvennogo tekhnicheskogo universiteta. Seriya: Upravlenie, vychislitel'naya tekhnika i informatika = Vestnik of Astrakhan State Technical University. Series: Management, Computer Science and Informatics*. 2020;2:84–94 (in Russ). https://doi.org/10.24143/2072-9502-2020-2-84-94, available from URL: https://elibrary.ru/owaldx
8. Kotenko I., Parashchuk I. An approach to modeling the decision support process of the security event and incident management based on Markov chains. *IFAC-PapersOnLine.* 2019;52(13):934–939. https://doi.org/10.1016/j.ifacol.2019.11.314, available from URL: https://elibrary.ru/eqccxc
9. Dohtieva I., Shyian A. Simulation of the work of the information security incident response team during cyberattacks. *Herald of Khmelnytskyi National University.* 2021;303(6):115–123.
10. Mikryukov A.A., Kuular A.V. Development of an incident management model in an enterprise information system based on a three-tier architecture using key (relevant) metrics. *Otkrytoe obrazovanie = Open Education*. 2020;24(3):78–86 (in Russ.). https://doi.org/10.21686/1818-4243-2020-3-78-86, available from URL: https://elibrary.ru/fcqjjr
11. Mouratidis H., Islam S., Santos-Olmo A., Sanchez L.E., Ismail U.M. Modelling language for cyber security incident handling for critical infrastructures. *Comput. Secur.* 2023;128(8):103139. https://doi.org/10.1016/j.cose.2023.103139

12. Renners L., Heine F., Kleiner C., Rodosek G. Design and evaluation of an approach for feedback-based adaptation of incident prioritization. In: *2019 2nd International Conference on Data Intelligence and Security* (*ICDIS*). IEEE: 2019. P. 28–35. https://doi.org/10.1109/ICDIS.2019.00012
13. Maksimova E., Sadovnikova N. Proactive modeling in the assessment of the structural functionality of the subject of critical information infrastructure. In: Kravets A.G., Shcherbakov M., Parygin D., Groumpos P.P. (Eds.). *Creativity in Intelligent Technologies and Data Science* (*CIT&DS 2021*). *Communications in Computer and Information Science*. Springer; 2021. V. 1448. P. 436–448. https://doi.org/10.1007/978-3-030-87034-8_31
14. Alin Z., Sharma R. Cybersecurity management for incident response. *Romanian Cyber Security Journal.* 2022;4(1):69–75. Available from URL: https://elibrary.ru/ihxntg

СПИСОК ЛИТЕРАТУРЫ

1. Żywiolek J., di Taranto A. Creating value added for an enterprise by managing information security incidents. *System Safety: Human – Technical Facility – Environment.* 2019;1(1):156–162. https://doi.org/10.2478/CZOTO-2019-0020
2. Zidan K., Alam A., Allison J., Al-sherbaz A. Assessing the challenges faced by Security Operations Centers (SOC). In: Arai K. (Ed.). *Advances in Information and Communication. FICC 2024. Lecture Notes in Networks and Systems*. Springer; 2024. V. 920. P. 256–271. https://doi.org/10.1007/978-3-031-53963-3_18
3. Sackey A. Information Security Incident Handling in the Cloud. In: *Book Chapter Series on Research Nexus in IT, Law, Cyber Security & Forensics*. 2022. P. 103–108. https://doi.org/10.22624/AIMS/CRP-BK3-P17
4. Дёмина А.К. Управление инцидентами информационной безопасности. *Международный журнал гуманитарных и естественных наук.* 2024;5–1(92):227–231. https://doi.org/10.24412/2500-1000-2024-5-1-227-231, URL: https://elibrary.ru/aizkwa
5. Khorev P.B., Karpeeva V.A. Software tools for analyzing information security incidents based on monitoring of information resources. In: *2022 6th International Conference on Information Technologies in Engineering Education* (*Inforino*). IEEE; 2022. https://doi.org/10.1109/Inforino53888.2022.9782979, URL: https://elibrary.ru/qjfmzi
6. Максимова Е.А. Когнитивное моделирование деструктивных злоумышленных воздействий на объектах критической информационной инфраструктуры. *Труды учебных заведений связи*. 2020;6(4):91–103. https://doi.org/10.31854/1813-324X-2020-6-4-91-103, URL: https://elibrary.ru/lirtxz
7. Котенко И.В., Паращук И.Б. Модель системы управления информацией и событиями безопасности. *Вестник Астраханского государственного технического университета. Серия: Управление, вычислительная техника и информатика*. 2020;2:84–94. https://doi.org/10.24143/2072-9502-2020-2-84-94, URL: https://elibrary.ru/owaldx
8. Kotenko I., Parashchuk I. An approach to modeling the decision support process of the security event and incident management based on Markov chains. *IFAC-PapersOnLine.* 2019;52(13):934–939. https://doi.org/10.1016/j.ifacol.2019.11.314, URL: https://elibrary.ru/eqccxc
9. Dohtieva I., Shyian A. Simulation of the work of the information security incident response team during cyberattacks. *Herald of Khmelnytskyi National University.* 2021;303(6):115–123.
10. Микрюков А.А., Куулар А.В. Разработка модели управления инцидентами в информационной системе предприятия на основе трехуровневой архитектуры с использованием ключевых (релевантных) метрик. *Открытое образование.* 2020;24(3):78–86. https://doi.org/10.21686/1818-4243-2020-3-78-86, URL: https://elibrary.ru/fcqjjr
11. Mouratidis H., Islam S., Santos-Olmo A., Sanchez L.E., Ismail U.M. Modelling language for cyber security incident handling for critical infrastructures. *Comput. Secur.* 2023;128(8):103139. https://doi.org/10.1016/j.cose.2023.103139
12. Renners L., Heine F., Kleiner C., Rodosek G. Design and evaluation of an approach for feedback-based adaptation of incident prioritization. In: *2019 2nd International Conference on Data Intelligence and Security* (*ICDIS*). IEEE: 2019. P. 28–35. https://doi.org/10.1109/ICDIS.2019.00012
13. Maksimova E., Sadovnikova N. Proactive modeling in the assessment of the structural functionality of the subject of critical information infrastructure. In: Kravets A.G., Shcherbakov M., Parygin D., Groumpos P.P. (Eds.). *Creativity in Intelligent Technologies and Data Science* (*CIT&DS 2021*). *Communications in Computer and Information Science*. Springer; 2021. V. 1448. P. 436–448. https://doi.org/10.1007/978-3-030-87034-8_31
14. Alin Z., Sharma R. Cybersecurity management for incident response. *Romanian Cyber Security Journal.* 2022;4(1):69–75. URL: https://elibrary.ru/ihxntg

About the authors

Evgeny S. Mityakov, Dr. Sci. (Econ.), Professor, Acting Head of the "Subject-Oriented Information Systems" Department, Institute of Cybersecurity and Digital Technologies, MIREA – Russian Technological University (78, Vernadskogo pr., Moscow, 119454 Russia). E-mail: mityakov@mirea.ru. Scopus Author ID 55960540500, RSCI SPIN-code 5691-8947, https://orcid.org/0000-0001-6579-0988

Elena A. Maksimova, Dr. Sci. (Eng.), Associate Professor, Head of the "Intelligent Information Security Systems" Department, Institute of Cybersecurity and Digital Technologies, MIREA – Russian Technological University (78, Vernadskogo pr., Moscow, 119454 Russia). E-mail: maksimova@mirea.ru. Scopus Author ID 57219701980, RSCI SPIN-code 6876-5558, https://orcid.org/0000-0001-8788-4256

Svetlana V. Artemova, Dr. Sci. (Eng.), Associate Professor, Head of the "Information Protection" Department, Institute of Cybersecurity and Digital Technologies, MIREA – Russian Technological University (78, Vernadskogo pr., Moscow, 119454 Russia). E-mail: artemova_s@mirea.ru. Scopus Author ID 6508256085, RSCI SPIN-code 3775-6241, https://orcid.org/0009-0006-8374-8197

Anatoly A. Bakaev, Dr. Sci. (Hist.), Cand. Sci. (Juri.), Associate Professor, Director of the Institute of Cybersecurity and Digital Technologies, MIREA – Russian Technological University (78, Vernadskogo pr., Moscow, 119454 Russia). E-mail: bakaev@mirea.ru. Scopus Author ID 57297341000, RSCI SPIN-code 5283-9148, https://orcid.org/0000-0002-9526-0117

Zhanna G. Vegera, Cand. Sci. (Phys.-Math.), Associate Professor, Head of the Department of Higher Mathematics, Institute of Cybersecurity and Digital Technologies, MIREA – Russian Technological University (78, Vernadskogo pr., Moscow, 119454 Russia). E-mail: vegera@mirea.ru. Scopus Author ID 57212931836, RSCI SPIN-code 9076-5678, https://orcid.org/0000-0001-7312-3341

Об авторах

Митяков Евгений Сергеевич, д.э.н., профессор, и.о. заведующего кафедрой КБ-9 «Предметно-ориентированные информационные системы», Институт кибербезопасности и цифровых технологий, ФГБОУ ВО «МИРЭА – Российский технологический университет» (119454, Россия, Москва, пр-т Вернадского, д. 78). E-mail: mityakov@mirea.ru. Scopus Author ID 55960540500, SPIN-код РИНЦ 5691-8947, https://orcid.org/0000-0001-6579-0988

Максимова Елена Александровна, д.т.н., доцент, заведующий кафедрой КБ-4 «Интеллектуальные системы информационной безопасности», Институт кибербезопасности и цифровых технологий, ФГБОУ ВО «МИРЭА – Российский технологический университет» (119454, Россия, Москва, пр-т Вернадского, д. 78). E-mail: maksimova@mirea.ru. Scopus Author ID 57219701980, SPIN-код РИНЦ 6876-5558, https://orcid.org/0000-0001-8788-4256

Артемова Светлана Валерьевна, д.т.н., доцент, заведующий кафедрой КБ-1 «Защита информации», Институт кибербезопасности и цифровых технологий, ФГБОУ ВО «МИРЭА – Российский технологический университет» (119454, Россия, Москва, пр-т Вернадского, д. 78). E-mail: artemova_s@mirea.ru. Scopus Author ID 6508256085, SPIN-код РИНЦ 3775-6241, https://orcid.org/0009-0006-8374-8197

Бакаев Анатолий Александрович, д.и.н., к.ю.н., доцент, директор Института кибербезопасности и цифровых технологий, ФГБОУ ВО «МИРЭА – Российский технологический университет» (119454, Россия, Москва, пр-т Вернадского, д. 78). E-mail: bakaev@mirea.ru. Scopus Author ID 57297341000, SPIN-код РИНЦ 5283-9148, https://orcid.org/0000-0002-9526-0117

Вегера Жанна Геннадьевна, к.ф.-м.н., доцент, заведующий кафедрой высшей математики, Институт кибербезопасности и цифровых технологий, ФГБОУ ВО «МИРЭА – Российский технологический университет» (119454, Россия, Москва, пр-т Вернадского, д. 78). E-mail: vegera@mirea.ru. Scopus Author ID 57212931836, SPIN-код РИНЦ 9076-5678, https://orcid.org/0000-0001-7312-3341

Translated from Russian into English by Lyudmila O. Bychkova
Edited for English language and spelling by Thomas A. Beavitt

Modern radio engineering and telecommunication systems

Современные радиотехнические и телекоммуникационные системы

UDC 004.932.4
https://doi.org/10.32362/2500-316X-2024-12-6-48-58
EDN NZQPFH

RESEARCH ARTICLE

Digital three-stage recursive-separable image processing filter with variable sizes of scanning multielement aperture

Andrey V. Kamenskiy,
Tatyana M. Akaeva [@],
Darya A. Grebenshchikova

Tomsk State University of Control Systems and Radioelectronics, Tomsk, 634050 Russia
[@] Corresponding author, e-mail: ttnakaeva@gmail.com

Abstract

Objectives. The main aim of digital image processing is to increase clarity while maintaining image quality and eliminate noise. However, the amount of information contained in digital image files is growing year after year. This circumstance negatively affects processing time, critical for systems with high load requirements on the computing platform. In this regard, the use of digital filters which enable a reduction to the processing time of incoming data is important. In order to resolve this issue, adaptive filters with different sizes of multielement processing aperture are being developed to improve image clarity and preserve image details. Filters with adaptive properties are able to change their parameters during data processing, and provide maximum performance as the aperture size increases. The aim of the work is to develop a type of recursively separable digital filter with variable sizes of a scanning multielement aperture which allows the number of computational operations to be reduced while maintaining the efficiency of filtering input data (images).

Methods. The work used recursive-separable methods and algorithms to construct digital filters.

Results. An algorithm for the recursive-separable implementation of a digital filter is described, and the final view of the processing aperture and its three-dimensional appearance are presented. In order to evaluate the performance of the filter, a comparison of the developed algorithm with the classical two-dimensional convolution algorithm was carried out. The experiment was performed using images of various sizes and consisted of determining the time spent on the process of processing the test image. The study established that the processing time of a test image using the developed filter is on average 5 times less than the time taken by the classical two-dimensional convolution algorithm. The optimal coefficients for magnifying the central element and raising the positive part of the aperture of a digital filter were determined, enabling the efficiency of its use to be enabled.

Conclusions. The studies show the effectiveness of using the developed recursive-separable two-dimensional filter to improve image clarity and reduce the time spent on processing.

Keywords: digital image processing, digital filters, recursion, separability, increased image clarity, speed

• **Submitted:** 29.09.2023 • **Revised:** 22.04.2024 • **Accepted:** 20.09.2024

For citation: Kamenskiy A.V., Akaeva T.M., Grebenshchikova D.A. Digital three-stage recursive-separable image processing filter with variable sizes of scanning multielement aperture. *Russ. Technol. J*. 2024;12(6):48–58. https://doi.org/10.32362/2500-316X-2024-12-6-48-58

Financial disclosure: The authors have no financial or proprietary interest in any material or method mentioned.

The authors declare no conflicts of interest.

НАУЧНАЯ СТАТЬЯ

Цифровой трехкаскадный рекурсивно-сепарабельный фильтр обработки изображений с изменяемыми размерами сканирующей многоэлементной апертуры

А.В. Каменский,
Т.М. Акаева [@],
Д.А. Гребенщикова

Томский государственный университет систем управления и радиоэлектроники, Томск, 634050 Россия
[@] Автор для переписки, e-mail: ttnakaeva@gmail.com

Резюме

Цели. Основными целями цифровой обработки изображений являются повышение их четкости при сохранении качества изображения и устранение шумов. Однако объемы информации, содержащейся в файлах цифровых изображений, растут из года в год. Это обстоятельство негативно сказывается на времени их обработки, что критично для систем с высокими требованиями к нагрузке на вычислительную платформу. В связи с этим актуальным становится применение цифровых фильтров, позволяющих сократить время обработки поступающих данных. Для решения этой задачи разрабатываются адаптивные фильтры с различными размерами многоэлементной апертуры обработки, которые позволяют повысить четкость и сохранить детали изображения. Фильтры с адаптивными свойствами способны изменять свои параметры в процессе обработки данных, обеспечивая максимальное быстродействие при увеличении размеров апертуры. Целью работы является разработка рекурсивно-сепарабельного цифрового фильтра с изменяемыми размерами сканирующей многоэлементной апертуры, позволяющего сократить количество вычислительных операций при сохранении эффективности фильтрации входных данных (изображений).

Методы. В работе использовались рекурсивно-сепарабельные методы и алгоритмы построения цифровых фильтров.

Результаты. Описан алгоритм рекурсивно-сепарабельной реализации цифрового фильтра, а также представлен итоговый вид апертуры обработки и ее трехмерный вид. Для оценки быстродействия фильтра проведено сравнение разработанного алгоритма с алгоритмом классической двумерной свертки. Эксперимент проводился с использованием изображений различных размеров и заключался в определении времени, затраченного на процесс обработки тестового изображения. Установлено, что время обработки тестового изображения с применением разработанного фильтра в среднем в 5 раз меньше, чем время, затрачиваемое алгоритмом классической двумерной свертки. Определены оптимальные коэффициенты увеличения центрального элемента и поднятия положительной части апертуры цифрового фильтра, позволяющие повысить эффективность его применения.

Выводы. Проведенные исследования показывают эффективность использования разработанного рекурсивно-сепарабельного двумерного фильтра для повышения четкости изображений и уменьшения затрачиваемого на обработку времени.

Ключевые слова: цифровая обработка изображений, цифровые фильтры, рекурсия, сепарабельность, повышение четкости изображений, быстродействие

• **Поступила:** 29.09.2023 • **Доработана:** 22.04.2024 • **Принята к опубликованию:** 20.09.2024

Для цитирования: Каменский А.В., Акаева Т.М., Гребенщикова Д.А. Цифровой трехкаскадный рекурсивно-сепарабельный фильтр обработки изображений с изменяемыми размерами сканирующей многоэлементной апертуры. *Russ. Technol. J*. 2024;12(6):48–58. https://doi.org/10.32362/2500-316X-2024-12-6-48-58

Прозрачность финансовой деятельности: Авторы не имеют финансовой заинтересованности в представленных материалах или методах.

Авторы заявляют об отсутствии конфликта интересов.

INTRODUCTION

The first preliminary step in image analysis is, as a rule, digital image processing. The quality of this stage can dramatically affect the results of subsequent analyses. Digital processing, including digital filtering, is used to resolve such problems as resolution enhancement, restoration of 'spoiled' objects in the image, clarity enhancement, and colourisation [1].

The main purpose of image filtering is to improve the clarity and quality of images and to remove noise. However, the amount of information contained in digital image files is growing from year to year [2]. This adversely affects the ability of digital filters to perform fast and high-quality processing of incoming data. One of the ways to resolve this problem is to increase the speed of digital filters by reducing the number of computational operations required for processing. It is also important to ensure the variability of their use and the possibility of parameter correction during operation. An effective solution is to develop adaptive filters which can change their parameters during image processing, in order to maintain performance while increasing the aperture size. In adaptive filters, the processing speed always remains constant for specific image sizes, regardless of the processing aperture size.

FILTERS WITH ADAPTIVE PROPERTIES

Adaptive filters are a class of filters in which the parameters are adjusted during operation according to the characteristics of the input data [3]. For each fixed set of parameters, an adaptive filter is a linear device, since there is a linear dependence between its input and output signals [4, 5].

Adaptive filters are of two types [6, 7]:

- transversal, i.e., filter with finite impulse response;
- recursive, i.e., filter with infinite impulse response.

Adaptive filters are widely used in various fields such as signal processing, computer vision, image processing, among others. In the latter two cases, their main purpose is to clean photo and video information from noise overlapping in spectrum with the useful signal, or when the noise bandwidth is undefined and cannot be specified initially [8]. The use of adaptive filters can significantly improve the efficiency and quality of data processing in various applications where automatic adjustment to changing conditions or requirements is necessary [4, 9].

CONSTITUENT ELEMENTS

Constituent recursive cells (recirculators) are used in the design of recursive filters. Recirculators are recursive cells which perform row-by-row (line recirculator, LR) and frame-by-frame (frame recirculator, FR) processing of the input image matrix [10]. Their functionality is to perform a two-dimensional discrete convolution procedure in which the input data is processed according to a given impulse response of the recirculator. The impulse response can be represented as a unit matrix (row or column of size $N \times 1$ elements). Figure 1 shows the forming recursive cells by n_1-row (LR) (a) and by n_2-frame (FR) (b), implementing the corresponding

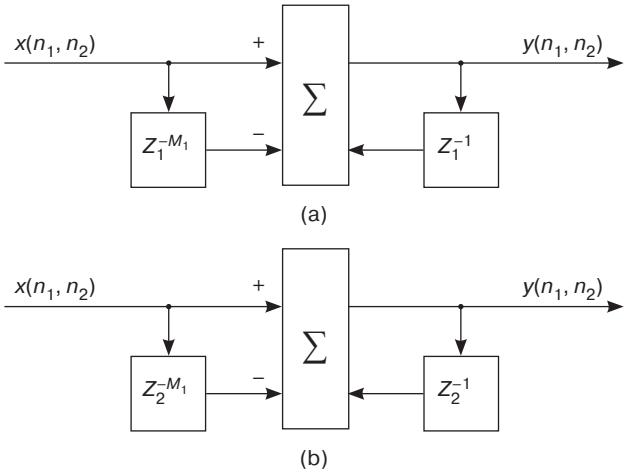

Fig. 1. Recirculator diagrams: (a) by n_1-row, (b) by n_2-frame

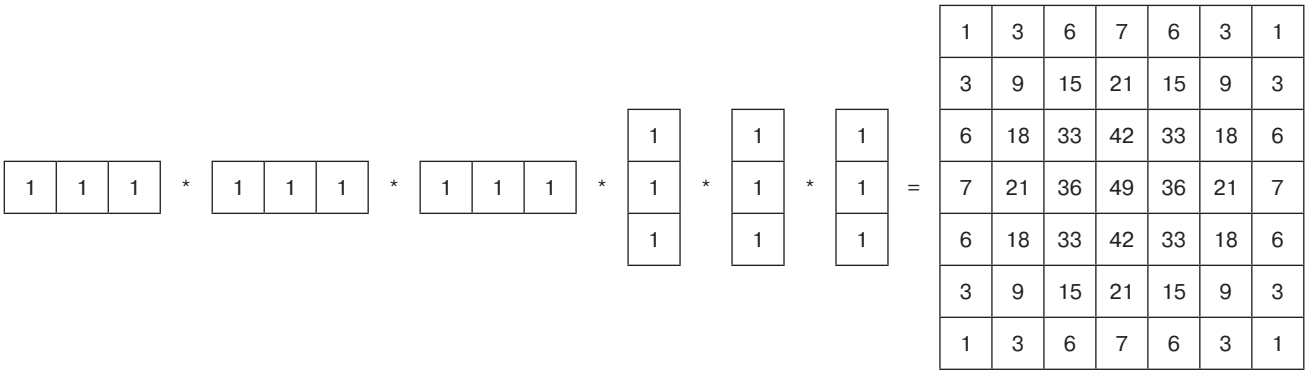

Fig. 2. Recursive-separable filter implementation algorithm

orthogonal directions of moving average processing. LR recirculator performs processing by the row of the input data matrix, and FR—by the column of this matrix; $x(n_1, n_2)$ is input data; $y(n_1, n_2)$ is output data; Z are delay elements; M_1 is the coefficient determining the delay value on the row (integer); M_2 is the coefficient determining the delay value on the column (integer) [11, 12].

INITIAL FILTER

Development of a two-dimensional filter is based on a sequence of certain processes. As an example, let us consider the process of forming a processing aperture of 7 × 7 elements of a two-dimensional three-cascade recursive-separable filter (TRSF).

The information sequence in the form of a unit matrix of 1 × 1 element is fed to the filter input. This action allows the TRSF mask to be formed which will further enable a correct comparison of the developed algorithm with the classical two-dimensional convolution (CTDC) algorithm. In order to form the main size of the processing aperture, the specified sequence passes through three row (a row of units of size 3 × 1 elements) and three frame (a column of units of size 1 × 3 elements) recirculators. This results in a matrix of 7 × 7 elements which is the basis for forming the final mask and undergoes further modifications. Figure 2 shows the algorithm of the recursive-separable filter implementation.

As a result of the operations taking place in the filter after the input of the test information sequence in the form of a unit matrix, a TRSF mask is formed. This is presented in Fig. 3 and a three-dimensional view is shown in Fig. 4 [13].

Figure 3 shows that the TRSF mask has a positive area in the center with the size of 3 × 3 elements. Its proportional increase resulting in the change of the initial sum of coefficients of the final mask will increase the efficiency of digital image processing. The same principle is used for processing by changing the center element of the matrix (for a mask of 7 × 7 elements it is the 4th element in the 4th row).

–1	–3	–6	–7	–6	–3	–1
–3	–9	–18	–21	–18	–9	–3
–6	–18	14	58	14	–18	–6
–7	–21	58	80	58	–21	–7
–6	–18	14	58	14	–18	–6
–3	–9	–18	–21	–18	–9	–3
–1	–3	–6	–7	–6	–3	–1

Fig. 3. TRSF 7 × 7 elements mask view

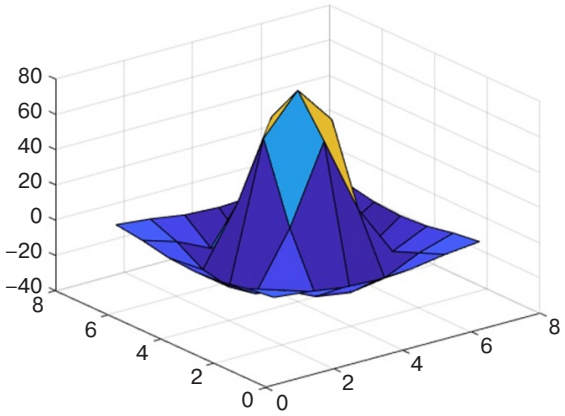

Fig. 4. Three-dimensional view of TRSF mask

The structural diagram of the TRSF with dimensionality of 7 × 7 elements is shown in Fig. 5. Here A_1 is the coefficient of increase in the values of the positive part of the mask, and A_2 is the coefficient of increase in the value of the center element of the mask. In the first branch of the TRSF, the formation of a mask of dimension 3 × 3 elements takes place. This is necessary, in order to compensate the negative part and form the positive center of the final mask due to the delay elements Z. The second branch of the filter forms the basic matrix of 7 × 7 elements. The third branch of the TRSF is necessary, in order to compensate the negative part of the mask by adding the residual to the center element of the main matrix, and to enable its

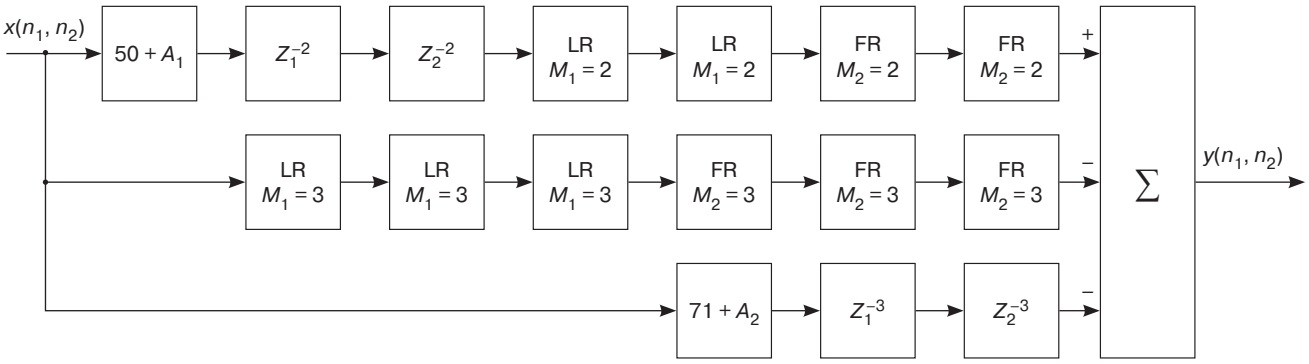

Fig. 5. Structural diagram of TRSF

adjustment by the user. The output data of the branches are aggregated, in order to form the filter output. For the second and third branches the aggregation is performed with sign inversion.

DESCRIPTION OF THE TRSF FILTER MODIFICATION PRINCIPLES

For the proper functioning of the adaptive TRSF, it is necessary to ensure its correct response to the user-defined value of the processing aperture dimensions. In this case, the operation takes place exclusively with odd values of dimensions (9 × 9, 11 × 11, 13 × 13, etc.). It is important to take into account the change of the coefficients of the center mask recirculators to the changes of the main filter mask recirculators in the ratio 1 : 2. Thus when the final size of the filter's main aperture changes, the size of its center mask also changes, albeit only every second increase in the size of the main mask. One recirculator always remains unchanged because the filter uses an odd number of recirculators. The size of the impulse response value matrix should be 3 × 1 or 1 × 3 elements. In this case, for a given dimensionality of 9 × 9, the coefficients of the line and frame recirculators will be equal to 4 (unit matrix of 4 × 1 elements) and 4 (unit matrix of 1 × 4 elements), respectively. For a dimensionality of 11 × 11, they will be equal to 5 (unit matrix of 5 × 1 elements) and 5 (unit matrix of 1 × 5 elements).

It is important to note that in the center part of the filter a smaller mask is generated when compared to the main one. This central part is necessary, in order to balance the sum of the outer and central parts of the final mask, to bring its sum to zero and to preserve normal brightness of the processed image. A similar balance of the outer and central parts of the final mask can be observed in the Laplacian filter for 'eight neighbors', where the sum of all coefficients is equal to zero [14]. When increasing the size of the mask, the normal ratio between the sizes of the outer and central regions must be maintained, in order to change its three-dimensional appearance proportionally. This is done by varying the size of the center mask in steps of 2. For example, a 3 × 3 center mask will be used for the 7 × 7 and 9 × 9 element matrices, followed by an increase of 2 elements to a 5 × 5 element matrix, which will be used for the final 11 × 11 and 13 × 13 element matrices. This is accomplished by automated calculation of the recirculator coefficients at the bottom of the filter by entering the size of the desired filter aperture. Thus, every other possible value of the mask size, starting at 3 × 3, will affect the change in the size of the inner mask. For example, at dimension 7 × 7, the upper left corner of the mask is at position $x(n_1 - 1, n_2 - 2)$. Then, at the next possible value of the mask dimension (starting at 5 × 5), the shift factor of the inner mask will change to 1. Thus, at 5 × 5, the shift will be 2 (instead of 1). This is because the size of the inner mask will also decrease by 1 cell and become 1 × 1. This process will continue, and when the dimension of the main mask is 9 × 9 and the inner mask is 3 × 3, the shift will be 3.

The dependence thus described can be programmatically expressed as a function using the parameters of matrix aperture sizes. The shift coefficient of the inner mask will be equal to the difference between the size of the main mask and the size of the center mask divided by two. For example, for a size of 17 × 17, we get: (17 − 7)/2 = 5. Consequently, the matrix is shifted by 5 elements.

This process works correctly for masks of any size. First, the total number of cells in the mask is calculated. For example, in the case of a 9 × 9 mask it is 81, and for a 7 × 7 mask it is 49. Then all elements of the mask are aggregated up, and this sum is divided by the previously calculated sum of elements of the positive center of the final mask. The result is used to create a new mask in the upper part of the filter. The initial mask is subtracted from it, and as a result, the final values are formed in the cells. Aggregating them makes the whole mask (its values) equal to 0.

Modified filter should be configurable using two input coefficients. One of these coefficients will be

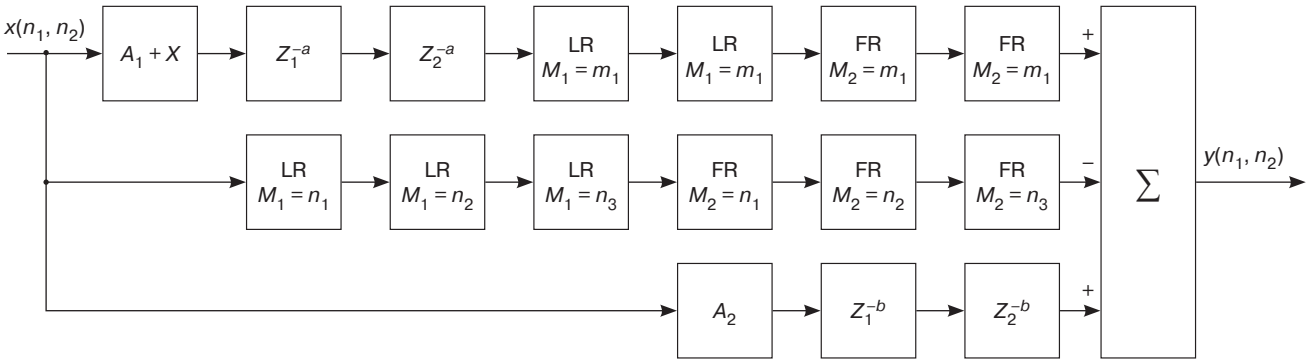

Fig. 6. Structural diagram of TRSF

Table 1. Dependence of filter parameters on the change of mask size

Set size	LR and FR coefficient	Inner mask size	LR and FR for the inner mask	Shift coefficient of the inner mask
5 × 5	2 and 2	1 × 1	1 and 1	3
7 × 7	3 and 3	3 × 3	3 and 3	3
9 × 9	4 and 4	3 × 3	3 and 3	4
11 × 11	5 and 5	5 × 5	5 and 5	4
13 × 13	6 and 6	5 × 5	5 and 5	5
15 × 15	7 and 7	7 × 7	7 and 7	5
17 × 17	8 and 8	7 × 7	7 and 7	6

used to increase the values of the center part of the mask by a specified amount. The second coefficient will be used to increase the value of the center element of the mask.

The patterns used to create the filter are illustrated in Table 1 which shows: the values of the recirculator coefficients; the size of the center mask; the number of recirculators for convolution; and the shift values of the center mask for different mask sizes from 5 × 5 to 17 × 17.

On the basis of the modification principles described above, a structural scheme of the filter, presented in Fig. 6, can be built: X is the coefficient of equalization of the sums of the central and external masks; A_1 is the coefficient of increase of the values of the positive part of the mask; A_2 is the coefficient of increase of the value of the central element of the mask; Z_1 and Z_2 are the mask shift coefficients (dependent on the variables $-a$ and $-b$, calculated automatically in the filter code); m are the row and frame recirculators coefficients for the positive branch; n are the row and frame recirculators coefficients for the negative branch.

STUDY OF THE DEVELOPED FILTER PERFORMANCE SPEED WHEN INCREASING THE SIZE OF THE PROCESSING APERTURE

Three images of different dimensionality were used for experimental studies: 640 × 480 elements of *tiff* format; 1280 × 720 elements of *bmp* format; and 3000 × 2000 elements of *jpeg* format. In the study, 7 × 7, 9 × 9 and 11 × 11 masks were used for each filter. Image processing was performed on a personal computer with the following characteristics: operating system—Windows 10; processor—12th Gen Intel(R) Core(TM) i5-12400F 2.50 GHz; RAM—32 GB. The measurement of the filter runtime was performed 10 times in each experiment and the average value was calculated.

The results of the experimental study determined the dependencies of processing speed on aperture size for each of the three images. The average values of processing time for CTDC and TRSF and their compiled MEX-functions[1] were estimated using the time

[1] Minimum EXcluded, algorithm for finding the minimum missing number.

Table 2. Average values of image processing time

Image 640 × 480, *tiff* format				
Filter mask size	Processing time, s			
	MATLAB		MEX	
	CTDC	TRSF	CTDC	TRSF
7 × 7	0.6318	0.0995	0.1187	0.0891
9 × 9	4.2060	0.0969	3.1092	0.0951
11 × 11	5.2562	0.0979	4.1090	0.0884
Image 1280 × 720, *bmp* format				
Filter mask size	Processing time, s			
	MATLAB		MEX	
	CTDC	TRSF	CTDC	TRSF
7 × 7	1.8361	0.3211	0.3622	0.2915
9 × 9	16.4342	0.3256	15.0594	0.2572
11 × 11	24.5264	0.3413	17.3964	0.2912
Image 3000 × 2000, *jpeg* format				
Filter mask size	Processing time, s			
	MATLAB		MEX	
	CTDC	TRSF	CTDC	TRSF
7 × 7	12.3788	2.4025	2.4289	2.1971
9 × 9	30.3757	2.3876	12.3612	2.1965
11 × 11	45.5701	2.2715	19.3326	2.1916

measurement procedure from *MATLAB*[2] software. The results of measuring the processing speed for the three images are presented in Table 2.

Figure 7 shows the graphs of processing time dependence on the filter aperture size for an image of 640 × 480 elements.

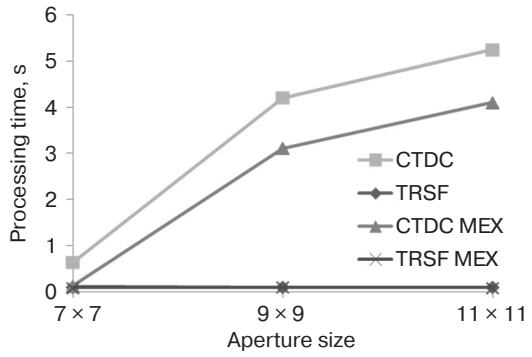

Fig. 7. Graph of performance dependence on the aperture size for 640 × 480 image (*tiff*)

Figure 8 shows the graphs of processing time dependence on the filter aperture size for a 1280 × 720 element image.

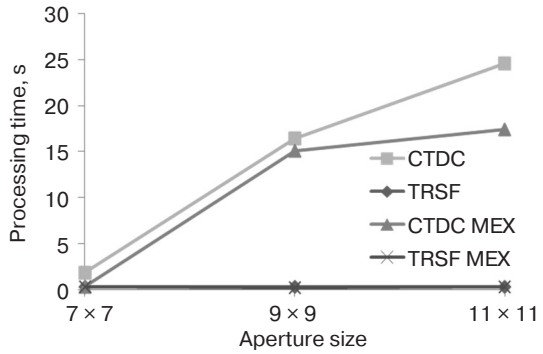

Fig. 8. Graph of performance speed dependence on the aperture size for 1280 × 720 image (*bmp*)

Figure 9 shows the graphs of processing time dependence on the filter aperture size for a 3000 × 2000 element image.

[2] https://www.mathworks.com/products/matlab.html. Accessed September 20, 2023.

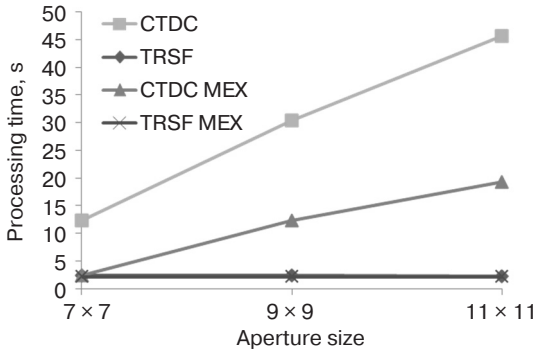

Fig. 9. Graph of performance speed dependence on the aperture size for 3000 × 2000 image (*jpeg*)

From the graphs presented above we can see the gain in performance of the developed filter when the processing aperture grows in comparison with the CTDC algorithm.

The next step is to evaluate the effect of TRSF aperture growth on its operating time. Values of aperture mask size from 7 to 25 in steps of 2, as well as 49, 75, and 99 were used. The values of coefficients in all calculations were the same and equal to: $A_1 = 10$, $A_2 = 0$. The results of measurements are summarized in Table 3.

Table 3. Time consumption for image filtering

Mask size	Processing time, s
7	2.46
9	2.39
11	2.24
13	2.27
15	2.33
17	2.29
19	2.31
21	2.32
23	2.31
25	2.33
49	2.56
75	2.62
99	2.49

It can be concluded that changing the filter aperture leads to insignificant changes in the speed of the TRSF algorithm in the range of 2.24 to 2.62 s.

ESTIMATION OF CHANGES IN THE NUMBER OF TV LINES IN THE PROCESSED IMAGES

When developing new algorithms for digital image processing, it is important not only to improve their performance, but also not to lose useful information stored in the images themselves, as well as to improve their quality (increase clarity, remove noise, etc.) to an ideal level.

The study was conducted by measuring the number of television lines (TVL) in the processed images while varying the coefficients A_1 and A_2. This is necessary, in order to test the filter's ability to keep fine details of images clear [15]. Formula [12] was used to convert the number of 'cycles per pixel' (modulation transfer function, MTF50) obtained when measuring resolution in *Imatest*[3] software into TVL:

$$\text{TVL} = \left(\frac{\text{CPP}}{0.5} \right) \times \text{limit resolution},$$

where CPP is the number of 'cycles per pixel', limit resolution (in TVL) is the value of the number of pixels in the width of the image.

The frame obtained by the active-pulse television measuring system[4] (Fig. 10) was taken as a test image [16, 17].

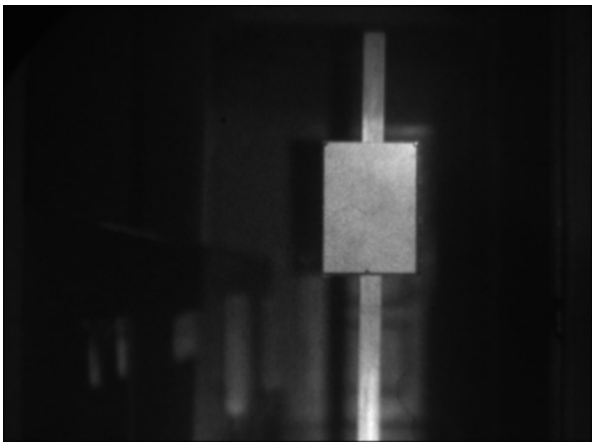

Fig. 10. Test image

This measurement was performed in order to determine the optimal values of the A_1 and A_2 coefficients, and to determine the fact of the best processing when changing either A_1, or A_2, since changing them independently of each other led to different results. Firstly, the A_1 coefficient was varied from 1 to 50, then

[3] https://www.imatest.com/. Accessed September 20, 2023.

[4] Kapustin V.V. *Active-impulse television measurement systems with increased immunity to optical interference*: Cand. Sci. (Eng.). Tomsk: 2017. 118 p. (in Russ.).

the A_2 coefficient was varied in the same range. The TVL value for the original image is 158. Figure 11 shows the dependence of TVL values on the A_1 coefficient.

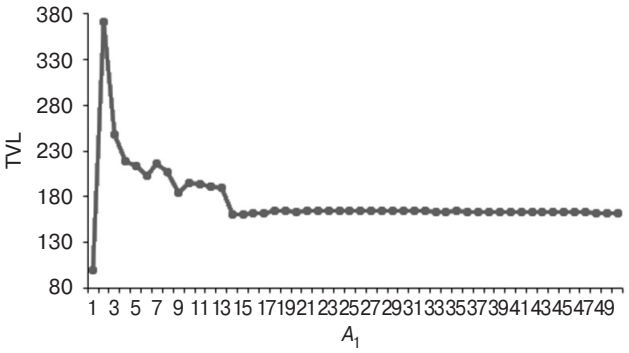

Fig. 11. Dependence of TVL values on the magnification factor of the positive part of the mask A_1

As can be seen from the results obtained, increasing the A_1 coefficient from 15 and more does not affect the final number of TVL. Image resolution before and after processing is practically unchanged, i.e., filtering loses its efficiency.

Figure 12 shows an example of processing the original image by a filter with the optimal value of the coefficient $A_1 = 1$.

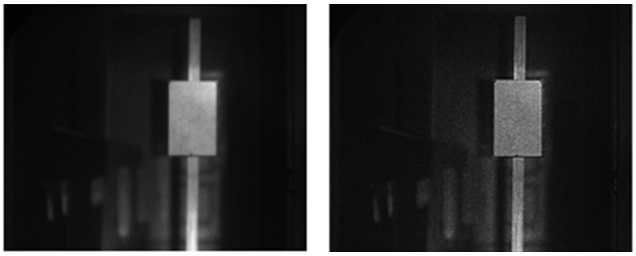

(a) (b)

Fig. 12. Images before (a) and after (b) processing with the filter with optimal coefficient A_1

Results of measurements of TVL quantity at change of A_2 coefficient are shown in Fig. 13.

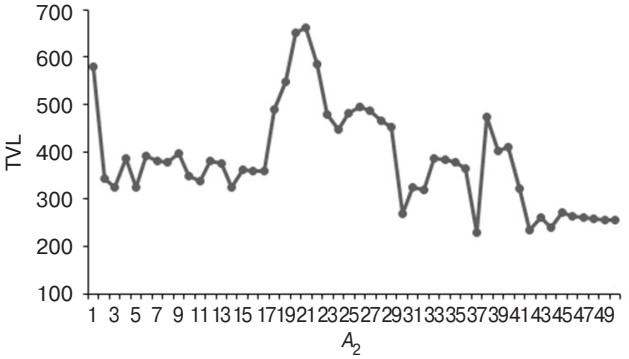

Fig. 13. Dependence of TVL values on the change of the magnification factor of the central element of the mask A_2

Figure 14 shows an example of processing the original image by a filter with the optimal value of the coefficient $A_2 = 21$.

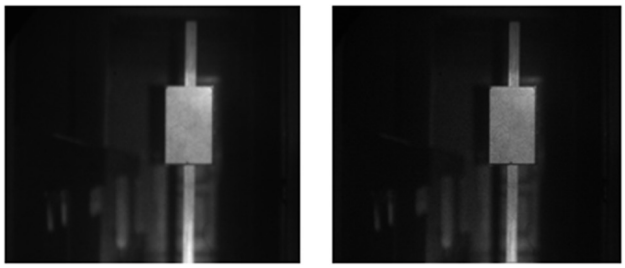

(a) (b)

Fig. 14. Images before (a) and after (b) processing with the filter with optimal A_2 coefficient

Based on the above graphs and images, it can be concluded that changing the A_2 coefficient gives good results over the whole range of values.

CONCLUSIONS

The paper presents a modified TRSF for image clarity enhancement. The principles of its modification are described and the structural scheme is given. A study of the speed and efficiency of image processing provided by the proposed modification of the filter is performed. The time spent on image processing is 5.3 times less on average than the time spent on processing for the CTDC.

The results of evaluating the influence of the coefficient of increasing the value of the positive central aperture and increasing the value of the central element of the filter mask on the characteristics of processed images are presented herein. This study established that the value of the central element of the mask has a stronger influence on the parameters of the processed image. Its change allows the image quality to be enhanced more significantly than when increasing the positive central aperture of the filter. The study also established the optimal values of filtering coefficients A_1 and A_2.

ACKNOLEDGMENTS

The study was carried out at the Tomsk State University of Control Systems and Radioelectronics under the Russian Science Foundation grant No. 21-79-10200.

Authors' contributions

A.V. Kamenskiy—setting the aim and objectives of the research, processing methods, scientific editing of the article.

T.M. Akaeva—planning the research, writing the text of the article, interpreting and summarizing the results.

D.A. Grebenshchikova—conducting research, writing the text of the article.

REFERENCES

1. Groshev I.V., Korol'kov V.I. *Sistemy tekhnicheskogo zreniya i obrabotki izobrazhenii* (*Technical Vision and Image Processing Systems*). Moscow: RUDN; 2008. 212 p. (in Russ.).
2. Abramov I.A., Kravchenko E.N. Multithreaded realization of the algorithm of local image filtering. *Vestnik Penzenskogo gosudarstvennogo universiteta = Vestnik of Penza State University.* 2016;3(15):66–71 (in Russ.).
3. Turulin I.I. *Osnovy teorii rekursivnykh KIKh-fil'trov* (*Recursive FIR Filters Theory Base*). Taganrog: Southern Federal University; 2016. 264 p. (in Russ.).
4. Ifeachor E.C., Jervis B.W. *Tsifrovaya obrabotka signalov. Prakticheskii podkhod* (*Digital Signal Processing: A Practical Approach*): transl. from Engl. Moscow: Williams; 2004. 992 p. (in Russ.).
[Ifeachor E.C., Jervis B.W. *Digital Signal Processing: A Practical Approach.* Prentice Hall; 2001. 933 p.]
5. Gol'denberg L.M., Matyushkin B.D., Polyak M.N. *Tsifrovaya obrabotka signalov* (*Digital Signal Processing*). Moscow: Radio i cvyaz'; 1990. 256 p. (in Russ.).
6. Kuryachii M.I., Gel'tser A.A., Abenov R.R., et al. *Tsifrovaya obrabotka signalov* (*Digital Signal Processing*). Tomsk: Tomsk State Univ. of Control Systems and Radioelectronics; 2018. 234 p. (in Russ.).
7. Lukin A. *Vvedenie v tsifrovuyu obrabotku signalov* (*Introduction to Digital Signal Processing*). Moscow: MSU, Laboratory of Computer Graphics and Multimedia; 2002. 44 p. (in Russ.).
8. Matveev Yu.N., Simonchik K.K., Tropchenko A.Yu., et al. *Tsifrovaya obrabotka signalov* (*Digital Signal Processing*). St. Petersburg: ITMO; 2013. 166 p. (in Russ.).
9. Bondina N.N., Murarov R.Yu. Adaptive algorithms of filtration and contrast changes of image. *Vestnik Natsional'nogo tekhnicheskogo universiteta "Khar'kovskii politekhnicheskii institute". Seriya: Informatika i modelirovanie = Bulletin of the National Technical University Kharkov Polytechnic Institute. Series: Informatics and Modeling*. 2014;35(1078):35–42 (in Russ.).
10. Kamenskiy A.V., Rylov K.A., Borodina N. Digital anti-aliasing trapezoidal recursively separable image processing filter with resizable scanning multielement aperture. *Omskii nauchnyi vestnik = Omsk Scientific Bulletin.* 2024;1(189):127–136 (in Russ.). https://doi.org/10.25206/1813-8225-2024-189-127-136
11. Say S.V., Kamenskiy A.V., Kuryachiy M.I. *Sovremennye metody analiza i povyshenie kachestva tsifrovykh izobrazhenii* (*Modern Methods of Analyzing and Improving the Quality of Digital Images:* monograph). Khabarovsk: Pacific National University; 2020. 173 p. (in Russ.).
12. Kamenskiy A.V. High-speed recursive-separable image processing filters. *Computer Optics.* 2022;46(4):659–665. http://doi.org/10.18287/2412-6179-CO-1063
13. Akaeva T.M., Kamenskiy A.V., Strumilova M.A. Recursive-separable filter image enhancement. *Voprosy radioelektroniki. Seriya: Tekhnika televideniya = Questions of Radio Electronics. Series: TV Technique*. 2023;1:138–145 (in Russ.).
14. Gonzalez R., Woods R. *Tsifrovaya obrabotka izobrazhenii* (*Digital Image Processing*): transl. from Engl. Moscow: Tekhnosfera; 2019. 1104 p. (in Russ.).
[Gonzalez R., Woods R. *Digital Image Processing.* Pearson/Prentice Hall; 2008. 954 p.]
15. Malanin M.Yu., Kamenskiy A.V., Kuryachiy M.I. Measurement of resolution and clarity of television images. In: *Optoelectronic Devices and Devices in Systems of Pattern Recognition, Image and Symbolic Information Processing*: Collection of materials of the 12th International Scientific and Technical Conference. Kursk; 2015. P. 235–237 (in Russ.).
16. Movchan A.K., Kapustin V.V., Kuryachiy M.I. Methods and means of tomographic vision of space by active-pulse television measuring systems. *Proceedings of the International Conference on Computer Graphics and Vision "Graficon".* 2018;28:222–225. http://www.graphicon.ru/html/2018/papers/proceedings.pdf
17. Zaytseva E.V. Integral and spectral sensitivity assessment of the active-pulse television systems. In: *2016 Dynamics of Systems, Mechanisms and Machines* (*Dynamics*). 2016:7819115. https://doi.org/10.1109/Dynamics.2016.7819115

СПИСОК ЛИТЕРАТУРЫ

1. Грошев И.В., Корольков В.И. *Системы технического зрения и обработки изображений*. М.: РУДН; 2008. 212 с.
2. Абрамов И.А., Кравченко Е.Н. Многопоточная реализация алгоритма локальной фильтрации изображений. *Вестник Пензенского государственного университета*. 2016;3(15):66–71.
3. Турулин И.И. *Основы теории рекурсивных КИХ-фильтров*. Таганрог: Южный федеральный университет; 2016. 264 с.
4. Айфичер Э.С., Джервис Б.У. *Цифровая обработка сигналов. Практический подход*: пер. с англ. М.: Вильямс; 2004. 992 с.
5. Гольденберг Л.М., Матюшкин Б.Д., Поляк М.Н. *Цифровая обработка сигналов*. М.: Радио и связь; 1990. 256 с.
6. Курячий М.И., Гельцер А.А., Абенов Р.Р., Рогожников Е.В., Попова К.Ю. *Цифровая обработка сигналов*. Томск: Изд-во Томск. гос. ун-т систем упр. и радиоэлектроники; 2018. 234 с.
7. Лукин А. *Введение в цифровую обработку сигналов*. М.: МГУ, Лаборатория компьютерной графики и мультимедиа; 2002. 44 с.
8. Матвеев Ю.Н., Симончик К.К., Тропченко А.Ю., Хитров М.В. *Цифровая обработка сигналов.* СПб.: СПбНИУ ИТМО; 2013. 166 с.

9. Бондина Н.Н., Мураров Р.Ю. Адаптивные алгоритмы фильтрации и изменения контраста изображения. *Вестник Национального технического университета «Харьковский политехнический институт». Серия: Информатика и моделирование*. 2014;35(1078):35–42.
10. Каменский А.В., Рылов К.А. Цифровой сглаживающий трапецеидальный рекурсивно-сепарабельный фильтр обработки изображений с изменяемыми размерами сканирующей многоэлементной апертуры. *Омский научный вестник.* 2024;1(189):127–136. https://doi.org/10.25206/1813-8225-2024-189-127-136
11. Сай С.В., Каменский А.В., Курячий М.И. *Современные методы анализа и повышение качества цифровых изображений:* монография. Хабаровск: Изд-во ТОГУ; 2020. 173 с.
12. Kamenskiy A.V. High-speed recursive-separable image processing filters. *Computer Optics.* 2022;46(4):659–665. http://doi.org/10.18287/2412-6179-CO-1063
13. Акаева Т.М., Каменский А.В., Струмилова М.А. Быстродействующий трапецеидальный рекурсивно-сепарабельный фильтр обработки изображений. *Вопросы радиоэлектроники. Серия: Техника телевидения*. 2023;1:138–145.
14. Гонсалес Р., Вудс Р. *Цифровая обработка изображений*: пер. с англ. М.: Техносфера; 2019. 1104 с.
15. Маланин М.Ю., Каменский А.В., Курячий М.И. Измерение разрешающей способности и четкости телевизионных изображений. В сб.: Оптико-*электронные приборы и устройства в системах распознавания образов, обработки изображений и символьной информации:* сборник материалов XII Международной научно-технической конференции. Курск; 2015. С. 235–237.
16. Мовчан А.К., Капустин В.В., Курячий М.И. Методы и средства томографического видения пространства активно-импульсными телевизионными измерительными системами. *Труды Международной конференции по компьютерной графике и зрению «Графикон».* 2018;28:222–225. http://www.graphicon.ru/html/2018/papers/proceedings.pdf
17. Zaytseva E.V. Integral and spectral sensitivity assessment of the active-pulse television systems. In: *2016 Dynamics of Systems, Mechanisms and Machines* (*Dynamics*). 2016:7819115. https://doi.org/10.1109/Dynamics.2016.7819115

About the authors

Andrey V. Kamenskiy, Cand. Sci. (Eng.), Associate Professor, Department of Television and Control, Tomsk State University of Control Systems and Radioelectronics (40, Lenina pr., Tomsk, 634050 Russia). E-mail: andru170@mail.ru. Scopus Author ID 57191031758, ResearcherID AAX-9780-2021, RSCI SPIN-code 9572-4278, https://orcid.org/0000-0001-6587-7776

Tatyana M. Akaeva, Postgraduate Student, Department of Television and Control, Tomsk State University of Control Systems and Radioelectronics (40, Lenina pr., Tomsk, 634050 Russia). E-mail: ttnakaeva@gmail.com. Scopus Author ID 58511241300, ResearcherID GZK-2362-2022, RSCI SPIN-code 3514-9658, https://orcid.org/0000-0002-4846-9508

Darya A. Grebenshchikova, Student, Department of Television and Control, Tomsk State University of Control Systems and Radioelectronics (40, Lenina pr., Tomsk, 634050 Russia). E-mail: gredasha9443@gmail.com. https://orcid.org/0009-0002-6576-6691

Об авторах

Каменский Андрей Викторович, к.т.н., доцент, кафедра телевидения и управления, ФГБОУ ВО «Томский государственный университет систем управления и радиоэлектроники» (634050, Россия, Томск, пр. Ленина, д. 40). E-mail: andru170@mail.ru. Scopus Author ID 57191031758, ResearcherID AAX-9780-2021, SPIN-код РИНЦ 9572-4278, https://orcid.org/0000-0001-6587-7776

Акаева Татьяна Максимовна, аспирант, кафедра телевидения и управления, ФГБОУ ВО «Томский государственный университет систем управления и радиоэлектроники» (634050, Россия, Томск, пр. Ленина, д. 40). E-mail: ttnakaeva@gmail.com. Scopus Author ID 58511241300, ResearcherID GZK-2362-2022, SPIN-код РИНЦ 3514-9658, https://orcid.org/0000-0002-4846-9508

Гребенщикова Дарья Александровна, студент, ФГБОУ ВО «Томский государственный университет систем управления и радиоэлектроники» (634050, Томск, пр. Ленина, д. 40). E-mail: gredasha9443@gmail.com. https://orcid.org/0009-0002-6576-6691

Translated from Russian into English by Lyudmila O. Bychkova
Edited for English language and spelling by Dr. David Mossop

Micro- and nanoelectronics. Condensed matter physics

Микро- и наноэлектроника. Физика конденсированного состояния

UDC 537.632
https://doi.org/10.32362/2500-316X-2024-12-6-59-68
EDN OEKZKM

RESEARCH ARTICLE

Contribution of interference to the magneto-optical transverse Kerr effect in white light

Igor V. Gladyshev,
Alexey N. Yurasov,
Maxim M. Yashin @

MIREA – Russian Technological University, Moscow, 119454 Russia
@ *Corresponding author, e-mail: yashin@mirea.ru*

Abstract

Objectives. When measuring the transverse Kerr effect on thin-film structures, interference effects have a great influence on the result obtained. In conference presentations, some researchers have reported on the use of white light in experiments. In their opinion, despite the thickness of the studied layers being much less than the wavelength of light, white light can help avoid interference effects and/or resonant excitation of plasmon waves. The aim of the present work is to verify the validity of such statements using simulation.

Methods. In order to solve this problem, the method of computer simulation was used. A numerical solution of equations was compiled for a model structure for various thicknesses and materials of layers.

Results. The simulation results show that interference effects in different parts of the spectrum when using white light sources do not neutralize each other. The magnitude of the effect is affected not only by the thickness of the structure layers, but also by the shape of the source emission spectrum, as well as the sensitivity curve of the photodetector. In this case, the output of the measured value of the effect to a plateau at relatively large thicknesses of the magneto-optical film is due to the light being absorbed in the thickness of the magneto-optical film and is negligibility of the back reflection of light from the substrate.

Conclusions. The presented technique takes into account the influence of interference effects when measuring the equatorial Kerr effect in white light or using other sources having a wide spectral range, thus improving the interpretation of experimental results. The results are relevant to the development and research of the physical foundations for creating new and improving existing devices in micro-, nano-, and solid-state electronics, as well as quantum devices, including optoelectronic devices and converters of physical quantities.

Keywords: magneto-optical transverse Kerr effect, dielectric constant tensor, interference, reflection coefficient, thin films

• **Submitted:** 14.03.2024 • **Revised:** 23.04.2024 • **Accepted:** 24.09.2024

For citation: Gladyshev I.V., Yurasov A.N., Yashin M.M. Contribution of interference to the magneto-optical transverse Kerr effect in white light. *Russ. Technol. J*. 2024;12(6):59–68. https://doi.org/10.32362/2500-316X-2024-12-6-59-68

Financial disclosure: The authors have no financial or proprietary interest in any material or method mentioned.

The authors declare no conflicts of interest.

НАУЧНАЯ СТАТЬЯ

Вклад интерференции в магнитооптический экваториальный эффект Керра в белом свете

И.В. Гладышев,
А.Н. Юрасов,
М.М. Яшин @

МИРЭА – Российский технологический университет, Москва, 119454 Россия
@ *Автор для переписки, e-mail: yashin@mirea.ru*

Резюме

Цели. При измерении экваториального эффекта Керра в тонкопленочных структурах большое влияние на полученный результат оказывают интерференционные эффекты. В выступлениях на конференциях некоторые исследователи сообщали об использовании белого света в экспериментах. На их взгляд, хотя толщина исследуемых слоев была много меньше длины волны света, белый свет может помочь избежать интерференционных эффектов и/или резонансного возбуждения плазмонных волн. Цель статьи – путем моделирования проверить обоснованность таких утверждений.

Методы. Для решения обозначенной задачи применялся метод компьютерного моделирования – численного решения уравнений, составленных для модельной структуры при различных толщине и материалах слоев.

Результаты. Результаты моделирования показывают, что интерференционные эффекты в разных частях спектра при использовании источников белого света не нейтрализуют друг друга, и на величину эффекта влияет не только толщина слоев структуры, но и форма спектра излучения источника, а также кривая чувствительности фотоприемника. При этом выход измеряемой величины эффекта на плато при относительно большой толщине магнитооптической пленки обуславливается тем, что при этом свет поглощается в толще магнитооптической пленки и обратное отражение света от подложки пренебрежимо мало.

Выводы. Представленная методика позволяет учитывать влияние интерференционных эффектов при измерении экваториального эффекта Керра в белом свете или с использованием других источников с широким спектральным диапазоном и более качественно интерпретировать экспериментальные результаты, что может быть весьма полезным для разработки и исследования физических основ создания новых и совершенствования существующих приборов, изделий микро- и наноэлектроники, твердотельной электроники, а также квантовых устройств, включая оптоэлектронные приборы и преобразователи физических величин.

Ключевые слова: магнитооптический экваториальный эффект Керра, тензор диэлектрической проницаемости, интерференция, коэффициент отражения, тонкие пленки

• **Поступила:** 14.03.2024 • **Доработана:** 23.04.2024 • **Принята к опубликованию:** 24.09.2024

Для цитирования: Гладышев И.В., Юрасов А.Н., Яшин М.М. Вклад интерференции в магнитооптический экваториальный эффект Керра в белом свете. *Russ. Technol. J.* 2024;12(6):59–68. https://doi.org/10.32362/2500-316X-2024-12-6-59-68

Прозрачность финансовой деятельности: Авторы не имеют финансовой заинтересованности в представленных материалах или методах.

Авторы заявляют об отсутствии конфликта интересов.

INTRODUCTION

The transverse magneto-optical Kerr effect (TMOKE) involves a change in the intensity of light reflected from a sample when it is remagnetized in the direction perpendicular to the plane of light incidence. As such, TMOKE represents an important and very effective method for studying the magnetic microstructure of homogeneous and inhomogeneous magnetics. By measuring the EEC value as a function of the radiation wavelength, the magneto-optical transitions reflecting the electronic, crystalline, and magnetic structures of a given local section of the sample can be evaluated. Magneto-optical thin-film systems are also widely studied for use in optical data storage devices, in which data are recorded using thermomagnetic processes, but read by measuring the change in polarization upon reflection using the polar magneto-optical Kerr effect. Researchers have been very active in applying this principle (see, for example, [1–8]), including for ultrathin [9] and multilayer (ferromagnetic material and thin film coating [10]) structures. In this case, TMOKE measurement is generally carried out using a source having a narrow, almost monochromatic spectrum. However, at the 8th Euro-Asian Symposium "Trends in MAGnetism" held in 2022 in Kazan, Skidanov [11] report the use of white light in conducting experiments on the influence on the magnitude of the magneto-optical effect of thin films of nonmagnetic metals deposited on top of a ferromagnetic layer. Hypothesizing that this would significantly reduce the influence of interference effects, the researcher concluded that the observed change in the Kerr effect was due to more fundamental physical processes. However, such an interpretation does not seem entirely convincing, since almost all quantities affecting the magnitude of the effect have a nonlinear dependence on the frequency of incident light. Although the report has not yet been published in full, the very fact of raising the question led us to the necessity of a more detailed consideration of the degree of influence of interference effects on TMOKE parameter in white light.

MATHEMATICAL MODEL AND CALCULATION METHODOLOGY

As already mentioned, TMOKE consists in changing the intensity of light reflected from the sample when an external magnetic field is applied to the sample in the direction perpendicular to the plane of light incidence. Accordingly, it is necessary to calculate the intensity of light reflected from the sample both with and without the application of a magnetic field. The geometry of the model structure is shown in Fig. 1. Here, the vector of magnetic field strength lies in the plane of the film perpendicular to the plane of light incidence.

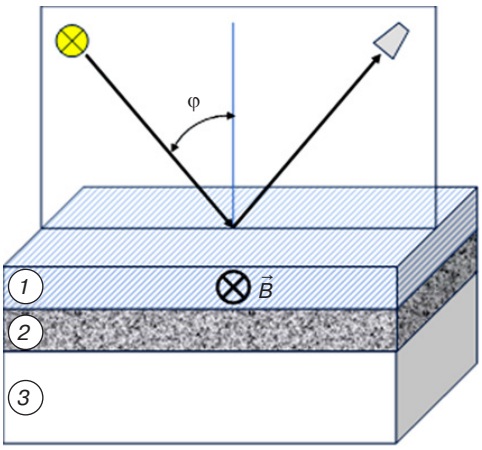

Fig. 1. Model structure geometry: (*1*) protective film (if any); (*2*) material with magneto-optical properties; (*3*) substrate, where φ is an angle of incidence of light, $\vec{B}$ is the magnetic field induction vector

The relation between the amplitudes of reflected R_j and incident A_j light can be expressed through their s- and p-components as in [12]:

$$\begin{pmatrix} R_s \\ R_p \end{pmatrix} = \begin{pmatrix} r_{ss} & r_{sp} \\ r_{ps} & r_{pp} \end{pmatrix} \begin{pmatrix} A_s \\ A_p \end{pmatrix}.$$

For an isotropic material, $r_{sp} = r_{ps} = 0$. While the application of an external magnetic field generally breaks the symmetry, in the geometry used in this work and shown in Fig. 1, i.e., when a non-zero magnetic field is applied to the magneto-optical material in the film plane perpendicular to the plane of light incidence, we also have $r_{sp} = r_{ps} = 0$. Therefore, in our case, the matrix of reflection coefficients has an invariant form:

$$\hat{r} = \begin{pmatrix} r_{ss} & 0 \\ 0 & r_{pp} \end{pmatrix}.$$

Then:

$$\begin{cases} R_s = r_{ss} A_s, \\ R_p = r_{pp} A_p. \end{cases} \quad (1)$$

During simulation, the spectral dependence of the source radiation intensity was taken into account. The model considered "natural" or circularly polarized light. In this case, the matrix of components of the incident light amplitude can be represented in the following form:

$$\begin{pmatrix} A_s \\ A_p \end{pmatrix} = |A| \begin{pmatrix} e^{i(\alpha+\pi/2)} \\ e^{i\alpha} \end{pmatrix},$$

where the initial phase α changes either arbitrarily ("natural" light) or cyclically at a given frequency (circularly polarized light); accordingly,

$$\begin{cases} R_s = |R_s| e^{i\chi}, \\ R_p = |R_p| e^{i\xi}. \end{cases}$$

Here $\chi = \alpha + \pi/2 + \Delta_s$ and $\xi = \alpha + \Delta_p$, and Δ_s and Δ_p are the phase run-ups as a result of light reflection from the investigated structure for s- and p-components, respectively. Due to the time-varying initial phase α, the resulting phases χ and ξ change in the same way.

Then the intensity of light falling on the photodiode will be equal to:

$$I = \left[|R_s|^2 \cos^2 \chi + |R_p|^2 \cos^2 \xi \right] \sin^2 \omega t,$$

where ω is the frequency of radiation; t is time.

Due to the inertia of the photodetector, the signal is averaged over time and, taking into account also the constant change of the initial phase α and, as a consequence, of the resulting χ and ξ, we obtain $\overline{\cos\chi} = \overline{\cos\xi} = \overline{\sin\omega t} = 0$ and

$$\overline{I} = \frac{|R_s|^2 + |R_p|^2}{4}. \quad (2)$$

As already noted, practically all quantities influencing the magnitude of the effect have a nonlinear dependence on the frequency of incident light. Therefore, the method of calculations in a wide spectral range was as follows. The spectral range was divided into small sections, within which the values of the used quantities were considered to be independent of frequency and corresponding to the value in the middle of this section. Figure 2 depicts an example of such partitioning for the relative spectrum of one of the radiation sources. The partition sections for all values simultaneously used in the calculation were taken to be identical; in case of insufficient experimental data, linear approximation was used. For nonlinear dependencies, the error of this method is smaller the narrower the partition section, leading to an increase in computation time. In the present work, the frequency partitioning into sections of $1 \cdot 10^{-3} - 3 \cdot 10^{-3}$ eV (240–720 GHz). For each partitioning section, the average intensity of radiation detected by the photodetector is determined by Eq. (2) taking into account its spectral sensitivity S_ω. Then, the total signal value is determined by summing over all partition areas:

$$\overline{I_\Sigma} = \sum\nolimits_\omega S_\omega \overline{I}_\omega, \quad (3)$$

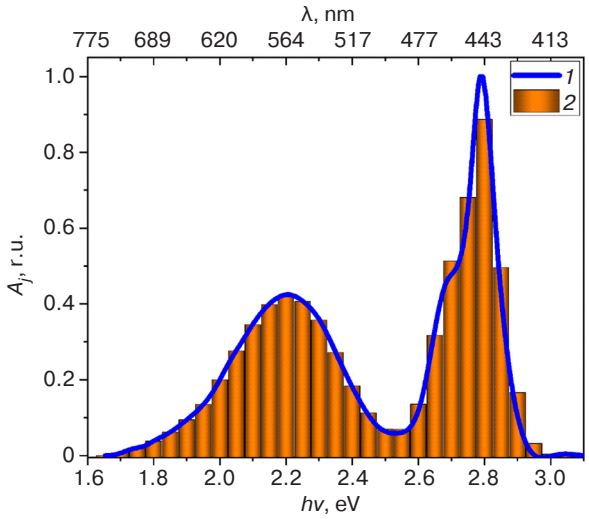

Fig. 2. Emission spectrum of white LED with color temperature T_c = 6500 K: (*1*) data taken from [13], (*2*) representation of the spectrum as a piecewise constant function. λ is the wavelength of light in a vacuum, which corresponds to a quantum of energy $h\nu$

The total signal magnitude is determined both in the absence of a magnetic field $\overline{I_\Sigma^0}$ and in its presence $\overline{I_\Sigma^M}$. Then the magnitude of the transverse magneto-optical effect δ is calculated:

$$\delta = \frac{\overline{I_\Sigma^M} - \overline{I_\Sigma^0}}{\overline{I_\Sigma^0}}. \quad (4)$$

In order to determine the amplitudes of the reflected signal (1), it is necessary to calculate the light reflection coefficients from the investigated structure in the absence of the magnetic field (r_{ss}^0, r_{pp}^0) and when it is switched on (r_{ss}^M, r_{pp}^M). This calculation was based on the well-known paper by V.M. Maevskiy "Theory of magneto-optical effects in multilayer systems with arbitrary magnetization orientation" [12], where the magneto-optical parameter $Q = i\varepsilon_{xy}\varepsilon_{xx}^{-1}$ linear in magnetization is considered as a small value ($|Q| << 1$). Here ε_{xx}, ε_{yy}, etc. are the elements of the dielectric tensor $\hat{\varepsilon}$, which for isotropic materials in our case can be represented as:

$$\hat{\varepsilon} = \begin{pmatrix} \varepsilon & -i\varepsilon Q & 0 \\ i\varepsilon Q & \varepsilon & 0 \\ 0 & 0 & \varepsilon \end{pmatrix} = \varepsilon \begin{pmatrix} 1 & -iQ & 0 \\ iQ & 1 & 0 \\ 0 & 0 & 1 \end{pmatrix}.$$

Taking into account that the magnetic permeability for the optical range $\mu \approx 1$, we can assume $n^2 \approx \varepsilon$. Here n is

the refractive index of the substance. All the mentioned quantities are complex in the general case. Then, for the reflection coefficients of s- and p-polarized wave at the boundary of media, j and k can be written as follows:

$$r_{jk}^{\mathrm{s}} = \frac{g_j - g_k}{g_j + g_k},\ r_{jk}^{\mathrm{p}} = \frac{g_j\varepsilon_k - g_k\varepsilon_j}{g_j\varepsilon_k + g_k\varepsilon_j}. \quad (5)$$

Here

$$g_j = \sqrt{\varepsilon_j - \sin^2\varphi}, \quad (6)$$

φ is the angle of incidence of light on the structure under study. Light falls from air, $\varepsilon_{\mathrm{air}} \approx 1$.

The following recurrence formulas can be used for the reflection coefficients of multilayer structures [12, 14]:

$$r_{jkl}^{\mathrm{s(p)}} = \frac{r_{jk}^{\mathrm{s(p)}} + F_k^2 r_{kl}^{\mathrm{s(p)}}}{1 + F_k^2 r_{jk}^{\mathrm{s(p)}} r_{kl}^{\mathrm{s(p)}}},\ r_{jklm}^{\mathrm{s(p)}} = \frac{r_{jk}^{\mathrm{s(p)}} + F_k^2 r_{klm}^{\mathrm{s(p)}}}{1 + F_k^2 r_{jk}^{\mathrm{s(p)}} r_{klm}^{\mathrm{s(p)}}}, \quad (7)$$

etc., where j, k, l, m are the numbers of layers (media), and the values F_k determine the phase run-up and amplitude attenuation at the thickness of the kth layer:

$$F_k = \mathrm{e}^{-2\pi g_k \frac{d_k}{\lambda}}. \quad (8)$$

Here d_k is the thickness of the layer, λ is the wavelength of light in vacuum, g_k is determined by the Eq. (6).

While these expressions are valid for coherent radiation, in the case of white-light measurements, the thickness of some layers (e.g., the substrate) may exceed it due to the small size of the coherence length. Since coherent and incoherent calculations are not generally mixed within the same model, the substrate could be excluded by treating it as a semi-infinite space. However, when conducting an experiment with illumination of the ferromagnetic film from the substrate side, it becomes impossible to take into account the influence of the thickness and absorption spectrum of the weakly absorbing substrate. Therefore, taking into account the inertia of the photodetector and the fact that the absorption practically does not change between two interference maxima for weakly absorbing materials, we averaged the coefficients (7) for a layer thickness much larger than the coherence length to "fix" the phase of the reflected light and ignore the influence of absorption. Thus, Eq. (7) for one layer can be written in the following form:

$$r_{jkl}^{\mathrm{s(p)}} = r_{jk}^{\mathrm{s(p)}}\left(\frac{1 + F_k^2 \dfrac{r_{kl}^{\mathrm{s(p)}}}{r_{jk}^{\mathrm{s(p)}}}}{1 + F_k^2 r_{jk}^{\mathrm{s(p)}} r_{kl}^{\mathrm{s(p)}}}\right). \quad (9)$$

Since any complex quantity can be represented as $Ye^{i\alpha}$, where Y and α are real numbers, the numerator and denominator of formula (9) contain expressions of the following form:

$$Y_1 e^{i\alpha_1} + Y_2 e^{i\alpha_2} = Z e^{i\beta},$$

where Y_1, Y_2, and $Z \geq 0$ are the modules of the complex numbers, and α_1, α_2, and β are their arguments.

Let us assume that $\gamma = \alpha_2 - \alpha_1$, then the resulting amplitude is

$$Z = \sqrt{Y_1^2 + Y_2^2 + 2Y_1Y_2\cos\gamma},$$

and for the argument β we can write:

$$\beta = \alpha_1 + \frac{\sin\gamma}{|\sin\gamma|}\arccos\left(\frac{Y_1 + Y_2\cos\gamma}{Z}\right). \quad (10)$$

The second summand in (10) is periodic and antisymmetric; when averaging over the phase difference, it can be easily shown that γ it converges to zero. Then:

$$\overline{Z} = \sqrt{Y_1^2 + Y_2^2},\ \overline{\beta} = \alpha_1.$$

In our case $\alpha_1 = 0$, since $1 = 1\cdot e^{i0}$. And then for the case when the thickness of the kth layer is much larger than the coherence length, Eq. (9) can be written as follows:

$$r_{jkl}^{\mathrm{s(p)}} = r_{jk}^{\mathrm{s(p)}}\sqrt{\frac{1 + |F_k^2 r_{kl}^{\mathrm{s(p)}} / r_{jk}^{\mathrm{s(p)}}|^2}{1 + |F_k^2 r_{jk}^{\mathrm{s(p)}} r_{kl}^{\mathrm{s(p)}}|^2}}. \quad (11)$$

Correspondingly,

$$r_{jklm}^{\mathrm{s(p)}} = r_{jk}^{\mathrm{s(p)}}\sqrt{\frac{1 + |F_k^2 r_{klm}^{\mathrm{s(p)}} / r_{jk}^{\mathrm{s(p)}}|^2}{1 + |F_k^2 r_{jk}^{\mathrm{s(p)}} r_{klm}^{\mathrm{s(p)}}|^2}},\ \text{etc.}$$

In order to demonstrate the advantages of such averaging over the use of expressions for coherent light for the substrate while the coherence condition is not fulfilled, Fig. 3 shows the results of calculations using the method considered for an absorbing substrate at a change of its thickness, performed using Eqs. (7) and (11).

Let us consider the structure shown in Fig. 1 surrounded by air. Then the reflection coefficients in the absence of magnetic field r_{ss}^0 and r_{pp}^0 can be calculated by Eqs. (5)–(8), (11) as follows:

$$r_{\mathrm{ss}}^0 = r_{\mathrm{a123a}}^{\mathrm{s}},\ r_{\mathrm{pp}}^0 = r_{\mathrm{a123a}}^{\mathrm{p}}. \quad (12)$$

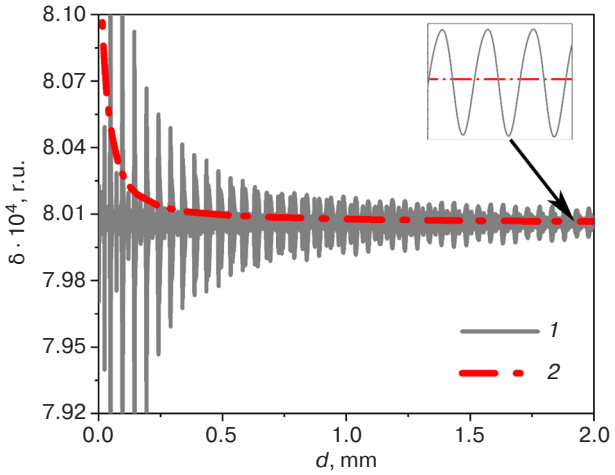

Fig. 3. Dependence of the effect value on the silicon substrate thickness for uncoated ferromagnetic film. The reflection coefficient from the substrate was calculated: (*1*) by Eq. (7), (*2*) by Eq. (11)

Here, index 'a' corresponds to air and the rest corresponds to the layer numbers in Fig. 1.

When taking into account the magneto-optical effect, reflection coefficients r_{ss}^{M} and r_{pp}^{M} can be expressed as follows:

$$r_{ss}^{M} = r_{ss}^{0}, \quad r_{pp}^{M} = r_{pp}^{0} W(1+\rho_p). \tag{13}$$

We define the multipliers W and ρ_p following [12], taking into account the geometry (Fig. 1) and the incidence of light on the structure from air. Then:

$$\rho_p = i(1-F_2^2)\times \times\left[\frac{r_{23a}^{p}-r_{21a}^{inv}}{1-F_2^2 r_{21a}^{inv} r_{23a}^{p}} - \frac{r_{23a}^{p}-r_{21a}^{p}}{1-F_2^2 r_{21a}^{p} r_{23a}^{p}}\right]\frac{Q\sin\varphi}{2g_2}, \tag{14}$$

where

$$r_{21a}^{inv} = \frac{r_{21}^{p} r_{1a}^{p} + F_1^2}{r_{1a}^{p} + F_1^2 r_{21}^{p}}. \tag{15}$$

For thin films, we can assume $W \approx 1$. Considering arbitrary thicknesses, following [12]:

$$W = \frac{1-F_2^2 a_p \sin^2\vartheta}{1+F_2^2 a_0 \sin^2\vartheta}, \tag{16}$$

where

$$\vartheta = \frac{\pi d_2 n_2 Q}{\lambda},$$

$$a_p = \frac{(r_{23a}^{p}-r_{23a}^{s})(1-r_{21a}^{inv} r_{21a}^{s})}{(r_{21a}^{inv}-F_2^2 r_{23a}^{p})(1-F_2^2 r_{21a}^{s} r_{23a}^{s})},$$

$$a_0 = \frac{(r_{23a}^{p}-r_{23a}^{s})(r_{21a}^{p}-r_{21a}^{s})}{(1-F_2^2 r_{21a}^{s} r_{23a}^{s})(1-F_2^2 r_{21a}^{p} r_{23a}^{p})}.$$

Considering Eqs. (1)–(4), we can write down:

$$\delta = \frac{\sum_\omega S_\omega(|r_{ss_\omega}^{M} A_{s_\omega}|^2 + |r_{pp_\omega}^{M} A_{p_\omega}|^2)}{\sum_\omega S_\omega(|r_{ss_\omega}^{0} A_{s_\omega}|^2 + |r_{pp_\omega}^{0} A_{p_\omega}|^2)} - \frac{\sum_\omega S_\omega(|r_{ss_\omega}^{0} A_{s_\omega}|^2 + |r_{pp_\omega}^{0} A_{p_\omega}|^2)}{\sum_\omega S_\omega(|r_{ss_\omega}^{0} A_{s_\omega}|^2 + |r_{pp_\omega}^{0} A_{p_\omega}|^2)}. \tag{17}$$

SIMULATION RESULTS

Since we were primarily interested in the presence or absence of the influence of interference effects, standard materials possessing magneto-optical properties were chosen: cobalt and a protective film of polyvinyl acetate (PVA). Two-layer (magneto-optical film on a substrate) and three-layer (a protective layer was applied to the film) structures were studied. Assuming the coherence length of radiation to be 500 nm, we took for calculations either thicknesses smaller (for the film and the protective layer) or much larger (for the substrate, the thickness of which was assumed to be 500 μm), which is close to the thicknesses of silicon wafers used in microelectronic production. White light was considered to be "natural" (circularly polarized), with the induction direction of the external magnetic field lying in the plane of the film perpendicular to the plane of light incidence (Fig. 1). As a photodetector, a silicon photodiode whose sensitivity curve was "averaged" according to the data [15, 16] was considered.

According to the performed numerical simulations, the assumption that interference effects in different parts of the spectrum when using white light sources do not neutralize each other was confirmed; here, the magnitude of the measured effect can strongly depend on the film thickness of the magneto-optical material up to the change of the effect sign (see, for example, curve *1* in Fig. 4). The measured value is also markedly affected by the shape of the emission spectrum of the source, which is also clearly visible in Fig. 4. The plateau of the measured value of the effect at relatively large thicknesses of the magneto-optical film is apparently caused by the absorption of light in the thickness of the magneto-optical film, while the back reflection of light from the substrate is negligible. This is confirmed by the fact that the substrate material does not play a role at such film thicknesses (Fig. 5).

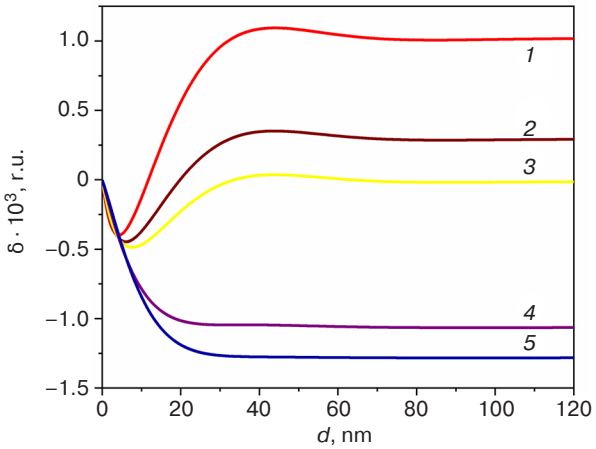

Fig. 4. Dependence of the effect size on the thickness of uncoated ferromagnetic film (light incidence angle 75°, silicon photodiode) for different white light sources: (*1*) 'A' type source (absolutely black body (ABB) with T = 2856 K), (*2*) 'B' type source (ABB with T = 4874 K), (*3*) 'sunlight' (ABB with T = 6000 K), (*4*) white LED with color temperature T_c = 3000 K, (*5*) white LED with color temperature T_c = 6500 K

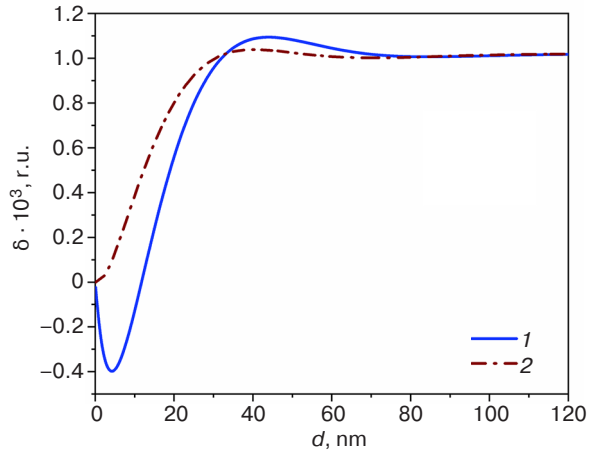

Fig. 5. Dependence of the effect value on the thickness of uncoated ferromagnetic film on SiO_2 (*1*) and Si (*2*) quartz substrates (light incidence angle 75°, 'A' type source, silicon photodiode)

If a protective film is applied on top of the structure, it will further complicate the observed picture. To verify this assumption, we performed calculations in which PVA was considered as a protective material. Since in this case the effect of changing the thickness of the magneto-optical film turned out to be much stronger than the effect of changing the thickness of the transparent film, Fig. 6 demonstrates the dependencies of the effect magnitude on the thickness of the protective film normalized to the effect magnitude in the absence of such a coating. An SiO_2 substrate was used, having a light incidence angle of 75°, an 'A' type source, and a silicon photodiode.

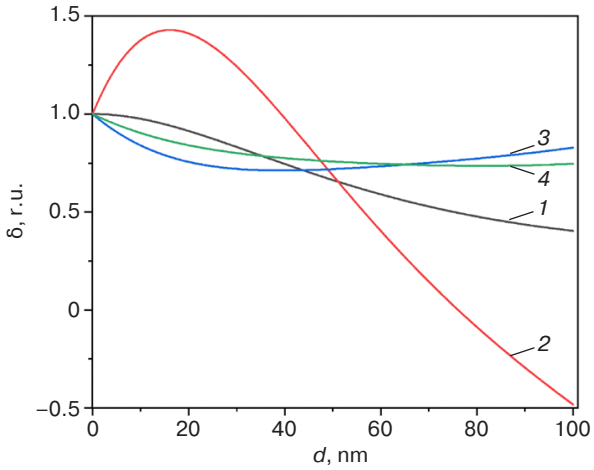

Fig. 6. Dependencies of the effect size on the thickness of the PVA protective layer on ferromagnetic films of different thickness, normalized to the effect size in the absence of such a layer: (*1*) 10 nm, (*2*) 20 nm, (*3*) 30 nm, (*4*) 60 nm

The curves in Fig. 7, which are in agreement with the theory of metallooptics (e.g., [17]), show that in order to obtain the maximum value of the measured effect, it is better to work in the geometry when light falls on the structure at an angle of around 70°–75°. The lack of dependence of the effect value on the thickness of the magneto-optical material at angles of incidence close to 90° (slip angle) is due to the fact that in this case light practically does not penetrate into the film and only the surface effect is registered. At the same time, we can see a clear influence of interference effects, which decreases with increasing thickness of the ferromagnetic film. This decrease is due to the absorption of light in the thickness of the ferromagnetic material and consequent decrease in the influence of light reflected from the interface with the substrate. An SiO_2 substrate was used having an 'A' type source and a silicon photodiode.

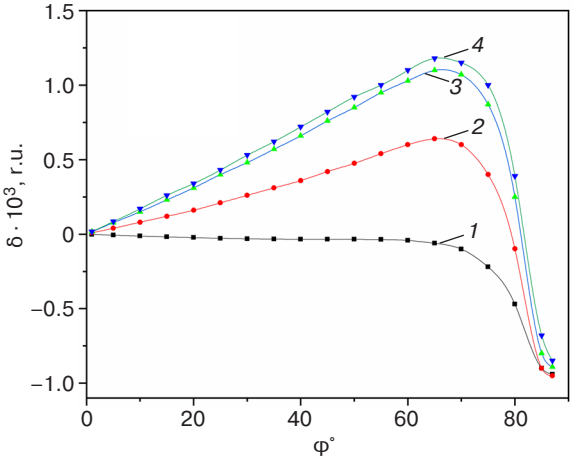

Fig. 7. Dependencies of the TMOKE value on the angle of incidence of light on ferromagnetic films of different thicknesses without a "protective layer": (*1*) 15 nm, (*2*) 30 nm, (*3*) 45 nm, (*4*) 60 nm

CONCLUSIONS

The performed calculations demonstrate the necessity of taking into account the influence of the spectral sensitivity of the photodetector when interpreting the obtained results on TMOKE measurement using white light sources. Here, it is also important to consider interference at small thicknesses of ferromagnetic and/or "protective" film. The developed technique allows us to take into account the influence of interference effects when measuring TMOKE in white light—or, using other sources, across a wide spectral range—and to interpret the experimental results more precisely.

Authors' contributions

I.V. Gladyshev—model proposal and development, calculation methodology development, creating a computer program, computer simulation, discussion of results, writing the text of the article.

A.N. Yurasov—computer simulation, discussion of results, writing and editing the text of the article.

M.M. Yashin—processing the literary sources, computer simulation, discussion of results, writing the text if the article.

REFERENCES

1. Gan'shina E.A., Garshin V.V., Perova N.N., et. al. Magnetooptical Kerr spectroscopy of nanocomposites. *J. Exp. Theor. Phys*. 2023;137(4):572–581. https://doi.org/10.1134/S1063776123100151
[Original Russian Text: Gan'shina E.A., Garshin V.V., Perova N.N, Pripechenkov I.M., Yurasov A.N., Yashin M.M., Ryl'kov V.V., Granovskii A.B. Magnetooptical Kerr spectroscopy of nanocomposites. *Zhurnal Eksperimental'noi i Teorieticheskoi Fiziki* (*ZhETF*). 2023;164(4):662–672 (in Russ.).]
2. Sato K., Ishibashi T. Fundamentals of Magneto-Optical Spectroscopy. *Front. Phys*. 2022;10:946515. https://doi.org/10.3389/fphy.2022.946515
3. Telegin A.V., Bessonova V.A., Suhorukov Yu.P., et. al. Magneticreflection and the Kerr effect in $La_{2/3}Ba_{1/3}MnO_3$ films with a variant structure. *Opt. Spectrosc.* 2020;128(1):42–48. https://doi.org/10.1134/S0030400X20010233
[Original Russian Text: Telegin A.V., Bessonova V.A., Suhorukov Yu.P., Nosov A.P., Gan'shina E.A. Magneticreflection and the Kerr effect in $La_{2/3}Ba_{1/3}MnO_3$ films with a variant structure. *Optika i spektroskopiya*. 2020;128(1):43–49 (in Russ.). https://doi.org/10.21883/OS.2020.01.48836.40-19]
4. Dyakov S.A., Fradkin I.M., Gippius N.A., Klompmaker L., Spitzer F., Yalcin E., Akimov I.A., Bayer M., Yavsin D.A., Pavlov S.I., Pevtsov A.B., Verbin S.Y., Tikhodeev S.G. Wide-band enhancement of the transverse magneto-optical Kerr effect in magnetite-based plasmonic crystals. *Phys. Rev. B*. 2019;100(21):214411. https://doi.org/10.1103/PhysRevB.100.214411
5. Gan'shina E.A., Pripechenkov I.M., Perova N.N., et al. Magneto-Optical Spectroscopy of GaSb–MnSb Composites. *Bull. Russ. Acad. Sci. Phys.* 2023;87(3):282–286. https://doi.org/10.3103/s1062873822701088
[Original Russian Text: Gan'shina E.A., Pripechenkov I.M., Perova N.N., Kanazakova E.S., Oveshnikov L.N., Dzhaloliddinzoda M., Ril' A.I., Granovskii A.B., Aronzon B.A. Magneto-optical spectroscopy of composites GaSb–MnSb. *Izvestiya Rossiiskoi akademii nauk. Seriya fizicheskaya.* 2023;87(3):328–332 (in Russ.). https://doi.org/10.31857/S0367676522700570]
6. Buchin E.Yu., Vaganova E.I., Naumov V.V., et al. Enhancement of the transversal magnetooptical Kerr effect in nanoperforated cobalt films. *Tech. Phys. Lett.* 2009;35(7):589–593. https://doi.org/10.1134/S1063785009070025
[Original Russian Text: Buchin E.Yu., Vaganova E.I., Naumov V.V., Paporkov V.A., Prokaznikov A.V. Enhancement of the transversal magnetooptical Kerr effect in nanoperforated cobalt films. *Pis'ma v Zhurnal Tekhnicheskoĭ Fiziki* (*Pis'ma v ZhTF*). 2009;35(13):8–17 (in Russ.).]
7. Gan'shina E.A., Kun'kova Z.E., Pripechenkov I.M., et al. Magneto-Optical Probing of the Magnetic State and Phase Composition of InFeAs Layers. *Phys. Metals Metallogr.* 2022;123(11):1098–1104. https://doi.org/10.1134/S0031918X22601287
[Original Russian Text: Gan'shina E.A., Kun'kova Z.E., Pripechenkov I.M., Markin Yu.V. Magneto-Optical Probing of the Magnetic State and Phase Composition of InFeAs Layers. *Fizika metallov i metallovedenie.* 2022;123(11):1168–1174 (in Russ.). https://doi.org/10.31857/S0015323022601222]
8. Li T., Luo L., Li X., Dove M.T., Zhang S., He J., Zhang Z. Observation of the mixed magneto-optical Kerr effects using weak measurement. *Opt. Express*. 2023;31(15):24469–24480. https://doi.org/10.1364/oe.492380
9. Sumi S., Awano H., Hayashi M. Interference induced enhancement of magneto-optical Kerr effect in ultrathin magnetic films. Sci. Rep. 2018;8(1):776. https://doi.org/10.1038/s41598-017-18794-w
10. Kaihara T., Ando T., Shimizu H., Zayets V., Saito H., Ando K., Yuasa S. Enhancement of magneto-optical Kerr effect by surface plasmons in trilayer structure consisting of double-layer dielectrics and ferromagnetic metal. *Opt. Express*. 2015;23(9):11537–11555. https://doi.org/10.1364/oe.23.011537
11. Skidanov V.A. Proximity induced long-range transformation of transverse magneto-optical Kerr effect in bilayers of magnetic and normal transition metals. In: *EASTMAG Conference*. 2022. Abstracts. V. 1. P. 415–416. URL: https://eastmag2022.knc.ru/wp-content/uploads/2023/10/EASTMAG-2022_Abstracts_volume-1-2.pdf

12. Maevskii V.M. Theory of magneto-optical effects in multilayer systems with arbitrary orientation of magnetization. *Fizika metallov i metallovedenie = Physics of Metals and Metallography)*. 1985;59(2):213–219 (in Russ.).
13. Deinego V., Kaptsov V., Gordienko V. Ten years of school LED lighting. Part 1. New threats. *Poluprovodnikovaya svetotekhnika = Solid-State Lighting*. 2021;3(71):22–28 (in Russ.).
14. Gorshkov M.M. *Ellipsometriya* (*Ellipsometry*). Moscow: Sovetskoe radio; 1974. 199 p. (in Russ.).
15. Lomakin L. Silicon photodiodes. The reference sheet. *Radio*. 1998;2:65–68 (in Russ.).
16. Aksenenko M.D., Baranochnikov M.L. *Priemniki opticheskogo izlucheniya. Spravochnik* (*Optical Radiation Receivers. Guide*). Moscow: Radio i svyaz'; 1987. 296 p. (in Russ.).
18. Born M., Wolf E. *Osnovy optiki* (*Principles of Optics*): transl. from Engl. Moscow: Nauka; 1973. 719 p. (in Russ.).
[Born M., Wolf E. *Principles of Optics*. Cambridge: Cambridge University Press; 2019. 992 p.]

СПИСОК ЛИТЕРАТУРЫ

1. Ганьшина Е.А., Гаршин В.В., Перова Н.Н., Припеченков И.М., Юрасов А.Н., Яшин М.М., Рыльков В.В., Грановский А.Б. Магнитооптическая Керр-спектроскопия нанокомпозитов. *Журнал экспериментальной и теоретической физики* (*ЖЭТФ*). 2023;164(4):662–672.
2. Sato K., Ishibashi T. Fundamentals of Magneto-Optical Spectroscopy. *Front. Phys*. 2022;10:946515. https://doi.org/10.3389/fphy.2022.946515
3. Телегин А.В., Бессонова В.А., Сухоруков Ю.П., Носов А.П., Ганьшина Е.А. Магнитоотражение и эффект Керра в пленках $La_{2/3}Ba_{1/3}MnO_3$ с вариантной структурой. *Оптика и спектроскопия*. 2020;128(1):43–49. https://doi.org/10.21883/OS.2020.01.48836.40-19
4. Dyakov S.A., Fradkin I.M., Gippius N.A., Klompmaker L., Spitzer F., Yalcin E., Akimov I.A., Bayer M., Yavsin D.A., Pavlov S.I., Pevtsov A.B., Verbin S.Y., Tikhodeev S.G. Wide-band enhancement of the transverse magneto-optical Kerr effect in magnetite-based plasmonic crystals. *Phys. Rev. B*. 2019;100(21):214411. https://doi.org/10.1103/PhysRevB.100.214411
5. Ганьшина Е.А., Припеченков И.М., Перова Н.Н., Каназакова Е.С., Овешников Л.Н., Джалолиддинзода М., Риль А.И., Грановский А.Б., Аронзон Б.А. Магнитооптическая спектроскопия композитов GaSb–MnSb. *Известия Российской академии наук. Серия физическая.* 2023;87(3):328–332. https://doi.org/10.31857/S0367676522700570
6. Бучин Э.Ю., Ваганова Е.И., Наумов В.В., Папорков В.А., Проказников А.В. Усиление экваториального эффекта Керра в наноперфорированных пленках кобальта. *Письма в ЖТФ*. 2009;35(13):8–17.
7. Ганьшина Е.А., Кунькова З.Э., Припеченков И.М., Маркин Ю.В. Магнитооптическое зондирование магнитного состояния и фазового состава слоев INFEAS. *Физика металлов и металловедение.* 2022;123(11):1168–1174. https://doi.org/10.31857/S0015323022601222
8. Li T., Luo L., Li X., Dove M.T., Zhang S., He J., Zhang Z. Observation of the mixed magneto-optical Kerr effects using weak measurement. *Opt. Express*. 2023;31(15):24469–24480. https://doi.org/10.1364/oe.492380
9. Sumi S., Awano H., Hayashi M. Interference induced enhancement of magneto-optical Kerr effect in ultrathin magnetic films. *Sci. Rep*. 2018;8(1):776. https://doi.org/10.1038/s41598-017-18794-w
10. Kaihara T., Ando T., Shimizu H., Zayets V., Saito H., Ando K., Yuasa S. Enhancement of magneto-optical Kerr effect by surface plasmons in trilayer structure consisting of double-layer dielectrics and ferromagnetic metal. *Opt. Express*. 2015;23(9):11537–11555. https://doi.org/10.1364/oe.23.011537
11. Skidanov V.A. Proximity induced long-range transformation of transverse magneto-optical Kerr effect in bilayers of magnetic and normal transition metals. In: *EASTMAG Conference*. 2022. Abstracts. V. 1. P. 415–416. URL: https://eastmag2022.knc.ru/wp-content/uploads/2023/10/EASTMAG-2022_Abstracts_volume-1-2.pdf
12. Маевский В.М. Теория магнетооптических эффектов в многослойных системах с произвольной ориентацией намагниченности. *Физика металлов и металловедение*. 1985;50(2):213–219.
13. Дейнего В., Капцов В., Гордиенко В. Десять лет школьному светодиодному освещению. Часть 1. Новые угрозы. *Полупроводниковая светотехника*. 2021;3(71):22–28.
14. Горшков М.М. *Эллипсометрия*. М.: Советское радио; 1974. 199 с.
15. Ломакин Л. Кремниевые фотодиоды. Справочный листок. *Радио*. 1998;2:65–68.
16. Аксененко М.Д., Бараночников М.Л. *Приемники оптического излучения. Справочник.* М.: Радио и связь; 1987. 296 с.
17. Борн М., Вольф Э. *Основы оптики*: пер. с англ. М.: Наука; 1973. 719 с.

About the authors

Igor V. Gladyshev, Cand. Sci. (Phys.–Math.), Associate Professor, Department of Nanoelectronics, Institute for Advanced Technologies and Industrial Programming, MIREA – Russian Technological University (78, Vernadskogo pr., Moscow, 119454 Russia). E-mail: i_gladyshev@mirea.ru. ResearcherID N-1535-2016, Scopus Author ID 6701612553, RSCI SPIN-code 6735-1887, https://orcid.org/0000-0002-7627-4978

Alexey N. Yurasov, Dr. Sci. (Phys.-Math.), Professor, Department of Nanoelectronics, Institute for Advanced Technologies and Industrial Programming, MIREA – Russian Technological University (78, Vernadskogo pr., Moscow, 119454 Russia). E-mail: alexey_yurasov@mail.ru, ResearcherID M-3113-2016, Scopus Author ID 6602974416, RSCI SPIN-code 4259-8885, https://orcid.org/0000-0002-9104-3529

Maxim M. Yashin, Cand. Sci. (Phys.-Math.), Associate Professor, Department of Nanoelectronics, Institute for Advanced Technologies and Industrial Programming, MIREA – Russian Technological University (78, Vernadskogo pr., Moscow, 119454 Russia). E-mail: ihkamax@mail.ru. ResearcherID G-6809-2017, Scopus Author ID 57210607470, RSCI SPIN-code 2438-6135, https://orcid.org/0000-0001-8022-9355

Об авторах

Гладышев Игорь Васильевич, к.ф.-м.н., доцент, кафедра наноэлектроники, Институт перспективных технологий и индустриального программирования, ФГБОУ ВО «МИРЭА – Российский технологический университет» (119454, Россия, Москва, пр-т Вернадского, д. 78). E-mail: i_gladyshev@mirea.ru. ResearcherID N-1535-2016, Scopus Author ID 6701612553, SPIN-код РИНЦ 6735-1887, https://orcid.org/0000-0002-7627-4978

Юрасов Алексей Николаевич, д.ф.-м.н., профессор, кафедра наноэлектроники, Институт перспективных технологий и индустриального программирования, ФГБОУ ВО «МИРЭА – Российский технологический университет» (119454, Россия, Москва, пр-т Вернадского, д. 78). E-mail: alexey_yurasov@mail.ru. ResearcherID M-3113-2016, Scopus Author ID 6602974416, SPIN-код РИНЦ 4259-8885, https://orcid.org/0000-0002-9104-3529

Яшин Максим Михайлович, к.ф.-м.н., доцент, кафедра наноэлектроники, Институт перспективных технологий и индустриального программирования, ФГБОУ ВО «МИРЭА – Российский технологический университет» (119454, Россия, Москва, пр-т Вернадского, д. 78). E-mail: ihkamax@mail.ru. ResearcherID G-6809-2017, Scopus Author ID 57210607470, SPIN-код РИНЦ 2438-6135, https://orcid.org/0000-0001-8022-9355

Translated from Russian into English by Lyudmila O. Bychkova
Edited for English language and spelling by Thomas A. Beavitt

Micro- and nanoelectronics. Condensed matter physics

Микро- и наноэлектроника. Физика конденсированного состояния

UDC 535.075.8
https://doi.org/10.32362/2500-316X-2024-12-6-69-79
EDN OHJNSF

RESEARCH ARTICLE

Reflections of linearly polarized electromagnetic waves from a multilayer periodic mirror

Dzamil Kh. Nurligareev [1, @], Iliya A. Nedospasov [1, 2], Kseniya Yu. Kharitonova [1]

[1] *MIREA – Russian Technological University, 119454 Russia*
[2] *Kotelnikov Institute of Radioengeneering and Electronics, Russian Academy of Sciences, Moscow, 125009 Russia*
[@] *Corresponding author, e-mail: nurligareev@mirea.ru*

Abstract

Objectives. The purpose of the article is to carry out a theoretical and experimental study of the angular reflection spectrum of linearly polarized electromagnetic waves from a multilayer periodic mirror on a transparent substrate to exact analytical expressions for reflection and transmission coefficients generalizing the cases of incidence of plane transverse electric (TE) and transverse magnetic (TM) modes on limited periodically structured media with a stepped refractive index profile.

Methods. The theoretical analysis of the reflection problem is based on the search for exact analytical solutions in the form of Floquet–Bloch waves presented in the form of inhomogeneous waves in the domain of periodically structured media. On the basis of the possible existence of a single Floquet–Bloch wave in a limited one-dimensional photonic crystal, it is proposed to search for exact solutions of the wave equation in the form of a linear combination of inhomogeneous waves propagating in different directions. By using the canonical forms of the considered periodic structures, it is possible to carry out the simple transition from the case of TE polarization to TM type in dispersion relations and expressions for the angular reflection spectrum.

Results. Cases of reflection of linearly polarized radiation are considered for the following cases: a flat boundary of two dielectrics, a thin plane-parallel plate, and a multilayer dielectric mirror. Exact analytical expressions for the reflection and transmission coefficients generalizing the cases of incidence of TE and TM polarizations waves on a limited one-dimensional photonic crystal are obtained. The transmission coefficients of a plane TE wave from a multilayer dielectric mirror sputtered on thin glass were experimentally measured.

Conclusions. A quantitative and qualitative agreement of experimental measurements of the transmission coefficient of a plane wave incident from a half-space on a confined photonic crystal with theoretical calculations is obtained. The obtained expressions for the transmission coefficient of a confined one-dimensional photonic crystal, which are shown to be determined by the interference of Floquet–Bloch waves presented in the form of inhomogeneous waves, can be reduced to a form analogous to the expression for the value of the transmission coefficient of a traditional Fabry–Pérot interferometer. In the case of TM polarization, when the Brewster condition is fulfilled at the interlayer boundaries, the Floquet–Bloch wave has the form of homogeneous plane waves in the layers of a photonic crystal.

Keywords: electromagnetic waves, periodic medium, multilayer mirror, one-dimensional photonic crystal, Floquet–Bloch waves

• **Submitted:** 31.05.2023 • **Revised:** 12.04.2024 • **Accepted:** 09.10.2024

For citation: Nurligareev D.Kh., Nedospasov I.A., Kharitonova K.Yu. Reflections of linearly polarized electromagnetic waves from a multilayer periodic mirror. *Russ. Technol. J.* 2024;12(6):69–79. https://doi.org/10.32362/2500-316X-2024-12-6-69-79

Financial disclosure: The authors have no financial or proprietary interest in any material or method mentioned.

The authors declare no conflicts of interest.

НАУЧНАЯ СТАТЬЯ

Отражение линейно поляризованных электромагнитных волн от многослойного периодического зеркала

Д.Х. Нурлигареев [1, @], И.А. Недоспасов [1, 2], К.Ю. Харитонова [1]

[1] *МИРЭА – Российский технологический университет, Москва, 119454 Россия*
[2] *Институт радиотехники и электроники им. В.А. Котельникова РАН, Москва, 125009 Россия*
[@] *Автор для переписки, e-mail: nurligareev@mirea.ru*

Резюме

Цели. Цель работы – теоретическое и экспериментальное исследование углового спектра отражения линейно поляризованных электромагнитных волн от многослойного периодического зеркала на прозрачной подложке, вывод точных аналитических выражений для коэффициентов отражения и прохождения, обобщающих случаи падения плоских TE-(transverse electric) и TM-мод (transverse magnetic) на ограниченные периодические структуры со ступенчатым профилем показателя преломления.

Методы. Теоретический анализ задачи отражения основан на поиске точных аналитических решений в виде волн Флоке – Блоха, представленных в форме неоднородных волн, в области периодически структурированных сред. На основе того факта, что в ограниченном одномерном фотонном кристалле возможно существование одиночной волны Флоке – Блоха, предлагается искать точные решения волнового уравнения в виде линейной комбинации волн Флоке – Блоха, бегущих в разные стороны. Канонические формы рассматриваемых периодических структур позволяют достаточно просто осуществлять переход от случая TE-поляризации к TM-типу в дисперсионных соотношениях и выражениях для углового спектра отражения.

Результаты. Рассмотрены случаи отражения линейно поляризованного излучения для следующих случаев: плоской границы двух диэлектриков, тонкой плоскопараллельной пластины и многослойного диэлектрического зеркала. Получены точные аналитические выражения для коэффициентов отражения и прохождения, обобщающие случаи падения волн TE- и TM-поляризаций на ограниченный одномерный фотонный кристалл. Экспериментально измерен коэффициент пропускания плоской TE-волны для многослойного диэлектрического зеркала, напыленного на тонкую стеклянную пластину.

Выводы. Получено количественное и качественное согласование экспериментальных измерений коэффициента пропускания плоской волны, падающей из полупространства на ограниченный фотонный кристалл с теоретическими вычислениями. Показано, что полученные выражения для коэффициента пропускания ограниченного одномерного фотонного кристалла определяются интерференцией волн Флоке – Блоха,

представленных в форме неоднородных волн, и могут быть приведены к виду, аналогичному для величины коэффициента прохождения традиционного интерферометра Фабри – Перо. В случае ТМ-поляризации при выполнении условия Брюстера на межслойных границах волна Флоке – Блоха имеет вид однородных плоских волн в слоях фотонного кристалла.

Ключевые слова: электромагнитные волны, периодическая среда, многослойное зеркало, одномерный фотонный кристалл, волны Флоке – Блоха

• **Поступила:** 31.05.2023 • **Доработана:** 12.04.2024 • **Принята к опубликованию:** 09.10.2024

Для цитирования: Нурлигареев Д.Х., Недоспасов И.А., Харитонова К.Ю. Отражение линейно поляризованных электромагнитных волн от многослойного периодического зеркала. *Russ. Technol. J*. 2024;12(6):69–79. https://doi.org/10.32362/2500-316X-2024-12-6-69-79

Прозрачность финансовой деятельности: Авторы не имеют финансовой заинтересованности в представленных материалах или методах.

Авторы заявляют об отсутствии конфликта интересов.

INTRODUCTION

The study of the peculiarities of light propagation in layered media whose properties are constant on planes perpendicular to a fixed direction is a well-known problem in optics. As a historical example, we can cite the classical works of Stokes [1] and Rayleigh [2], in which the phenomena arising from the passage of light through crystalline periodic structures were considered. The wave equation in layered periodic media is known to be reducible to Hill's differential equation; in such media, there may exist transmission and non-transmission windows for the passing radiation [2]. In the one-dimensional case, the solution of the wave equation in layered periodic media is written in the Floquet form [3], while in the three-dimensional case it is written in the Bloch wave form [4]. A fairly detailed background is given in the review [5]. The relatively recent and still growing interest in the study of wave propagation through one-dimensional periodic structures in optics is due to the possibility for such structures, with relative simplicity of fabrication, to provide a complete reflection in a given frequency range of frequencies and angles of incidence for different polarization states [6, 7]. In this connection, one-dimensional periodic structures can be considered as one-dimensional photonic crystals (1D-PC); as such, light propagation in them can be described using the Floquet–Bloch approach [8–13]. However, since the elements of the Floquet–Bloch wave (FBW) theory are not currently developed in sufficient detail, numerical methods are usually used to describe the propagation of electromagnetic waves through such structures. Numerical calculations performed using complex transfer matrices do not provide a clear picture of the explicit quantitative dependence of the studied physical processes on the geometrical and material parameters of the periodic structure [14–16]. In [8, 9], for the case of transverse electric (TE) polarized radiation[1], the FBW in the 1D-PC is represented in the form of an inhomogeneous wave. In particular, the functions describing the amplitude and phase profiles of the wave and the reflection coefficient of a plane wave at the boundary of the 1D-PC were obtained.

At present, various questions on the application of 1D-PC are being actively investigated in the literature. In particular, the transmission spectra of 1D-PC having a complex sequence of superconductor-semiconductor layers are investigated in [17]; the application of photonic crystal as a biosensor based on graphene is considered in [18]. Studies of 1D-PC seem to be particularly relevant due to the possibility of experimental realization of bound or localized states in a continuous spectrum [19]. Thus, the use of birefringent media in combination with 1D-PC was recently proposed, where the existence of such modes is supported at the Brewster angle of incidence.

Therefore, the main objectives of the present work are to extend the developed representation of the FBW in the form of an inhomogeneous wave to the case of transverse magnetic (TM) polarized radiation[2], as well as to experimentally demonstrate the effect of the FBW interference on the magnitude of reflection and transmission coefficients for the case of incidence of a plane linearly polarized wave from a homogeneous medium on a bounded 1D-PC.

[1] Transverse electric, linearly (plane) polarized wave with the electric field intensity vector $\vec{E}$ oriented perpendicular to the plane of incidence.

[2] Transverse magnetic, linearly (plane) polarized wave with the magnetic field intensity vector $\vec{H}$ oriented perpendicular to the plane of incidence.

1. REFLECTION OF A PLANE WAVE AT THE BOUNDARY OF TWO DIELECTRICS AND FROM A THIN PLATE

In the present work, we consider the conditions for the passage of a plane electromagnetic wave through the interface of two media for three characteristic cases (Fig. 1): reflection at the boundary of two homogeneous dielectrics, reflection from a thin dielectric plate, and reflection from a multilayer dielectric mirror (bounded by an 1D-PC).

Let us write the field distribution $E(x, z, t)$ ($H(x, z, t)$) of the waves propagating in the x-z-plane (plane of incidence) as a scalar function $\Psi(x, z, t)$:

$$\left.\begin{matrix} E(x,z,t) \\ H(x,z,t) \end{matrix}\right\} = \Psi(x,z,t) = \Psi(x)\mathrm{e}^{i(\omega t-\beta z)}. \qquad (1)$$

When the plane wave $\hat{P}_a$

$$\hat{P}_a = P_a \exp[i(\phi_p + \omega t - \kappa_a x - \beta z)]$$

is incident on the interface of dielectrics with refractive indices n_a, n_b ($n_a{}^2 = \varepsilon_a$, $n_b{}^2 = \varepsilon_b$) and dielectric permittivities $\varepsilon_a, \varepsilon_b$, the parameter β is the longitudinal component of the wave vectors ($\beta = k_0 n_a \sin\varphi$) determined by the angle of incidence φ counted from the normal to the interface (x = 0) of the media. The amplitude Q_a of the reflected wave $\hat{Q}_a$

$$\hat{Q}_a = Q_a \exp[i(\phi_q + \omega t + \kappa_a x - \beta z)]$$

is determined by the Fresnel reflection coefficient r_a and the amplitude P_a of the incident wave ($Q_a = r_a P_a$), while the amplitude G_b of the refracted wave

$$\hat{G}_b = G_b \exp[i(\phi_g + \omega t - \kappa_b x - \beta z)]$$

is determined by the amplitude transmission coefficient t_b ($G_b = t_b P_a$). Here ϕ_p, ϕ_q, ϕ_g are the initial phases, κ_a, κ_b are the transverse components of wave vectors ($\kappa_a = \sqrt{k_0^2 n_a^2 - \beta^2}$, $\kappa_b = \sqrt{k_0^2 n_b^2 - \beta^2}$), t is time, $k_0 = \omega/c$ is the wave vector of radiation in vacuum, and ω is the frequency of radiation.

Considering the component of the field-vector $\vec{E}$ ($\vec{H}$) perpendicular to the plane of incidence in case of TE- or TM-polarized waves, it is convenient to introduce parameters χ_a, χ_b, which are associated with transverse wave vectors: $\chi_a = \kappa_a / (\varepsilon_a)^\tau$, $\chi_b = \kappa_b / (\varepsilon_b)^\tau$, where τ is the efficient polarization parameter equal to zero (unity) in this case. The Fresnel formulas for the amplitudes of reflected and refracted light can be presented in the same form for the cases of TE- and TM-polarized wave:

$$\begin{gathered} r_a = Q_a / P_a = (\chi_a - \chi_b)/(\chi_a + \chi_b), \\ t_a = G_b / P_a = 2\chi_a / (\chi_a + \chi_b), \\ t_a - r_a = 1. \end{gathered} \qquad (2)$$

If the parameters χ_a, χ_b are real, the amplitude coefficient t_a is always positive, and the phase of the refracted wave at the interface coincides with the phase of the incident wave. At $\chi_a > \chi_b$ and $r_a > 0$, the phase of the reflected wave also coincides with the phase of the incident wave, while at $\chi_a < \chi_b$ and $r_a < 0$, a phase shift equal to π occurs for the reflected wave. It is convenient to equate the initial phases of the numerical values ϕ_p, ϕ_q, ϕ_g, which coincide to the nearest 2π multiplied by an arbitrary integer, to zero. In this case, the coefficients r_a, t_a are real. However, in the general case, when the initial phases are ϕ_p, ϕ_q, ϕ_g we will use the parameter $\hat{r}_a$ ($\hat{r}_a = r_a \exp(i\phi_{ra})$, $\phi_{ra} = \phi_q - \phi_p$) to denote the complex reflection coefficient. The energy coefficients of reflection R_a and transmission T_a are represented as follows:

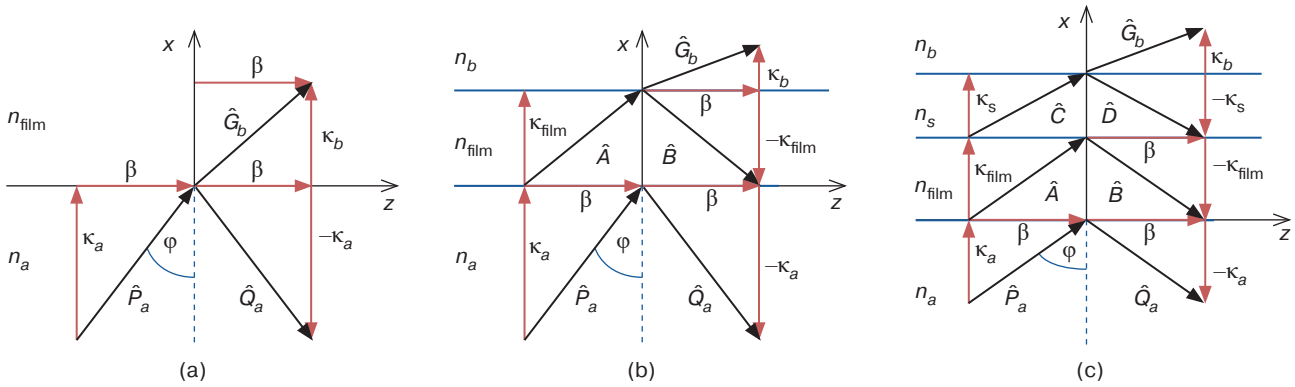

Fig. 1. Directions of the wave vector components $\kappa_a, \kappa_b, \kappa_{film}, \beta$ at the reflection: (a) at the interface of two dielectrics, (b) from a thin dielectric plate, (c) from the 1D-PC

$$R_a = Q_a^2 / P_a^2 = |r_a|^2 = (\chi_a - \chi_b)^2 / (\chi_a + \chi_b)^2;$$
$$T_a = |t_a|^2 \cdot (\chi_b / \chi_a) = 4\chi_a\chi_b / (\chi_a + \chi_b)^2. \quad (3)$$

The energy coefficients R_a and T_a are equal to the ratio of the average energy flux of the reflected and transmitted waves to the average energy flux of the incident wave, respectively. Here, only transverse (i.e., parallel to the x-axis) components of the energy fluxes in the medium layers are considered. The condition of continuity of the transverse energy flux is satisfied:

$$\chi_a(P_a^2 - Q_a^2) = \chi_b G_b^2. \quad (4)$$

In the case of a plane wave $\hat{P}_a$ incident from a medium with refractive index n_a ($x < 0$) onto a dielectric plate of thickness h and refractive index n_{film} ($n_{\text{film}}^2 = \varepsilon_{\text{film}}$, $\varepsilon_{\text{film}}$ is the dielectric permittivity of the plate material) (Fig. 1b), a reflected wave $\hat{Q}_a$, appears in the area $x < 0$, while in the area $x > h$ the wave $\hat{G}_b$ is refracted into the medium having a refractive index n_b. The field inside the plate can be represented by a forward and an inverse waves $\hat{A}, \hat{B}$

$$\hat{A} = A\exp[i(\phi_a + \omega t - \kappa_{\text{film}} x - \beta z)],$$
$$\hat{B} = B\exp[i(\phi_b + \omega t + \kappa_{\text{film}} x - \beta z)],$$

where $\kappa_{\text{film}} = \sqrt{k_0^2 n_{\text{film}}^2 - \beta^2}$. These waves are called partial waves.

For complex amplitudes $\hat{A}, \hat{B}, \hat{G}_b$, the equations $B = \hat{r}_b A$, $G_b = A + B$, where $\hat{r}_b = r_b \exp(i\phi_{rb})$ is the Fresnel reflection coefficient at the $x = h$, are valid:

$$\hat{r}_b = (\chi_{\text{film}} - \chi_b) / (\chi_{\text{film}} + \chi_b),$$
$$\chi_{\text{film}} = \kappa_{\text{film}} / (\varepsilon_{\text{film}})^\tau,\ \chi_b = \kappa_b / (\varepsilon_b)^\tau. \quad (5)$$

Initial phases ϕ_a, ϕ_b, ϕ_g coincide with an accuracy up to the value of 2π multiplied by an arbitrary integer; here it is convenient to select their numerical values equal to $\phi_g = 0$. In this case, the phases of waves $\hat{A}, \hat{B}$ at the boundary $x = 0$ will be equal, respectively, to $\pm\phi_h$ (where $\phi_h = \kappa_{\text{film}} h$ is the phase delay arising for a partial wave during the passage of a layer of thickness h).

Now we will write down formulas for the reflection coefficient r_a at the boundary $x = 0$ both reflectance (R_a) and transmittance (T_a) of the plate:

$$r_a = \frac{Q_a}{P_a} = \left(\frac{\left(1 - \frac{\chi_b}{\chi_a}\right)^2 + \left(\frac{\chi_b}{\chi_{\text{film}}} - \frac{\chi_{\text{film}}}{\chi_a}\right)^2 \text{tg}^2\phi_h}{\left(1 + \frac{\chi_b}{\chi_a}\right)^2 + \left(\frac{\chi_b}{\chi_{\text{film}}} + \frac{\chi_{\text{film}}}{\chi_a}\right)^2 \text{tg}^2\phi_h} \right)^{1/2}, \quad (6)$$
$$R_a = \frac{Q_a^2}{P_a^2} = r_a^2, \quad T_a = 1 - R_a.$$

Formulas (6) are in agreement with the well-known Airy formulas obtained when considering multipath wave interference in a transparent plate [20]. Thus, according to (6), at values $2\phi_h = 2\pi m$ and $\pi(2m + 1)$ for R_a, extreme values equal to $(\chi_a - \chi_b)^2 / (\chi_a + \chi_b)^2$ and $(\chi_a\chi_b - \chi_{\text{film}}^2)^2 / (\chi_a\chi_b + \chi_{\text{film}}^2)^2$, respectively, are reached. In particular, in the interference reflection minima that arise, for example, when the simultaneous fulfillment of conditions (1) $2\phi_h = 2\pi m$ and $\chi_a = \chi_b$ or (2) $2\phi_h = \pi(2m+1)$ and $\chi_a \neq \chi_b$, $\chi_{\text{film}}^2 = \chi_a\chi_b$ must be reached, the values of R_a are equal to zero. In the general case of variation of the angle of incidence φ of the incident wave $\hat{P}_a$, alternating maxima and minima of the intensity of the reflected $\hat{Q}_a$ and refracted $\hat{G}_b$ waves should be observed.

2. PLANE WAVE REFLECTION FROM A MULTILAYER DIELECTRIC MIRROR

Let us consider a multilayer dielectric mirror (Fig. 1c) consisting of alternating f- and s-layers having refractive indices n_f and n_s and thicknesses h and s, respectively, which have been placed between homogeneous dielectric media having refractive indices n_a ($x < 0$) и n_b ($x > H$). It is convenient to represent this structure as an 1D-PC framed by two homogeneous dielectric media, which are formed by multiple repetition of a cell composed of two layers (f- and s-layers) of the size Λ ($\Lambda = h + s$). Figure 1c shows one such cell framed by two homogeneous media. When a plane wave $\hat{P}_a$ is incident on the lower boundary ($x = 0$) of the 1D-PC, reflected $\hat{Q}_a$ and refracted $\hat{G}_b$, respectively, plane waves are generated in the regions $x < 0$ and $x > H$ to excite forward and backward FBW in the region $H > x > 0$. We will give a description of TE-polarized FBW for the case of unbounded 1D-PC in [8, 9]. In this article, we present these waves for the cases of TE- and TM-polarized radiation in a single inhomogeneous wave form $\Psi_u(x, z, t)$:

$$\Psi_u(x,z,t) = \Psi_u(x)\exp\{i[(\omega t + \Phi(x,z)]\}. \quad (7)$$

Here, the functions $\Psi_u(x)$ and $\Phi(x, z)$ define the distribution of the amplitude and phase of the wave, respectively. Surfaces of constant amplitude are planes perpendicular to the x-axis. Function $\Psi_u(x)$ is periodic with a period equal to Λ, so that by introducing local coordinates $\xi_f = x - h/2 - \Lambda m$ and $\xi_s = x - s/2 - h - \Lambda m$ (where m is the number of the 1D-PC cell), which are counted from the centers of the corresponding layers, we can write for it:

$$\Psi_u(x)=\begin{cases}\Psi_f(\xi_f)=\left(A^2+B^2+2AB\cdot\cos(2\kappa_f\xi_f)\right)^{1/2}, \\ \qquad -h/2<\xi_f<h/2, \\ \Psi_s(\xi_s)=\left(C^2+D^2+2CD\cdot\cos(2\kappa_s\xi_s)\right)^{1/2}, \\ \qquad -s/2<\xi_s<s/2.\end{cases} \quad (8)$$

The phase function $\Phi(x, z)$ depends on two coordinates; in general, the FBW is non-planar:

$$\Phi(x,z)=\phi_0-K\Lambda(m+\varsigma)-\beta z-\phi_u(x), \quad (9)$$

where ϕ_0 has the meaning of the initial phase of the wave, the phase parameter $\varsigma=0$ in *f*-layers at $\Lambda m<x<\Lambda m+h$ and $\varsigma=1/2$ in *s*-layers at $\Lambda m+h<x<\Lambda(m+1)$, while $\phi_u(x)$ is the nonlinear component of the phase function $\Phi(x, z)$, which sets the shape of the profile of the FBW wave surfaces. The constant *K* (Bloch wave number) can be found from the dispersion equation [8]:

$$\cos K\Lambda=\cos(\kappa_f h)\cos(\kappa_s s)- \\ -\frac{1}{2}\left(\frac{\chi_s}{\chi_f}+\frac{\chi_f}{\chi_s}\right)\sin(\kappa_f h)\sin(\kappa_s s),\ \beta<k_0 n_s. \quad (10)$$

Distribution (8) of the FBW field in the 1D-PC layers is given by the amplitude coefficients *A*, *B*, *C*, *D* of the partial waves, which are also real at real κ_f, κ_s, and *K,* and depend on the parameters of the medium cell and the Bloch wave number [8, 9]:

$$\begin{cases}A=A_0\sin\left((\kappa_f h-\kappa_s s+K\Lambda)/2\right)\times \\ \qquad\times\sin\left((\kappa_f h+\kappa_s s+K\Lambda)/2\right), \\ B=A_0\sin\left((\kappa_f h-\kappa_s s+K\Lambda)/2\right)\times \\ \qquad\times\sin\left((\kappa_f h-\kappa_s s-K\Lambda)/2\right)\times \\ \qquad\times(\chi_s-\chi_f)/(\chi_s+\chi_f), \\ C=A_0\sin\left((\kappa_f h+\kappa_s s+K\Lambda)/2\right)\times \\ \qquad\times\sin(\kappa_f h)(\chi_s+\chi_f)/2\chi_s, \\ D=A_0\sin\left((\kappa_f h-\kappa_s s+K\Lambda)/2\right)\times \\ \qquad\times\sin(\kappa_f h)(\chi_s-\chi_f)/2\chi_s.\end{cases} \quad (11)$$

Formulas (11), which are a generalization of formulas (12) of [8], are used to describe the features of TM-polarized waves, which have not been considered earlier. For example, according to (11) for the case of TM-polarized radiation, if the condition $\chi_s=\chi_f$ is fulfilled, the *B* and *D* amplitudes of the partial waves are equal to zero, while the coefficients *A* and *C* are equal to each other. FBW in *f*- and *s*-layers of the photonic crystal has the form of homogeneous plane waves for which the angles of incidence α_f, α_s on the interlayer boundaries are in agreement with the Brewster condition $\mathrm{tg}\alpha_f=n_s/n_f$, $\mathrm{tg}\alpha_s=n_f/n_s$. The dispersion equation (10) reduces to the following equations: $\cos K\Lambda=(\kappa_f h+\kappa_s s)$.

Parameter A_0 in (11) plays the role of the FBW amplitude. In a confined 1D-PC for forward and backward waves, this parameter may differ. It makes sense to introduce into consideration the amplitude reflection coefficient r_u at the boundary $x = H$ as the ratio of the amplitudes A_{down} and A_{up} (in this case we consider these parameters to be valid) of the backward and forward FBW, respectively. Considering the continuity conditions of the tangential components of the wave fields at the interlayer boundaries inside the 1D-PC and at the boundaries of the 1D-PC with the adjacent media, we can obtain for the coefficient r_u:

$$r_u=\frac{A_{\mathrm{down}}}{A_{\mathrm{up}}}=\frac{1-F_u}{1+F_u}, \\ F_u=\frac{\chi_b}{\chi_f}\left(\frac{A-B}{A+B}+\frac{4AB}{A^2-B^2}\cos^2\phi_h\right). \quad (12)$$

The modulus of the amplitude reflection coefficient r_{au} and the energy coefficients of reflection R_{au} and transmittance T_{au} of the plane wave $\hat{P}_a$, which are obtained for the 1D-PC taking into account the interference of the forward and backward FBW, are found from the following formulas:

$$r_{au}=\frac{Q_a}{P_a}= \\ =\left(\frac{r_a^2+r_u^2+2r_a r_u\cos(2\phi_{\text{p.-q.}}+2\phi_{\text{p.-d.}})}{1+r_a^2r_u^2+2r_a r_u\cos(2\phi_{\text{p.-q.}}+2\phi_{\text{p.-d.}})}\right)^{1/2}, \quad (13) \\ R_{au}={r_{au}}^2,\ T_{au}=1-R_{au},$$

where r_a is the modulus of the amplitude reflection coefficient from the semi-infinite 1D-PC:

$$r_a=\left(\frac{(\chi_a-\chi_f)^2A^2+(\chi_a+\chi_f)^2B^2+2AB(\chi_a^2-\chi_f^2)\cos\kappa_f h}{(\chi_a+\chi_f)^2A^2+(\chi_a-\chi_f)^2B^2+2AB(\chi_a^2-\chi_f^2)\cos\kappa_f h}\right)^{1/2}, \quad (14)$$

$2\phi_{\text{p.-q.}}$, $2\phi_{\text{p.-d.}}$ are the wave phase matching parameters[3] at the boundaries $x = 0$ and $x = h$:

$$2\phi_{\text{p.-q.}} = \\ = \operatorname{arctg}\frac{(\chi_f^2 - \chi_a^2)(A^2 - B^2)\sin 2\phi_h}{(\chi_f^2 - \chi_a^2)(A^2 + B^2) - 2AB(\chi_f^2 + \chi_a^2)\cos 2\phi_h} + \\ + \pi m_{\text{p.-q.}}, \quad (15)$$

$$2\phi_{\text{p.-d.}} = 2K\Lambda N + 2\operatorname{arctg}\left(\operatorname{tg}\phi_h (A - B)/(A + B)\right). \quad (16)$$

Here, parameter $\phi_{\text{p.-d.}}$ with an accuracy to the value 2π multiplied by an integer is equal to the phase delay arising for the FBW at the double passage of the confined 1D-PC; parameter N sets the number of cells of the confined 1D-PC; parameter $\phi_{\text{p.-q.}}$ is equal to the average value of the phases of the incident and reflected waves at the boundary $x = 0$; numerical values of the parameter $m_{\text{p.-q.}}$ variation of the cell parameters of the 1D-PC and FBW can take values 0 ± 1. Analysis of the formulas (13–16) shows that, at variation of the angle of incidence φ of a plane wave on the 1D-PC, interference maxima and minima of intensities for the reflected and refracted waves should occur.

3. EXPERIMENTAL DESIGN AND RESULTS

In the experiments, the multilayer interference dielectric mirror used as the structure under study was produced on a high-vacuum unit for ion-beam deposition of dielectric layers Aspira-150 (Izovac, Belarus)[4]. This structure (sample) was a glass substrate (standard slide glass was used as a substrate material; substrate thickness is 0.7 mm; refractive index is 1.52) with 10 pairs of alternating layers of Nb_2O_5 (niobium oxide (V); thickness is 0.11 μm; refractive index is 2.27) and SiO_2 (quartz glass; thickness is 0.18 μm; refractive index is 1.48) deposited on its surface. Material parameters of the structure layers and substrate were provided by the manufacturer. In the experiments, the dependence of the transmission coefficient T_a of the sample on the angle of incidence φ of the laser light beam was studied. Figure 2 shows the scheme of the experiment. The intensity of helium-neon laser radiation (*1*), which passed through the polarizer (*2*) and the sample (*4*) mounted on the goniometer stage (*3*), was measured by the photodetector (*5*).

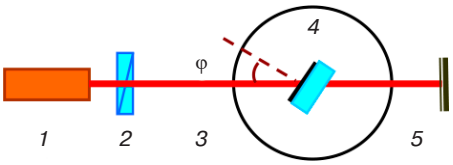

Fig. 2. Experimental design

According to preliminary estimates made by the formulas (6), the angular distance between neighboring maxima of the transmitted light intensity should be the largest at incidence angles close to zero (normal incidence mode) and incidence angles close to 90° (sliding incidence mode). The angular width of interference resonances in these modes is the largest, which should also significantly simplify the confident registration of the maxima and minima of the intensity of transmitted radiation at variation of the angle of incidence φ.

For the case of TE-polarized radiation at variation of the angle of incidence φ within the range from 0° to 8°, Fig. 3 shows the measured intensity of I_{trans} radiation (in arbitrary units, a.u.) that passed through the sample together with the transmittance coefficient of the T_a glass plate calculated by the formulas (6). In full accordance with the preliminary calculations, the angular distance between the resonances and their angular width decrease as the angle of incidence increases from 0° to 8°.

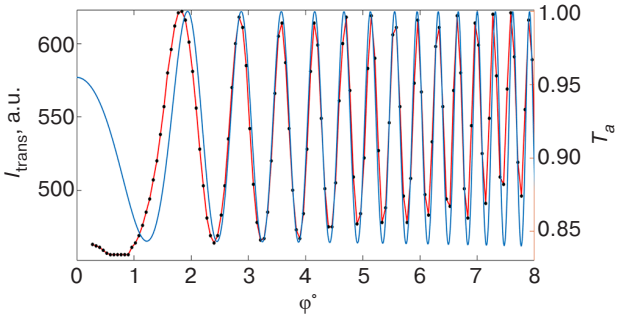

Fig. 3. Measured I_{trans} intensity (red line with dots) and calculated transmittance function T_a of a plate with $n_b = 1.52$ and $d = 0.7$ mm (solid blue line) as a function of the angle of incidence φ. Emission wavelength is 0.6328 μm

Figure 4 depicts the measured intensity of I_{trans} radiation (in a.u.), which passed through the sample, and the transmittance T_a of the glass plate calculated by the formulas (6) as a function of the slip angle θ $(\theta = \pi/2 - \varphi)$ for the case of TE-polarized radiation.

[3] Index p.-d. is a phase delay; in p.-q. index the letter p indicates the P_a wave, and the letter q indicates the Q_a wave.
[4] http://izovac.by/ (in Russ.). Accessed September 27, 2024.

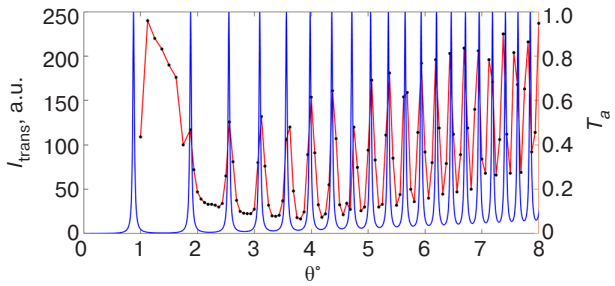

Fig. 4. Measured I_{trans} intensity (red line with dots) and calculated transmission function T_a of a plate with n_b = 1.52 and d = 0.7 mm (solid blue line) as a function of slip angle θ. Emission wavelength is 0.6328 μm

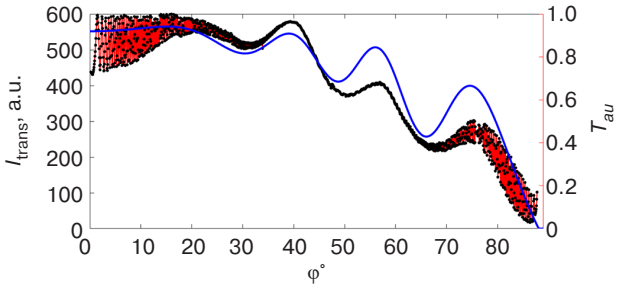

Fig. 5. 1D-PC transmittance function T_{au} (solid blue line) and measured I_{trans} intensity as a function of the angle of incidence φ (red color, black dots). The wavelength is 0.6328 μm

In this slip-fall mode, a marked decrease in the angular width and angular distance between the observed resonances is clearly recorded when increasing the slip angle θ in the presented range from 0° to 8°, which is also in full agreement with the preliminary estimates.

The dependencies presented in Figs. 3 and 4 clearly demonstrate the presence of interference resonances of a thin dielectric plate. At the same time, for the presented I_{trans} dependencies, the presence of a significant increase in transmittance in the intensity maxima and minima both at increasing the angle of incidence φ (in the regime close to normal incidence) and at increasing the slip angle θ (in the regime close to slip incidence) should be noted. These features are explained by the influence of Nb_2O_5 and SiO_2 layers deposited on the glass plate, the interference of waves in which should lead to additional modulations of the intensity of radiation passing through the sample.

Figure 5 shows the measured intensity of I_{trans} TE-polarized He-Ne laser radiation (in a.u.) that passed through the sample (red line, black dots) and the 1D-PC transmittance function of T_{au} with the following cell parameters (13): h = 0.11 μm, s = 0.18 μm, n_f = 2.27, n_s = 1.48 (solid blue line) for the case of variation of the angle of incidence φ in the range from 0° to 90°. The crystal consists of 10 cells framed by two homogeneous media with refractive indices: n_a = 1, n_b = 1.52. According to the calculations, four interference transmission maxima should be observed as a result of FBW interference in the 1D-PC at the variation of the angle of incidence φ in the range from 0° to 90°.

The transmittance of the considered sample is determined by superposition of the interference resonances of the glass plate on the interference resonances of the 1D-PC. Here, the transmittance resonances and their corresponding reflection resonances for the glass plate are clearly registered with the used laser only in a limited range of incidence angles φ and slip angles θ not exceeding 20° (Figs. 6a and 6b).

(a) (b) (c)

Fig. 6. Images of the reflected laser beam at the values of the angle of incidence φ: (a) 12°; (b) 75°; (c) 50°

Within the range of incidence angles φ from 30° to 70°, the angular width of the glass plate resonances is significantly smaller than the angular divergence of the laser beam (Fig. 6c); moreover, these fast intensity modulations are not resolved. At the same time, the slow intensity modulations due to FBW interference are in full agreement with the theory.

The obtained results of the experiments and theoretical simulation agree quite well to demonstrate the presence of interference of FBW in 1D-PC, as a result of which the radiation intensity in the maxima and minima of interference resonances of a thin glass plate can change significantly. Thus, the representation of FBW in the form of inhomogeneous waves can be useful for calculating and optimizing the parameters of optical elements and devices that use interference effects in multilayer periodic structures.

CONCLUSIONS

In this article, the exact expressions for the reflection and transmission coefficients for the case of a confined 1D-PC with a stepped refractive index profile are obtained on the basis of wave representation in the form of a linear combination of Floquet and Bloch waves. A qualitative agreement of experimental measurements of the transmission coefficient of a plane TE-wave incident from a half-space on a confined photonic crystal with the theoretical calculations has been established. The graph (Fig. 5) clearly depicts fast intensity modulations, which is in agreement with the well-known Airy functions

obtained in the case of multipath wave interference in a transparent plate at a variation of the angle of incidence of the wave. Since the thickness of the glass substrate is many times greater than the thickness of the photonic crystal and the wavelength of the laser radiation, which leads to a large phase delay, rapidly alternating maxima and minima of intensity should be observed, which are difficult to resolve in measurements. Slow intensity modulations, in turn, are due to the interference of the FBW in the photonic crystal, where the phase lag is much smaller at a small Bloch wave vector.

ACKNOWLEDGMENTS

I.A. Nedospasov thanks the Russian Science Foundation (grant No. 22-79-10267) for financial support.

Authors' contributions

D.Kh. Nurligareev—derivation of exact formulas for reflection and transmission coefficients for the cases of a limited one-dimensional photonic crystal with a stepped refractive index profile and a multilayer dielectric mirror; writing the Introduction, Conclusions, and the 1st and 2nd sections of the article.

I.A. Nedospasov—performing calculations and plotting dependencies of intensities and transmission functions of the studied structures; writing the Abstract and the 3rd section of the article.

K.Yu. Kharitonova—performing measurements and constructing experimental dependencies of radiation intensities; writing the 3rd section of the article.

REFERENCES

1. Lord Rayleigh. On the maintenance of vibrations by forces of double frequency, and on the propagation of waves through a medium endowed with periodic structure. *Phyl. Mag. Ser. 5.* 1887;24(147):145–159. https://doi.org/10.1080/14786448708628074
2. Lord Rayleigh. On the remarkable phenomenon of crystalline reflection described by Prof. Stokes. *Phyl. Mag. Ser. 5.* 1888;26(160):256–265. https://doi.org/10.1080/14786448808628259
3. Floquet G. Sur les equations differentielles linearies a coeffients periodiques. (*Annales scientifiques de l'École Normale Supérieure, Serie 2*) *Ann. Ecole Norm. Sup.* 1883;12:47–88. https://doi.org/10.24033/asens.220
4. Bloch F. Uber die Quantenmechanic der elektronen in kristallgittern. *Z. Phys.* 1929;52(85):555–600. https://doi.org/10.1007/BF01339455
5. Elachi C. Waves in active and passive periodical structures: A review. *Proc. IEEE.* 1976;64(12):1666–1698. https://doi.org/10.1109/PROC.1976.10409, available from URL: https://core.ac.uk/download/pdf/216300643.pdf
6. Winn J.N., Fink Y., Fan S., Joannopoulos J.D. Omnidirectional reflection from a one-dimensional photonic crystal. *Opt. Lett.* 1998;23(20):1573–1575. https://doi.org/10.1364/OL.23.001573
7. Chigrin D.N., Lavrinenko A.V., Yarotsky D.A., Gaponenko S.V. Observation of total omnidirectional reflection from a one-dimensional dielectric lattice. *Appl. Phys. A.* 1999;68(1):25–28. https://doi.org/10.1007/s003390050849
8. Nurligareev D.K., Sychugov V.A. Propagation of light in a one-dimensional photonic crystal: analysis by the Floquet–Bloch function method. *Quantum Electron*. 2008;38(5):452–461. https://doi.org/10.1070/QE2008v038n05ABEH013653
[Original Russian Text: Nurligareev D.K., Sychugov V.A. Propagation of light in a one-dimensional photonic crystal: analysis by the Floquet–Bloch function method. *Kvantovaya elektronika*. 2008;38(5):452–461. Available from URL: https://www.elibrary.ru/tteynf]
9. Nurligareev D.K. Floquet-Bloch waves of a one-dimensional photonic crystal: a general theory. *Naukoemkie tekhnologii.* 2009;10(9):12–23 (in Russ.).
10. Nurligareev D.K., Sychugov V.A. Technique for determining the cell parameters of the confined one-dimensional photonic crystal, based on the Floquet-Bloch formalism. *Bull. Lebedev Phys. Inst.* 2012;39(2):33–37. https://doi.org/10.3103/S1068335612020017
[Original Russian Text: Nurligareev D.K., Sychugov V.A. Technique for determining the cell parameters of the confined one-dimensional photonic crystal, based on the Floquet-Bloch formalism. *Kratkie soobshcheniya po fizike*. 2012;2:3–10 (in Russ.). Available from URL: https://www.elibrary.ru/ouillp]
11. Caffrey S., Morozov G.V., Sprung D.W., Martorell J. Floquet–Bloch solutions in a sawtooth photonic crystal. *Opt. Quantum Electron.* 2017;49(3):112. https://doi.org/10.1007/s11082-017-0939-1
12. Ibrahim A., Sprung D.W.L., Morozov G.V. Construction and Floquet–Bloch analysis of analytically solvable Hill equations with smooth potentials. *J. Opt. Soc. Am. B.* 2018;35(6):1223–1232. https://doi.org/10.1364/JOSAB.35.001223
13. Shmat'ko A.A., Mizernik V.N., Odarenko E.N. Floquet-Bloch waves in magnetophotonic crystals with transverse magnetic field. *J. Electromagn. Waves Appl.* 2020;34(12):1667–1679. https://doi.org/10.1080/09205071.2020.1780955
14. Yeh P., Yariv A., Hong C.S. Electromagnetic propagation in periodic stratified media. 1. General theory. *J. Opt. Soc. Am.* 1977;67(4):423–438. https://doi.org/10.1364/JOSA.67.000423
15. Walpita L.M. Solutions for planar optical waveguide equations by selecting zero elements in a characteristic matrix. *J. Opt. Soc. Am. A.* 1985;2(4):595–602. https://doi.org/10.1364/JOSAA.2.000595
16. Konopsky V. Design of 1D Photonic Crystals Sustaining Optical Surface Modes. *Coatings.* 2022;12(10):1489. https://doi.org/10.3390/coatings12101489

17. Segovia-Chaves F., Vinck-Posada H., Trabelsi Y., Ali N.B. Transmittance spectrum in a one-dimensional photonic crystal with Fibonacci sequence superconductor–semiconductor. *Optik.* 2020;217:164803. https://doi.org/10.1016/j.ijleo.2020.164803
18. Panda A., Pukhrambam P.D., Wu F., Belhadj W. Graphene-based 1D defective photonic crystal biosensor for real-time detection of cancer cells. *Eur. Phys. J. Plus.* 2021;136(8):809. https://doi.org/10.1140/epjp/s13360-021-01796-z
19. Liu Z., Li X., Chen C., Wang X., Gao W., Ye W., Li L., Liu J. Bound states in the continuum in asymmetric one-dimensional photonic crystal systems guided by anisotropy. *Opt. Express.*2023;31(5):8384–8392. https://doi.org/10.1364/OE.482894
20. Born M., Wolf E. *Osnovy optiki* (*Principles of Optics*). Transl. from Engl. Moscow: Nauka; 1970. 856 p. (in Russ.). [Born M., Wolf E. *Principles of Optics*. Oxford, London, Edinburg, New York, Paris, Frankfurt: Pergamon Press; 1964, 856 p.]

СПИСОК ЛИТЕРАТУРЫ

1. Lord Rayleigh. On the maintenance of vibrations by forces of double frequency, and on the propagation of waves through a medium endowed with periodic structure. *Phyl. Mag. Ser. 5.* 1887;24(147):145–159. https://doi.org/10.1080/14786448708628074
2. Lord Rayleigh. On the remarkable phenomenon of crystalline reflection described by Prof. Stokes. *Phyl. Mag. Ser. 5.* 1888;26(160):256–265. https://doi.org/10.1080/14786448808628259
3. Floquet G. Sur les equations differentielles linearies a coeffients periodiques. (*Annales scientifiques de l'École Normale Supérieure, Serie 2*) *Ann. Ecole Norm. Sup.* 1883;12:47–88. https://doi.org/10.24033/asens.220
4. Bloch F. Uber die Quantenmechanic der elektronen in kristallgittern. *Z. Phys.* 1929;52(85):555–600. https://doi.org/10.1007/BF01339455
5. Elachi C. Waves in active and passive periodical structures: A review. *Proc. IEEE.* 1976;64(12):1666–1698. https://doi.org/10.1109/PROC.1976.10409, URL: https://core.ac.uk/download/pdf/216300643.pdf
6. Winn J.N., Fink Y., Fan S., Joannopoulos J.D. Omnidirectional reflection from a one-dimensional photonic crystal. *Opt. Lett.* 1998;23(20):1573–1575. https://doi.org/10.1364/ol.23.001573
7. Chigrin D.N., Lavrinenko A.V., Yarotsky D.A., Gaponenko S.V. Observation of total omnidirectional reflection from a one-dimensional dielectric lattice. *Appl. Phys. A.* 1999;68(1):25–28. https://doi.org/10.1007/s003390050849
8. Нурлигареев Д.Х., Сычугов В.А. Распространение света в одномерном фотонном кристалле: анализ методом функции Флоке-Блоха. *Квантовая электроника.* 2008;38(5):452–461. URL: https://www.elibrary.ru/tteynf
9. Нурлигареев Д.Х. Волны Флоке-Блоха одномерного фотонного кристалла: общая теория. *Наукоемкие технологии.* 2009;10(9):12–23.
10. Нурлигареев Д.Х., Сычугов В.А. Методика определения параметров ячейки ограниченного одномерного фотонного кристалла, основанная на формализме функций Флоке-Блоха. *Краткие сообщения по физике Физического института им. П.Н. Лебедева РАН*. 2012;2:3–10. URL: https://www.elibrary.ru/ouillp
11. Caffrey S., Morozov G.V., Sprung D.W.L., Martorell J. Floquet–Bloch solutions in a sawtooth photonic crystal. *Opt. Quantum Electron.* 2017;49(3):112. https://doi.org/10.1007/s11082-017-0939-1
12. Ibrahim A., Sprung D.W.L., Morozov G.V. Construction and Floquet–Bloch analysis of analytically solvable Hill equations with smooth potentials. *J. Opt. Soc. Am. B.* 2018;35(6):1223–1232. https://doi.org/10.1364/JOSAB.35.001223
13. Shmat'ko A.A., Mizernik V.N., Odarenko E.N. Floquet-Bloch waves in magnetophotonic crystals with transverse magnetic field. *J. Electromagn. Waves Appl.* 2020;34(12):1667–1679. https://doi.org/10.1080/09205071.2020.1780955
14. Yeh P., Yariv A., Hong C.S. Electromagnetic propagation in periodic stratified media. 1. General theory. *J. Opt. Soc. Am.* 1977;67(4):423–438. https://doi.org/10.1364/JOSA.67.000423
15. Walpita L.M. Solutions for planar optical waveguide equations by selecting zero elements in a characteristic matrix. *J. Opt. Soc. Am. A.* 1985;2(4):595–602. https://doi.org/10.1364/JOSAA.2.000595
16. Konopsky V. Design of 1D Photonic Crystals Sustaining Optical Surface Modes. *Coatings.* 2022;12(10):1489. https://doi.org/10.3390/coatings12101489
17. Segovia-Chaves F., Vinck-Posada H., Trabelsi Y., Ali N.B. Transmittance spectrum in a one-dimensional photonic crystal with Fibonacci sequence superconductor–semiconductor. *Optik.* 2020;217:164803. https://doi.org/10.1016/j.ijleo.2020.164803
18. Panda A., Pukhrambam P.D., Wu F., Belhadj W. Graphene-based 1D defective photonic crystal biosensor for real-time detection of cancer cells. *Eur. Phys. J. Plus.* 2021;136(8):809. https://doi.org/10.1140/epjp/s13360-021-01796-z
19. Liu Z., Li X., Chen C., Wang X., Gao W., Ye W., Li L., Liu J. Bound states in the continuum in asymmetric one-dimensional photonic crystal systems guided by anisotropy. *Opt. Express.*2023;31(5):8384–8392. https://doi.org/10.1364/OE.482894
20. Борн М., Вольф Э. *Основы оптики*: пер с англ. М.: Наука; 1970. 856 с.

About the authors

Dzamil Kh. Nurligareev, Dr. Sci. (Phys.-Math.), Professor, Department of Physics, Institute for Advanced Technologies and Industrial Programming, MIREA – Russian Technological University (78, Vernadskogo pr., Moscow, 119454 Russia). E-mail: nurligareev@mirea.ru. Scopus Author ID 6602356533, ResearcherID L-5323-2018, RSCI SPIN-code 3651-6149, https://orcid.org/0009-0006-6412-0580

Iliya A. Nedospasov, Cand. Sci. (Phys.–Math.), Senior Researcher, Kotelnikov Institute of Radio engeneering and Electronics, Russian Academy of Sciences (11, Mokhovaya ul., Moscow, 125009 Russia); Associate Professor, Department of Physics, Institute for Advanced Technologies and Industrial Programming, MIREA – Russian Technological University (78, Vernadskogo pr., Moscow, 119454 Russia). E-mail: nedospasov@mirea.ru. Scopus Author ID 56415098900, ResearcherID G-6191-2016, RSCI SPIN-code 4300-8750, https://orcid.org/0000-0002-8185-5072

Kseniya Yu. Kharitonova, Cand. Sci. (Phys.–Math.), Associate Professor, Department of Physics, Institute for Advanced Technologies and Industrial Programming, MIREA – Russian Technological University (78, Vernadskogo pr., Moscow, 119454 Russia). E-mail: kharitonova_k@mirea.ru. Scopus Author ID 6603407254. https://orcid.org/0009-0008-2967-8372

Об авторах

Нурлигареев Джамиль Хайдарович, д.ф.-м.н., профессор, кафедра физики, Институт перспективных технологий и индустриального программирования, ФГБОУ ВО «МИРЭА – Российский технологический университет» (119454, Россия, Москва, пр-т Вернадского, д. 78). E-mail: nurligareev@mirea.ru. Scopus Author ID 6602356533, ResearcherID L-5323-2018, SPIN-код РИНЦ 3651-6149, https://orcid.org/0009-0006-6412-0580

Недоспасов Илья Александрович, к.ф.-м.н., старший научный сотрудник, ФГБУН «Институт радиотехники и электроники им. В.А. Котельникова Российской академии наук» (ИРЭ РАН) (125009, Россия, Москва, ул. Моховая, д. 11); доцент, кафедра физики, Институт перспективных технологий и индустриального программирования, ФГБОУ ВО «МИРЭА – Российский технологический университет» (119454, Россия, Москва, пр-т Вернадского, д. 78). E-mail: nedospasov@mirea.ru. Scopus Author ID 56415098900, ResearcherID G-6191-2016, SPIN-код РИНЦ 4300-8750, https://orcid.org/0000-0002-8185-5072

Харитонова Ксения Юрьевна, к.ф.-м.н., доцент, кафедра физики, Институт перспективных технологий и индустриального программирования, ФГБОУ ВО «МИРЭА – Российский технологический университет» (119454, Россия, Москва, пр-т Вернадского, д. 78). E-mail: kharitonova_k@mirea.ru. Scopus Author ID 6603407254. https://orcid.org/0009-0008-2967-8372

Translated from Russian into English by Lyudmila O. Bychkova
Edited for English language and spelling by Thomas A. Beavitt

Mathematical modeling

Математическое моделирование

UDC 539.3; 536.2
https://doi.org/10.32362/2500-316X-2024-12-6-80-90
EDN VWASPO

RESEARCH ARTICLE

Development of model representations of thermal reaction viscoelastic bodies on the temperature field

Eduard M. Kartashov @

MIREA – Russian Technological University, 119454 Russia
@ *Corresponding author, e-mail: professor.kartashov@gmail.com*

Abstract

Objectives. In recent decades, the relevance of research into the thermal response of solids to a temperature field has increased in connection with the creation of powerful energy emitters and their use in technological operations. There is a significant number of publications describing these processes using mathematical models of dynamic or quasi-static thermoelasticity, mainly for most technically important materials that obey Hooke's law. However, at elevated temperatures and higher stress levels, the concept of an elastic body becomes insufficient: almost all materials exhibit more or less clearly the phenomenon of viscous flow. The real body begins to exhibit elastic and viscous properties and becomes viscoelastic. A rather complex problem arises: the development of dynamic (quasi-static) thermoviscoelasticity within the framework of the corresponding mathematical models of classical applied thermomechanics and mathematics. The purpose of the work is to consider the open problem of the theory of thermal shock in terms of a generalized model of thermoviscoelasticity under the conditions of classical Fourier phenomenology on the propagation of heat in solids. Three types of intense heating are considered: temperature, thermal, and medium heating. Intensive cooling modes can be equally considered. The task is posed: to develop model representations of dynamic (quasi-static) thermoviscoelasticity that allow accurate analytical solutions of the corresponding boundary value problems on their basis. This direction is practically absent in the scientific literature.

Methods. Methods and theorems of operational calculus were used.

Results. Model representations of the thermal response of viscoelastic bodies using the proposed new compatibility equation in displacements have been developed.

Conclusions. New integro-differential relations are proposed based on linear rheological models for the Maxwell medium and the Kelvin medium, including both dynamic and quasi-static models for viscoelastic and elastic media, generalizing the results of previous studies. The proposed constitutive relations of the new form are applicable to describe the thermal response of quasi-elastic bodies of a canonical shape simultaneously in three coordinate systems with a system-defining parameter, which makes it possible to identify the influence of the topology of the region on the value of the corresponding temperature stresses.

Keywords: heat stroke, thermoviscoelasticity, generalized dynamic models, analytical solutions, thermal stresses

• **Submitted:** 26.03.2024 • **Revised:** 10.04.2024 • **Accepted:** 10.10.2024

For citation: Kartashov E.M. Development of model representations of thermal reaction viscoelastic bodies on the temperature field. *Russ. Technol. J*. 2024;12(6):80–90. https://doi.org/10.32362/2500-316X-2024-12-6-80-90

Financial disclosure: The author has no financial or proprietary interest in any material or method mentioned.

The author declares no conflicts of interest.

НАУЧНАЯ СТАТЬЯ

Развитие модельных представлений термической реакции вязкоупругих тел на температурное поле

Э.М. Карташов @

МИРЭА – Российский технологический университет, Москва, 119454 Россия
@ *Автор для переписки, e-mail: professor.kartashov@gmail.com*

Резюме

Цели. В последние десятилетия в связи с созданием мощных излучателей энергии и их использованием в технологических операциях возросла актуальность исследований термической реакции твердых тел на температурное поле. Существует значительное количество публикаций, описывающих эти процессы математическими моделями динамической или квазистатической термоупругости, в основном для большинства технически важных материалов, подчиняющихся закону Гука. Однако при повышенных температурах и более высоком уровне напряжений понятие об упругом теле становится недостаточным: почти у всех материалов обнаруживается более или менее отчетливо явление вязкого течения. Реальное тело начинает проявлять упругие и вязкие свойства и становится вязкоупругим. Возникает достаточно сложная проблема – развитие динамической (квазистатической) термовязкоупругости в рамках соответствующих математических моделей классической прикладной термомеханики и математики. Цель работы – рассмотреть открытую проблему теории теплового удара в терминах обобщенной модели термовязкоупругости в условиях классической феноменологии Фурье о распространении теплоты в твердых телах. Рассматриваются три вида интенсивного нагрева: температурный, тепловой, нагрев средой. В равной мере могут быть рассмотрены режимы интенсивного охлаждения. Ставится задача: разработать модельные представления динамической (квазистатической) термовязкоупругости, допускающие точные аналитические решения соответствующих краевых задач на их основе. Указанное направление в научной литературе практически отсутствует.

Методы. Использованы методы и теоремы операционного исчисления.

Результаты. Развиты модельные представления термической реакции вязкоупругих тел с использованием предложенного нового уравнения совместности в перемещениях.

Выводы. Предложены новые интегро-дифференциальные соотношения на базе линейных реологических моделей для среды Максвелла и среды Кельвина, включающие одновременно динамические и квазистатические модели для вязкоупругих и упругих сред, обобщающие результаты предыдущих исследований. Предложенные определяющие соотношения новой формы применимы для описания термической реакции квазиупругих тел канонической формы одновременно в трех системах координат с определяющим систему параметром, что позволяет выявить влияние топологии области на величину соответствующих температурных напряжений.

Ключевые слова: тепловой удар, термовязкоупругость, обобщенные динамические модели, аналитические решения, термические напряжения

• **Поступила:** 26.03.2024 • **Доработана:** 10.04.2024 • **Принята к опубликованию:** 10.10.2024

Для цитирования: Карташов Э.М. Развитие модельных представлений термической реакции вязкоупругих тел на температурное поле. *Russ. Technol. J.* 2024;12(6):80–90. https://doi.org/10.32362/2500-316X-2024-12-6-80-90

Прозрачность финансовой деятельности: Автор не имеет финансовой заинтересованности в представленных материалах или методах.

Автор заявляет об отсутствии конфликта интересов.

INTRODUCTION

The paper continues previous research [1, 2] into the development of generalized local-equilibrium and local-non-equilibrium heat transfer processes. Here, the open problem of the thermal response of viscoelastic bodies to heating of a massive body bounded internally by a flat surface (elastic half-space in the Cartesian coordinate system), a cylindrical surface (elastic space in the cylindrical coordinate system with an internal cylindrical cavity), or a spherical surface (elastic space in the spherical coordinate system with an internal spherical cavity). The developed approach based on integro-differential relations including simultaneously dynamic and quasi-static models for viscoelastic and elastic media generalizes the results of previous studies. New model representations are based on linear Maxwell and Kelvin rheological models, allowing the impact of viscous flow in an elastic medium on temperature elastic stresses to be distinctly traced. The reported results open a new scientific direction in applied thermomechanics and mathematics comprising a study of the thermal response of viscoelastic bodies to intensive heating (cooling) within the framework of dynamic and quasi-static models. At the first stage, the research is carried out under the conditions of the commonly used local equilibrium heat transfer based on the traditional Fourier phenomenology [3] in terms of the linear gradient relations that relate heat flux density vector $\bar{q}(M,t)$ (t is time) with thermal gradient $T(M,t)$: $\bar{q}(M,t) = -\lambda_T \mathrm{q}\mathrm{rad} T(M,t)$, where λ_T is the thermal conductivity coefficient. Three cases of intensive heating of boundary S of region $\bar{\Omega} = \{M(x,y,z) \in \bar{D} = D + S,\ t > 0\}$ describing a real solid are considered: thermal heating $T(M,t) = T_{am}(t)$, $M \in S,\ t > 0$ ($T_{am}(t) > T_0$; T_0 is the initial temperature at which the region is in unstressed and undeformed state); thermal heating $\partial T(M,t)/\partial n = -(1/\lambda_T) q_0(t), M \in S,\ t > 0$ ($q_0(t)$ is heat flux value, $\bar{n} = (n_1, n_2, n_3)$ is external normal to S and is the vector continuous at S); and heating by medium $\partial T(M,t)/\partial n = -h\left[T(M,t) - T_{am}\right], M \in S,\ t > 0$ (where h – relative heat exchange coefficient; T_{am} – ambient temperature ($T_{am}(t) > T_0$). Within the described approach, cases of abrupt cooling can also be considered, as well as the effect of heat internal sources (heat sinks).

DEFINING RELATIONS OF DYNAMIC THERMOELASTICITY

Let $\sigma_{ij}(M,t)$, $\varepsilon_{ij}(M,t)$, $U_i(M,t)$ be tensor components of the stress, strain, and displacement vector, respectively, satisfying basic equations of (uncoupled) thermoelasticity (in index notation) [1–6]:

$$\sigma_{ij,j}(M,t) + F_i(M,t) = \rho^* U_i(M,t), \quad (1)$$

$$\varepsilon_{ij}(M,t) = (1/2)\left[U_{i,j}(M,t) + U_{j,i}(M,t)\right], \quad (2)$$

$$\sigma_{ij}(M,t) = 2\mu\varepsilon_{ij}(M,t) + \left[\lambda\varepsilon_{ii}(M,t) - (3\lambda + 2\mu)\alpha_T(T(M,t) - T_0)\right]\delta_{ij}, \quad (3)$$
$$M \in D,\ t > 0,$$

where ρ^* is density; λ, μ are Lamé isothermal coefficients; G is the shear modulus; $\lambda = 2Gv/(1-2v)$; v is the Poisson ratio, with $2G(1+v) = E$, E is the Young's modulus; λ_T is the linear thermal expansion coefficient, δ_{ij} is the Kronecker symbol, $F_i(M, t)$ are volumetric force components; $e(M, t) = U_{i,i}(M, t) = \varepsilon_{ii}(M, t)$ is the volumetric strain related to the sum of normal stresses $\sigma(M,t) = \sigma_{nn}(M,t)$, $(n = x, y, z)$ described by the following relation:

$$e(M,t) = \frac{1-2v}{E}\sigma(M,t) + 3\alpha_T\left[T(M,t) - T_0\right]. \quad (4)$$

Boundary conditions $\sum_j \sigma_{ji}(M,t)n_j = f_i(M,t)$, $M \in S,\ t > 0$ should be added to Eqs. (1)–(4) on the part of the surface where stresses are known and boundary conditions $U_i(M,t) = \varphi_i(M,t), M \in S,\ t > 0$ on the part of the surface where displacements are given. For a partially bounded region, the condition of boundedness of all functions included in (1)–(4) should be added. The temperature function $T(M, t)$ included in (3) is derived from the solution to the boundary value problem of nonstationary thermal conductivity of the following form:

$$\left.\begin{aligned}\frac{\partial T}{\partial t} = a\Delta T(M,t) + (1/c\rho^*)f(M,t), M \in D,\ t>0,\\ T(M,t)\big|_{t=0} = T_0, M \in S,\\ \gamma_1\frac{\partial T(M,t)}{\partial n} + \gamma_2 T(M,t) = \gamma_3\varphi(M,t), M \in S,\ t>0,\end{aligned}\right\} \quad (5)$$

where a is thermal diffusivity; c is heat capacity; γ_1, γ_2, and γ_3 are coefficients under the boundary condition.

Relations (1)–(4) are general relations of dynamic thermoelasticity that relate stress, strain, displacement, and temperature. When passing to specific cases, Eq. (1)–(4) should be transformed into the so-called compatibility equations, either in stresses or in displacements, and the corresponding problem of dynamic thermoelasticity should be written for these equations. For the case considered in the paper, the impact of the boundary surface curvature of solid body on the temperature and corresponding temperature stresses should be taken into account. Here, a more convenient mathematical model is the equation of compatibility in displacements that simultaneously covers cylindrical, spherical, and Cartesian coordinate systems only within the framework of the generalized model involving numerous practical applications.

Substituting right parts of (3) into (1) (without volumetric forces) and then using (2) and (4), following a number of long transforms we arrive at the following three equations:

$$\Delta U_i(M,t) + \frac{1}{(1-2\nu)}\cdot\frac{\partial\bar{e}(M,t)}{\partial i} - (\rho^*/G)\frac{\partial^2 U_i(M,t)}{\partial t^2} = \\ = \frac{2(1+\nu)\alpha_T}{(1-2\nu)}\frac{\partial\left[T(M,t)-T_0\right]}{\partial i}, (i=x,y,z),$$

which can be formally written as the following vector equality:

$$\Delta\bar{U}(M,t) + \frac{1}{(1-2\nu)}\mathrm{grad}\left[\mathrm{div}\,\bar{U}(M,t)\right] - \\ - (\rho^*/G)\frac{\partial^2\bar{U}(M,t)}{\partial t^2} = \\ = \frac{2(1+\nu)}{(1-2\nu)}\alpha_T\,\mathrm{grad}\left[T(M,t)-T_0\right], M \in D,\ t>0. \quad (6)$$

Note that during the reverse transition, the appropriate components in vector entries in the left and right parts of (6) should be equated.

We consider further practical cases of dynamic thermoelasticity based on Eq. (6). In the first case, region $z > R$, $t > 0$ is considered in Cartesian coordinates (x, y, z), bounded by flat surface whose temperature state is described by function $T_i(z, t)$, $(i = 1, 2, 3)$; thus, $U_x = U_y = 0$, $U_z = U_z(z, t)$, and Eq. (6) has the following form:

$$\frac{\partial^2 U_z(z.t)}{\partial z^2} - \frac{1}{v_{ew}^2}\cdot\frac{\partial^2 U_z(z,t)}{\partial t^2} = \\ = \frac{1+\nu}{1-\nu}\alpha_T\frac{\partial\left[T_i(z,t)-T_0\right]}{\partial z}, z>R,\ t>0. \quad (7)$$

Here, $v_{ew} = \sqrt{\frac{2G(1-\nu)}{\rho^*(1-2\nu)}} = \sqrt{(\lambda+2\mu)/\rho^*}$ is the velocity of the expansive wave (EW) propagation in an elastic medium that is close to the speed of sound.

The stress component $\sigma_{zz}(z, t)$ that interests us is connected to the displacement by the following relation:

$$\sigma_{zz}(z,t) = \frac{2G(1-\nu)}{(1-2\nu)}\times \\ \times\left\{\frac{\partial U_z}{\partial z} - \frac{1+\nu}{1-\nu}\alpha_T\left[T_i(z,t)-T_0\right]\right\}. \quad (8)$$

The temperature function satisfies three heating conditions:

$$\left.\begin{aligned}\frac{\partial T_i}{\partial t} = a\frac{\partial^2 T_i}{\partial z^2},\ z>R,\ t>0,\ (i=1,2,3),\\ T_i(z,t)\big|_{t=0} = T_0,\ z \ge R,\\ T_1(z,t)\big|_{z=R} = T_{am},\ t>0,\\ \frac{\partial T_2}{\partial z}\Big|_{z=R} = -(1/\lambda_T)q_0,\ t>0,\\ \frac{\partial T_3}{\partial z}\Big|_{z=R} = -h(T_3 - T_{am}),\ t>0,\\ \left|T_i(z,t)\right| < \infty,\ z \ge R,\ t \ge 0.\end{aligned}\right\} \quad (9)$$

In the second case, region $\rho > R$, $t > 0$ having an internal spherical cavity is considered according to spherical coordinates (ρ, φ, θ) when heated under central symmetry conditions $T_i = T_i(\rho, t)$ so that $U_\varphi = U_\theta = 0$, $U_\rho = U_\rho(\rho, t)$, and (6) is written in the following form:

$$\frac{\partial U_\rho(\rho,t)}{\partial\rho^2} + \frac{2}{\rho}\cdot\frac{\partial U_\rho(\rho,t)}{\partial\rho} - \\ - \frac{2}{\rho^2}U_\rho(\rho,t) - \frac{1}{v_{ew}^2}\cdot\frac{\partial^2 U_\rho(\rho,t)}{\partial t^2} = \\ = \frac{1+\nu}{1-\nu}\alpha_T\frac{\partial\left[T_i(\rho,t)-T_0\right]}{\partial\rho},\ \rho>R,\ t>0. \quad (10)$$

In this case,

$$\sigma_{\rho\rho}(\rho,t)=\frac{2G(1-\nu)}{(1-2\nu)}\times \times\left\{\frac{\partial U_\rho(\rho,t)}{\partial\rho}+\frac{2\nu}{1-\nu}\cdot\frac{1}{\rho}U_\rho(\rho,t)- -\frac{1+\nu}{1-\nu}\alpha_T\left[T_i(\rho,t)-T_0\right]\right\}, \quad (11)$$

$$\left.\begin{aligned}\frac{\partial T_i(\rho,t)}{\partial t}=a\left(\frac{\partial^2 T_i}{\partial\rho^2}+\frac{2}{\rho}\cdot\frac{\partial T_i}{\partial\rho}\right),\ \rho>R,\ t>0,\\ T_1(\rho,t)\big|_{\rho=R}=T_{am},\ t>0,\\ \frac{\partial T_2(\rho,t)}{\partial\rho}\Big|_{\rho=R}=-(1/\lambda_T)q_0,\ t>0,\\ \frac{\partial T_3(\rho,t)}{\partial\rho}\Big|_{\rho=R}=-h\left[T_3(\rho,t)\big|_{\rho=R}-T_{am}\right],\ t>0,\\ \left|T_i(\rho,t)\right|<\infty,\ \rho\ge R,\ t\ge 0.\end{aligned}\right\} \quad (12)$$

In the third case, region $\rho > R$, $t > 0$ with an internal cylindrical cavity is considered in cylindrical coordinates (r, φ, z) under radial temperature conditions $T_i = T_i(\rho, t)$ so that $U_\varphi = U_z = 0$, $U_r = U_r(r, t)$, and Eq. (6) has the following form:

$$\frac{\partial^2 U_r(r,t)}{\partial r^2}+\frac{1}{r}\cdot\frac{\partial U_r(r,t)}{\partial r}-\frac{1}{r^2}U_r(r,t)- -\frac{1}{v_{ew}^2}\cdot\frac{\partial^2 U_r(r,t)}{\partial t^2}=\frac{1+\nu}{1-\nu}\alpha_T\frac{\partial\left[T_i(r,t)-T_0\right]}{\partial r},\quad r>R,\ t>0. \quad (13)$$

Here,

$$\sigma_{rr}(r,t)=\frac{2G(1-\nu)}{(1-2\nu)}\left\{\frac{\partial U_r(r,t)}{\partial r}+\frac{\nu}{1-\nu}\cdot\frac{1}{r}U_r(r,t)- -\frac{1+\nu}{1-\nu}\alpha_T\left[T_i(r,t)-T_0\right]\right\}, \quad (14)$$

$$\left.\begin{aligned}\frac{\partial T_i}{\partial t}=a\left(\frac{\partial^2 T_i}{\partial r^2}+\frac{1}{r}\cdot\frac{\partial T_i}{\partial r}\right),\ r>R,\ t>0,\\ T_i(r,t)\big|_{t=0}=T_0,\ r\ge R,\\ T_1(r,t)\big|_{r=R}=T_{am},\ t>0,\\ \frac{\partial T_2(r,t)}{\partial r}\Big|_{r=R}=-(1/\lambda_T)q_0,\ t>0,\\ \frac{\partial T_3(r,t)}{\partial r}\Big|_{r=R}=-h\left[T_3(r,t)\big|_{r=R}-T_{am}\right],\ t>0,\\ \left|T_i(r,t)\right|<\infty,\ r\ge R,\ t\ge 0.\end{aligned}\right\} \quad (15)$$

It would be useful to simultaneously cover all three cases in all three coordinate systems within the framework of the generalized model, which could be of practical significance in the theory of thermal shock. For convenient recording of the generalized model, the generalized coordinate μ is introduced: μ = z in Cartesian coordinates, μ = ρ in spherical coordinates, and μ = r in cylindrical coordinates. Here, $U_\mu = U_\mu(\mu, t)$, $\sigma_{\mu\mu} = \sigma_{\mu\mu}(\mu, t)$, $T_i = T_i(\mu, t)$.

Then Eqs. (7)–(15) for elastic body can be written in the generalized form, as follows:

$$\frac{\partial^2 U_\mu}{\partial\mu^2}+\frac{2m+1}{\mu}\left(\frac{\partial U_\mu}{\partial\mu}-\frac{1}{\mu}U_\mu\right)-\frac{1}{v_{ew}^2}\cdot\frac{\partial^2 U_\mu}{\partial t^2}= =\frac{1+\nu}{1-\nu}\alpha_T\frac{\partial}{\partial\mu}\left[T_i(\mu,t)-T_0\right],\ \mu>R,\ t>0, \quad (16)$$

$$\sigma_{\mu\mu}(\mu,t)=\frac{2G(1-\nu)}{(1-2\nu)}\left\{\frac{\partial U_\mu}{\partial\mu}+\frac{(2m+1)\nu}{(1-\nu)}\cdot\frac{1}{\mu}U_\mu- -\frac{1+\nu}{1-\nu}\alpha_T\left[T_i(\mu,t)-T_0\right]\right\},\ \mu>R,\ t>0, \quad (17)$$

$$\left.\begin{aligned}\frac{\partial T_i(\mu,t)}{\partial t}=a\left(\frac{\partial^2 T_i}{\partial\mu^2}+\frac{2m+1}{\mu}\cdot\frac{\partial T_i}{\partial\mu}\right),\ \mu>R,\ t>0,\\ T_i(\mu,t)\big|_{t=0}=T_0,\ \mu\ge R,\\ T_1(\mu,t)\big|_{\mu=R}=T_{am},\ t>0,\\ \frac{\partial T_2(\mu,t)}{\partial\mu}\Big|_{\mu=R}=-(1/\lambda_T)q_0,\ t>0,\\ \frac{\partial T_3(\mu,t)}{\partial\mu}\Big|_{\mu=R}=-h\left[T_3(\mu,t)\big|_{\mu=R}-T_{am}\right],\ t>0,\\ \left|T_i(\mu,t)\right|<\infty,\ \mu\ge R,\ t\ge 0.\end{aligned}\right\} \quad (18)$$

Here,

$$\mu=\begin{cases}z,\ z>R,\ m=-1/2 & \text{for Cartesian coordinates,}\\ \rho,\ \rho>R,\ m=1/2 & \text{for spherical coordinates,}\\ r,\ r>R,\ m=0 & \text{for cylindrical coordinats.}\end{cases} \quad (19)$$

In order to completely formulate the dynamic problem for displacements in elastic region (in the latter case, the boundary of the region is assumed stress free), the initial and boundary conditions should be added:

$$U_\mu(\mu,t)\Big|_{t=0},\ \frac{\partial U_\mu(\mu,t)}{\partial t}\Big|_{t=0}=0,\ \mu\ge R, \quad (20)$$

$$\left[\frac{\partial U_\mu(\mu,t)}{\partial\mu}+\frac{(2m+1)v}{(1-v)}\cdot\frac{1}{\mu}U_\mu(\mu,t)\right]\Bigg|_{\mu=R}= \\ =\frac{1+v}{1-v}\alpha_T\left[T_i(\mu,t)-T_0\right]_{\mu=R},\ t>0, \quad (21)$$

$$\left|U_\mu(\mu,t);\sigma_{\mu\mu}(\mu,t)\right|<\infty,\ \mu\geq R,\ t\geq 0. \quad (22)$$

STRESS–STRAIN RELATIONS IN RHEOLOGICAL MODELS

Numerous studies on the thermal response of solids have been carried out mainly for the majority of technically important materials that obey Hooke's law. At relatively low temperature and stress levels, the behavior of a wide class of materials is believed to be in good agreement with the above-described theory of thermoelasticity.

At higher temperatures and stress levels, the concept of an elastic body becomes insufficient due to almost all materials exhibiting more or less distinct viscous flow phenomena. In this case, the behavior of a real body is called viscoelastic since the body simultaneously exhibits elastic and viscous properties. In order to mathematically describe the inelastic behavior of a body under given heating and stress conditions, the stress–strain Eqs. (3) and (4) should be appropriately generalized.

Rheological models that simultaneously account for elastic deformation and viscous flow processes due to the sufficient simplicity of the adopted stress–strain relations permit a mathematical analysis of the behavior of real bodies under different loading conditions. In this connection, when designing structural elements exposed to high temperatures, accounting for the rheological effects becomes of great importance.

We write all necessary relations for the rheological laws relating stresses $\sigma_{ij}(M, t)$ and strains $\varepsilon_{ij}(M, t)$, $(i, j = x, y, z)$. For this, stress deviator $s_{ij}(M, t)$ along with strain deviator $e_{ij}(M, t)$ are introduced by the following relations:

$$s_{ij}(M, t) = \sigma_{ij}(M, t) - \sigma^*(M, t)\delta_{ij}, \quad (23)$$

$$e_{ij}(M, t) = \varepsilon_{ij}(M, t) - \varepsilon^*(M, t)\delta_{ij}, \quad (24)$$

where σ^* and ε^* are average normal stress and average elongation:

$$\sigma^*(M,t)=\frac{1}{3}\sum_i\sigma_{ii}(M,t),\ \varepsilon^*(M,t)=\frac{1}{3}\sum_i\varepsilon_{ii}(M,t). \quad (25)$$

Using these deviators, Eqs. (3) and (4) can be written in the following form:

$$s_{ij}(M,t)=2Ge_{ij}(M,t), \quad (26)$$

$$\varepsilon^*(M,t)=\frac{1-2v}{2G(1+v)}\sigma^*(M,t)+ \\ +\alpha_T\left[T(M,t)-T_0\right]. \quad (27)$$

These equations describe the behavior of a linear elastic medium. Adding the summand expressing Newton's law of viscosity (series or parallel connection of spring and viscous resistance) to Hooke's law relations, the resulting dependencies would yield the Maxwell medium, as follows:

$$\frac{\partial s_{ij}(M,t)}{\partial t}+\frac{1}{\tau_{rlx}}s_{ij}(M,t)=2G\frac{\partial e_{ij}(M,t)}{\partial t} \quad (28)$$

and the Kelvin medium, as follows:

$$s_{ij}(M,t)=2G\left[e_{ij}(M,t)+\tau_{rlx}\frac{\partial e_{ij}(M,t)}{\partial t}\right]. \quad (29)$$

In this case, Eq. (27) remains unchanged. The latter means that under hydrostatic compression or tension, the body behaves as a fully elastic body. The constant $\tau_{rlx} = \eta/G$ is referred to as the relaxation time in (28) and the lag time in (29), while η is the material viscosity. Certainly, an actual behavior of materials is more complicated than in hypothetical cases (28) and (29); however, when based on applying the simplest models, the Maxwell scheme can be used for metals at high temperatures, as well as for polymers combining elastic deformation and viscous flow, while the Kelvin scheme can be used for materials with internal friction in studying damped oscillations.

Note that at $\tau_{rlx} = 0$ ($\eta = \infty$), Eq. (28) yields Hooke's medium, while at $\tau_{rlx} = 0$ ($\eta = 0$) in (29), Kelvin's law reduces to Eq. (26).

At thermal shock (instant heating or cooling of the boundary surface), the stresses immediately change by value $\Delta=\left|E\alpha_T\left(T_{am}-T_0\right)\right|$ [3]. In an elastic medium, these stresses remain unchanged, while in a Maxwell medium, viscous flow begins, as a result of which the stress continuously decreases to asymptotically approach a zero value. In contrast, in the Kelvin medium, the stress jump exceeds the appropriate elastic value toward which this stress then approaches asymptotically.

NEW INTEGRAL RELATIONS FOR DYNAMIC THERMOVISCOELASTICITY

Since stress–strain relations for viscoelastic materials contain variable t (time), the corresponding mathematical models are nonstationary and therefore dynamic. The above relations can be used to describe the thermal response of canonically shaped viscoelastic bodies (an infinite plate; a half-space bounded by a flat surface; cylindrical and spherical bodies, and etc.) under given heating (or cooling) conditions as part of the corresponding boundary value problem of nonstationary thermal conductivity. For this purpose, the differential equation of dynamic thermoviscoelasticity should be obtained at the initial stage. We start considering this issue in Cartesian coordinates for viscoelastic half-space $z \geq l$ (l is left boundary of the region) of temperature $T(z, t)$ whose boundary is stress-free. In this case, $U_x = U_y = 0$, $U_z = U_z(z, t)$, $\varepsilon_{xx} = \varepsilon_{yy} = 0$, $e_{zz} = \varepsilon_{zz}$, stresses $\sigma_{ij} = \sigma_{ij}(z, t)$ for $i = j$, $\sigma_{ij} = 0$ for $i \neq j$, $(i, j = x, y, z)$.

Then we have the following:

$$\left.\begin{aligned} &\frac{\partial s_{zz}(z,t)}{\partial t}+\frac{1}{\tau_{\text{rlx}}}s_{zz}(z,t)=\frac{4G}{3}\cdot\frac{\partial \varepsilon_{zz}(z,t)}{\partial t},\ t>0,\\ &s_{zz}(z,t)\big|_{t=0}=0, \end{aligned}\right\} \tag{30}$$

$$\left.\begin{aligned} &\varepsilon_{zz}(z,t)=\frac{\partial U_z(z,t)}{\partial z},\\ &\frac{\partial \sigma_{zz}(z,t)}{\partial z}=\rho\frac{\partial^2 U_z(z,t)}{\partial t^2},\ z>l,\ t>0, \end{aligned}\right\} \tag{31}$$

$$\sigma_{zz}=s_{zz}+\sigma^*=s_{zz}+\frac{2G(1+\nu)}{3(1-2\nu)}\varepsilon_{zz}-\\ -\frac{2G(1+\nu)}{(1-2\nu)}\alpha_{\text{T}}(T_i-T_0). \tag{32}$$

We find the solution to the Cauchy problem (30):

$$s_{zz}=\frac{4G}{3}\varepsilon_{zz}-\frac{4G}{3\tau_{\text{rlx}}}\int_0^t\exp\left[-\frac{(t-\tau)}{\tau_{\text{rlx}}}\right]\varepsilon_{zz}(z,\tau)d\tau. \tag{33}$$

Then we find σ_{zz} from (32) and (33) and substitute it into (31). As a result, the following relation for the Maxwell medium is obtained:

$$\frac{\partial^2 U_z}{\partial z^2}-\frac{1}{v_{\text{ew}}^2}\cdot\frac{\partial^2 U_z}{\partial t^2}=\frac{(1+\nu)}{(1-\nu)}\alpha_{\text{T}}\frac{\partial\left[T_i(z,t)-T_0\right]}{\partial z}+\\ +\frac{2(1-2\nu)}{3\tau_{\text{rlx}}(1-\nu)}\int_0^t\exp\left[-\frac{(t-\tau)}{\tau_{\text{rlx}}}\right]\frac{\partial^2 U_z(z,\tau)}{\partial z^2}d\tau. \tag{34}$$

In this case,

$$\sigma_{zz}(z,t)=\frac{2G(1-\nu)}{(1-2\nu)}\cdot\frac{\partial U_z}{\partial z}-\\ -\frac{4G}{3\tau_{\text{rlx}}}\int_0^t\exp\left[-\frac{(t-\tau)}{\tau_{\text{rlx}}}\right]\frac{\partial U_z(z,\tau)}{\partial z}d\tau-\\ -\frac{2G(1+\nu)}{(1-2\nu)}\alpha_{\text{T}}\left[T_i(z,t)-T_0\right]. \tag{35}$$

Using similar reasoning in the spherical coordinate system (central symmetry $T_i = T_i(\rho, t)$ for the viscoelastic region $\rho > R$, $t > 0$, relations for the Maxwell medium are obtained:

$$\frac{\partial^2 U_\rho}{\partial\rho^2}+\frac{2}{\rho}\cdot\frac{\partial U_\rho}{\partial\rho}-\frac{2}{\rho^2}U_\rho-\frac{1}{v_{\text{ew}}^2}\cdot\frac{\partial^2 U_\rho}{\partial t^2}=\\ =\frac{1+\nu}{1-\nu}\alpha_{\text{T}}\frac{\partial\left[T_i(\rho,t)-T_0\right]}{\partial\rho}+\frac{2(1-2\nu)}{3\tau_{\text{rlx}}(1-\nu)}\times\\ \times\int_0^t\exp\left[-\tau\frac{(t-\tau)}{\tau_{\text{rlx}}}\right]\left(\frac{\partial^2 U_\rho}{\partial\rho^2}+\frac{2}{\rho}\cdot\frac{\partial U_\rho}{\partial\rho}-\frac{2}{\rho^2}U_\rho(\rho,\tau)\right)d\tau, \tag{36}$$

$$\sigma_{\rho\rho}(\rho,t)=\frac{2G(1-\nu)}{(1-2\nu)}\times\\ \times\left\{\frac{\partial U_\rho}{\partial\rho}+\frac{2\nu}{1-\nu}\cdot\frac{1}{\rho}U_\rho-\frac{(1+\nu)}{(1-\nu)}\alpha_{\text{T}}\left[T_i(\rho,t)-T_0\right]-\right.\\ \left.-\frac{2}{3\tau_{\text{rlx}}}\int_0^t\exp\left[-\frac{(t-\tau)}{\tau_{\text{rlx}}}\right]\left(\frac{\partial U_\rho}{\partial\rho}-\frac{1}{\rho}U_\rho(\rho,\tau)\right)d\tau\right\}. \tag{37}$$

In cylindrical coordinates (radial flux $T_i = T_i(r, t)$) for viscoelastic region $r > R$, $t > 0$, similar reasoning produces the following:

$$\frac{\partial^2 U_r}{\partial r^2}+\frac{1}{r}\cdot\frac{\partial U_r}{\partial r}-\frac{1}{r^2}U_r-\\ -\frac{1}{v_{\text{ew}}^2}\cdot\frac{\partial^2 U_r}{\partial t^2}=\frac{(1+\nu)}{(1-\nu)}\alpha_{\text{T}}\frac{\partial\left[T_i(r,t)-T_0\right]}{\partial r}+\frac{2(1-2\nu)}{3\tau_{\text{rlx}}(1-\nu)}\times\\ \times\int_0^t\exp\left[-\frac{(t-\tau)}{\tau_{\text{rlx}}}\right]\left(\frac{\partial^2 U_r}{\partial r^2}+\frac{1}{r}\cdot\frac{\partial U_r}{\partial r}-\frac{1}{r^2}U_r(r,\tau)\right)d\tau, \tag{38}$$

$$\sigma_{rr}(r,t)=\frac{2G(1-\nu)}{(1-2\nu)}\times\\ \times\left\{\frac{\partial U_r}{\partial r}+\frac{\nu}{1-\nu}\cdot\frac{1}{r}U_r-\frac{(1+\nu)}{(1-\nu)}\alpha_{\text{T}}\left[T_i(r,t)-T_0\right]-\right.\\ \left.-\frac{2}{3\tau_{\text{rlx}}}\int_0^t\exp\left[-\frac{(t-\tau)}{\tau_{\text{rlx}}}\right]\left(\frac{\partial U_r}{\partial r}-\frac{1}{2r}U_r(r,\tau)\right)d\tau\right\}. \tag{39}$$

Thus, the generalized model of dynamic thermoviscoelasticity can be written in coordinates (μ, *t*) for all three coordinate systems simultaneously.

For the Maxwell medium:

$$\frac{\partial^2 U_\mu}{\partial \mu^2}+\frac{2m+1}{\mu}\left(\frac{\partial U_\mu}{\partial \mu}-\frac{1}{\mu}U_\mu\right)-$$
$$-\frac{1}{v_{ew}^2}\cdot\frac{\partial^2 U_\mu}{\partial t^2}=\frac{(1+\nu)}{(1-\nu)}\alpha_T\frac{\partial\left[T_i(\mu,t)-T_0\right]}{\partial \mu}+\frac{2(1-2\nu)}{3\tau_{rlx}(1-\nu)}\times \quad (40)$$
$$\times\int_0^t\exp\left[-\frac{(t-\tau)}{\tau_{rlx}}\right]\left[\frac{\partial^2 U_\mu}{\partial \mu^2}+\frac{2m+1}{\mu}\left(\frac{\partial U_\mu}{\partial \mu}-\frac{1}{\mu}U_\mu(\mu,\tau)\right)\right]d\tau,$$

$$\sigma_{\mu\mu}(\mu,t)=\frac{2G(1-\nu)}{(1-2\nu)}\times$$
$$\times\left\{\frac{\partial U_\mu}{\partial \mu}+\frac{(2m+1)\nu}{(1-\nu)}\cdot\frac{1}{\mu}U_\mu-\frac{(1+\nu)}{(1-\nu)}\alpha_T\left[T_i(\mu,t)-T_0\right]\right\}- \quad (41)$$
$$-\frac{4G}{3\tau_{rlx}}\int_0^t\exp\left[-\frac{(t-\tau)}{\tau_{rlx}}\right]\left[\frac{\partial U_\mu}{\partial \mu}-\frac{2m+1}{2\mu}U_\mu(\mu,\tau)\right]d\tau.$$

The specific coordinate system in Eqs. (40) and (41) is fixed by (19).

For the Kelvin medium:

$$\frac{\partial^2 U_\mu}{\partial \mu^2}+\frac{2m+1}{\mu}\left(\frac{\partial U_\mu}{\partial \mu}-\frac{1}{\mu}U_\mu\right)-\frac{1}{v_{ew}^2}\cdot\frac{\partial^2 U_\mu}{\partial t^2}=$$
$$=\frac{(1+\nu)}{(1-\nu)}\alpha_T\frac{\partial\left[T_i(\mu,t)-T_0\right]}{\partial \mu}-\frac{2\tau_{rlx}}{3}\cdot\frac{(1-2\nu)}{1-\nu}\times \quad (42)$$
$$\times\frac{\partial}{\partial t}\left[\frac{\partial^2 U_\mu}{\partial \mu^2}+\frac{2m+1}{\mu}\left(\frac{\partial U_\mu}{\partial \mu}-\frac{1}{\mu}U_\mu\right)\right].$$

$$\sigma_{\mu\mu}(\mu,t)=\frac{2G(1-\nu)}{(1-2\nu)}\times$$
$$\times\left\{\frac{\partial U_\mu}{\partial \mu}+\frac{\nu}{1-\nu}\cdot\frac{2m+1}{\mu}U_\mu-\frac{1+\nu}{1-\nu}\alpha_T\left[T_i(\mu,t)-T_0\right]\right\}+ \quad (43)$$
$$+\frac{4G\tau_{rlx}}{3}\cdot\frac{\partial}{\partial t}\left(\frac{\partial U_\mu}{\partial \mu}-\frac{2m+1}{2\mu}U_\mu\right).$$

As in (41) above, the corresponding coordinate system is defined by conditions (19). Functions $T_i(\mu, t)$, (i = 1, 2, 3) correspond to statements (18). For writing boundary value problems for Eq. (40) and (42), initial conditions (20), boundedness conditions (22), and the boundary condition for the boundary of region $\mu \geq R$, $t \geq 0$ free of stresses (41) and (43) should be added. When conducting numerical experiments for different thermal heating (or cooling) conditions specified in (18), Eqs. (40) and (42) admit Laplace transforms that permit passage to linear boundary value problems for displacements in the image space and, after finding them, writing all (nonzero) components of stress and strain tensors out. Following passage to the originals, it becomes possible to reproduce the complete picture of the dynamic response of viscoelastic body to thermal shock. For such purposes, partial differential equations (34), (36), (38) can also be used; moreover, it then becomes possible (which is more interesting) to go straight to generalized models for Eqs. (40) and (42). In [2], the analytical method for finding exact operational solutions to such generalized equations is developed, which ultimately permits a description of the impact of the region topology (by fixing m in the problem solution) on the magnitude of viscoelastic temperature stresses. In practical terms, the latter is of considerable interest for many fields of science and technology [3–6].

Another new approach based on deviatoric relations, which also provides a dynamic formulation of the thermoviscoelastic problem, can be mentioned here. We consider this approach for Cartesian coordinates. From (32) and (33), the following is obtained:

$$\sigma_{zz}(z,t)=\frac{2G(1-\nu)}{(1-2\nu)}\varepsilon_{zz}-\frac{2G(1+\nu)}{(1-2\nu)}\times$$
$$\times\alpha_T\left[T_i(z,t)-T_0\right]-\frac{4G}{3\tau_{rlx}}\times \quad (44)$$
$$\times\int_0^t\exp\left[-\frac{(t-\tau)}{\tau_{rlx}}\right]\varepsilon_{zz}(z,\tau)d\tau.$$

We use the operational method to find $\overline{\varepsilon}_{zz}(z,p)$ from (44) and substitute the resulting relation into the operational form of the equation as follows:

$$\frac{\partial^2\sigma_{zz}}{\partial z^2}=\rho^*\frac{\partial^2}{\partial t^2}(\varepsilon_{zz}).$$

After long transforms, the following equation of a new type is obtained:

$$\frac{\partial^2\sigma_{zz}}{\partial z^2}-\frac{1}{v_{ew}^2}\cdot\frac{\partial^2\sigma_{zz}}{\partial t^2}=$$
$$=\frac{1+\nu}{1-\nu}\alpha_T\rho^*\frac{\partial^2\left[T_i(z,t)-T_0\right]}{\partial t^2}+\frac{m_1}{v_{ew}^2\tau_{rlx}}\times$$
$$\times\frac{\partial^2}{\partial t^2}\int_0^t\exp\left[-(m_2/3\tau_{rlx})(t-\tau)\right]\sigma_{zz}(z,\tau)d\tau+\frac{m_1m_2}{\tau_{rlx}(1/\rho^*)}\times \quad (45)$$
$$\times\frac{\partial^2}{\partial t^2}\int_0^t\exp\left[-(m_2/3\tau_{rlx})(t-\tau)\right]\alpha_T\left[T_i(z,\tau)-T_0\right]d\tau,$$
$$z>l,\ t>0.$$

Here, $m_1=\frac{2(1-2\nu)}{3(1-\nu)}$, $m_2=\frac{1+\nu}{1-\nu}$.

Equation (45), which generalizes the well-known Danilovskaya equation for elastic bodies [7] to viscoelastic bodies, provides further development of the above problem (within the Maxwell medium framework). For the Kelvin medium, we have the following equation:

$$\frac{\partial^2\sigma_{zz}}{\partial z^2}=\frac{1}{m_1\tau_{\text{rlx}}v_{\text{ew}}^2}\times$$
$$\times\frac{\partial^2}{\partial t^2}\int_0^t\exp\left[-\frac{(t-\tau)}{m_1\tau_{\text{rlx}}}\right]\sigma_{zz}(z,\tau)d\tau+\frac{m_2\rho^*}{m_1\tau_{\text{rlx}}}\times \quad (46)$$
$$\times\frac{\partial^2}{\partial t^2}\int_0^t\exp\left[-\frac{(t-\tau)}{m_1\tau_{\text{rlx}}}\right]\alpha_{\text{T}}\left[T_i(z,\tau)-T_0\right]d\tau.$$

For numerical calculations, for example, based on Eq. (45), it is reasonable to pass to dimensionless quantities using the following formulas:

$$\xi=\frac{v_{\text{ew}}(z-l)}{a},\ \tau=\frac{v_{\text{ew}}^2t}{a},$$
$$\beta_1=\frac{2(1-2\nu)}{3(1-\nu)\tau_{\text{rlx}}(v_{\text{ew}}^2/a)},\ \beta_2=\frac{(1+\nu)}{(1-\nu)3\tau_{\text{rlx}}(v_{\text{ew}}^2/a)},$$
$$S_{\text{T}}=\frac{2G\alpha_{\text{T}}(T_{\text{am}}-T_0)(1+\nu)}{(1-2\nu)},\ \sigma_{\xi\xi}(\xi,\tau)=\frac{\sigma_{zz}(z,t)}{S_{\text{T}}},$$
$$W_i(\xi,\tau)=\frac{T_i(z,t)-T_0}{T_{\text{am}}-T_0}.$$

Then Eq. (45) takes the following form:

$$\frac{\partial^2\sigma_{\xi\xi}}{\partial\xi^2}-\frac{\partial^2\sigma_{\xi\xi}}{\partial\tau^2}=\frac{\partial^2W}{\partial\tau^2}+$$
$$+\beta_1\int_0^\tau\exp\left[-\beta_2(\tau-\tau')\right]\left[\sigma_{\xi\xi}(\xi,\tau')+W(\xi,\tau')\right]d\tau'. \quad (47)$$

In this form, the equation seems more convenient for Laplace transforms in the image space since it contains a convolution-type summand (which is convenient for applying the Laplace transform).

We find the operational solution of Eq. (47):

$$\overline{\sigma}_{\xi\xi}(\xi,p)=\frac{1}{2}p\sqrt{\frac{p+\beta_1+\beta_2}{p+\beta_2}}\overline{W}(0,p)\times$$
$$\times\int_0^\infty\exp\left[-p(\xi+\xi')\sqrt{\frac{p+\beta_1+\beta_2}{p+\beta_2}}\right]d\xi'-$$
$$-\frac{1}{2}p\sqrt{\frac{p+\beta_1+\beta_2}{p+\beta_2}}\overline{W}(\xi,p)\times$$
$$\times\int_\xi^\infty\exp\left[-p(\xi'-\xi)\sqrt{\frac{p+\beta_1+\beta_2}{p+\beta_2}}\right]d\xi'- \quad (48)$$
$$-\frac{1}{2}p\sqrt{\frac{p+\beta_1+\beta_2}{p+\beta_2}}\overline{W}(\xi,p)\times$$
$$\times\int_0^\xi\exp\left[-p(\xi-\xi')\sqrt{\frac{p+\beta_1+\beta_2}{p+\beta_2}}\right]d\xi'.$$

The given representation, which is characteristic for dynamic problems of thermoviscoelasticity, differs from conventional representations (with originals) in tables [8]. The key issue in finding the original of the complex representation (48) is the preliminary obtaining of its origin

$$\overline{\Psi}_i(\xi,\xi',p)=\frac{1}{p}\exp\left[-\gamma_i(\xi,\xi')\sqrt{\frac{p+\beta_1+\beta_2}{p+\beta_2}}\right]. \quad (49)$$

Here, the approach developed in [2] for complex representations can be used. For this, the Riemann–Mellin integral is applied with allowance for function (49) having two branching points. We omit long calculations and provide the final result:

$$\Psi_i(\xi,\xi',\tau)=\left\{1-\frac{1}{\pi}\int_0^{\beta_1}\frac{1}{x+\beta_2}\exp\left[-(x+\beta_2)\tau\right]\times\right.$$
$$\left.\times\sin\left[\gamma_i(\xi,\xi')(x+\beta_2)\sqrt{\frac{\beta_1-x}{x}}\right]dx\right\}\times \quad (50)$$
$$\times\eta\left[\tau-\gamma_i(\xi,\xi')\right].$$

Here,

$$\gamma_i(\xi,\xi')=\begin{cases}(\xi+\xi'),\ i=1,\\(\xi'-\xi),\ i=2,\\(\xi-\xi'),\ i=3,\end{cases}$$

$\eta(z)$ is the Heaviside function. Then the origin of representation (48) can be written out:

$$\sigma_{\xi\xi}(\xi,\tau)=-W(\xi,\tau)-$$
$$-\frac{1}{2}\cdot\frac{\partial}{\partial\xi}\int_0^\infty d\xi'\int_0^\tau\frac{\partial W(0,\tau')}{\partial\tau'}\Psi_1(\xi,\xi',\tau-\tau')d\tau'-$$
$$-\frac{1}{2}\cdot\frac{\partial}{\partial\xi}\int_\xi^\infty d\xi'\int_0^\tau\frac{\partial W(\xi,\tau')}{\partial\tau'}\Psi_2(\xi,\xi',\tau-\tau')d\tau'+ \quad (51)$$
$$+\frac{1}{2}\cdot\frac{\partial}{\partial\xi}\int_0^\xi d\xi'\int_0^\tau\frac{\partial W(\xi,\tau')}{\partial\tau'}\Psi_3(\xi,\xi',\tau-\tau')d\tau'.$$

Other coordinate systems can be considered similarly.

Finishing this part of the theory of dynamic thermoviscoelasticity, generalized Eqs. (16) and (17) for the elastic medium should be compared with Eqs. (40), (41) for the Maxwell model and (42), (43) for the Kelvin model for a viscoelastic medium. Here, the influence of viscosity and its contribution to generalized thermomechanics is clearly shown. In fact, the above relations (as well as (45), (46), and (51)) open a promising

scientific direction related to investigation of the thermal response of viscoelastic media to heating (or cooling) in terms of dynamic viscoelasticity. For example, (51) can consider numerous cases of heating (cooling) in the framework of model problems (9) with different kinds of heat flow: homogeneous, inhomogeneous, pulsed, pulsating, periodic, aperiodic, etc. Each case of this study represents independent scientific research involving not only thermomechanics, but also computational mathematics, and especially operational calculus in finding the origins of complex representations. Here it should be noted that such solutions to dynamic problems are practically not covered in the literature. Further studies of the above problem consist in developing generalized model representations of the thermal reaction of viscoelastic media for locally nonequilibrium heat transfer processes [9–15].

CONCLUSIONS

In the paper, new model representations of integro-differential form for dynamic and quasi-static thermoviscoelasticity are simultaneously proposed for various cases of thermal effect on viscoelastic bodies in Cartesian, cylindrical, and spherical coordinate systems. The given relations permit the study of analytically numerous practical cases of thermal reaction of viscoelastic medium (viscoelastic bodies of canonical form) within the framework of linear rheological Maxwell and Kelvin models in terms of conventional Fourier phenomenology on heat propagation in solids. They can be automatically extended to locally nonequilibrium heat transfer processes in terms of the Maxwell–Cattaneo–Lykov–Vernott phenomenology.

REFERENCES

1. Kartashov E.M. Model representations of heat shock in terms of dynamic thermal elasticity. *Russ. Technol. J*. 2020;8(2): 85–108 (in Russ.). https://doi.org/10.32362/2500-316X-2020-8-2-85-108
2. Kartashov E.M. New operational relations for mathematical models of local nonequilibrium heat transfer. *Russ. Technol. J*. 2022;10(1):68–79 (in Russ.). https://doi.org/10.32362/2500-316X-2022-10-1-68-79
3. Kartashov E.M., Kudinov V.A. *Analiticheskaya teoriya teploprovodnosti i prikladnoi termouprugosti* (*Analytical Theory of Thermal Conductivity and Applied Thermoelasticity*). Moscow: URSS; 2012. 670 p. (in Russ.). ISBN 978-5-397-02750-2
4. Zarubin V.S., Kuvyrkin G.N. *Matematicheskie modeli termomekhaniki* (*Mathematical Thermomechanics Models*). Moscow: FIZMATLIT; 2002. 168 p. (in Russ.).
5. Zarubin V.S., Kuvyrkin G.N. *Matematicheskie modeli mekhaniki i elektrodinamiki sploshnoi sredy* (*Mathematical Models of Mechanics and Electrodynamics of a Continuous Medium*. Moscow: Bauman Press; 2008. 512 p. (in Russ.). ISBN 978-5-7038-3162-5
6. Boley B., Weiner J. *Teoriya temperaturnykh napryazhenii* (*Theory of Thermal Stresses*): transl. from Engl. Moscow: Mir; 1964. 517 p. (in Russ.).
   [Boley B., Weiner J. *Theory of Thermal Stresses.* N.Y., London: Wiley & Sons; 1960. 608 p.]
7. Danilovskaya V.I. Temperature stresses in an elastic half-space arising due to sudden heating of its boundary. *Prikladnaya matematika i mehanika = J. Appl. Math. Mech*. 1950;14(3):316–324 (in Russ.).
8. Ditkin V.A., Prudnikov A.P. *Spravochnik po operatsionnomu ischisleniyu* (*Handbook of Operational Calculus*). Moscow: Vysshaya shkola; 1965. 467 p. (in Russ.).
9. Kudinov I.V., Kudinov V.A. Mathematical Simulation of the Locally Nonequilibrium Heat Transfer in a Body with Account for its Nonlocality in Space and Time. *J. Eng. Phys. Thermophy.* 2015;88(2):406–422. https://doi.org/10.1007/s10891-015-1206-6
   [Original Russian Text: Kudinov I.V., Kudinov V.A. Mathematical Simulation of the Locally Nonequilibrium Heat Transfer in a Body with Account for its Nonlocality in Space and Time. *Inzhenerno-Fizicheskii Zhurnal.* 2015;88(2):393–408 (in Russ.).]
10. Kudinov V.A., Eremin A.V., Kudinov I.V. The development and investigation of a strongly non-equilibrium model of heat transfer in fluid with allowance for the spatial and temporal non-locality and energy dissipation. *Thermophys. Aeromech.* 2017;24(6):901–907. https://doi.org/10.1134/S0869864317060087
    [Original Russian Text: Kudinov V.A., Eremin A.V., Kudinov I.V. The development and investigation of a strongly non-equilibrium model of heat transfer in fluid with allowance for the spatial and temporal non-locality and energy dissipation. *Teplofizika i Aeromekhanika*. 2017;24(6):929–935 (in Russ.).]
11. Baumeister K., Hamill T. Hyperbolic heat equation. Solving the problem of a semi-infinite body. *Teploperedacha = J. Heat Transfer*. 1969;4:112–119 (in Russ.).
12. Sobolev S.L. Local Non-Equilibrium Transport Models. *Phys. Usp*. 1997;40(10):1043. https://doi.org/10.1070/PU1997v040n10ABEH000292
    [Original Russian Text: Sobolev S.L. Local Non-Equilibrium Transport Models. *Uspekhi Fizicheskikh Nauk.* 1997;167(10):1095–1106 (in Russ). https://doi.org/10.3367/UFNr.0167.199710f.1095]

13. Savelyeva I.Yu. Variational formulation of a mathematical model of stationary thermal heat conduction with account spatial nonlocality. *Herald of the Bauman Moscow State University. Series Natural Sciences.* 2022;2(101):68–86 (in Russ.). https://doi.org/10.18698/1812-3368-2022-2-68-86
14. Kudinov V.A., Kudinov I.V. Studying heat conduction taking into account the finite rate of heat propagation. *High Temp.* 2013;51(2):268–276. https://doi.org/10.1134/S0018151X1204013X
[Original Russian Text: Kudinov V.A., Kudinov I.V. Studying heat conduction taking into account the finite rate of heat propagation. *Teplofizika Vysokikh Temperatur*. 2013;51(2):301–310 (in Russ.).]
15. Podstrigach Ya.S., Kolyano Yu.M. *Obobshchennaya termomekhanika* (*Generalized Thermomechanics*). Kiev: Naukova dumka; 1976. 312 p. (in Russ.).

СПИСОК ЛИТЕРАТУРЫ

1. Карташов Э.М. Модельные представления теплового удара в динамической термоупругости. *Russ. Technol. J.* 2020;8(2):85–108. https://doi.org/10.32362/2500-316X-2020-8-2-85-108
2. Карташов Э.М. Новые операционные соотношения для математических моделей локально-неравновесного теплообмена. *Russ. Technol. J*. 2022;10(1):68–79. https://doi.org/10.32362/2500-316X-2022-10-1-68-79
3. Карташов Э.М., Кудинов В.А. *Аналитическая теория теплопроводности и прикладной термоупругости*. М.: URSS; 2012. 670 с. ISBN 978-5-397-02750-2
4. Зарубин В.С., Кувыркин Г.Н. *Математические модели термомеханики*. М.: ФИЗМАТЛИТ; 2002. 168 с.
5. Зарубин В.С., Кувыркин Г.Н. *Математические модели механики и электродинамики сплошной среды*. М.: Изд-во МГТУ им. Н.Э. Баумана; 2008. 512 с. ISBN 978-5-7038-3162-5
6. Боли Б., Уэйнер Дж. *Теория температурных напряжений*: пер. с англ. М.: Мир; 1964. 517 с.
7. Даниловская В.И. Температурные напряжения в упругом полупространстве, возникающие вследствие внезапного нагрева его границы. *Прикладная математика и механика.* 1950;14(3):316–324.
8. Диткин В.А., Прудников А.П. *Справочник по операционному исчислению*. М.: Высшая школа; 1965. 467 с.
9. Кудинов И.В., Кудинов В.А. Математическая модель локально-неравновесного теплопереноса с учетом пространственно-временной нелокальности. *Инженерно-физический журнал*. 2015;88(2):393–408.
10. Кудинов В.А., Еремин А.В., Кудинов И.В. Разработка и исследование сильно неравновесной модели теплообмена в жидкости с учетом пространственно-временной нелокальности и диссипации энергии. *Теплофизика и аэромеханика*. 2017;24(6):929–935.
11. Баумейстер К., Хамилл Т. Гиперболичесое уравнение теплопроводности. Решение задачи о полубесконечном теле. *Теплопередача.* 1969;4:112–119.
12. Соболев С.Л. Локально-неравновесные модели процессов переноса. *Успехи физ. наук*. 1997;167(10):1095–1106. https://doi.org/10.3367/UFNr.0167.199710f.1095
13. Савельева И.Ю. Вариационная формулировка математической модели процесса стационарной теплопроводности с учетом пространственной нелокальности. *Вестник МГТУ им. Н.Э. Баумана. Серия: Естественные науки*. 2022;2(101):68–86. https://doi.org/10.18698/1812-3368-2022-2-68-86
14. Кудинов В.А., Кудинов И.В. Исследование теплопроводности с учетом конечной скорости распространения теплоты. *Теплофизика высоких температур*. 2013;51(2):301–310.
15. Подстригач Я.С., Коляно Ю.М. *Обобщенная термомеханика*. Киев: Наукова думка; 1976. 312 с.

About the author

Eduard M. Kartashov, Dr. Sci. (Phys.-Math.), Honored Scientist of the Russian Federation, Honorary Worker of Higher Professional Education of the Russian Federation, Honorary Worker of Science and Technology of the Russian Federation, Honorary Professor of the Lomonosov Moscow State University of Fine Chemical Technology, Laureate of the Golden Medal of the Academy of Sciences of Belarus in Thermophysics, Professor, Department of Higher and Applied Mathematics, M.V. Lomonosov Institute of Fine Chemical Technologies, MIREA – Russian Technological University (78, Vernadskogo pr., Moscow, 119454 Russia). E-mail: professor.kartashov@gmail.com. Scopus Author ID 7004134344, ResearcherID Q-9572-2016, https://orcid.org/0000-0002-7808-4246

Об авторе

Карташов Эдуард Михайлович, д.ф.-м.н., Заслуженный деятель науки Российской Федерации, Почетный работник высшего профессионального образования Российской Федерации, Почетный работник науки и техники Российской Федерации, Почетный профессор МИТХТ им. М.В. Ломоносова, Лауреат Золотой медали Академии наук Беларуси по теплофизике, профессор, кафедра высшей и прикладной математики, Институт тонких химических технологий им. М.В. Ломоносова, ФГБОУ ВО «МИРЭА – Российский технологический университет (119454, Россия, Москва, пр-т Вернадского, д. 78). E-mail: professor.kartashov@gmail.com. Scopus Author ID 7004134344, ResearcherID Q-9572-2016, https://orcid.org/0000-0002-7808-4246

Translated from Russian into English by K. Nazarov
Edited for English language and spelling by Thomas A. Beavitt

Mathematical modeling

Математическое моделирование

UDC 535.375.5
https://doi.org/10.32362/2500-316X-2024-12-6-91-101
EDN ZHLMCM

RESEARCH ARTICLE

Structural transitions in systems with a triple-well potential

Liliya M. Ozherelkova [@], Evgeniy S. Savin, Irina R. Tishaeva, Valentin V. Shevelev

MIREA – Russian Technological University, 119454 Russia
[@] Corresponding author, e-mail: ozherelkova@mirea.ru

Abstract

Objectives. Recently studied phenomena in condensed matter physics have prompted new insights into the dynamic theory of crystals. The results of numerous experimental data demonstrate the impossibility of their explanation within the framework of linear models of the dynamics of many-particle systems, resulting in the necessity to account for nonlinear effects. Analyzing the dynamics of systems in condensed matter physics containing a sufficiently large number of particles shows that modes of motion can undergo changes depending on the potential of interparticle interaction. This is also reflected in the presence of domains with essentially chaotic phase space having a number of degrees of freedom $N \geqslant 1.5$ and a certain set of interparticle interaction parameters. However, it is not only the dynamic model that appears to be strongly nonlinear. A similar nature of motion can be also observed in a static nonlinear many-particle system. The paper aims to study the influence of the external field specified by the interatomic triple-well potential on the equilibrium structure of a chain of interacting atoms.

Methods. Methods of Hamiltonian mechanics are used.

Results. Analytical expressions are obtained and analyzed for determining the phase portrait of the equilibrium structure of a chain of interacting atoms for various values of the parameter characterizing the local potential of the field in which each atom of the chain moves. Phase portraits of the equilibrium structure of the system are constructed in continuous and discrete representations of the equilibrium equations for various values of the parameter characterizing the local potential of the field in which each atom of the chain moves.

Conclusions. It is shown that both periodic and random chaotic arrangements of atoms are implemented depending on the magnitude of the external field.

Keywords: triple-well potential, chain, interaction, atom, phase portrait, chaos, structure

• **Submitted:** 22.03.2024 • **Revised:** 15.04.2024 • **Accepted:** 27.09.2024

For citation: Ozherelkova L.M., Savin E.S., Tishaeva I.R., Shevelev V.V. Structural transitions in systems with a triple-well potential. *Russ. Technol. J*. 2024;12(6):91–101. https://doi.org/10.32362/2500-316X-2024-12-6-91-101

Financial disclosure: The authors have no financial or proprietary interest in any material or method mentioned.

The authors declare no conflicts of interest.

НАУЧНАЯ СТАТЬЯ

Структурные переходы в системах с трехминимумным потенциалом

Л.М. Ожерелкова [@], **Е.С. Савин**, **И.Р. Тишаева**, **В.В. Шевелев**

МИРЭА – Российский технологический университет, Москва, 119454 Россия
[@] *Автор для переписки, e-mail: ozherelkova@mirea.ru*

Резюме

Цели. Явления, которые в последнее время изучаются физикой конденсированного состояния, привели к новым взглядам на проблемы динамической теории кристаллов. Результаты многочисленных экспериментальных данных показывают, что их невозможно объяснить, оставаясь в рамках линейных моделей динамики многочастичных систем. Необходимо учитывать существенно нелинейные эффекты. Анализ динамики систем в физике конденсированного состояния, содержащих достаточно большое число частиц, показывает, что они могут, в зависимости от потенциала межчастичного взаимодействия, испытывать смену режимов движения. Это проявляется и в том, что в фазовом пространстве такой системы с числом степеней свободы $N \geqslant 1.5$ при определенном наборе параметров межчастичного взаимодействия имеются области, в которых движение является по существу хаотическим. Однако не только динамическая модель оказывается сильно нелинейной. Подобный характер движения может проявляться и в статической нелинейной многочастичной системе. Цель работы – исследовать влияние внешнего поля, задаваемого межатомным трехъямным потенциалом, на равновесную структуру цепочки взаимодействующих атомов.

Методы. Использованы методы гамильтоновой механики.

Результаты. Получены и проанализированы аналитические выражения, определяющие фазовый портрет равновесной структуры цепочки взаимодействующих атомов при различных значениях параметра потенциала межчастичного взаимодействия, в котором движется каждый атом цепочки. Построены фазовые портреты равновесной структуры системы в континуальном и дискретном представлениях уравнений равновесия при различных значениях параметра, характеризующего межчастичный потенциал, в котором движется каждый атом цепочки.

Выводы. Показано, что в зависимости от величины внешнего поля реализуется как периодическое, так и случайное, хаотическое расположение атомов цепочки.

Ключевые слова: трехъямный потенциал, цепочка, взаимодействие, атом, фазовый портрет, хаос, структура

• **Поступила:** 22.03.2024 • **Доработана:** 15.04.2024 • **Принята к опубликованию:** 27.09.2024

Для цитирования: Ожерелкова Л.М., Савин Е.С., Тишаева И.Р., Шевелев В.В. Структурные переходы в системах с трехминимумным потенциалом. *Russ. Technol. J.* 2024;12(6):91–101. https://doi.org/10.32362/2500-316X-2024-12-6-91-101

Прозрачность финансовой деятельности: Авторы не имеют финансовой заинтересованности в представленных материалах или методах.

Авторы заявляют об отсутствии конфликта интересов.

INTRODUCTION

Recently studied phenomena in condensed state physics have prompted new approaches to problems in the dynamical theory of crystals [1, 2]. In order to explain numerous experimental data [3, 4], it has become necessary to allow for essentially nonlinear effects. However, it is not only the dynamical model that is strongly nonlinear. For example, it has been revealed [4, 5] that the type of crystal lattice depends on nonlinear properties of the interaction potential between crystal atoms even at absolute temperature $T = 0$ K.

From analyzing the dynamics of systems consisting of a sufficiently large number of particles shows [1–5] that a system can undergo a number of bifurcations occurring in the change of different types of motion depending on the nature and magnitude of interactions between particles. This is also reflected in the existence of regions in the phase space of such system having a number of degrees of freedom $N \geq 1.5$ at a certain set of parameters of the interparticle interaction potential, where motion is essentially chaotic [6–12].

This implies that the character of the system motion in such regions determinized by dynamic equations is such that it can be hardly distinguished from a random process. In addition, the presence of such regions implies that either deterministic or stochastic trajectories of motion can be realized in the system when the parameters of the interparticle interaction potential or initial conditions are changed. Such effects are best understood as a manifestation of the interparticle interaction potential nonlinearity.

The bifurcation phenomenon may also occur in a static system where the potential of interparticle interaction is nonlinear. In this case, such bifurcations imply the presence of structural transitions of different degrees of regularity up to chaotic.

In [3, 5], possible types of one-dimensional structures and transitions between them are studied. Distinguishing one-dimensional systems from their non-dimensional counterparts significantly simplifies the solution to the problem of atomic chain equilibrium due to the arrangement of atoms along one coordinate giving the meaning of "time" to this coordinate. The model of atomic one-dimensional chain in the periodic field and U(4) model are discussed in [13, 14] and [13], respectively. In the present work, the U(6) model is considered.

MATHEMATICAL MODEL

Following [4], we consider a one-dimensional chain of atoms interacting with their nearest neighbors in external field $V(u_n)$ determined by the atom number n in the chain interacting with the lattice atoms surrounding it. The Hamilton function (Hamiltonian) for this chain (system) has the following form (the atomic mass is assumed equal to 1):

$$H = \sum_{n=1}^{N}\left[\frac{1}{2}p_n^2 + \frac{1}{2}\chi a^2\left(u_n - u_{n-1} - 1\right)^2 + V\left(u_n\right)\right]. \quad (1)$$

Here u_n is displacement of the nth atom in units of interatomic distance a in the unperturbed chain, since at $V = 0$, the condition of minimum potential energy gives $u_{n+1} - u_n = 1$ for all numbers n; $p_n = a\dot{u}_n$, χ is the force interaction constant of chain atoms; $V(u_n)$ is the external potential field in which the nth atom moves. We define potential field $V(u_n)$ as the following function (the U(6) model):

$$V(u) = \varepsilon_0 u^2(u^2 - 1)^2, \quad (2)$$

where $|\varepsilon_0|$ is the potential barrier value. The function has three minima and two maxima at $\varepsilon_0 > 0$ (Fig. 1), while two minima and three maxima occur at $\varepsilon_0 < 0$ (Fig. 2).

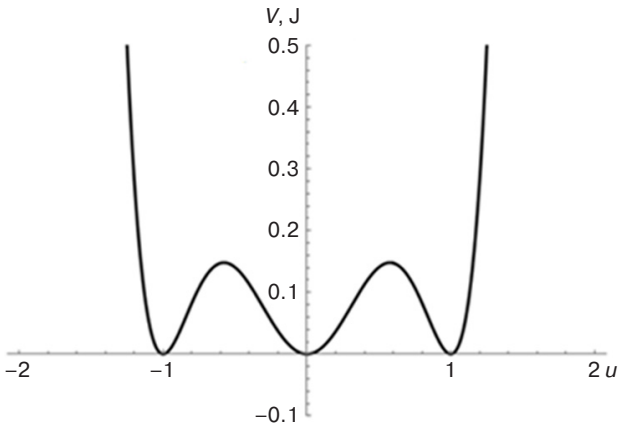

Fig. 1. Potential $V(u)$ at $\varepsilon_0 > 0$

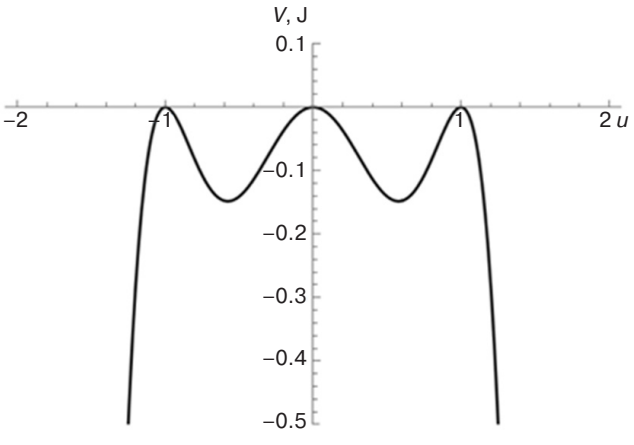

Fig. 2. Potential $V(u)$ at $\varepsilon_0 < 0$

ANALYZING THE MATHEMATICAL MODEL: CONTINUUM APPROXIMATION

1. Special points on a phase plane. The relative value of potential barrier $|\varepsilon_0|$ and energy of interatomic coupling $\approx \chi a^2$ between atoms in neighboring nodes of the chain are essential parameters affecting the properties of the chain having Hamiltonian (1) with external potential (2). If inequality $\chi a^2 \gg |\varepsilon_0|$ is satisfied, the equilibrium position of chain atoms would take the form of a spatial periodic wave. For $\chi a^2 \ll |\varepsilon_0|$, bonds between particles become insignificant so that the chain forms a "gas" of particles that are chaotically scattered over potential wells of the external field.

All possible configurations of the chain are solutions to equation

$$\chi a^2 \left(u_{n+1} - 2u_n + u_{n-1}\right) = \frac{dV}{du_n}. \qquad (3)$$

Expression (3) is a difference equation. In the continuum approximation, where displacement values of atoms u_n slightly depend on index n, we have

$$u_{n+1} = u_n + \frac{du}{dx} + \frac{1}{2!}\cdot\frac{d^2u}{dx^2} + \ldots,$$
$$u_{n-1} = u_n - \frac{du}{dx} + \frac{1}{2!}\cdot\frac{d^2u}{dx^2} + \ldots,$$

while the equation describing the equilibrium form of the chain has the following form:

$$\chi a^2 \frac{d^2u}{dx^2} = \frac{dV}{du}. \qquad (4)$$

For function $W = -V$, formula (4) is the equation of motion of a nonlinear oscillator provided that variable x is understood as time. This is equivalent to a system of two first-order equations:

$$\begin{cases} \chi a^2 \dfrac{du}{dx} = v, \\ \dfrac{dv}{dx} = \varepsilon_0\left(6u^5 - 8u^3 + 2u\right). \end{cases}$$

Special points on phase plane (u, du/dx) are defined by conditions ($v = 0$, $dv/dx = 0$), i.e., by the following system of equations:

$$\begin{cases} v = 0, \\ 6u^5 - 8u^3 + 2u = 0. \end{cases}$$

This system defines five special points: $u = 0$, $u = \pm 1/\sqrt{3}$, $u = \pm 1$. At $\varepsilon_0 > 0$, points $u = 0, \pm 1$ are saddle points, while points $u = \pm 1/\sqrt{3}$ are centers. Conversely, points $u = 0, \pm 1$ are centers and points $u = \pm 1/\sqrt{3}$ are saddles at $\varepsilon_0 < 0$.

2. Phase trajectories of motion. Integrating Eq. (4) for once, the equation defining phase trajectories on plane (u, du/dx) is obtained:

$$\sqrt{\frac{\chi a^2}{2}}\cdot\frac{du}{dx} = \pm\sqrt{\varepsilon_0\left(u^6 - 2u^4 + u^2\right) + E}, \qquad (5)$$

where E – integration constant. The trajectories of the system motion (phase portrait) significantly depend on the sign of parameter ε_0. Therefore, we consider two cases.

2.1. Parameter $\varepsilon_0 > 0$. As follows from (5), at $\varepsilon_0 > 0$ in the finite depth potential well, periodic oscillations of atoms (periodic structures) exist only under condition $-4\varepsilon_0/27 \le E \le 0$.

Periodic oscillations and their corresponding periodic (ordered) chain structures are impossible within interval $E > 0$.

For $\varepsilon_0 > 0$, phase trajectories of the system motion on phase plane, based on Eq. (5), have the form shown in Fig. 3. It can be seen from the figure that the system phase portrait contains five main elements: special points of the "center" type at $u = \pm 1/\sqrt{3}$ and three special saddle points $u = 0, \pm 1$. The selected motion trajectory leaving one saddle and entering another is a separatrix. This curve separates the regions of phase plane with substantially different nature of motion: the separatrix separates periodic motions of the chain from aperiodic motions, i.e., ordered structures from disordered ones.

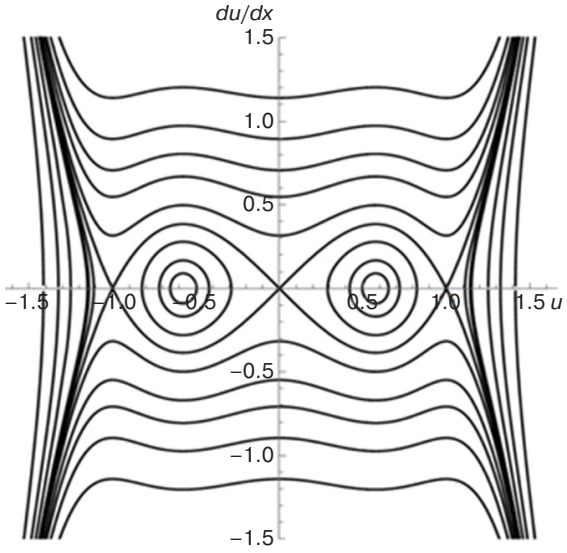

Fig. 3. Phase portrait of the system at $\varepsilon_0 > 0$

2.2. Parameter $\varepsilon_0 < 0$. Phase trajectories of the system motion on phase plane at $\varepsilon_0 < 0$ are shown in Fig. 4. It is evident from the figure that all phase trajectories in this case are closed, thus responding to the oscillatory motion of atoms in the chain and corresponding to the existence of its periodic structures. Here, separatrices have the form of loops beginning and ending in the same saddle to distinguish trajectories that correspond to oscillations of the chain with different nature; small-amplitude oscillations near minima $u = 0, \pm 1$ are separated by the separatrix from large-amplitude oscillations near the origin.

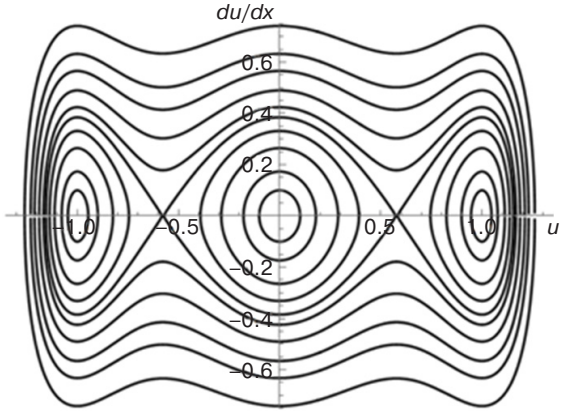

Fig. 4. Phase portrait of the system at $\varepsilon_0 < 0$

3. Analyzing solutions to Eq. (5). Next we consider solutions to Eq. (5) separately depending on the sign of parameter ε_0 in Eq. (2).

3.1. Parameter $\varepsilon_0 > 0$. After integrating Eq. (5) in this case, we denote $E_0 = E/\varepsilon_0$ and obtain the following

$$\int_{u_1}^{u_2} \frac{du}{\sqrt{u^6 - 2u^4 + u^2 + E_0}} = \\ = \int_{u_1}^{u_2} \frac{du}{\sqrt{P_6(u, E_0)}} = \pm \int_{x_0}^{x} \sqrt{\frac{2\varepsilon_0}{\chi a^2}}\, dx. \tag{6}$$

Here, value $P_6(u, E_0) = u^6 - 2u^4 + u^2 + E_0$. Limits of integration u_1, u_2 should satisfy condition $P_6(u, E_0) > 0$. We introduce a new integration variable using relation $u^2 = y$ and then transform expression (6) to the following form:

$$\int_{y_1}^{y_2} \frac{dy}{\sqrt{P_4(y, E_0)}} = \pm 2\sqrt{\frac{2\varepsilon_0}{\chi a^2}}\,(x - x_0). \tag{7}$$

Here, $P_4(y, E_0) = y^4 - 2y^3 + y^2 + E_0 y$. The graphs of function $P_4(y, E_0)$ for two different values of E_0 are shown in Fig. 5.

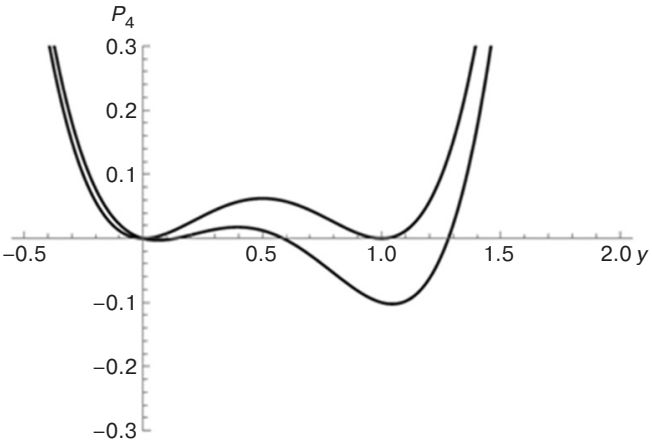

Fig. 5. Graphs of function $P_4(y, E_0)$ at $\varepsilon_0 > 0$

We study all possible cases of representing polynomial $P_4(y, E_0)$ in the form of a product of cofactors. At $E < -4\varepsilon_0/27$, polynomial $P_4(y, E_0)$ has two real and two complex conjugate roots. Given this, Eq. (7) takes the following form:

$$\int_{C_1}^{y} \frac{dy}{\sqrt{y(y - C_1)\left[(y - \alpha)^2 + \beta^2\right]}} = \\ = \pm 2\sqrt{\frac{2\varepsilon_0}{\chi a^2}}\,(x - x_0). \tag{8}$$

Here, C_1 is the real root of polynomial $P_4(y, E_0)$, the second real root $y = 0$, and complex roots $\alpha \pm i\beta$. The integral in the left part of Eq. (8) is expressed through elliptic Jacobi functions [15, 16], as follows:

$$\int_{C_1}^{y} \frac{dy}{\sqrt{y(y - C_1)\left[(y - \alpha)^2 + \beta^2\right]}} = \\ = \frac{1}{\sqrt{pq}} F\left(2\operatorname{arctg}\sqrt{\frac{q(y - C_1)}{py}};\ \frac{1}{2}\sqrt{\frac{(p+q)^2 + C_1^2}{pq}}\right). \tag{9}$$

Here, $p^2 = (C_1 - \alpha)^2 + \beta^2$, $q^2 = (2C_1 - \alpha)^2 + \beta^2$.

Introducing new variable $z = 2\sqrt{\frac{2\varepsilon_0 pq}{\chi a^2}}\,(x - x_0)$, the following is obtained from Eqs. (8) and (9):

$$z = \pm F(\gamma, k). \tag{10}$$

Here, $\gamma = 2\operatorname{arctg}\sqrt{\frac{q(y - C_1)}{py}}$, $k = \frac{1}{2}\sqrt{\frac{(p+q)^2 + C_1^2}{pq}}$, while $F(\gamma, k)$ is an elliptic integral of the first kind.

It follows from Eq. (10) that

$$\mathrm{sn}(z,k)=\sin(\gamma)=\sin\left(2\,\mathrm{arctg}\sqrt{\frac{q(y-C_1)}{py}}\right)= \\ =2\sqrt{\frac{q(y-C_1)}{py}}\left[1+\frac{q(y-C_1)}{py}\right]^{-1}. \quad (11)$$

Then

$$y=\frac{C_1 q\,\mathrm{sn}^2(z,k)}{q\,\mathrm{sn}^2(z,k)-p\left(1\pm\mathrm{cn}(z,k)\right)^2}. \quad (12)$$

Here, sn(z, k) and cn(z, k) are elliptic sine and cosine, respectively.

Function y defined by Eq. (12) is an even function with period $T = 4K(k)/\delta$, where $K(k)$ is the complete elliptic integral of the first kind, $\delta = 8|\varepsilon_0|pq/(\chi a^2)$. Hence,

$$u=\pm\frac{\mathrm{sn}(z,k)\sqrt{\alpha q}}{\sqrt{q\,\mathrm{sn}^2(z,k)-p\left(1\pm\mathrm{cn}(z,k)\right)^2}}. \quad (13)$$

In domain $-4/27 \le E_0 \le 0$, polynomial $P_4(y, E_0)$ has four real roots, $C_1 > C_2 > C_3 > C_4 = 0$. Roots C_1, C_2, C_3, and C_4 should satisfy the following conditions:

$$\begin{cases} C_1+C_2+C_3+C_4=-2, \\ C_1C_2+C_3C_4+(C_1+C_2)(C_3+C_4)=-1, \\ C_1C_2(C_3+C_4)+C_3C_4(C_1+C_2)=E_0, \\ -C_1C_2C_3C_4=0. \end{cases}$$

With allowance for the location of roots C_1, C_2, C_3, and C_4 on the real axis, polynomial $P_4(y, E_0) > 0$ in intervals $y \in (C_3, C_2)$ and

On interval $y \in (C_3, C_2)$, the integral on the left side of Eq. (7) has the following form:

$$\int_{C_3}^{y}\frac{dy}{\sqrt{(C_1-y)(C_2-y)(y-C_3)y}}= \\ =\frac{2F(\gamma,q)}{\sqrt{(C_1-C_3)C_2}}. \quad (14)$$

Here, $\gamma=\arcsin\sqrt{\frac{C_2(y-C_3)}{(C_2-C_3)y}}$, $q=\sqrt{\frac{(C_2-C_3)C_1}{(C_1-C_3)C_2}}$.

We denote

$$z=\sqrt{\frac{2\varepsilon_0(C_1-C_3)C_2}{\chi a^2}}(x-x_0). \quad (15)$$

Then from (14), (15), we obtain that $z = \pm F(\gamma, q)$, so

$$\mathrm{sn}(z,q)=\sin\gamma=\sqrt{\frac{C_2(y-C_3)}{(C_2-C_3)y}}.$$

Hence,

$$u=\pm\left[\frac{C_2C_3}{C_2-(C_2-C_3)\mathrm{sn}^2(z,q)}\right]^{1/2}. \quad (16)$$

As above, function u is an even function with period $T = 4K(k)/\delta$, where

$$\delta=\sqrt{\frac{2\varepsilon_0(C_1-C_3)C_2}{\chi a^2}}.$$

If we assume $C_1 = C_2$ in (16), then parameter $q = 1$ and solution (16) is a soliton solution having the following form:

$$u=\pm\sqrt{\frac{C_2C_3}{C_2-(C_2-C_3)\mathrm{th}^2 z}}. \quad (17)$$

Within the interval of values $y > C_1$, polynomial $P_4(y, E_0) > 0$. Substituting the necessary limits of integration into (8), periodic solutions at $E_0 > 0$ are obtained. Thus, we have the following:

$$\int_{C_1}^{y}\frac{dy}{\sqrt{(y-C_1)(y-C_2)(y-C_3)y}}= \\ =\frac{2}{\sqrt{(C_1-C_3)C_2}}F(\varphi,k)=\pm2\sqrt{\frac{2\varepsilon_0}{\chi a^2}}(x-x_0), \quad (18)$$

where $\varphi=\arcsin\sqrt{\frac{C_2(y-C_1)}{C_1(y-C_2)}}$, $k=\sqrt{\frac{(C_2-C_3)C_1}{(C_1-C_3)C_2}}$.

Let $z=\sqrt{\frac{2\varepsilon_0(C_1-C_3)C_2}{\chi a^2}}(x-x_0)$.

Then $z = \pm F(\varphi, k)$ and hence,

$$\mathrm{sn}(z,k)=\sin\varphi=\sqrt{\frac{C_2(y-C_1)}{C_1(y-C_2)}}. \quad (19)$$

Given that $u = \pm y^{1/2}$, we obtain the following:

$$u=\pm\left[\frac{C_1C_2(1-\mathrm{sn}^2(z,k))}{C_2-C_1\,\mathrm{sn}^2(z,k)}\right]^{1/2}. \quad (20)$$

For $C_1 = C_2$ ($k = 1$) from (20), the solution is bell-shaped:

$$u = \pm\left[\frac{C_1C_2\left(1-\text{th}^2(z)\right)}{C_2 - C_1\,\text{th}^2(z)}\right]^{1/2}.$$

At $z = 0$, u has the form of $u = \pm C_1^{1/2}$, while $u = 0$ at $z \to \pm\infty$.

3.2 Parameter $\varepsilon_0 < 0$. For $\varepsilon_0 < 0$, Eq. (5) has the following form:

$$\sqrt{\frac{\chi a^2}{2|\varepsilon_0|}}\frac{du}{dx} = \pm\sqrt{-u^6 + 2u^4 - u^2 + E_0}, \qquad (21)$$

where $E_0 = E/|\varepsilon_0|$.

Three points of stable equilibrium positions $u = 0, \pm1$ and two points $u = \pm1/\sqrt{3}$ corresponding to unstable positions are observed on the oscillator phase plane (u, du/dx).

We integrate Eq. (21):

$$\int_{u_1}^{u_2}\frac{du}{\sqrt{-u^6 + 2u^4 - u^2 + E_0}} = \int_{u_1}^{u_2}\frac{du}{\sqrt{P_6(u, E_0)}} = \pm\sqrt{\frac{2|\varepsilon_0|}{\chi a^2}}\int_{x_0}^{x} dx, \qquad (22)$$

where $P_6(u, E_0) = -u^6 + 2u^4 - u^2 + E_0$.

We introduce a new integration variable, $u^2 = y$, $du = dy/2\sqrt{y}$. Then (22) takes the following form:

$$\int_{u_3}^{u_4}\frac{dy}{\sqrt{P_4(y, E_0)}} = \pm2\sqrt{\frac{2|\varepsilon_0|}{\chi a^2}}(x - x_0). \qquad (23)$$

Here, $P_4(y, E_0) = -y^4 + 2y^3 - y^2 + E_0 y$. The graphs of function $P_4(y, E_0)$ at two different values of E_0 are shown in Fig. 6.

As before, different cases of decomposing polynomial $P_4(y, E_0)$ into multipliers are also studied here. When polynomial $P_4(y, E_0)$ has two real $y = 0$, $y = C_1$ and two complex conjugate roots $y = \alpha \pm i\beta$, expression (23) is transformed to:

$$\int_0^{y}\frac{dy}{\sqrt{y(C_1 - y)\left[(y-\alpha)^2 + \beta^2\right]}} = \pm2\sqrt{\frac{2|\varepsilon_0|}{\chi a^2}}(x - x_0),\ 0 < y < C_1. \qquad (24)$$

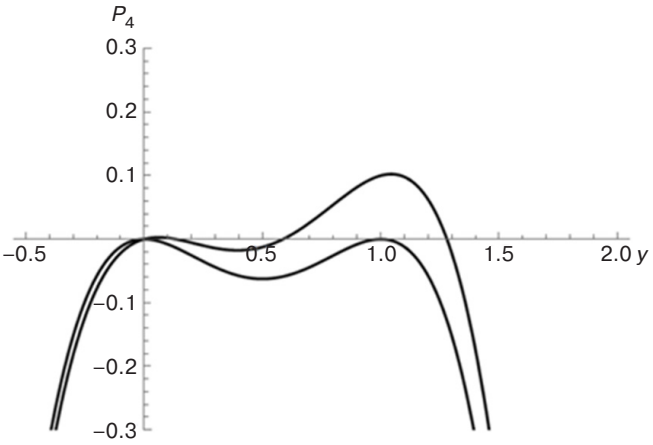

Fig. 6. Graphs of function $P_4(y, E_0)$ at $\varepsilon_0 < 0$

Since the integral in the left part of Eq. (24) is an elliptic Jacobi function, this equation can be represented as follows:

$$z = \pm F(\gamma, k), \qquad (25)$$

where $z = 2\sqrt{\frac{2|\varepsilon_0|}{\chi a^2}pq}(x - x_0)$, $\gamma = 2\,\text{arcctg}\sqrt{\frac{q(C_1 - y)}{py}}$, $k = \frac{1}{2}\sqrt{\frac{-(p-q)^2 + C_1^2}{pq}}$, $q^2 = \alpha^2 + \beta^2$, $p^2 = (\alpha - C_1)^2 + \beta^2$, $F(\gamma, k)$ is the Jacobi elliptic function.

It follows from Eq. (25) that

$$\text{sn}(z, k) = \sin\gamma = \sin\left(2\,\text{arcctg}\sqrt{\frac{q(C_1 - y)}{py}}\right) = \frac{\sqrt{qpy(C_1 - y)}}{py + q(C_1 - y)}.$$

Hence, we obtain that $y = u^2$ and

$$y = \frac{qC_1\,\text{sn}^2(z, k)}{p\left(1 \pm \text{cn}(z, k)\right)^2 + q\,\text{sn}^2(z, k)}. \qquad (26)$$

Function y is an even periodic function with period $T = 4K(k)/\delta$. At $x = x_0$, the function becomes zero. Thus,

$$u = \pm\frac{\text{sn}(z, k)\sqrt{qC_1}}{\sqrt{p\left(1 \pm \text{cn}(z, k)\right)^2 + q\,\text{sn}^2(z, k)}}. \qquad (27)$$

It follows from (27) that function u can be either even with period $T = 4K(k)/\delta$ or odd with period $T = 8K(k)/\delta$, $\delta = 8|\varepsilon_0|pq/(\chi a^2)$.

We consider the case when all roots C_1, C_2, C_3, and C_4 of polynomial $P_4(y, E_0)$ are real, where

$C_1 > C_2 > C_3 > C_4 = 0$. Then the integral in the left-hand part of (23) is transformed to the form under condition $0 < y < C_3$, as follows:

$$\int_0^y \frac{dy}{\sqrt{(C_1-y)(C_2-y)(C_3-y)y}} = \frac{2}{\sqrt{(C_1-C_3)C_2}}F(\beta,r) = \pm 2\sqrt{\frac{2|\varepsilon_0|}{\chi a^2}}(x-x_0). \quad (28)$$

Here, $\beta = \arcsin\sqrt{\frac{(C_1-C_3)y}{(C_1-y)C_3}}$, $r = \sqrt{\frac{C_3(C_1-C_2)}{C_2(C_1-C_3)}}$, $0 < y < C_3$.

It follows from expression (28) that

$$u = \pm\frac{\sqrt{C_1C_3}\,\mathrm{sn}(z,r)}{\sqrt{(C_1-C_3)+C_3\,\mathrm{sn}^2(z,r)}}. \quad (29)$$

Here, $z = \sqrt{\frac{2|\varepsilon_0|}{\chi a^2}(C_1-C_3)C_2}\,(x-x_0)$.

Equation (29) has a soliton solution in case of $C_2 = C_3$, with parameter $r = 1$. This solution has the following form:

$$u = \pm\frac{\sqrt{C_1C_3}\,\mathrm{th}\,z}{\sqrt{C_1-C_3+C_3\,\mathrm{th}^2 z}}. \quad (30)$$

Note that $u = 0$ at $z = 0$ while $u = \pm\sqrt{C_3}$ at $z \to \pm\infty$.

The polynomial $P_4(y, E_0)$ is also positive within interval $C_2 < y < C_1$.

Substituting the desired limits of integration from (23), we obtain:

$$\int_{C_2}^y \frac{dy}{\sqrt{y(C_1-y)(y-C_2)(y-C_3)}} = \frac{2}{\sqrt{(C_1-C_3)C_2}}F(\lambda,r) = \pm\sqrt{\frac{2|\varepsilon_0|}{\chi a^2}}(x-x_0), \quad (31)$$

where $\lambda = \arcsin\sqrt{\frac{(C_1-C_3)(y-C_2)}{(C_1-C_2)(y-C_3)}}$, $r = \sqrt{\frac{C_3(C_1-C_2)}{C_2(C_1-C_3)}}$.

With allowance for (31), we obtain the following:

$$u = \pm\sqrt{\frac{C_3(C_1-C_2)\mathrm{sn}^2(z,r)-C_2(C_1-C_3)}{(C_1-C_2)\mathrm{sn}^2(z,r)-(C_1-C_3)}}, \quad (32)$$

where $z = \sqrt{\frac{2|\varepsilon_0|}{\chi a^2}(C_1-C_3)C_2}\,(x-x_0)$.

Thus, the results obtained in the continuum approximation (under conditions of weak external field) indicate that phase curves are closed and have the form of slightly deformed ellipses in the neighborhood of stable position points regardless of the ε_0 sign. Each curve corresponds to the equilibrium position of the chain in the form of a spatial periodic wave. Separatrices connecting the points of unstable position and limiting the domain of closed curves correspond to the equilibrium in the form of a bell-shaped solitary wave.

ANALYSING THE MATHEMATICAL MODEL: DISCRETE APPROXIMATION

When the external field potential is sufficiently large, function u_n cannot be considered to be weakly dependent on n, so it is necessary to return to difference equations.

Equation (3) can be visualized as a representation given the introduction of variable $I_n = (u_n - u_{n-1})$. Then Eq. (3) transforms into the universal representation [3]:

$$\begin{cases} I_{n+1} = I_n + \dfrac{dV_0}{du_n}, \\ u_{n+1} = u_n + I_{n+1}, \end{cases} \quad (33)$$

where $V_0 = V/(\chi a^2)$.

Representation (33) has periodic and chaotic solutions that determine the corresponding arrangements of atoms in the chain, i.e., its structure. Thus, studying equilibrium forms of the chain is reduced to studying sequences of points $\{u_n, I_n\}$ plotted on a plane. Depending on initial values (u_0, I_0), this sequence either regularly fits into closed lines or appears chaotically scattered in some domain on the coordinate plane.

Numerical solutions to the system of equations (33) with function V in form (2) are shown in Figs. 7 and 8 as phase portraits of the system at different values of parameter $\varepsilon_0' = \varepsilon_0/(\chi a^2)$.

The solution to system (33) in coordinates (u, I) at any initial values (u_0, I_0) is a straight line parallel to the u axis. At sufficiently small ε_0' (Fig. 7), the most of phase space is occupied by the sequence of points fitting into closed curves.

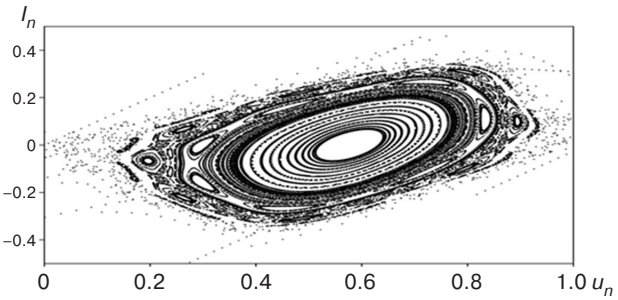

Fig. 7. Phase portrait of the system at $\varepsilon_0' = 0.4$

However, a disorderly distribution of sequential pairs (u_n, I_n) on the plane occurs in a minor part of the phase space, thus demonstrating the chaotic phenomenon for model (33). In the phase space, these pairs occupy narrow stochastic layers separated from each other by invariant curves. Separate domains on the phase plane are not occupied by stochastic trajectory points. Since these domains contain a finite measure of periodic trajectories, the conditions of KAM-theory (Kolmogorov–Arnold–Moser theory) are fulfilled in central parts of the domains [13]. This means that in case of ε_0' smallness, the stochastic layers are not connected to each other. This is the direct consequence of the KAM-theory [13] for the number of degrees of freedom $N \le 2$.

According to [3], the stochastic layer width δh can be estimated for $\varepsilon_0' \ll 1$:

$$\delta h \approx 2(2\pi)^4 e^{-\frac{\pi}{\sqrt{\varepsilon_0'}}}. \qquad (34)$$

It follows from (34) that at arbitrarily small perturbations, an exponentially small stochastic layer appears that can be interpreted as a germ of structural chaos in the arrangement of chain atoms.

An increase in values of parameter ε_0' results in the growth of the stochastic layer width, thus leading, in turn, to the destruction of KAM curves and merging of stochastic layers and the subsequent formation of a stochastic sea containing islands of stability.

The system phase portrait at $\varepsilon_0' = 0.7$ is shown in Fig. 8.

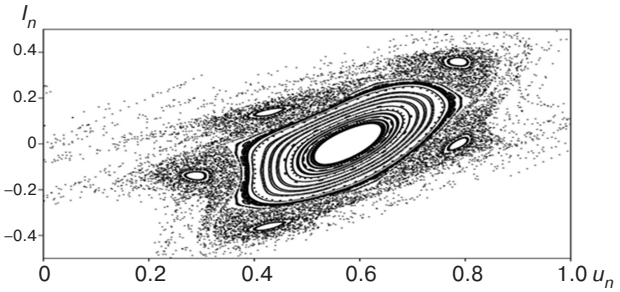

Fig. 8. Phase portrait of the system at $\varepsilon_0' = 0.7$

It is evident from Fig. 8 that the largest object of the phase portrait is the separatrix cell with saddle $u = \pm 1/\sqrt{3}$, which is destroyed to allow a stochastic structural layer to be formed in its place. The domain limited by this main layer contains a family of nested invariant curves that span point $I = 0$. Outside the domain limited by the main stochastic layer, a group of separatrix cells containing narrower stochastic layers is located. Invariant curves are beyond the cells. Thus, the system phase portrait consists of an infinite number of alternating invariant curves and stochastic layers. At $\varepsilon_0' \sim 1$, the merging of stochastic layers and formation of a common stochastic sea is observed indicating a transition to the formation of the chain chaotic structure.

At $|\varepsilon_0'| \gg 1$, almost the entire domain of phase space becomes the domain of stochastic motion. The exceptions are islands of stability, whose size is of $1/|\varepsilon_0'|$ order at $|\varepsilon_0'| \gg 1$. These islands are located in the neighborhood of elliptic points (points of stable equilibrium position) of the representation.

CONCLUSIONS

In the present paper, it is shown that closed phase curves in the continuum approximation under the conditions of a small external field have the form of slightly deformed ellipses in the neighborhood of stable position points regardless of the ε_0 sign. Each curve corresponds to the equilibrium position of the chain having the form of a spatial periodic wave. Separatrices connecting the points of unstable position and limiting the area of closed curves correspond to the chain equilibrium in the form of a bell-shaped solitary wave.

The numerical solutions to the system of equilibrium equations also demonstrate the implementation of that both periodic and random chaotic arrangements of chain atoms depending on the external field strength.

Authors' contribution. All authors equally contributed to the research work.

REFERENCES

1. Gleick J. *Khaos. Sozdanie novoi nauki* (*Chaos. Making a New Science*). Transl. from Engl. Moscow: AST: Corpus; 2022. 432 p. (in Russ.). ISBN 978-5-17-138645-0
[Gleick J. *Chaos: Making a New Science*. Open Road Medea; 2011. 360 p.]
2. Grinchenko V.T., Matsypura V.T., Snarskii A.A. *Vvedenie v nelineinuyu dinamiku: Khaos i fraktaly* (*Introduction to Nonlinear Dynamics: Chaos and Fractals*). M.: LENAND; 2021. 280 p. (in Russ.). ISBN 978-5-9710-6410-7
3. Zaslavskii G.M. *Fizika khaosa v gamil'tonovykh sistemakh* (*Physics of Chaos in Hamiltonian Systems*). Moscow, Izhevsk: Institute of Computer Research; 2004. 286 p. (in Russ.). ISBN 5-93972-342-X
4. Akhmadulina E.N., Savin E.S. Proton oscillation in a three-minimum potential. *Fine Chem. Technol*. (*Vestnik MITHT*). 2012;7(6):88–91 (in Russ.). Available from URL: https://www.elibrary.ru/pnmfxv
5. Ragushina M.D., Savin E.S. Dynamics of systems allowing structural phase transitions. *Fine Chem. Technol*. 2016;11(2): 81–85 (in Russ.). https://doi.org/10.32362/2410-6593-2016-11-2-81-85, available from URL: https://www.elibrary.ru/tugqvj
6. Ivanchenko M.V., Kozinov E.A., Volokitin V.D., Liniov A.V., Meyerov I.B., Denisov S.V. Classical bifurcation diagrams by quantum means. *Ann. Der Phys.* 2017;529(8):1600402. https://doi.org/10.1002/andp.201600402
7. Ivanchenko M.V. Dissipative quantum chaos. In: *Nanoelectronics, Nanophotonics and Nonlinear Physics: Collection of proceedings of the 14th All-Russian Conference of Young Scientists*. Saratov: Techno-Décor; 2019. P. 96 (in Russ.). Available from URL: https://www.elibrary.ru/pdgagn
8. Arnold L., Boxier P. Stochastic bifurcation: instructive examples in dimension one. In: M. Pinsky and V. Wihstutz (Eds.). *Diffusion Processes and Related Problems in Analysis. Volume II: Stochastic Flows. Volume 27: Progress in Probability*. Birkhäuser, Boston Basel Stuttgart; 1992. P. 241–255. https://doi.org/10.1007/978-1-4612-0389-6_10
9. Yusipov I.I., Denisov S.V., Ivanchenko M.V. Bifurcations and chaos in open quantum systems. *Radiophys. Quantum El.* 2023;66(1):63–76. https://doi.org/10.1007/s11141-023-10276-6, available from URL: https://www.elibrary.ru/skhwmx
[Original Russian Text: Yusipov I.I., Denisov S.V., Ivanchenko M.V. Bifurcations and chaos in open quantum systems. *Izvestiya vysshikh uchebnykh zavedenii. Radiofizika.* 2023;66(1):71–85 (in Russ.). Available from URL: https://www.elibrary.ru/zmnges]
10. Poot M., van der Zant H.S.J. Mechanical systems in the quantum regime. *Phys. Rep.* 2012;511(5):273–335. http://doi.org/10.1016/j.physrep.2011.12.004
11. Savin E.S. Model of the transition of polyethylene to a mesophase state. *Polym. Sci. Ser. A.* 2000;42(6):637–641. Available from URL: https://www.elibrary.ru/lfybdp
[Original Russian Text: Savin E.S. Model of the transition of polyethylene to a mesophase state. *Vysokomole-kulyarnye Soedineniya. Seriya A.* 2000; 42(6):974–979 (in Russ.). Available from URL: https://www.elibrary.ru/mpggtv]
12. Haken H. *Sinergetika. Ierarkhiya neustoichivostei v samoorganizuyushchikhsya sistemakh i ustroistvakh* (*Synergetics. Hierarchy of Instabilities in Self-Organizing Systems and Devices*). Transl. from Engl. Moscow: Mir; 1985. 424 p. (in Russ.).
[Haken H. *Synergetics: An Introduction*. Berlin: Springer Verlag; 1978. 394 p.]
13. Beloshapkin V.V., Tretyakov A.G., Zaslavsky G.M. Disorder of Particle Chains as a Dynamical Problem of Transition to Chaos: Analogy to Simulation Induced Chaos. *Communications on Pure and Applied Mathematics.* 1994;47(1):39–46. https://doi.org/10.1002/cpa.3160470104, available from URL: https://www.elibrary.ru/zztesn
14. Chernikov A.A., Natenzon M.Ya., Petrovichev B.A., Sagdeev R.Z., Zaslavsky G.M. Strong changing of adiabatic invariants, KAM-tori and Web-tori. *Phys. Lett. A.* 1988;129(7):377–380. https://doi.org/10.1016/0375-9601(88)90006-0
15. Gradshtein M.S., Ryzhik I.M. *Tablitsy integralov, summ, ryadov i proizvedenii* (*Tables of Integrals, Sums, Series and Products*). Moscow: Fizmatgiz; 1971. 1108 p. (in Russ.).
16. Baterman H., Erdelyi A. *Vysshie transtsendentnye funktsii. Ellipticheskie i avtomorfnye funktsii. Funktsii Lame i Mat'e* (*Higher transcendental functions. Elliptic and automorphic functions. Lamé and Mathieu functions*). Transl. from Engl. Moscow: Nauka; 1967. 300 p. (in Russ.).
[Baterman H., Erdelyi A. *Higher Transcendental Functions.* V. 3. McGraw Hill; 1955. 312 p.]

СПИСОК ЛИТЕРАТУРЫ

1. Глик Д. *Хаос. Создание новой науки*: пер. с англ. М.: АСТ: Corpus; 2022. 432 с. ISBN 978-5-17-138645-0
2. Гринченко В.Т., Мацыпура В.Т., Снарский А.А. *Введение в нелинейную динамику: Хаос и фракталы.* М.: ЛЕНАНД; 2021. 280 с. ISBN 978-5-9710-6410-7
3. Заславский Г.М. *Физика хаоса в гамильтоновых системах.* Москва, Ижевск: Институт компьютерных исследований; 2004. 286 с. ISBN 5-93972-342-X
4. Ахмадулина Э.Н., Савин Е.С. Колебание протона в трех-минимумном потенциале. *Тонкие химические технологии* (*Вестник МИТХТ им. М.В. Ломоносова*). 2012;7(6):88–91. URL: https://www.elibrary.ru/pnmfxv
5. Рагушина М.Д., Савин Е.С. Динамика систем, допускающих структурные фазовые переходы. *Тонкие химические технологии.* 2016;11(2):81–85. https://doi.org/10.32362/2410-6593-2016-11-2-81-85, URL: https://www.elibrary.ru/tugqvj
6. Ivanchenko M.V., Kozinov E.A., Volokitin V.D., Liniov A.V., Meyerov I.B., Denisov S.V. Classical bifurcation diagrams by quantum means. *Ann. Der Phys.* 2017;529(8):1600402. https://doi.org/10.1002/andp.201600402

7. Иванченко М.В. Диссипативный квантовый хаос. В сб.: *Наноэлектроника, нанофотоника и нелинейная физика: Сборник трудов XIV Всероссийской конференции молодых ученых.* Саратов: Техно-Декор; 2019. С. 96. URL: https://www.elibrary.ru/pdgagn
8. Arnold L., Boxier P. Stochastic bifurcation: instructive examples in dimension one. In: Pinsky M., Wihstutz V. (Eds.). *Diffusion Processes and Related Problems in Analysis. Volume II: Stochastic Flows. Volume 27: Progress in Probability*. Birkhäuser, Boston Basel Stuttgart; 1992. P. 241–255. https://doi.org/10.1007/978-1-4612-0389-6_10
9. Юсипов И.И., Денисов С.В., Иванченко М.В. Бифуркации и хаос в открытых квантовых системах. *Известия вузов. Радиофизика.* 2023;66(1):71–85. URL: https://www.elibrary.ru/zmnges
10. Poot M., van der Zant H.S.J. Mechanical systems in the quantum regime. *Phys. Rep.* 2012;511(5):273–335. http://doi.org/10.1016/j.physrep.2011.12.004
11. Савин Е.С. Модель перехода полиэтилена в мезофазное состояние. *Высокомолекулярные соединения. Серия А*. 200;42(6):974–979. URL: https://www.elibrary.ru/mpggtv
12. Хакен Г. *Синергетика. Иерархия неустойчивостей в самоорганизующихся системах и устройствах*: пер. с англ. М.: Мир; 1985. 424 с.
13. Beloshapkin V.V., Tretyakov A.G., Zaslavsky G.M. Disorder of Particle Chains as a Dynamical Problem of Transition to Chaos: Analogy to Simulation Induced Chaos. *Communications on Pure and Applied Mathematics.* 1994;47(1):39–46. https://doi.org/10.1002/cpa.3160470104, URL: https://www.elibrary.ru/zztesn
14. Chernikov A.A., Natenzon M.Ya., Petrovichev B.A., Sagdeev R.Z., Zaslavsky G.M. Strong changing of adiabatic invariants, KAM-tori and Web-tori. *Phys. Lett. A.* 1988;129(7):377–380. https://doi.org/10.1016/0375-9601(88)90006-0
15. Градштейн М.С., Рыжик И.М. *Таблицы интегралов, сумм, рядов и произведений.* М.: Физматгиз; 1971. 1108 с.
16. Бейтмен Г., Эрдейи А. *Высшие трансцендентные функции. Эллиптические и автоморфные функции. Функции Ламе и Матье:* пер. с англ. М.: Наука; 1967. 300 с.

About the authors

Liliya M. Ozherelkova, Cand. Sci. (Eng.), Associate Professor, Department of Higher and Applied Mathematics, M.V. Lomonosov Institute of Fine Chemical Technologies, MIREA – Russian Technological University (86, Vernadskogo pr., Moscow, 119571 Russia). E-mail: lilom@list.ru. Scopus Author ID 57212531310, https://orcid.org/0009-0004-5680-5040

Evgeniy S. Savin, Cand. Sci. (Phys.-Math.), Associate Professor, Department of Higher and Applied Mathematics, M.V. Lomonosov Institute of Fine Chemical Technologies, MIREA – Russian Technological University (86, Vernadskogo pr., Moscow, 119571 Russia). E-mail: savin@mirea.ru. Scopus Author ID 57214433156, https://orcid.org/0009-0001-1402-5845

Irina R. Tishaeva, Cand. Sci. (Eng.), Associate Professor, Department of Higher and Applied Mathematics, M.V. Lomonosov Institute of Fine Chemical Technologies, MIREA – Russian Technological University (86, Vernadskogo pr., Moscow, 119571 Russia). E-mail: irina.tishaeva@rambler.ru. Scopus Author ID 57212526831, https://orcid.org/0000-0003-1866-6866

Valentin V. Shevelev, Dr. Sci. (Phys.-Math.), Professor, Department of Higher and Applied Mathematics, M.V. Lomonosov Institute of Fine Chemical Technologies, MIREA – Russian Technological University (86, Vernadskogo pr., Moscow, 119571 Russia). E-mail: valeshevelev@yandex.ru. Scopus Author ID 7006985545, RSCI SPIN-code 3007-0334, https://orcid.org/0000-0002-9285-5772

Об авторах

Ожерелкова Лилия Мухарамовна, к.т.н., доцент, кафедра высшей и прикладной математики, Институт тонких химических технологий им. М.В. Ломоносова, ФГБОУ ВО «МИРЭА – Российский технологический университет» (119571, Россия, Москва, пр-т Вернадского, д. 86). E-mail: lilom@list.ru. Scopus Author ID 57212531310, https://orcid.org/0009-0004-5680-5040

Савин Евгений Степанович, к.ф.-м.н., доцент, кафедра высшей и прикладной математики, Институт тонких химических технологий им. М.В. Ломоносова, ФГБОУ ВО «МИРЭА – Российский технологический университет» (119571, Россия, Москва, пр-т Вернадского, д. 86). E-mail: savin@mirea.ru. Scopus Author ID 57214433156, https://orcid.org/0009-0001-1402-5845

Тишаева Ирина Романовна, к.т.н., доцент, кафедра высшей и прикладной математики, Институт тонких химических технологий им. М.В. Ломоносова, ФГБОУ ВО «МИРЭА – Российский технологический университет» (119571, Россия, Москва, пр-т Вернадского, д. 86). E-mail: irina.tishaeva@rambler.ru. Scopus Author ID 57212526831, https://orcid.org/0000-0003-1866-6866

Шевелев Валентин Владимирович, д.ф.-м.н., профессор, кафедра высшей и прикладной математики, Институт тонких химических технологий им. М.В. Ломоносова, ФГБОУ ВО «МИРЭА – Российский технологический университет» (119571, Россия, Москва, пр-т Вернадского, д 86). E-mail: valeshevelev@yandex.ru. Scopus Author ID 7006985545, SPIN-код РИНЦ 3007-0334, https://orcid.org/0000-0002-9285-5772

Translated from Russian into English by K. Nazarov
Edited for English language and spelling by Thomas A. Beavitt

Mathematical modeling

Математическое моделирование

UDC 519.673
https://doi.org/10.32362/2500-316X-2024-12-6-102-112
EDN YBOYBL

RESEARCH ARTICLE

Neural operators for hydrodynamic modeling of underground gas storage facilities

Daniil D. Sirota [@], Kirill A. Gushchin, Sergey A. Khan, Sergey L. Kostikov, Kirill A. Butov

Gazprom, St. Petersburg, 197229 Russia
[@] Corresponding author, e-mail: D.Sirota@adm.gazprom.ru

Abstract

Objectives. Much of the research in deep learning has focused on studying mappings between finite-dimensional spaces. While hydrodynamic processes of gas filtration in underground storage facilities can be described by partial differential equations (PDE), the requirement to study the mappings between functional spaces of infinite dimension distinguishes this problem from those solved using traditional mapping approaches. One of the most promising approaches involves the construction of neural operators, i.e., a generalization of neural networks to approximate mappings between functional spaces. The purpose of the work is to develop a neural operator to speed up calculations involved in hydrodynamic modeling of underground gas storages (UGS) to an acceptable degree of accuracy.

Methods. In this work, a modified Fourier neural operator was built and trained for hydrodynamic modeling of gas filtration processes in underground gas storages.

Results. The described method is shown to be capable of successful application to problems of three-dimensional gas filtration in a Cartesian coordinate system at objects with many wells. Despite the use of the fast Fourier transform algorithm in the architecture, the developed model is also effective for modeling objects having a nonuniform grid and complex geometry. As demonstrated not only on the test set, but also on artificially generated scenarios with significant changes made to the structure of the modeled object, the neural operator does not require a large training dataset size to achieve high accuracy of approximation of PDE solutions. A trained neural operator can simulate a given scenario in a fraction of a second, which is at least 10^6 times faster than a traditional numerical simulator.

Conclusions. The constructed and trained neural operator demonstrated efficient hydrodynamic modeling of underground gas storages. The resulting algorithm reproduces adequate solutions even in the case of significant changes in the modeled object that had not occurred during the training process. The model can be recommended for use in planning and decision-making purposes regarding various aspects of UGS operation, such as optimal control of gas wells, pressure control, and management of gas reserves.

Keywords: mathematical modeling, deep learning, artificial intelligence, neural networks, neural operators, Fourier neural operators, hydrodynamic modeling, underground gas storage facilities

• **Submitted:** 31.05.2024 • **Revised:** 12.07.2024 • **Accepted:** 25.09.2024

For citation: Sirota D.D., Gushchin K.A., Khan S.A., Kostikov S.L., Butov K.A. Neural operators for hydrodynamic modeling of underground gas storage facilities. *Russ. Technol. J*. 2024;12(6):102–112. https://doi.org/10.32362/2500-316X-2024-12-6-102-112

Financial disclosure: The authors have no financial or proprietary interest in any material or method mentioned.

The authors declare no conflicts of interest.

НАУЧНАЯ СТАТЬЯ

Нейронные операторы для гидродинамического моделирования подземных хранилищ газа

Д.Д. Сирота [@],
К.А. Гущин,
С.А. Хан,
С.Л. Костиков,
К.А. Бутов

ПАО «Газпром», Санкт-Петербург, 197229 Россия
[@] *Автор для переписки, e-mail: D.Sirota@adm.gazprom.ru*

Резюме

Цели. Значительная часть исследований в области глубокого обучения сосредоточена на изучении отображений между конечномерными пространствами. Гидродинамические процессы фильтрации газа в подземных хранилищах, описываемые дифференциальными уравнениями в частных производных (ДУЧП), требуют изучения отображений между функциональными пространствами бесконечной размерности, что отличает данную задачу от традиционных. Одним из перспективных подходов является построение нейронных операторов – обобщение нейронных сетей для аппроксимации отображений между функциональными пространствами. Цель работы – создание нейронного оператора для ускорения расчетов гидродинамического моделирования подземных хранилищ газа (ПХГ) при допустимых потерях точности.

Методы. В работе построен и обучен модифицированный нейронный оператор Фурье для гидродинамического моделирования процессов фильтрации газа в ПХГ.

Результаты. Показано, что данный метод может быть успешно применен для задач трехмерной фильтрации газа в декартовой системе координат на объектах с множеством скважин. Разработанная модель обеспечивает высокое качество при моделировании объектов с неравномерной сеткой дискретизации и сложной геометрией, несмотря на использование в архитектуре алгоритма быстрого преобразования Фурье. При этом нейронному оператору не требуется большой размер обучающей выборки для достижения высокой точности аппроксимации решений ДУЧП, что демонстрируется не только на тестовой выборке, но и на искусственно сгенерированных сценариях с внесением существенных изменений в структуру моделируемого объекта. Обученный нейронный оператор осуществляет моделирование заданного сценария за доли секунды, что, по меньшей мере, в 10^6 раз быстрее, чем традиционный численный симулятор.

Выводы. Построенный и обученный нейронный оператор показал хорошую эффективность в задаче гидродинамического моделирования ПХГ. Полученный алгоритм воспроизводит адекватные решения даже в случае существенных изменений в моделируемом объекте, которых не было в процессе обучения. Все это делает возможным применение данной модели в задачах планирования и принятия решений в отношении различных аспектов эксплуатации ПХГ, таких как оптимальное использование скважин, контроль давления и управление запасами газа.

Ключевые слова: математическое моделирование, глубокое обучение, искусственный интеллект, нейронные сети, нейронные операторы, нейронные операторы Фурье, гидродинамическое моделирование, подземные хранилища газа

• **Поступила:** 31.05.2024 • **Доработана:** 12.07.2024 • **Принята к опубликованию:** 25.09.2024

Для цитирования: Сирота Д.Д., Гущин К.А., Хан С.А., Костиков С.Л., Бутов К.А. Нейронные операторы для гидродинамического моделирования подземных хранилищ газа. *Russ. Technol. J*. 2024;12(6):102–112. https://doi.org/10.32362/2500-316X-2024-12-6-102-112

Прозрачность финансовой деятельности: Авторы не имеют финансовой заинтересованности в представленных материалах или методах.

Авторы заявляют об отсутствии конфликта интересов.

INTRODUCTION

Underground gas storage facilities (UGS) are technological complexes designed for gas injection, storage and withdrawal. They typically comprise the following functional components: aboveground engineering and technical facilities; a subsurface area limited by a mining allotment; a gas storage facility; control reservoirs; a gas buffer volume; a stock of wells for various purposes. Hydrodynamic modeling of UGS reservoirs, which is required to improve the accuracy and reliability of predicting UGS behavior, represents an integral part of the planning and decision-making processes for various aspects of UGS operation, such as optimal well utilization, pressure control, and gas reserve management.

Simplified balance models and more accurate numerical hydrodynamic models (HDMs) can be used in modeling of filtration processes of underground gas storage. Balance models are typically used where there is a lack of sufficient initial data to build three-dimensional numerical models or limited computing power. Such models solve the reservoir-filtration equation using simplified dependencies without considering complex geological and hydrodynamic processes that can have a significant impact on the behavior of UGS. Modern hydrodynamic simulators for numerical modeling of gas filtration processes are used to obtain more detailed information on the distribution of parameters in UGS reservoir beds and assess the impact of various factors on the processes of underground gas storage. However, the use of the finite volume method to approximate the system of differential equations in space, as well as an implicit scheme for time approximation for modeling, can be a computationally expensive procedure.

At present, numerical HDMs are mainly used to solve the problems of hydrodynamic modeling of UGS facilities. Due to the possibility of adapting such models to the accumulated history of field development (in the case of UGS in depleted fields) and the actual history of UGS operation, the modeling and model adaptation horizon can exceed 60 years. Moreover, taking into account the considerable amount of geological and field data supplied to the HDM as input data (geophysical survey results, pressure measurements, gas flow rates, etc.), the time of a single calculation can reach several hours.

Thus, the speed of calculations is one of the determining factors affecting managerial decisions related to the distribution of gas injection/withdrawal by wells and by area. One of the most promising approaches for accelerating hydrodynamic calculations involves the use of contemporary deep learning methods.

A substantial part of works in the field of deep learning is devoted to the construction of mappings between finite-dimensional (e.g., Euclidean) spaces [1, 2]. However, the use of partial differential equations (PDE) to describe physical processes of gas filtration in UGS distinguishes this problem due to the requirement to learn mappings between function spaces of infinite dimensionality [3].

According to the universal approximation theorem [4, 5], a fully connected network with a *sufficient* number of parameters can approximate any continuous function defined on a compact set to a predetermined accuracy. In [6–8], theoretical possibilities for approximating nonlinear mappings between function spaces are demonstrated. In addition, [9] provides estimates of the complexity bounds of the approximation error of neural networks, relating the number of model parameters and the dimensionality of the problem to the value of the approximation error.

However, the theoretical possibility to approximate mappings between infinite-dimensional spaces does not imply information on how to do it efficiently in practice. It is known that existing neural network architectures vary in terms of their performance when solving specific problems. For example, the same fully connected networks show significantly lower quality in image processing compared to the widely used convolutional architectures [2]. In order to further investigate the issue of effective training of neural

networks, [10] decomposes the overall model error into three components: approximation error, optimization error, and generalization error. The approximation error depends on the number of network parameters and the dimensionality of the problem, while the optimization error is related to the loss function, and the generalization error depends on the training sample size [11].

One of the important points in generalizing the dependencies described by the PDE using neural networks is the problem of dimensionality ("curse of dimensionality") [12, 13], especially when modeling objects having complex UGS geometry or equations with multidimensional parameter spaces (the basic gas filtration equation) [3]. In order to generalize the basic dependencies and relations, deep learning models require a sufficiently large training sample size. According to [11], the upper bound on the generalization error is: $E_{\text{gen}} \sim \frac{1}{\sqrt{N}}$, where N is the number of training samples. Consequently, to obtain a relative generalization error of 1%, a sample size of $O(10^4)$ is required.

In the case of modeling hydrodynamic processes in reservoir systems, obtaining a data set of similar size can be a difficult task, since the data set is formed from calculations on a numerical simulator, representing a computationally expensive procedure. Consequently, when taking into account the above features, the development of neural network architecture for the effective solution of problems of this type becomes a nontrivial and relevant issue.

Over the last few years, deep learning has actively penetrated the field of scientific computing to become a new paradigm.[1, 2] Many novel methods have emerged to offer faster alternatives to numerical simulation.

Of course, there are works based on traditional deep learning approaches in the form of constructing finite-dimensional operators, which use the results of numerical simulations as a training set. For example, convolutional-, recurrent- and generative-adversarial architectures for solving fluid dynamics problems are investigated in [14–16]. However, due to their failure to use knowledge about the structure of the simulated dependencies, the presented methods are demanding on the object geometry and discretization grid, thus requiring a large amount of data.

A group of methods [17–19] belongs to a specialized class of algorithms known as *physically informed neural networks*. While this approach is also based on finite-dimensional mappings, it incorporates the PDE directly into the algorithm's error function using the automatic differentiation mechanism [20]. In this way, physics is taken into account in the learning process as the model seeks to minimize the discrepancies between the left and right parts of the equation, representing initial and boundary conditions. However, the main disadvantage of this approach is its limitation to approximate a particular realization of the PDE. Consequently, physically informed neural networks do not provide a significant speed advantage relative to traditional numerical methods for many applied problems.

An alternative and relatively new approach is to train *neural operators*, which represent mappings between function spaces [21–23]. Since trained neural operators can approximate any nonlinear continuous operators, do not depend on the sampling grid, and require only a single training, they can be trained and evaluated on different sampling grids and PDE implementations. These methods demonstrate better efficiency when approximating PDEs in comparison with other existing approaches based on deep learning, including for hydrodynamic modeling problems.

Operator learning in spaces of infinite dimensionality is currently an active area of research. Work is ongoing to improve the efficiency and applicability of this approach in various applications.

1. TASK STATEMENT

Mathematical model of gas filtration process

The present work considers the process of hydrodynamic modeling of porous-type UGS facilities. For such objects, various parameters describing gas motion in porous medium (filtration) have a strong time dependence [3]. Such processes are called unsteady (nonstationary).

The basic equation of three-dimensional unsteady single-phase filtration of a compressible fluid (gas) in a porous medium is obtained by substituting the law of conservation of momentum (Darcy's law of filtration) into the law of conservation of mass [24]:

$$\frac{\partial}{\partial x}\left(\frac{A_x k_x}{\mu_g B_g}\frac{\partial p}{\partial x}\right)\Delta x + \frac{\partial}{\partial y}\left(\frac{A_y k_y}{\mu_g B_g}\frac{\partial p}{\partial y}\right)\Delta y + \\ + \frac{\partial}{\partial z}\left(\frac{A_z k_z}{\mu_g B_g}\frac{\partial p}{\partial z}\right)\Delta z = \frac{V_{\text{bulk}}\phi T_{\text{sc}}}{p_{\text{sc}}}\frac{\partial}{\partial t}\left(\frac{p}{Z}\right) - q_{\text{gsc}}, \quad (1)$$

where p is pressure; q_{gsc} is the gas flow rate under standard conditions; $B_g = \frac{p_{\text{sc}} TZ}{T_{\text{sc}} p}$ is the gas phase

[1] Lavin A., Krakauer D., Zenil H., et al. *Simulation Intelligence: Towards a New Generation of Scientific Methods*. 2022. http://arxiv.org/abs/2112.03235. Accessed April 25, 2023.

[2] Cuomo S., di Cola V.S., Giampaolo F., et al. *Scientific Machine Learning through Physics-Informed Neural Networks: Where we are and What's next*. 2022. http://arxiv.org/abs/2201.05624. Accessed April 25, 2023.

volume coefficient; Z is the gas supercompressibility coefficient; μ_g is the gas viscosity; T_{sc} is the temperature under standard conditions; p_{sc} is the pressure under standard conditions; V_{bulk} is the rock volume; ϕ is porosity; k is permeability; A is the cross-sectional area of rock perpendicular to the filtration direction; Δx, Δy, Δz are length, width, and height of rock volume (final volume), respectively.

The PDE (1) is nonlinear due to the dependence of μ_g, B_g, and Z on pressure and is similar to the diffusion equation, however, by its dynamic characteristics the flow described by this relation is not diffusion but filtration flow.

Neural operator training

The purpose of the present work is to approximate the gas filtration equation in UGS (1) by constructing a neural operator that maps between two infinite-dimensional spaces from a finite set of pairs of pairs of initial, boundary conditions, and PDE solutions.

Let us fix the spatiotemporal dimension $d \in \mathbb{N}$ and denote by $D \subset \mathbb{R}^d$ the area in $\mathbb{R}^d$. Then we can consider a mapping that is inherently an operator of the solution of PDE:

$$G : A(D;\mathbb{R}^{d_a}) \to U(D;\mathbb{R}^{d_u}),$$
$$a \to u := G(a), \qquad (2)$$

$a \in A(D;\mathbb{R}^{d_a})$ is the function of the input data of the type $a : D \to \mathbb{R}^{d_a}$; $u \in U(D;\mathbb{R}^{d_u})$ is the function of the output data of the type $u : D \to \mathbb{R}^{d_u}$. $A(D;\mathbb{R}^{d_a})$ and $U(D;\mathbb{R}^{d_u})$ are Banach spaces.

In order to train the operator, it is necessary to assume a finite set of pairs of initial, boundary conditions and solutions of PDE $\{a_j, u_j\}_{j=1}^N$, where $a_j \sim \mu$ (μ is a probability measure) is a sequence of probability measures defined on A and $u_j = G(a_j)$. These pairs are obtained from the HDM of the current UGS, which uses a finite volume method to approximate the system of differential equations in space and an implicit scheme to approximate in time. Thus, the training of the neural operator can be formulated as follows. The input data generated by the numerical simulator is essentially the result of a nonlinear mapping satisfying the gas filtration equation: $G(a_j) = u_j$. Consequently, it is possible to construct a neural operator N_{θ^*} by selecting the parameters $\theta \in \Theta$ in such a way as to approximate the initial mapping $N_{\theta^* \approx G}$. Then the learning process, which can be reduced to the problem of minimizing the loss function C: U × U → $\mathbb{R}$, has the following form:

$$\min_{\theta} E_{a\sim\mu}[C(N_\theta(a), G(a))], \qquad (3)$$

where $E_{a\sim\mu}$ is the mathematical expectation.

2. CONSTRUCTION OF A NEURAL OPERATOR MODEL

In accordance with the problem statement, a neural operator should be trained to approximate the solution of the gas filtration PDE in UGS. When developing such methods, it is convenient to adhere to the following sequence of steps in the model architecture [23]:

1. P is the operator of transformation of input data into the hidden space of higher dimensionality;
2. Iterative application of the kernel of the integral operator L;
3. Q is the projection operator from the hidden space to the initial output space.

Thus, the structure of the neural operator has the form (4):

$$N(a) = Q \circ L_L \circ L_{L-1} \circ \ldots \circ L_1 \circ P(a), \qquad (4)$$

where the given depth of layers is $L \in \mathbb{N}$, $P : A(D;\mathbb{R}^{d_a}) \to$ $\to U(D;\mathbb{R}^{d_v})$, $d_v \geq d_a$, $Q : U(D;\mathbb{R}^{d_v}) \to U(D;\mathbb{R}^{d_u})$.

By analogy with classical finite-dimensional neural networks, $L_1, \ldots, L_L$ are nonlinear layers of the operator, $L_l : U(D;\mathbb{R}^{d_v}) \to U(D;\mathbb{R}^{d_u})$, $v \to L_l(v)$, which can be written as:

$$L_l(v)(x) = \sigma(W_l v(x) + (K(a;\theta_l)v)(x)), \forall x \in D, \qquad (5)$$

where σ is the activation function, W_l is the linear transformation, $K : A \times \Theta \to L(U(D;\mathbb{R}^{d_v}), U(D;\mathbb{R}^{d_v}))$.

Operator $K(a, \theta_l)$ [22] is an integral operator of the form:

$$(K(a,\theta_l)v)(x) =$$
$$= \int_D \kappa_\theta(x, y, a(x), a(y))v(y)dy, \forall x \in D. \qquad (6)$$

The kernel κ_θ, which is a neural network with parameters $\theta \in \Theta$, can have various structures. Different kinds of neural operator are derived from this, for example, graph neural operators (GNO) and multipole graph neural operators (MGNO) [22], as well as low-rank neural operators (LNO) and Fourier neural operators (FNO).

At present, one of the promising methods for approximating solutions of filtration equations is FNO, which is used to parameterize the kernel of the integral operator in Fourier space [25]. This method demonstrates better efficiency in fluid filtration problems in porous media as compared to traditional neural network algorithms and other operator architectures (GNO, MGNO, LNO, DeepONet) [23]. At the same time, [26] shows, using the example of the approximation of the transport equation, that the complexity of FNO grows *logarithmically*

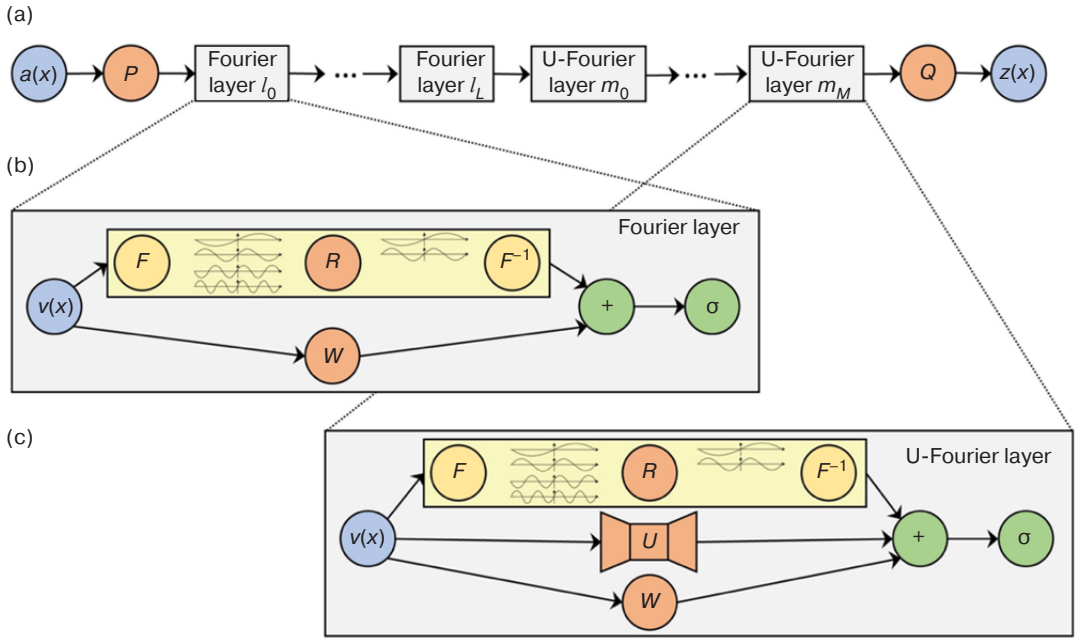

Fig. 1. (a) Model architecture: *P* and *Q* are fully connected layers, *z*(*x*) is the model output; (b) Fourier layer: *R* represents the parameterization in Fourier space, *W* is the linear displacement; (c) modified Fourier layer: *U* is the U-Net operator, other notations have the same meaning as in the Fourier layer

to achieve a given error; this contrasts with the alternative DeepONet architecture [21], which grows *quadratically*.

The Fourier neural operator [25] belongs to the class of neural operators in which the kernel can be written as a convolution:

$$(\mathrm{K}(a,\theta_l)v)(x) = \int_{\mathrm{D}} \kappa_\theta(x-y)v(y)dy,\ \forall x \in \mathrm{D}. \quad (7)$$

In order to parameterize the kernel efficiently according to the convolution theorem, this method considers the image v in Fourier space using the fast Fourier transform F and the inverse Fourier transform F^{-1}:

$$(\mathrm{K}(\theta)v)(x) = F^{-1}(R_\theta(k)\cdot F(v)(k))(x),\ \forall x \in \mathrm{D}, \quad (8)$$

where $R_\theta(k) = F(\kappa_\theta)(k)$ is the matrix of Fourier transform coefficients from κ_θ.

Thus, the layers of the Fourier operator will have the form:

$$L_l(v)(x) = \sigma(W_l v(x) + F^{-1}(R_l(k)\cdot F(v)(k))(x)). \quad (9)$$

The key difference between (9) and the traditional neural network architecture is the direct definition of all operations in feature space, which obviates a dependence on the discretization of the data.

We have developed a method for hydrodynamic modeling of UGS, consisting in a modified Fourier neural operator in which the layers of the neural operator include a convolution neural network U-Net operator to enhance expressiveness by processing high-frequency information that is not captured by the Fourier basis[3]. Such an algorithm involves the following three steps (Fig. 1):

1. Transformation of input data $a(x)$ into a hidden space of higher dimensionality $v_{l_0} = P(a(x))$;
2. Iterative application of Fourier layers and subsequent application of modified Fourier layers: $v_{l_0} \to \ldots \to v_{l_L} \to v_{m_0} \to \ldots \to v_{m_M}$, where v_{l_j} for $j = \overline{0,L}$ and v_{m_k} for $k = \overline{0,M}$;
3. Projection v_{m_M} from the hidden space into the original exit space $z(x) = Q(v_{m_M}(x))$.

The modified Fourier layer of the neural operator has the following form:

$$v_{m_{k+1}}(x) = \sigma(W(v_{m_k}(x)) + (Kv_{m_k})(x) + Uv_{m_k}(x)),\ \forall x \in \mathrm{D}, \quad (10)$$

where W is a linear operator; $Kv_{m_k}(x) = F^{-1}(R\cdot F(v_{m_k}))(x)$ is the integral transformation operator; U is the operator of the U-Net convolutional neural network.

It is important to note that the neural Fourier operator is an infinite-dimensional operator capable of generating invariant solutions regardless of the sampling grid on training and test samples. However, by adding a U-Net

[3] Wen G., Li Z., Azizzadenesheli K., et al. *U-FNO – An enhanced Fourier neural operator-based deep-learning model for multiphase flow*. 2022. http://arxiv.org/abs/2109.03697. Accessed April 25, 2023.

block, which inherently lacks the flexibility of training and testing at different sampling, the authors of the architecture sacrifice flexibility in favor of higher accuracy. This architecture is expected to provide acceptable accuracy even with a relatively small training sample.

Data configuration

In this work, the data from the HDM are used to form the dataset. The approximation period is chosen to be equal to the gas withdrawal season. The whole data set is formed from 70 different withdrawal scenarios with a time step of 10 days. The considered UGS has more than 100 active wells and a complex geometry.

The final dataset consists of 2850 input-output pairs. For training, 2250 images were allocated for the training sample and 300 each for the validation and test samples.

3. RESULTS

Relative error is used as a loss function

$$L(y,\hat{y}) = \frac{\| y - \hat{y} \|_2}{| y |_2}, \qquad (11)$$

since formation pressure in UGS in different periods has a different scale; $\hat{y}$ is the value obtained from the model

During training, the initial learning rate coefficient, assumed to be 0.001, decreases gradually as the number of passed epochs increases. Training stops when the loss on the validation sample does not decrease any more (Fig. 2).

The quality of the trained model was evaluated on a test sample. Statistical parameters of model errors are as follows: mean = 0.006; standard deviation = 0.2.

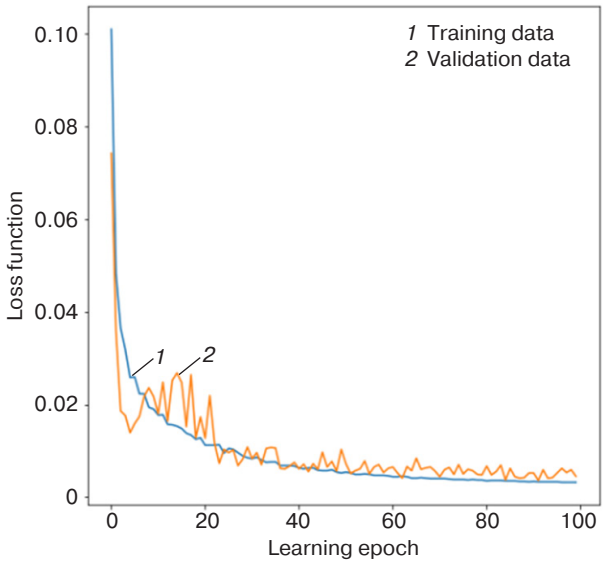

Fig. 2. Diagram of model error during the learning process

The trained model is able to reproduce the reservoir pressure dynamics for the period of sampling seasons to an acceptable degree of accuracy. Figure 3 shows the scatter diagram of normalized (scaled to the range from 0 to 1) formation pressure between the trained neural operator and the results of numerical simulations. The coefficient of determination $R^2 = 0.999$.

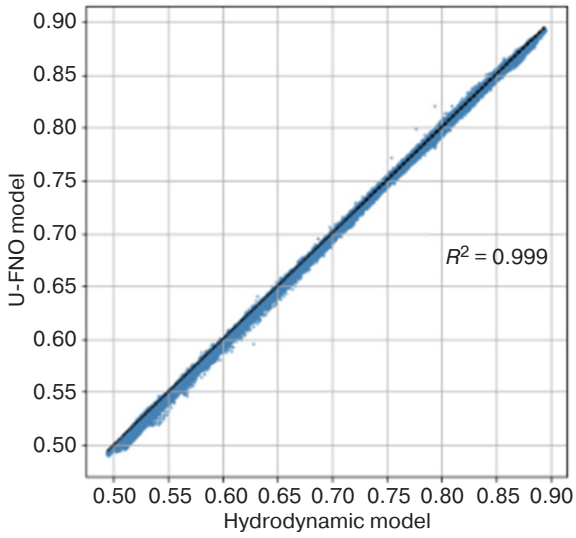

Fig. 3. Normalized reservoir pressure scatter diagram

Based on the scatter plot, it follows that the distribution generated by the neural operator on the test sample in each reservoir cell is very close to the distribution from the HDM.

A visualization of the comparison of simulation results of reservoir pressure field dynamics modeling by means of neural operator and HDM is presented in Figs. 4–6. The time step means the ordinal number of the ten-day period (decade) within the gas withdrawal season.

The trained neural operator demonstrated good performance on the test sample. Moreover, the obtained model calculates a given scenario in a fraction of a second, which is at least 10^6 times faster than a traditional numerical simulator.

In spite of the small number of PDE implementations in the training sample, we evaluated the generalization ability of the model on the example of reproducing the reservoir pressure dynamics in case of significant changes in the object itself involving variations in the number and location of wells. Since the use of the developed neural operator at this stage does not imply calculations or optimization of various well placement schemes, the scenario calculated on the operating HDM was taken as a reference scenario reproducing the situation with near-zero withdrawals from UGS during the entire period. Then, all wells were removed, 11 new production wells were placed in reservoir cells where they had never been before, and the scenario of forced gas withdrawals through these wells was modeled. The results are shown in Fig. 7.

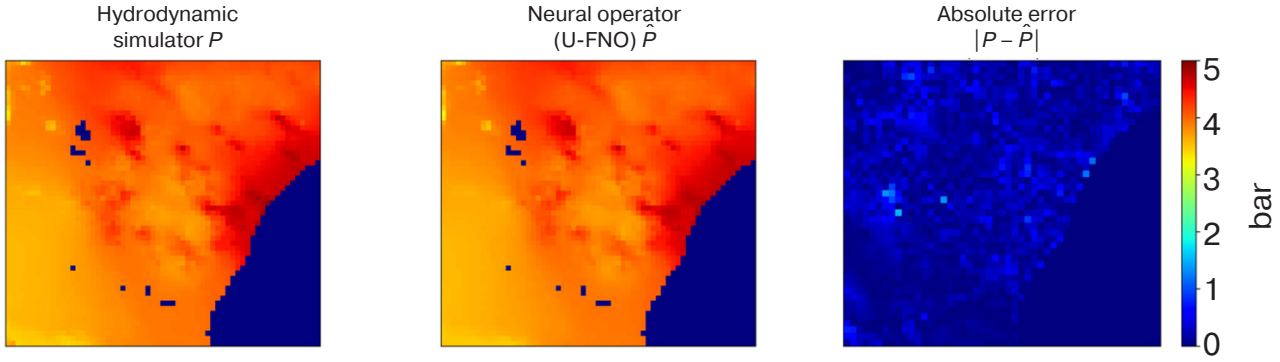

Fig. 4. Visualization of reservoir pressure from HDM, U-FNO model and absolute error on test sample (time step 4/16)

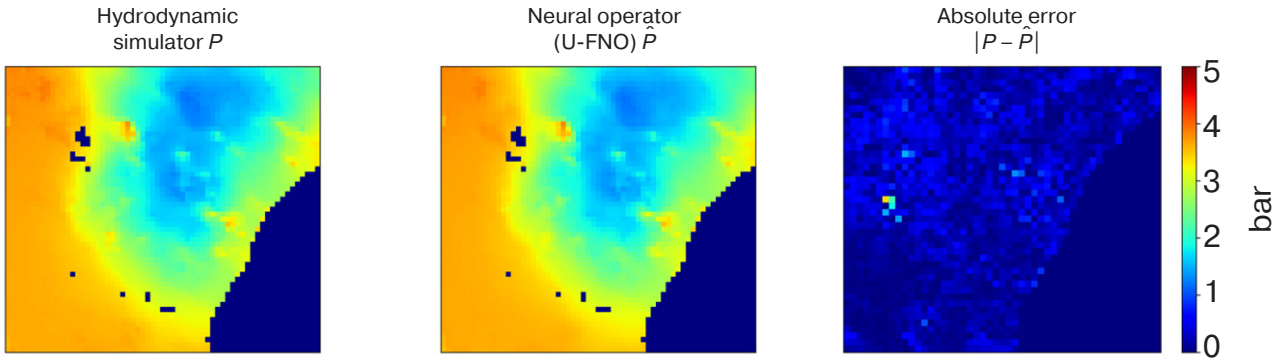

Fig. 5. Visualization of reservoir pressure from HDM, U-FNO model and absolute error on test sample (time step 10/16)

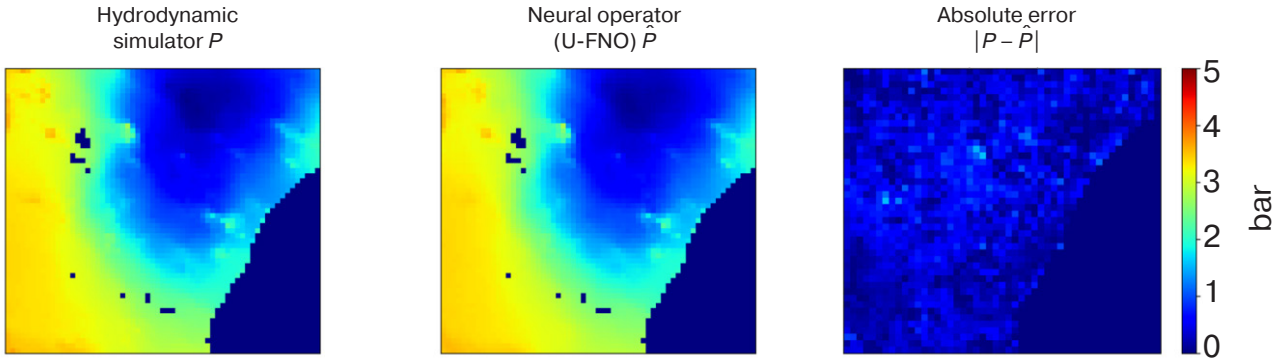

Fig. 6. Visualization of reservoir pressure from HDM, U-FNO model and absolute error on test sample (time step 16/16)

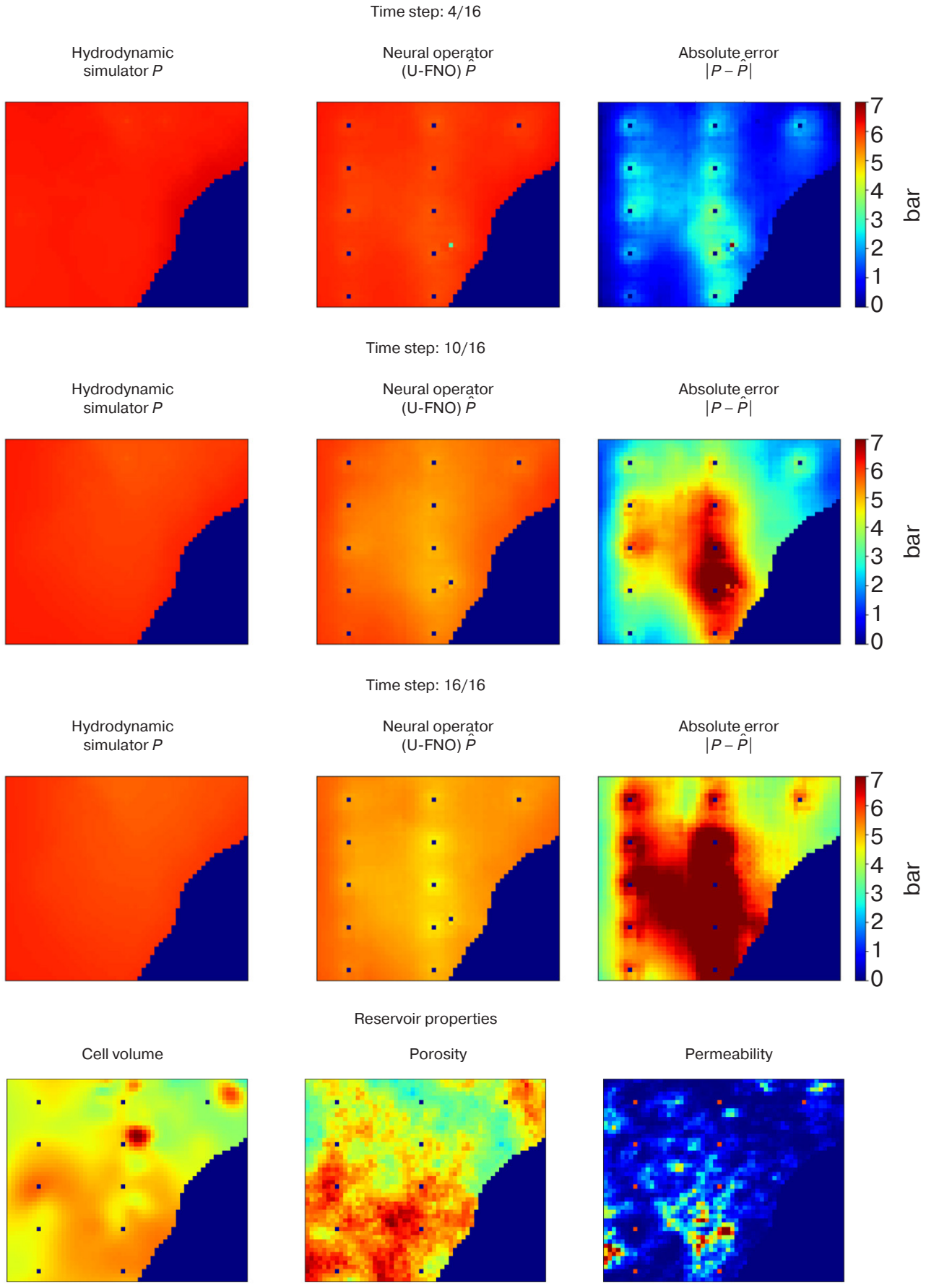

Fig. 7. Visualization of simulation results taking into account changes in well stock and visualization of formation properties (cells with placed wells are highlighted in color)

The lower part of Fig. 7 depicts visualizations of discretized reservoir cell volumes, porosity and permeability. Based on the obtained results, we conclude that the model responds adequately to such significant changes: the reservoir pressure field in the near-wellbore space changes taking into account the distribution of formation properties.

CONCLUSIONS

The reported study demonstrates the possibility of successfully applying the modified neural Fourier operator not only to the problems of modeling gas filtration in a cylindrical coordinate system with a single well, but also to the problems of three-dimensional gas filtration in a Cartesian coordinate system on objects with multiple wells. In addition, despite the use of the fast Fourier transform algorithm in the architecture, the developed model provides high quality modeling of objects with non-uniform sampling grid and complex geometry.

At the same time, the neural operator does not need a large training sample size to achieve high accuracy of approximation of PDE solutions, which is demonstrated not only on the test sample, but also on artificially generated scenarios involving significant changes in the structure of the modeled object. Based on the experiments, the trained neural operator simulates a given scenario in a fraction of a second, which is at least 10^6 times faster than a traditional numerical simulator. This makes the model suitable for application in tasks of planning and decision-making with respect to various aspects of UGS operation, such as optimal well utilization, pressure control and gas reserves management.

Authors' contributions
All authors equally contributed to the research work.

REFERENCES

1. LeCun Y., Bengio Y., Hinton G. Deep learning. *Nature.* 2015;521(7553):436–444. https://doi.org/10.1038/nature14539
2. Goodfellow I., Bengio Y., Courville A. *Deep Learning*. Cambridge, Massachusetts: The MIT Press; 2016. 775 p.
3. Aziz K., Settari A. *Petroleum Reservoir Simulation*. London, New York: Applied Science Publ.; 1979. 497 p.
4. Cybenko G. Approximation by superpositions of a sigmoidal function. *Math. Control Signals Syst.* 1989;2:303–314. https://doi.org/10.1007/BF02551274
5. Hornik K., Stinchcombe M., White H. Multilayer feedforward networks are universal approximators. *Neural Netw.* 1989;2(5):359–366. https://doi.org/10.1016/0893-6080(89)90020-8
6. Chen T., Chen H. Approximations of continuous functionals by neural networks with application to dynamic systems. *IEEE Trans. Neural Netw.* 1993;4(6):910–918. https://doi.org/10.1109/72.286886
7. Chen T., Chen H. Approximation capability to functions of several variables, nonlinear functionals, and operators by radial basis function neural networks. *IEEE Trans. Neural Netw.* 1995;6(4):904–910. https://doi.org/10.1109/72.392252
8. Chen T., Chen H. Universal approximation to nonlinear operators by neural networks with arbitrary activation functions and its application to dynamical systems. *IEEE Trans. Neural Netw.* 1995;6(4):911–917. https://doi.org/10.1109/72.392253
9. Yarotsky D. Error bounds for approximations with deep ReLU networks. *Neural Netw.* 2017;94:103–114. https://doi.org/10.1016/j.neunet.2017.07.002
10. Jin P., Lu L., Tang Y., et al. Quantifying the generalization error in deep learning in terms of data distribution and neural network smoothness. *Neural Netw.* 2020;130:85–99. https://doi.org/10.1016/j.neunet.2020.06.024
11. Jakubovitz D., Giryes R., Rodrigues M.R.D. Generalization Error in Deep Learning. Epub ahead of print 2018. https://doi.org/10.48550/ARXIV.1808.01174
12. Bellman R. *Dynamic Programming*. Princeton: Princeton University Press; 2010. 392 p.
13. Han J., Jentzen A., Weinan E. Solving high-dimensional partial differential equations using deep learning. *Proc. Natl. Acad. Sci.* 2018;115(34):8505–8510. https://doi.org/10.1073/pnas.1718942115
14. Guo X., Li W., Iorio F. Convolutional Neural Networks for Steady Flow Approximation. In: *Proceedings of the 22nd ACM SIGKDD International Conference on Knowledge Discovery and Data Mining*. San Francisco California USA: ACM; 2016. P. 481–490. https://doi.org/10.1145/2939672.2939738
15. Tang M., Liu Y., Durlofsky L.J. A deep-learning-based surrogate model for data assimilation in dynamic subsurface flow problems. *J. Comput. Phys.* 2020;413(1):109456. https://doi.org/10.1016/j.jcp.2020.109456
16. Zhong Z., Sun A.Y., Jeong H. Predicting CO_2 Plume Migration in Heterogeneous Formations Using Conditional Deep Convolutional Generative Adversarial Network. *Water Resour. Res.* 2019;55(7):5830–5851. https://doi.org/10.1029/2018WR024592
17. Berg J., Nyström K. A unified deep artificial neural network approach to partial differential equations in complex geometries. Epub ahead of print 2017. https://doi.org/10.48550/ARXIV.1711.06464, Related DOI: https://doi.org/10.1016/j.neucom.2018.06.056
18. Raissi M., Perdikaris P., Karniadakis G.E. Physics Informed Deep Learning (Part I): Data-driven Solutions of Nonlinear Partial Differential Equations. Epub ahead of print 2017. https://doi.org/10.48550/ARXIV.1711.10561

19. Raissi M., Perdikaris P., Karniadakis G.E. Physics-informed neural networks: A deep learning framework for solving forward and inverse problems involving nonlinear partial differential equations. *J. Comput. Phys.* 2019;378:686–707. https://doi.org/10.1016/j.jcp.2018.10.045
20. Baydin A.G., Pearlmutter B.A., Radul A.A., et al. Automatic differentiation in machine learning: a survey. Epub ahead of print 2015. https://doi.org/10.48550/ARXIV.1502.05767
21. Lu L., Jin P., Pang G., Zhang Z., Karniadakis G.E. Learning nonlinear operators via DeepONet based on the universal approximation theorem of operators. *Nat. Mach. Intell.* 2021;3(3):218–229. https://doi.org/10.1038/s42256-021-00302-5
22. Li Z., Kovachki N., Azizzadenesheli K., et al. Neural Operator: Graph Kernel Network for Partial Differential Equations. Epub ahead of print 2020. https://doi.org/10.48550/ARXIV.2003.03485
23. Kovachki N., Li Z., Liu B., et al. Neural Operator: Learning Maps Between Function Spaces. Epub ahead of print 2021. https://doi.org/10.48550/ARXIV.2108.08481
24. Ertekin T., Abou-Kassem J.H., King G.R. *Basic Applied Reservoir Simulation*. Richardson, Tex.: Society of Petroleum Engineers; 2001. 406 p.
25. Li Z., Kovachki N., Azizzadenesheli K., et al. Fourier Neural Operator for Parametric Partial Differential Equations. Epub ahead of print 2020. https://doi.org/10.48550/ARXIV.2010.08895
26. Lanthaler S., Molinaro R., Hadorn P., et al. Nonlinear Reconstruction for Operator Learning of PDEs with Discontinuities. Epub ahead of print 2022. https://doi.org/10.48550/ARXIV.2210.01074

About the authors

Daniil D. Sirota, Deputy Head of Division, PJSC Gazprom (2/3, Lakhtinsky pr., St. Petersburg, 197229 Russia). E-mail: D.Sirota@adm.gazprom.ru. ResearcherID KUF-1969-2024, RSCI SPIN-code 1137-2827, https://orcid.org/0009-0009-9663-6188

Kirill A. Gushchin, Deputy Head of Department – Head of Directorate, PJSC Gazprom (2/3, Lakhtinsky pr., St. Petersburg, 197229 Russia). E-mail: K.Gushchin@adm.gazprom.ru. https://orcid.org/0009-0006-2181-3272

Sergey A. Khan, Cand. Sci. (Eng.), Deputy Head of Department – Head of Directorate, PJSC Gazprom (2/3, Lakhtinsky pr., St. Petersburg, 197229 Russia). E-mail: S.Khan@adm.gazprom.ru. Scopus Author ID 27172181100, RSCI SPIN-code 2591-5980

Sergey L. Kostikov, Deputy Head of Directorate – Head of Division, PJSC Gazprom (2/3, Lakhtinsky pr., St. Petersburg, 197229 Russia). E-mail: S.Kostikov@adm.gazprom.ru. Scopus Author ID 58283384300, https://orcid.org/0009-0007-7298-3586

Kirill A. Butov, Cand. Sci. (Eng.), Chief Technologist of the Division, PJSC Gazprom (2/3, Lakhtinsky pr., St. Petersburg, 197229 Russia). E-mail: K.Butov@adm.gazprom.ru. https://orcid.org/0009-0008-3444-2049

Об авторах

Сирота Даниил Дмитриевич, заместитель начальника отдела, Публичное акционерное общество «Газпром» (ПАО «Газпром») (197229, Россия, Санкт-Петербург, Лахтинский пр., д. 2, корп. 3, стр. 1). E-mail: D.Sirota@adm.gazprom.ru. ResearcherID KUF-1969-2024, SPIN-код РИНЦ 1137-2827, https://orcid.org/0009-0009-9663-6188

Гущин Кирилл Андреевич, заместитель начальника Департамента – начальник Управления, Публичное акционерное общество «Газпром» (ПАО «Газпром») (197229, Россия, Санкт-Петербург, Лахтинский пр., д. 2, корп. 3, стр. 1). E-mail: K.Gushchin@adm.gazprom.ru. https://orcid.org/0009-0006-2181-3272

Хан Сергей Александрович, к.т.н., заместитель начальника Департамента – начальник Управления, Публичное акционерное общество «Газпром» (ПАО «Газпром») (197229, Россия, Санкт-Петербург, Лахтинский пр., д. 2, корп. 3, стр. 1). E-mail: S.Khan@adm.gazprom.ru. Scopus Author ID 27172181100, SPIN-код РИНЦ 2591-5980

Костиков Сергей Леонидович, заместитель начальника Управления – начальник отдела, Публичное акционерное общество «Газпром» (ПАО «Газпром») (197229, Россия, Санкт-Петербург, Лахтинский пр., д. 2, корп. 3, стр. 1). E-mail: S.Kostikov@adm.gazprom.ru. Scopus Author ID 58283384300, https://orcid.org/0009-0007-7298-3586

Бутов Кирилл Андреевич, к.т.н., главный технолог отдела, Публичное акционерное общество «Газпром» (ПАО «Газпром») (197229, Россия, Санкт-Петербург, Лахтинский пр., д. 2, корп. 3, стр. 1). E-mail: K.Butov@adm.gazprom.ru. https://orcid.org/0009-0008-3444-2049

Translated from Russian into English by Lyudmila O. Bychkova
Edited for English language and spelling by Thomas A. Beavitt

Economics of knowledge-intensive and high-tech enterprises and industries. Management in organizational systems

Экономика наукоемких и высокотехнологичных предприятий и производств. Управление в организационных системах

UDC 332.05
https://doi.org/10.32362/2500-316X-2024-12-6-113-126
EDN QPTLBD

RESEARCH ARTICLE

Short-term stock indices as a tool for assessing and forecasting scientific and technological security

Andrey I. Ladynin @

MIREA – Russian Technological University, Moscow, 119454 Russia
@ *Corresponding author, e-mail: ladynin@mirea.ru*

Abstract

Objectives. Ensuring scientific and technological sovereignty, defined as one of the objectives of the Concept of Technological Development for the period until 2030, approved by the Order of the Government of the Russian Federation No. 1315-r dated May 20, 2023, implies the use of effective mechanisms for managing the country's economy. Under contemporary conditions, technology is a crucial element in the country's economic development and a key component of scientific and technological security. Thus, the aim of the present work is to develop existing methods for analyzing economically significant information relating to the monitoring and diagnostics of scientific and technological security at the meso- and macrolevels.

Methods. The developed method for scientific and technological security level monitoring and forecasting, which is based on the dynamics analysis of the values of corporate securities, includes economic and statistical analysis methods, machine learning and time series analysis tools.

Results. The approach towards information processing and enhancement of analysis mechanisms in managerial decisions, which relies on diagnostic, analysis, and forecasting tools for socioeconomic system scientific and technological security, is based on information-processing, economic, and mathematical methods. The presented results constitute a developed method for the analysis of systemically important enterprises stock indices, supporting research and development to assess and predict scientific and technological security dynamics at meso- and macro levels of the economy. In order to verify the methodology, a numerical experiment was carried out using statistical data from systemically important companies.

Conclusions. The developed methodology is aimed at improved managerial decision-making accuracy and speed when solving problems connected with scientific and technological security underpinning socioeconomic systems. The experimental results quantitatively confirm the significant contribution made by systemically important companies to Russian Federation's scientific and technological security ensuring.

Keywords: scientific and technological safety, information analysis methods, economic and mathematical modeling, scientific development, stock indices, decision support tools

• **Submitted:** 12.02.2024 • **Revised:** 04.04.2024 • **Accepted:** 23.09.2024

For citation: Ladynin A.I. Short-term stock indices as a tool for assessing and forecasting scientific and technological security. *Russ. Technol. J*. 2024;12(6):113–126. https://doi.org/10.32362/2500-316X-2024-12-6-113-126

Financial disclosure: The author has no financial or proprietary interest in any material or method mentioned.

The author declares no conflicts of interest.

НАУЧНАЯ СТАТЬЯ

Краткосрочные биржевые индексы как инструмент оценки и прогнозирования научно-технологической безопасности

А.И. Ладынин [@]

МИРЭА – Российский технологический университет, Москва, 119454 Россия
[@] *Автор для переписки, e-mail: ladynin@mirea.ru*

Резюме

Цели. Обеспечение научно-технологического суверенитета, определенное как одна из задач Концепции технологического развития на период до 2030 г., утвержденной Распоряжением Правительства Российской Федерации от 20 мая 2023 г. № 1315-р, предполагает использование эффективных механизмов управления экономикой страны. В современных условиях технологическое развитие экономики является императивом развития страны и ключевой составляющей научно-технологической безопасности. Цель работы – развитие существующих инструментальных методов анализа экономически значимой информации для мониторинга и диагностики научно-технологической безопасности на мезо- и макроуровне.

Методы. Использована авторская методика мониторинга и прогнозирования уровня научно-технологической безопасности на основе анализа динамики стоимости ценных бумаг компаний, включающая методы экономико-статистического анализа, инструменты машинного обучения и анализа временных рядов.

Результаты. Представлен авторский подход к совершенствованию механизмов обработки и анализа информации в ходе принятия управленческих решений. Для этого осуществлена разработка инструмента диагностики научно-технологической безопасности социально-экономической системы на основе экономико-математических методов обработки информации. Предложена методика интегральной оценки научно-технологической безопасности на макроуровне на основе анализа и прогнозирования стоимости ценных бумаг экономических агентов – системообразующих компаний. Научный результат – разработанная методика анализа биржевых индексов системообразующих предприятий, осуществляющих исследования и разработки для оценки и прогнозирования динамики научно-технологической безопасности на мезо- и макроуровне экономики. Для верификации методики проведен численный эксперимент с использованием статистических данных системообразующих компаний.

Выводы. Разработанная методика направлена на повышение точности и быстродействия управления в задачах обеспечения научно-технологической безопасности социально-экономических систем. Результаты эксперимента количественно подтверждают предположение о значительном вкладе системообразующих предприятий в обеспечение научно-технологической безопасности Российской Федерации.

Ключевые слова: научно-технологическая безопасность, методика анализа информации, экономико-математическое моделирование, научное развитие, биржевые индексы, инструменты поддержки принятия решений

• **Поступила:** 12.02.2024 • **Доработана:** 04.04.2024 • **Принята к опубликованию:** 23.09.2024

Для цитирования: Ладынин А.И. Краткосрочные биржевые индексы как инструмент оценки и прогнозирования научно-технологической безопасности. *Russ. Technol. J.* 2024;12(6):113–126. https://doi.org/10.32362/2500-316X-2024-12-6-113-126

Прозрачность финансовой деятельности: Автор не имеет финансовой заинтересованности в представленных материалах или методах.

Автор заявляет об отсутствии конфликта интересов.

INTRODUCTION

Contemporary tools for monitoring, analyzing, and forecasting the state of the economy imply the use of relevant information processing tools. The conducting of scientific research and development of large enterprises under the jurisdiction of the Russian Federation plays a key role in ensuring economic security. At the same time, the activity of science-based enterprises is characterized by uncertainty due to the complexity of the tasks to be solved, the variety of influencing factors, and the dynamics of changes in the influence of the external environment.

Under such conditions, it is advisable to consider not only methods for directly assessing scientific and technological security (STS) on the basis of indicators of scientific activity of an enterprise or a company, but also the more general processes underpinning its improvement. For example, in order to establish a quantitative relationship between the value of securities of large technology companies at the STS level, indirect evaluation mechanisms are required. For example, the generally recognized indicator systems include characteristics for determining the level of innovation activity, as well as costs and results of enterprise functions carried out in the field of scientific activity and the development of high technology. An additional factor determining the possibility of such an assessment is the significant participation of the state in large businesses—for example, for many large companies, including those carrying out research and development within the framework of business interests, state institutions are included among the shareholders.

Key factors in the efficiency of management decision-making are accuracy and speed. However, reliance on statistical assessments, which include indicators significant for STS, involve significant intervals between the periods of receipt of statistical data. Under the conditions of dynamic changes in the indicators characterizing the socioeconomic system, it is advisable to consider tools with greater sensitivity and less time delays. Hence, there is a need to use methodological approaches based on the analysis of rapidly changing data, as well as to improve existing and develop new tools for processing and analyzing information.

LITERATURE REVIEW

While considering the tasks of ensuring STS, it is necessary to determine its position in the structure of modern economy. It seems reasonable to consider STS as an integral part of economic security. The current understanding of a competitive national economy assumes a close relationship with scientific and technological progress. The concept of ensuring scientific and technological sovereignty, defined as one of the priorities of Russia's development[1], also implies the actualization of the existing independent scientific and technological basis, as well as its further development. STS plays an important role in the specialized literature. A.E. Varshavskii in [1] postulated the principles of STS provision. In the study by M.S. Vlasova, O.S. Stepchenkova, indicators of economic security in the scientific and technological sphere are considered [2]. A.Yu. Pinchuk considers scientific and technological development in the context of digitalization of the economy and industrial development [3]. A.A. Afanasev considers the role of STS in the tasks of ensuring technological sovereignty [4].

The relationship between innovation activity and STS is reasonable assumed to have a fundamental character [5]. The articles [6, 7] are focused on the problems of methodological support of innovation activity. Studies in the field of assessing the effectiveness of innovation activity of organizations in the context of digitalization of the economy are presented in [8]. A significant layer of works is devoted to analyzing the problems of innovative business development in modern Russia [9–12].

Problems associated with ensuring innovative development are closely related to the competitiveness of organizations under contemporary conditions. The development of innovations, representing one of the main factors of production, involves both a stimulus and a requirement to improve the production toolkit. M.P. Kalinichenko considers the management of enterprise competitiveness through innovation activity [13]. T.A. Burtseva presents approaches to analyzing the evaluation of the effectiveness of information support of innovation management [14]. A.V. Babkin and L. Chen evaluated the efficiency of innovation of high-tech industry on the example of a province in the People's Republic of China [15]. The problems of management of knowledge-intensive organizations were considered in the works of A.M. Batkovsky [16, 17], D.Yu. Fraimovich [18]. I.L. Berezin considers the institutional forms of innovation activity management and their limitations [19], while S.A. Filin discusses the principles of management in the context of transition to the digital economy [20]. It should be noted the actualization

[1] Decree of the President of the Russian Federation No. 145, dated February 28, 2024, On the Strategy for Scientific and Technological Development of the Russian Federation. http://www.kremlin.ru/acts/bank/50358 (in Russ.). Accessed April 03, 2024.

of research in the field of ensuring scientific activity and economic security in the context of sanctions pressure [21]. The authors [22] consider approaches to overcoming Russia's technological dependence. The available mechanisms and tools of transition to the sixth technological mode are studied in [23].

Researchers note the need to transition to a sovereign, import-independent model of scientific and technological development. For example, T.D. Stepanova in [24] identified the key threats to technological development and, consequently, economic security. Staffing problems represent an important aspect of scientific discussions. Noting the need to improve personnel training in the context of economic security, V.I. Avdiyskiy offers recommendations that facilitate this process [25].

An acknowledged mechanism for ensuring economic security is the monitoring of key indicators of socioeconomic development [26]. Current studies are devoted to various aspects of monitoring and evaluation of economic security. Thus, A.P. Suvorova and N.Yu. Sudakova consider the scientific and technological development of Russia through the prism of the effectiveness of the implementation of state programs [27]. In [28] the theoretical and methodological approaches to the study of economic security, the development of theory and practice of information processing in the context of its provision are improved. The works by V.K. Senchagov, S.N. Mityakov [29] describe the approach to the application of short-term indicators assessment models for analyzing economic security. The authors consider the monitoring of regional innovation activity in the context of ensuring economic security and scientific sovereignty. Other studies are devoted to assessing the effects and implementation of projects in production systems as part of the scientific potential of the country [30]. The paper [31] presents conceptual aspects of STS ensuring and tools for STS monitoring of the regions of Russia.

The review of scholarly publications demonstrates the relevance of the topic under consideration in the context of ensuring economic security at the regional and federal levels. Thus, most of the works are devoted to the formation of an instrumental and methodological basis for the study of STS on the basis of existing statistical information. While this is certainly justified in the context of data collection and the possibility of their further comparative and retrospective analysis, existing approaches can be supplemented on the basis of alternative assessment methods. Moreover, such tools, which are based on indirect indicators of economic activity that have a significant impact on the state of STS, enable additional verification of existing official statistical data.

METHODOLOGY FOR MONITORING AND FORECASTING STS LEVEL ON THE BASIS OF ANALYZING THE DYNAMICS OF THE VALUE OF COMPANIES' SECURITIES

With the development of data transmission networks, mechanisms for organizing, storing, and presenting information, many Russian and foreign researchers use stock exchange quotations to analyze the financial component, assess the prospects of development of industries of the real sector of the economy, and clarify the parameters of developed simulation models. Here, the system of indicators is based on short-term indices. While such an approach is applicable to the tasks of selective assessment and forecasting of the constituent elements of the economic security structure, it seems reasonable to switch to monitoring changes in key indicators in the medium term when setting out to improve its scientific and technological component. This is due to more complex properties of the impact of changes in financial instruments of companies and corporations engaged in research and development at the STS level of the socioeconomic system. It is also due to the presence of deferred influence of innovation processes, which effectiveness affects the overall STS level as well as influencing the value of the company's shares on the stock exchange.

Relevant methods of predictive modeling used for evaluation and analysis of time series on the basis of machine learning can be combined with formal models of mathematical statistics to predict dynamics of changes in the value of securities of companies with a certain degree of probability. In other words, the methodology of STS monitoring based on the analysis of the dynamics of the value of companies' securities includes two key components: (1) a system of indicators formed on the basis of a set of leaders of scientific and technological progress for the direct construction of an integral index and (2) methods of time series analysis for forecasting (Figure).

Let us consider a methodology for monitoring and forecasting the STS level based on the analysis of the dynamics of the value of securities of Russia's leading companies. The methodology involves analyzing the value of securities of companies grouped by types of economic activity where there is a direct relation to research and development on top of science and technology investments. Thus, we will consider companies engaged in mining, manufacturing, as well as those belonging to the collective classification grouping of economic activities "Information and Communication Technologies Sector."

The formal component of the methodology includes tools for time series analysis, which are used to build predictive models in the presence of a sufficient amount

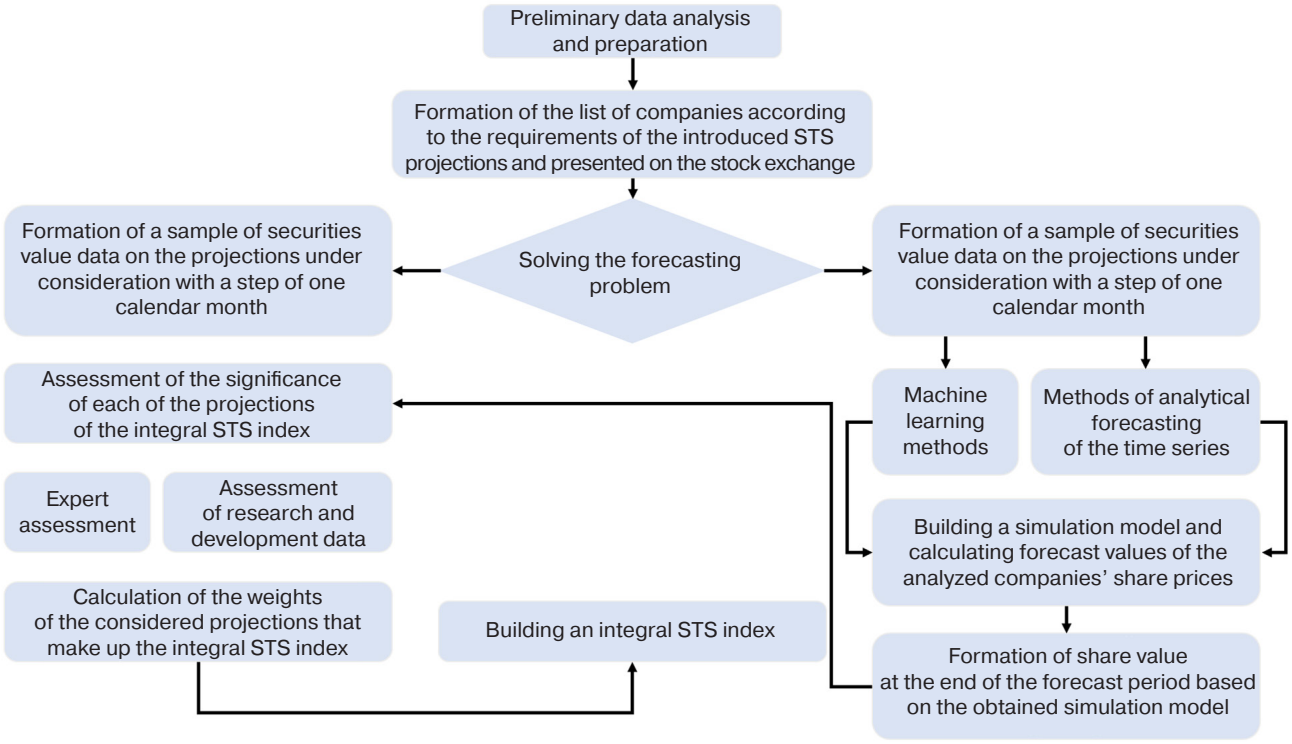

Figure. Structural scheme of the methodology for monitoring and forecasting the STS level on the basis of analyzing the dynamics of the value of the companies' securities

of initial data. While providing opportunities to select the most appropriate mechanisms for the characteristics of the initial data, the existing models require a comparative analysis of the results to select those most adequate to the initial data. Thus, in [32] an example of forecasting short-term economic security indices based on machine learning and time series tools is presented. The authors conduct a comparative analysis of modeling results for various macroeconomic indicators using autoregressive integrated moving average and Holt models, as well as neural network models. With regard to the assessment of STS on the basis of analyzing the value of shares of companies engaged in research and development, it seems appropriate to use a combination of methods of forecasting time series based on the Holt–Winters and Box–Jenkins models, taking into account the importance of comparative analysis of the resulting forecasts. It is also advisable to use machine learning models, which allows us to compare the final results, for example, the long short-term memory network known as the long short-term memory model.

While the described methods are not a mandatory guide to action when forecasting the values of a time series, they can be used to conduct a comparative analysis of forecast accuracy. The analytical component of the proposed methodology involves iterative comparison of the obtained values in accordance with certain accuracy criteria, as well as adaptation of the selected models to solve specific practical problems. The use of machine learning and time series apparatus illustrates the diversity of approaches to forecasting and forms the possibility of selecting the most appropriate of them to solve the specific task of analyzing the dynamics of STS change.

Let us consider the determining ratios necessary for quantitative assessment of changes in the STS level in accordance with the presented methodology. For this purpose, we propose to use the author's formula based on the assumption of a pronounced direct impact of the investment attractiveness of a high-tech company on the research and development sector, and, consequently, on the STS level.

Let us proceed to the construction of an integral STS index on the basis of analyzing the value of companies' shares. For this purpose, it is advisable to use the following ratio:

$$S = \frac{\sum_{i=1}^{n} \beta_i \sum_{j=1}^{m} (1-\rho_j)\alpha_j \frac{x_t}{\overline{x}_\tau}}{\sum_{i=1}^{n} \sum_{j=1}^{m} \frac{x_t}{\overline{x}_\tau}}, \quad (1)$$

where n is the number of projections of companies' economic activities; m is the number of companies in the projection being analyzed; $0 \le \beta_i \le 1$ is the projection significance coefficient for STS; $0 \le \alpha_j \le 1$ is the

company's significance coefficient in the projection; $0 \le \rho_j \le 1$ is the risk assessment of the asset under consideration; x_t is the value of the company's financial instrument (e.g., shares) in the last analyzed period; $\overline{x}_\tau$ is the average value of the financial instrument's value at some time interval equal to several periods t preceding the one under consideration.

While the coefficient of the company's significance αj can be determined on the basis of expert assessment, if the initial data is available, its calculation lies in the assessment of statistical indicators of the analyzed organization in the field of completed research and development. Thus, the significance of a particular company can be determined in the context of ensuring STS on the basis of the relative contribution in terms of research and R&D within the scope of the industrial sector. In this case, it is proposed to normalize the values of α_j for the formula under consideration according to the condition of maximum, where $\alpha_j = 1$ is assigned to the most innovative and active company, and the rest are normalized in descending order. In other words, after obtaining the relative weights of the contribution of each of the companies to the number of research and R&D of the industrial sector, the values are proportionally scaled to match the relative weight of the leader of the considered distribution to one.

While the coefficient β_i can also be determined on the basis of expert evaluation, it is advisable to consider its values on the basis of the assessment of statistical data on innovation activity by sector, defined as the ratio of the number of research and R&D of the type of economic activity under consideration to the total number of scientific works performed by all its types. The normalization of β_i value is assumed to be consistent with α_j, i.e., the largest value of the coefficient in the distribution is equivalent to one, and other values are calculated proportionally. For the correct functioning of the methodology, it is necessary to have appropriate statistical data for calculating the coefficients β_i and α_j by types of economic activity and the number of new products and technologies, respectively.

The risk component, represented by the corresponding component $(1 - \rho_j)$ and normalized from 0 to 1, should be specially noted. An assessment of the impact of the dynamics of changes in the value of securities on the STS level must be carried out when taking into account the risks that characterize the investment attractiveness of the selected asset. While the assessment of risks in the proposed methodology refers to the volatility of securities, it can also include the risks of reducing the impact of the dynamics of analyzed financial instruments on the change in the STS level. At the same time, this conflict situation can be resolved in the model by increasing or decreasing the expert values of the significance coefficients of the influence of the dynamics of the analyzed asset on the STS level.

When considering some practically important tasks in detail, it is advisable to resort to differentiated methods of assessing the risk component. Thus, the present methodology does not imply restrictions on the type of securities, which in the context of the assessment implies appropriate adaptation of the risk measure. For the selected time periods, measures based on the value at risk commonly used in financial analysis, calculated specifically for each type of securities under consideration, can be used, along with probabilistic risk assessment, expert assessment or methods based on more complex factor models. The method used in a particular practical task to assess the risk component of a financial instrument is primarily based on the requirements of the study, taking into account available statistical data, as well as time and material and technical resources, in the analysis.

In the basic version of the methodology, the calculation of the relevant component is based on generally known methods of financial risk assessment. Here, the coefficient of variation may serve as a measure. If necessary, the tool used may be supplemented and modified in accordance with the requirements of a particular study. The coefficient of variation used in this methodology is calculated according to the following formula:

$$\rho_j = \frac{SD_j}{M_j}, \quad (2)$$

where SD_j is the standard deviation based on statistical data for the period under consideration; M_j is the average value of the financial instrument under consideration for the time interval under evaluation.

Thus, the final formula includes a conservative assessment of risks while taking into account the coefficient of variation, allows the characteristics of the analyzed set of financial instruments to be further clarified. Formalizing the set of actions defining the methodology of monitoring and forecasting the STS level based on the analysis of the dynamics of the value of securities of companies, the following stages can be outlined:

1. Selection of time interval for STS level assessment.
2. Formation of the list of companies-issuers of financial instruments, according to the directions of their R&D activities and types of economic activities.
3. Preparation of statistical data on selected companies: determination of the current x_t and average value $\overline{x}_\tau$ of a financial instrument, as well as its risk measure ρ_j.

4. Calculation of weights β_i characterizing the contribution of the industry corresponding to the selected companies to the scientific and technological progress of the state.
5. Assessment of company importance in the projection α_j.
6. Building the *S*—integral STS index based on the analysis of the value of companies' shares.

COMPUTATIONAL EXPERIMENT

In order to illustrate the practical application of the presented methodology, let us turn to the rating of the largest companies in Russia by sales volume. Let us select the companies occupying leading positions by this indicator according to the RAEX-Analytica[2] rating agency in accordance with the highlighted evaluation projections. Coefficients β_i were calculated on the basis of the Federal State Statistics Service data, in particular, in accordance with the report[3] on the number of fundamentally new developed advanced production technologies by types of economic activity. Coefficients α_j in the example represent the expert opinion on the importance of a particular company in the context of providing STS. In order to analyze stock exchange quotations and calculate parameters x_t, $\overline{x}_\tau$, we used open data on the value of financial instruments of the companies under consideration using open services such as Investing.com[4], Yahoo Finance[5], Moscow Exchange[6], and others.

In order to assess the STS level for the period of 2022 (Table 1), the data aggregated by means of comparative analysis and mutual verification of the value of financial assets on international platforms were used. For the period of spring 2024 (Table 3), the data of the Moscow Exchange were employed in the calculations due to the delisting of financial instruments of Russian companies from global trading platforms. Under the conditions of an isolated national financial market, the risk component expressed by the volatility of instruments issued by companies is lower on average, as evidenced by a comparative analysis of the relevant statistical data given in the numerical experiment in Tables 1 and 3. In this regard, in further practical calculations it is advisable to supplement the risk component of this methodology with factors that have a quantitative expression.

After preparing the initial data, as well as calculating the coefficients β_i and α_j and the ratio $\frac{x_t}{\overline{x}_\tau}$ for each of the companies under consideration, we proceed to the construction of an integral assessment of the STS level of the socioeconomic system. Using the formula (1), we obtain the value of the integral STS index, which is 0.64. In this case, according to the considered assessment model, the values of the private contribution of companies for each type of economic activity are 26%, 60%, and 14%, respectively (Table 2).

To ensure that the results of the numerical experiment correspond to the actual time interval, it is necessary to use the data of the Moscow Exchange. This is partly due to the exclusion of Russian companies from the list of organizations represented on international exchanges, and partly to the restricted access to statistical reporting of systemically important companies[7]. For some statistical data (for example, the number of fundamentally new developed advanced production technologies), on the basis of which, in particular, the coefficient β_i of the methodology was calculated, the period of values is also 2022. The numerical experiment based on the updated statistical information is presented below (Tables 3 and 4).

Now, based on formula (1), the value of the integral STS index is 0.22. At the same time, according to the evaluation model under consideration, the values of private contribution of companies for each of the economic activities are 24%, 61%, and 15%, respectively (Table 4).

It should be noted that the calculation mechanism of the presented results does not include Rostec State Corporation structures; in particular, Kalashnikov Concern and Russian Helicopters Holding, since their financial instruments are not listed on the Moscow Exchange. To enable a comparative analysis of the results over the reporting period interval (data for February 2022 and April 2024), *S*—STS integral index for the period of February 2022 without participation of the above companies—was calculated. The corresponding value was 0.20, while the private contribution indices of the companies for each of the economic activities were 15%, 61%, and 24%, respectively. This indicates a decrease in the contribution of mining companies and the role of manufacturing, as well as an increase in the importance of the information and communication technology sector.

[2] Rating of Russia's largest companies by sales volume—RAEX-600. https://raex-rr.com/largest/RAEX-600/biggest_companies/2022/ (in Russ.). Accessed April 03, 2024.

[3] Technological development of economic sectors. Federal State Statistics Service. https://rosstat.gov.ru/folder/11189 (in Russ.). Accessed April 02, 2024.

[4] https://www.investing.com. Accessed April 02, 2024.

[5] https://finance.yahoo.com. Accessed April 02, 2024.

[6] https://www.moex.com (in Russ.). Accessed April 02, 2024.

[7] Federal Law No. 55-FZ dated February 28, 2023 "On Amending Article 5 and Suspending Part 7 of Article 8 of the Federal Law "On Official Statistical Accounting and the System of State Statistics in the Russian Federation" and on the Specifics of Official Statistical Accounting in the Territories of Certain Constituent Entities of the Russian Federation." http://publication.pravo.gov.ru/Document/View/0001202302280031 (in Russ.). Accessed April 03, 2024.

Table 1. Data for STS level assessment based on stock market analysis of large R&D companies, February 2022

Company performance / Type of economic activity	Company name		Financial instrument cost in the last analyzed period, x_t (February 2022), RUR	Average value of a financial instrument cost at a certain time interval, $\overline{x}_\tau$ (January 2021 – January 2022), RUR	β_i coefficient calculated on the basis of statistical data given by the maximum value rule	α_j coefficient—expert estimation given by the maximum value rule	Risk assessment $(1 - \rho_j)$
Mining	Gazprom		324.30	287.57	0.21	0.5	0.82
	LUKOIL		70.41	63.48		0.5	0.92
	RUSAL United Company		67.07	77.47		0.25	0.85
	Norilsk Nickel, mining and metallurgical company		21919	23683		0.25	0.94
Manufacturing, mechanic engineering	Rostec State Corporation, structures represented on the financial market	Kalashnikov Concern	99.8	101.27	1	0.75	0.99
		Russian Helicopters	96.48	99.26		0.75	0.97
		KAMAZ	106.08	87.01		0.5	0.76
	Rosseti		1.01	1.36		0.5	0.86
	SIBUR Holding		94.5	98.00		0.25	0.97
Cumulative classification grouping of economic activities “Information and Communication Technology Sector”	AFK Sistema		19.44	29.31	0.46	0.5	0.84
	Rostelekom		71.42	95.45		0.5	0.88

Table 2. Integral STS index values based on the analysis of the securities market of large companies engaged in R&D activities, February 2022

Type of economic activity	Percentage expression of companies’ contribution to the integral STS index for each of the analyzed types of economic activity
Mining	26%
Manufacturing, mechanic engineering	60%
Cumulative classification grouping of economic activities “Information and Communication Technology Sector”	14%

Table 3. Data for STS level assessment based on stock market analysis of large R&D companies, April 2024

Company performance / Type of economic activity	Company name		Financial instrument cost in the last analyzed period, x_t (April 2024), RUR	Average value of a financial instrument cost at a certain time interval, $\bar{x}_\tau$ (April 2023 – April 2024), RUR	β_i coefficient calculated on the basis of statistical data given by the maximum value rule	α_j coefficient—expert estimation given by the maximum value rule	Risk assessment $(1 - \rho_j)$
Mining	Gazprom		92.53	95.44	0.35	0.5	0.97
	LUKOIL		94.08	90.29		0.5	0.95
	RUSAL United Company		100.59	70.36		0.25	0.57
	Norilsk Nickel, mining and metallurgical company		93.45	97.54		0.25	0.96
Manufacturing, mechanic engineering	Rostec State Corporation, structures represented on the financial market	Kalashnikov Concern	Non-traded instrument[8]	–	1	0.75	0.99
		Russian Helicopters	Non-traded instrument[9]	–		0.75	0.97
		KAMAZ	100.50	99.98		0.5	1.00
	Rosseti		99.87	97.09		0.5	0.97
	SIBUR Holding		93.52	96.98		0.25	0.96
Cumulative classification grouping of economic activities “Information and Communication Technology Sector”	Rostelekom		92.47	96.11	0.33	0.5	0.96
	Rostelekom		91.22	95.52		0.5	0.96

Table 4. Integral STS index values based on the analysis of the securities market of large companies engaged in R&D activities, April 2024

Type of economic activity	Percentage expression of companies’ contribution to the integral STS index for each of the analyzed types of economic activity
Mining	24%
Manufacturing, mechanic engineering	61%
Cumulative classification grouping of economic activities “Information and Communication Technology Sector”	15%

[8] On Amendments to the List of Securities Admitted to Trading. Moscow Exchange. https://www.moex.com/n47168?print=1 (in Russ.). Accessed April 03, 2024.

[9] On Keeping Securities on the List of Securities Admitted to Trading. Moscow Exchange. https://www.moex.com/n67495?print=1 (in Russ.). Accessed April 03, 2024.

The comparative analysis of the obtained results shows that the methodology is stable in relation to the number of selected companies within the grouping "Type of economic activity." At the same time, it remains certain that with the increase in the number of organizations-representatives of each of the considered areas of economic activity, influencing the change in the STS level, the objectivity of the assessment increases proportionally. The conducted computational experiment at different time intervals quantitatively shows that the most significant contribution to the integral STS level is made by manufacturing and machine-building enterprises. This allows us to justify the need to increase the industrial potential to ensure scientific and technological sovereignty of the Russian Federation.

CONCLUSIONS

The developed methodology for monitoring and forecasting the STS level on the basis of analyzing the dynamics of the value of company securities is part of a comprehensive toolkit for processing significant retrospective and instantaneous information on the state, dynamics of changes, and forecasting of important indicators of scientific and technological development in the context of ensuring economic and national security. Tools of statistical analysis and economic and mathematical modeling used in this methodology are used to provide an objective assessment of the state of research and development of the socioeconomic system. The presented methodology combines the simulation modeling of complex systems into a unified structure to conduct operational monitoring of the research and development sphere on the basis of assessing the dynamics of the integral index for selected industries and spheres of economic activity.

A distinctive feature of the presented methodology is its high adaptability and the possibility to build the main or additional sources of information into the functioning mechanisms of management decision support. Given a statistical sample of sufficient volume and quality, it is possible to build an integral assessment of the STS level using tools from exclusively formal methods, which positively affects the accuracy of the results in comparison with the accepted expert or probabilistic approaches. In the context of monitoring, this contributes to improved accuracy and speed of management—and consequently increased level of economic security.

REFERENCES

1. Varshavskii A.E. Methodological principles of evaluating Russia's technological security. *Vestnik Moskovskogo universiteta. Seriya 25: Mezhdunarodnye otnosheniya i mirovaya politika = Moscow University Bulletin of World Politics*. 2015;7(4): 73–100 (in Russ.). https://fmp.msu.ru/attachments/article/361/VARSHAVSKII_2015_4.pdf, available from URL: https://www.elibrary.ru/vrnhyr
2. Vlasova M.S., Stepchenkova O.S. Indicators of economic security in the scientific and technological sphere. *Voprosy statistiki*. 2019;26(10):5–17 (in Russ.). https://doi.org/10.34023/2313-6383-2019-26-10-5-17, available from URL: https://www.elibrary.ru/lyzokw
3. Pinchuk A.Yu. On the relationship between the national security and the transformation of sociopolitical processes in the scientific and technological development of Russia. *Voprosy upravleniya = Management Issues*. 2020;6(67):6–14 (in Russ.). https://doi.org/10.22394/2304-3369-2020-6-6-14, available from URL: https://www.elibrary.ru/ronggn
4. Afanasev A.A. Technological sovereignty: a question of essence. *Kreativnaya ekonomika = J. Creative Economy*. 2022;16(10):3691–3708 (in Russ.). https://doi.org/10.18334/ce.16.10.116406, available from URL: https://www.elibrary.ru/ecahwb
5. Ladynin A.I. *Razvitie instrumentariya analiza nauchno-tekhnologicheskoi bezopasnosti Rossii* (*Development of Tools for Analyzing Scientific and Technological Security of Russia*: monograph). Nizhny Novgorod: Nizhny Novgorod State Technical University; 2023. 92 p. (in Russ.). ISBN 978-5-502-01711-4
6. Glazkova V.V. Methodical approach to assessing effectiveness of innovation implementation in unified heat supply organizations. *Vestnik Universiteta*. 2023;8:30–39 (in Russ.). https://doi.org/10.26425/1816-4277-2023-8-30-39, available from URL: https://www.elibrary.ru/yolcba
7. Alenkova I.V., Mityakova O.I. System of indicators for assessment efficiency of introduction of ecological innovations. *Fundamental'nye issledovaniya = Fundamental Research*. 2019;12(2):237–241 (in Russ.). Available from URL: https://www.elibrary.ru/rfwyrz
8. Tishchenko I.A. The system of indicators for evaluating innovations in the context of digital transformation of the economy. *Ekonomicheskie i gumanitarnye nauki = Economic and Humanitarian Sciences*. 2022;5(364):3–9 (in Russ.). https://doi.org/10.33979/2073-7424-2022-364-5-3-9, available from URL: https://www.elibrary.ru/mgvbmb
9. Milyuchikhina O.A. Innovation management in Russian Federation: main challenges and perspectives of innovative business. *Russian Economic Bulletin.* 2020;3(4):252–255 (in Russ.). Available from URL: https://www.elibrary.ru/gnklkt

10. Mitrofanov A.S., Pastukhov M.V. Performance indicators of the Innovation Assistance Fund Programs as a tool for evaluating the effectiveness of budgetary investment. *Kachestvo. Innovatsii. Obrazovanie = Quality. Innovation. Education*. 2019;6(164):58–66 (in Russ.). https://doi.org/10.31145/1999-513x-2019-6-58-66, available from URL: https://www.elibrary.ru/tlfndu
11. Glukhov V.V., Babkin A.V., Shkarupeta E.V. Digital strategizing of industrial systems based on sustainable eco-innovation and circular business models in the context of the transition to Industry 5.0. *Ekonomika i upravlenie = Economics and Management*. 2022;28(10):1006–1020 (in Russ.). https://doi.org/10.35854/1998-1627-2022-10-1006-1020
12. Rybakov F.F. The economy of research and development: evolution of views and modernity. *Innovatsii = Innovations*. 2014;4(186):62–64 (in Russ.). Available from URL: https://www.elibrary.ru/TJDBFR
13. Kalinichenko M.P. Management of strategic competitiveness of industrial enterprises: assessment, implementation of technological and management innovations. *Izvestiya Yugo-Zapadnogo gosudarstvennogo universiteta. Seriya: Ekonomika. Sotsiologiya. Menedzhment = Proceedings of the Southwest State University. Series: Economics. Sociology. Management.* 2022;12(1):80–91 (in Russ.). https://doi.org/10.21869/2223-1552-2022-12-1-80-91, available from URL: https://www.elibrary.ru/bhgnjk
14. Burtseva T.A. Evaluating the effectiveness of information support for innovation management. *Vestnik Moskovskogo universiteta im. S.Yu. Vitte. Seriya 1: Ekonomika i upravlenie = Moscow Witte University Bulletin. Series 1: Economics and Management*. 2020;1(32):78–86 (in Russ.). https://doi.org/10.21777/2587-554X-2020-1-78-86, available from URL: https://www.elibrary.ru/cegzcw
15. Babkin A.V., Chen L. Evaluation of the efficiency of innovations in the high-tech industry. *Estestvenno-gumanitarnye issledovaniya = Natural-Humanitarian Studies*. 2022;41(3):42–50 (in Russ.). Available from URL: https://www.elibrary.ru/EZNQAV
16. Batkovsky A.M., Kravchuk P.V., Fomina A.V. Management of innovative active enterprises of the radioelectronic industry under conditions their diversifications. *Dnevnik nauki = Science Deiary.* 2020;1(37):31 (in Russ.). Available from URL: https://www.elibrary.ru/uelshj
17. Batkovsky A.M., Batkovsky M.A., Ermakova Ya.M., Omelchenko A.N. Formalization of the initial information needed to model the diversification of production. *Original'nye issledovaniya = Original Research.* 2023;13(1):175–187 (in Russ.). Available from URL: https://www.elibrary.ru/tvausg
18. Fraimovich D.Yu., Alekseev V.A. Improving the mechanism for managing innovation activities on the basis of public-private partnership. *Mezhdunarodnyi Ekspeditor.* 2021;4:20–23 (in Russ.). Available from URL: https://www.elibrary.ru/TWBMGU
19. Berezin I.L., Lukyanova A.A. Institutional forms of innovation management and their limitations. *Kreativnaya ekonomika = J. Creative Economy*. 2023;17(4):1211–1230 (in Russ.). https://doi.org/10.18334/ce.17.4.117687, available from URL: https://www.elibrary.ru/lukyhd
20. Filin S.A., Kuzina A.A. Principles for managing innovative activities of entities in Russia during the transition to the digital economy. *Daidzhest-finansy = Digest Finance*. 2021;26(1–257):107–122 (in Russ.). https://doi.org/10.24891/df.26.1.107, available from URL: https://elibrary.ru/wsrrqf
21. Frolova O.V., Donchevskaya L.V. Scientific and technological development in the economic security system of Russia under sanctions. *Sotsial'nye i ekonomicheskie sistemy = Social and Economic Systems*. 2023;3–2(44):136–154 (in Russ.). Available from URL: https://elibrary.ru/nqrwwr
22. Nikitina I.A., Kruglova I.A., Potemkin A.S. Global sanctions in the context of Russia's economic security. *Regional'naya ekonomika: teoriya i praktika = Regional Economics: Theory and Practice)*. 2023;21(8–515):1478–1504 (in Russ.). https://doi.org/10.24891/re.21.8.1478, available from URL: https://www.elibrary.ru/lpivji
23. Topunova I.R. Ensuring the economic security of the Russian Federation in the conditions of external sanctions. *Ekonomika: vchera, segodnya, zavtra = Economics: Yesterday, Today and Tomorrow).* 2023;13(3–1):242–250 (in Russ.). Available from URL: https://elibrary.ru/ofwbbg
24. Stepanova T.D. Economic security of Russia after 2022: technological sovereignty and human potential. *Rossiiskii ekonomicheskii zhurnal = Russian Economic J.* 2023;4:107–119 (in Russ.). Available from URL: https://elibrary.ru/quzgbj
25. Avdiyskiy V.I. Modern approaches to personnel training as an element of ensuring national security in the context of political and economic sanctions. *Vestnik Evraziiskoi nauki = The Eurasian Scientific J.* 2023;15(1):64 (in Russ.). Available from URL: https://elibrary.ru/xzplfw
26. Mironova O.A. Development of economic security as a science: problems and prospects. *Innovatsionnoe razvitie ekonomiki = Innovative Development of Economy.* 2019;2(50):332–338 (in Russ.). Available from URL: https://elibrary.ru/ikbsiy
27. Suvorova A.P., Sudakova N.Yu. Formation of monitoring of scientific and technological development as a factor of threats to the social and economic security of the Russian Federation. *Innovatsionnoe razvitie ekonomiki = Innovative Development of Economy.* 2020;6(60):358–370 (in Russ.). Available from URL: https://elibrary.ru/ghwsrk
28. Boboshko V.I., Mironova O.A., Mironov A.A. The Concept of formation and development of accounting and analytical information in the conditions of spatial development of the Russian economy. *Innovatsionnoe razvitie ekonomiki = Innovative Development of Economy.* 2022;5(71):225–230 (in Russ.). https://doi.org/10.51832/2223798420225225, available from URL: https://elibrary.ru/bdwkmu
29. Senchagov V.K., Mityakov S.N. Using the index method to assess the level of economic security. *Vestnik akademii ekonomicheskoi bezopasnosti MVD Rossii = Vestnik of Academy of Economic Security of the Ministry of Internal Affairs of Russia*. 2011;5:41–50 (in Russ.). Available from URL: https://elibrary.ru/ogxljl

30. Abdulkadyrov M.A., Ignatov A.N., Kulikova N.N., Mityakov E.S. Assessment of the effects of production system development projects: Case study of Lytkarino Optical Glass Factory. *Russ. Technol. J*. 2023;11(6):76–88. https://doi.org/10.32362/2500-316X-2023-11-6-76-88
31. Mityakov S.N., Murashova N.A., Mityakov E.S., Ladynin A.I. Russian regions scientific and technological security monitoring: Conceptual aspects. *Innovatsii = Innovations*. 2022;1(279):58–65 (in Russ.). Available from URL: https://elibrary.ru/hfqgti
32. Shmeleva A.G., Mityakov E.S., Ladynin A.I. Neural Networks Usability Analysis in Economic Security Indicators Dynamics Forecasting. In: *Proceedings of the International Scientific-Practical Conference "Ensuring the Stability and Security of Socio-Economic Systems: Overcoming the Threats of the Crisis Space."* Kirov: 2021. P. 149–155. ISBN: 978-989-758-546-3. https://doi.org/10.5220/0000148100003169

СПИСОК ЛИТЕРАТУРЫ

1. Варшавский А.Е. Методические принципы оценивания научно-технологической безопасности России. *Вестник Московского университета. Серия 25: Международные отношения и мировая политика*. 2015;7(4):73–100. https://fmp.msu.ru/attachments/article/361/VARSHAVSKII_2015_4.pdf, URL: https://www.elibrary.ru/vrnhyr
2. Власова М.С., Степченкова О С. Показатели экономической безопасности в научно-технологической сфере. *Вопросы статистики*. 2019;26(10):5–17. https://doi.org/10.34023/2313-6383-2019-26-10-5-17, URL: https://www.elibrary.ru/lyzokw
3. Пинчук А.Ю. О взаимосвязи обеспечения национальной безопасности и трансформации социально-политических процессов в научно-технологическом развитии России. *Вопросы управления*. 2020;6(67):6–14. https://doi.org/10.22394/2304-3369-2020-6-6-14, URL: https://www.elibrary.ru/ronggn
4. Афанасьев А.А. Технологический суверенитет: к вопросу о сущности. *Креативная экономика*. 2022;16(10):3691–3708. https://doi.org/10.18334/ce.16.10.116406, URL: https://www.elibrary.ru/ecahwb
5. Ладынин А.И. *Развитие инструментария анализа научно-технологической безопасности России*: монография. Нижний Новгород: Нижегород. гос. техн. ун-т. им. Р.Е. Алексеева; 2023. 92 с. ISBN 978-5-502-01711-4
6. Глазкова В.В. Методический подход к оценке эффективности внедрения инноваций в единые теплоснабжающие организации. *Вестник университета*. 2023;8:30–39. https://doi.org/10.26425/1816-4277-2023-8-30-39, URL: https://www.elibrary.ru/yolcba
7. Аленкова И.В., Митякова О.И. Система показателей оценки эффективности внедрения экологических инноваций. *Фундаментальные исследования.* 2019;12(2):237–241. URL: https://www.elibrary.ru/rfwyrz
8. Тищенко И.А. Система показателей по оценке инноваций в условиях цифровой трансформации экономики. *Экономические и гуманитарные науки*. 2022;5(364):3–9. https://doi.org/10.33979/2073-7424-2022-364-5-3-9, URL: https://www.elibrary.ru/mgvbmb
9. Милючихина О.А. Управление инновациями в Российской Федерации: оценка основных проблем и перспектив развития инновационного бизнеса на современном этапе. *Russian Economic Bulletin*. 2020;3(4):252–255. URL: https://www.elibrary.ru/gnklkt
10. Митрофанов А.С., Пастухов М.В. Показатели результативности Программ Фонда содействия инновациям как инструмент оценки эффективности вложения бюджетных средств. *Качество. Инновации. Образование*. 2019;6(164):58–66. https://doi.org/10.31145/1999-513x-2019-6-58-66, URL: https://www.elibrary.ru/tlfndu
11. Глухов В.В., Бабкин А.В., Шкарупета Е.В. Цифровое стратегирование промышленных систем на основе устойчивых экоинновационных и циркулярных бизнес-моделей в условиях перехода к Индустрии 5.0. *Экономика и управление*. 2022;28(10):1006–1020. https://doi.org/10.35854/1998-1627-2022-10-1006-1020
12. Рыбаков Ф.Ф. Экономика исследований и разработок: эволюция взглядов и современность. *Инновации.* 2014;4(186):62–64. URL: https://www.elibrary.ru/TJDBFR
13. Калиниченко М.П. Управление стратегической конкурентоспособностью промышленных предприятий: оценка, внедрение технологических и управленческих инноваций. *Известия Юго-Западного государственного университета. Серия: Экономика. Социология. Менеджмент*. 2022;12(1):80–91. https://doi.org/10.21869/2223-1552-2022-12-1-80-91, URL: https://www.elibrary.ru/bhgnjk
14. Бурцева Т.А. Оценка эффективности информационного обеспечения управления инновациями. *Вестник Московского университета им. С.Ю. Витте. Серия 1: Экономика и управление.* 2020;1(32):78–86. https://doi.org/10.21777/2587-554X-2020-1-78-86, URL: https://www.elibrary.ru/cegzcw
15. Бабкин А.В., Чэнь Л. Оценка эффективности инноваций высокотехнологичной промышленности. *Естественно-гуманитарные исследования*. 2022;41(3):42–50. URL: https://www.elibrary.ru/EZNQAV
16. Батьковский А.М., Кравчук П.В., Фомина А.В. Управление инновационно-активными предприятиями радиоэлектронной промышленности в условиях их диверсификации. *Дневник науки*. 2020;1(37):31. URL: https://www.elibrary.ru/UELSHJ
17. Батьковский А.М., Батьковский М.А., Ермакова Я.М., Омельченко А.Н. Анализ и формализация информации, необходимой для моделирования диверсификации производства. *Оригинальные исследования*. 2023;13(1):175–187. URL: https://www.elibrary.ru/TVAUSG
18. Фраймович Д.Ю., Алексеев В.А. Развитие механизма управления инновационной деятельностью. *Международный экспедитор*. 2021;4:20–23. URL: https://www.elibrary.ru/TWBMGU

19. Березин И.Л., Лукьянова А.А. Институциональные формы управления инновационной деятельностью и их ограничения. *Креативная экономика*. 2023;17(4):1211–1230. https://doi.org/10.18334/ce.17.4.117687, URL: https://www.elibrary.ru/LUKYHD
20. Филин С.А., Кузина А.А. Принципы управления инновационной деятельностью предприятий в России при переходе к «цифровой» экономике. *Дайджест-финансы*. 2021;26(1-257):107–122. https://doi.org/10.24891/df.26.1.107, URL: https://www.elibrary.ru/WSRRQF
21. Фролова О.В., Дончевская Л.В. Научно-технологическое развитие в системе обеспечения экономической безопасности России в условиях санкций. *Социальные и экономические системы*. 2023;3–2(44):136–154. URL: https://www.elibrary.ru/NQRWWR
22. Никитина И.А., Круглова И.А., Потемкин А.С. Глобальные санкции в контексте экономической безопасности России. *Региональная экономика: теория и практика.* 2023;21(8-515):1478–1504. https://doi.org/10.24891/re.21.8.1478, URL: https://www.elibrary.ru/LPIVJI
23. Топунова И.Р. Обеспечение экономической безопасности РФ в условиях внешних санкций. *Экономика: вчера, сегодня, завтра*. 2023;13(3-1):242–250. URL: https://www.elibrary.ru/OFWBBG
24. Степанова Т.Д. Экономическая безопасность России после 2022 года: технологический суверенитет и человеческий потенциал. *Российский экономический журнал*. 2023;4:107–119. URL: https://www.elibrary.ru/QUZGBJ
25. Авдийский В.И. Современные подходы подготовки кадров как элемент обеспечения национальной безопасности в условиях политических и экономических санкций. *Вестник Евразийской науки*. 2023;15(1):64. URL: https://www.elibrary.ru/XZPLFW
26. Миронова О.А. Развитие экономической безопасности как науки: проблемы и перспективы. *Инновационное развитие экономики*. 2019;2(50):332–338. URL: https://www.elibrary.ru/IKBSIY
27. Суворова А.П., Судакова Н.Ю. Формирование мониторинга научно-технологического развития как фактора угроз социально-экономической безопасности Российской Федерации. *Инновационное развитие экономики*. 2020;6(60): 358–370. URL: https://www.elibrary.ru/GHWSRK
28. Бобошко В.И., Миронова О.А., Миронов А.А. Концепция формирования и развития учетно-аналитической информации в условиях пространственного развития экономики России. *Инновационное развитие экономики*. 2022;5(71): 225–230. https://doi.org/10.51832/2223798420225225, URL: https://www.elibrary.ru/BDWKMU
29. Сенчагов В.К., Митяков С.Н. Использование индексного метода для оценки уровня экономической безопасности. *Вестник академии экономической безопасности МВД России.* 2011;5:41–50. URL: https://elibrary.ru/ogxljl
30. Абдулкадыров М.А., Игнатов А.Н., Куликова Н.Н., Митяков Е.С. Оценка эффектов реализации проектов развития производственной системы (на примере АО «Лыткаринский завод оптического стекла»). *Russian Technological Journal*. 2023;11(6):76–88. https://doi.org/10.32362/2500-316X-2023-11-6-76-88
31. Митяков С.Н., Мурашова Н.А., Митяков Е.С., Ладынин А.И. Мониторинг научно-технологической безопасности регионов России: концептуальные аспекты. *Инновации*. 2022;1(279):58–65. URL: https://www.elibrary.ru/HFQGTI
32. Shmeleva A.G., Mityakov E.S., Ladynin A.I. Neural Networks Usability Analysis in Economic Security Indicators Dynamics Forecasting. In: *Proceedings of the International Scientific-Practical Conference "Ensuring the Stability and Security of Socio-Economic Systems: Overcoming the Threats of the Crisis Space."* Kirov: 2021. P. 149–155. ISBN 978-989-758-546-3. https://doi.org/10.5220/0000148100003169

About the author

Andrey I. Ladynin, Cand. Sci. (Econ.), Associate Professor, Informatics Department, Institute of Cybersecurity and Digital Technologies, MIREA – Russian Technological University (78, Vernadskogo pr., Moscow, 119454 Russia). E-mail: ladynin@mirea.ru. Scopus Author ID 57202347343, ResearcherID HJP-8030-2023, RSCI SPIN-code 8762-8534, https://orcid.org/0000-0001-7659-2581

Об авторе

Ладынин Андрей Иванович, к.э.н., доцент, кафедра информатики, Институт кибербезопасности и цифровых технологий, ФГБОУ ВО «МИРЭА – Российский технологический университет» (119454, Россия, Москва, пр-т Вернадского, д. 78). E-mail: ladynin@mirea.ru. Scopus Author ID 57202347343, ResearcherID HJP-8030-2023, SPIN-код РИНЦ 8762-8534, https://orcid.org/0000-0001-7659-2581

Translated from Russian into English by Lyudmila O. Bychkova
Edited for English language and spelling by Thomas A. Beavitt

MIREA – Russian Technological University.
78, Vernadskogo pr., Moscow, 119454 Russian Federation.
Publication date November 28, 2024.
Not for sale.

МИРЭА – Российский технологический университет.
119454, РФ, г. Москва, пр-т Вернадского, д. 78.
Дата опубликования 28.11.2024 г.
Не для продажи.

https://www.rtj-mirea.ru